THE SENSORY AND COGNITIVE BASIS OF DISTANCE ESTIMATION IN TELEOST FISH.



Helena Cecilia Lovisa Karlsson
St John's College
University of Oxford

A thesis presented for the degree of
Doctor of Philosophy

Trinity Term 2020

Acknowledgements

I would first like to thank the BBSRC and St John's College, Oxford for funding this project. I would also like to thank the Department of Zoology for their financial support in the final year of my DPhil.

I am sincerely grateful to my supervisor Theresa Burt de Perera for her guidance and advice throughout my time at Oxford. Thank you for giving me this opportunity, and for teaching me the value of patience and perseverance.

This work was greatly improved by feedback from members of the OxNav community. I would especially like to thank Tim Guilford, Ollie Padget, Dora Biro, Graham Taylor, Joseph Bartram, Sarah Skeels, and Caitlin Newport for their help with experiment design, statistical analyses, and fish care.

Thanks must also go to John and Jason Hogg, and the maintenance staff for keeping the fish labs running both in the ailing Tinbergen building and at the Field Station in Wytham. I am especially grateful to Christine and Helen for their help with fish husbandry.

To Jay Willis, my honourary supervisor and friend, thank you for all your help with experiment design, construction, statistics and paper writing. I have deeply enjoyed our weekly meetings, including the odd joy-ride on the canal.

I thank friends from LMH, St John's, Zoology, OUWLRC, and OUTriC who helped to make my time at Oxford as enriching, challenging, and joyful as I always imagined.

I extend my deepest gratitude to my family. To Fredrika, thank you for being the most enthusiastic and conscientious lab assistant. To Amelie, thank you for all the training camp weekends, providing valuable breaks amidst endless lab work. To my wonderful parents, Helena and Håkan, I will be forever grateful for the childhood you gave the three of us, and your continued faith and support (including frequent reminders that time off is just as important as hard work). Special thanks must also go to my mum for proof-reading all of my drafts over the years.

Finally, Mati, thank you for seeing me through the past 5 years, including endless help with statistics, writing, and coding. This DPhil would have been much harder without your kindness and support.

Declaration

The work within this thesis is primarily my own. Three co-authors contributed towards one or more chapters. Their contributions are as follows:

Theresa Burt de Perera oversaw the project and provided feedback on all chapters of this thesis.

Jay Willis aided with experiment design and construction of experiment set-ups, and provided feedback on chapter 2.

Matishalin Patel assisted with analyses in chapters 2 and 4.

This thesis is submitted in integrated format. Chapters therefore have stand-alone introductions and may differ stylistically for submission to different journals.

Abstract

The ability to measure travel distances is central to navigating by path integration. A path integrating animal constantly and automatically sums movement vectors containing distance and direction self-motion information, providing it with a global vector home to a starting position. This allows the animal to at any time compute novel shortcuts through its familiar area, and reduces the reliance on external positional information to navigate.

Distance estimation has been widely documented in terrestrial animals at the sensory and neural mechanistic levels. In contrast, nothing is known about how freely-swimming aquatic animals such as the large vertebrate group - the teleost fish - collect and compute information on distance travelled. Understanding odometry in teleost fish is important first, for understanding the evolution of vertebrate spatial cognition from an aquatic common ancestor, and second, for understanding how aquatic animals more generally collect metric spatial information under the constraints and challenges of navigating underwater.

In this thesis, I study distance estimation in teleost fish for the first time. Using the Picasso triggerfish, *Rhinecanthus aculeatus*, I aim to answer two key questions: (i) Can teleost fish estimate distance travelled, and with what accuracy? (ii) What sensory mechanisms do teleost fish use to estimate distance travelled?

Using an operant conditioning task, I show that teleost fish can learn and remember travel distances with remarkable accuracy. This internal representation of distance travelled is also preferentially used over previously learned landmark cues when the two sources of information are in conflict.

I proceed to explore the sensory mechanisms underlying distance estimation in *Rhinecanthus aculeatus*. I show that *Rhinecanthus* is unlikely to use mechanosensory inputs from finbeats or measures of travel time for odometry. However, like many terrestrial animals, *Rhinecanthus aculeatus* relies strongly on self-induced optic flow to reproduce travel distances. Visual motion information is also used more broadly to control swimming speeds and to maintain straight, stable swimming trajectories. Therefore, despite the physical constraints water places on the scope of such sensory information, visual motion information can be as important for navigating underwater as it is on land. Unlike many terrestrial animals, teleost fish also have access to a second frame of reference from which they can measure travel distances: the water through which they swim. I finish by presenting preliminary evidence suggesting that in the absence of visual information *Rhinecanthus* can use sensory information from the water column itself to measure relative distance travelled.

This work provides an important baseline for understanding the mechanisms underlying distance estimation in teleost fish. Using the operant conditioning task developed in this thesis, we can study the neural basis of the teleost odometer and continue to test hypotheses about how metric spatial information is collected and encoded by teleost fish that are free to move without constraint through a volume.

Contents

1 General Introduction. 1
- 1.1 Background . . . 2
- 1.2 Odometry in terrestrial species . . . 7
- 1.3 Finding the fish odometer: the importance of fish as a model system . . . 13
- 1.4 Study species . . . 17
- 1.5 Structure of Thesis . . . 19
- 1.6 References . . . 23

2 Teleost fish can accurately estimate distance travelled. 35
- 2.1 Abstract . . . 36
- 2.2 Introduction . . . 37
- 2.3 Methods . . . 41
  - 2.3.1 Subjects . . . 41
  - 2.3.2 Behavioural Task . . . 41
  - 2.3.3 Behavioural Analysis . . . 47
- 2.4 Results . . . 49
- 2.5 Discussion . . . 59
- 2.6 Conclusions . . . 64
- 2.7 Acknowledgements and Approvals . . . 65
- 2.8 References . . . 66

3 Visual odometry in a freely-swimming fish. 71
- 3.1 Summary . . . 72
- 3.2 Main . . . 73
- 3.3 References . . . 83
- 3.4 Acknowledgements and Approvals . . . 87
- 3.5 Methods . . . 88
  - 3.5.1 Behavioural apparatus . . . 88
  - 3.5.2 Behavioural training . . . 88
  - 3.5.3 Testing . . . 89
  - 3.5.4 Video analysis . . . 90
  - 3.5.5 Statistical analyses . . . 91

4 Visual swimming control in the marine fish, *Rhinecanthus aculeatus*. 93
4.1 Abstract . . . 94
4.2 Introduction . . . 95
4.3 Methods . . . 99
4.3.1 Subjects . . . 99
4.3.2 Experiment set-up . . . 99
4.3.3 Training . . . 100
4.3.4 Behavioural data collection . . . 102
4.3.5 Behavioural analysis . . . 104
4.3.6 Statistical analyses . . . 109
4.4 Results . . . 111
4.5 Discussion . . . 126
4.6 Conclusions . . . 131
4.7 References . . . 133

5 A fish's frame of reference: distance estimation in variable flows. 137
5.1 Abstract . . . 138
5.2 Introduction . . . 139
5.3 Methods . . . 142
5.3.1 Subjects . . . 142
5.3.2 Experiment set-up . . . 142
5.3.3 Training . . . 144
5.3.4 Testing . . . 145
5.3.5 Statistical analysis . . . 147
5.4 Results . . . 149
5.5 Discussion and future directions . . . 158
5.6 References . . . 162

6 Development of methods: designing and testing a behavioural task for studying distance estimation in teleost fish. 165
6.1 Background . . . 166
6.2 Experiment 1: Odometry in *Astyanax fasciatus* . . . 170
6.2.1 Methods . . . 170
6.2.2 Results . . . 174
6.2.3 Conclusion and next steps . . . 179
6.3 Experiment 2: Odometry in *Rhinecanthus aculeatus* . . . 181
6.3.1 Methods . . . 181
6.3.2 Results . . . 187
6.3.3 Conclusion and next steps . . . 191
6.4 Experiment 3: Continuous distance task with *Rhinecanthus aculeatus* . . . 191
6.4.1 Methods . . . 192
6.4.2 Results . . . 196
6.4.3 Conclusion . . . 199
6.5 Discussion and Implications . . . 200
6.6 References . . . 202

7 General Discussion **205**
7.1 Summary . . . 206
7.2 Key findings and future directions . . . 207
7.2.1 Distance estimation in a teleost fish . . . 207
7.2.2 Sensory mechanisms underlying distance estimation in *Rhinecanthus aculeatus* . . . 209
7.2.3 Navigating in three dimensions . . . 217
7.2.4 The neural basis of odometry in teleost fish . . . 219
7.3 Concluding remarks . . . 221
7.4 References . . . 223

Appendices **229**

A Supplementary Information: Teleost fish can accurately estimate distance travelled. **231**
A.1 Methods: additional information . . . 233
A.2 Individual fish learning curves . . . 237
A.3 Individual fish distance estimates . . . 239
A.4 Testing assumptions . . . 241
A.5 Use of external cues for distance estimation . . . 243

B Supplementary Information: Visual odometry in a freely swimming fish. **245**
B.1 Methods: additional information . . . 247
B.1.1 Controlling for use of external cues . . . 247
B.1.2 Study species and population sampling . . . 248
B.1.3 Full distance training protocol . . . 250
B.2 Results: additional information . . . 252
B.2.1 Distance estimates across visual treatments . . . 252
B.2.2 Absolute turning position by start area across visual treatments . . . 253
B.2.3 Distance estimate variability . . . 256
B.2.4 Swimming speed across visual treatments . . . 257

C Supplementary Information: Visual swimming control in the marine fish, *Rhinecanthus aculeatus*. **261**
C.1 Sample size and power analysis . . . 263
C.2 Individual fish tracks . . . 265
C.3 Statistical model summaries . . . 271
C.4 Testing model assumptions . . . 273

D Supplementary Information: A fish's frame of reference: distance estimation in variable flows. **275**
D.1 Apparatus . . . 277
D.2 Fish illness report . . . 281

E Supplementary Information: Development of methods - designing and testing a behavioural task for studying distance estimation in teleost fish. 287
E.1 Arduino set-up 289

F Pilot experiment: Metric spatial memory in *Lamprologus ocellatus*. 291
F.1 Background and aims 293
F.2 Methods 294
F.3 Preliminary results 299
F.4 Future work 304

$\sim$ Page left blank intentionally $\sim$

Chapter 1

General Introduction.

General Introduction

1 Background

Navigation refers to the ability to plan and execute a route to a goal [1], and is central to the survival and success of many, if not all, animals. It has been studied across almost all spatial scales and complexities in animals from both the vertebrate and invertebrate clades. Examples extend from the comparatively simple navigational feats of chitons returning to their home scar after a day of foraging [2], through to the long distance migration of American eels, *Anguilla rostrata*, navigating 2400 miles across the continental shelf to the Sargasso Sea [3], and various avian migrants including the arctic tern, *Sterna paradisaea*, [4] Balearchic shearwater, *Puffinus mauretanicus*, [5] and bar-tailed godwit, *Limosa lapponica*, [6] navigating seasonally sometimes across the entire globe.

Navigation can broadly be split into 'learning-based' and 'true' navigation. True navigation, often referred to as 'map and compass' navigation, is distinguished by an animal's ability to return home even after experimental displacement into an unknown environment. It is argued that birds and turtles are capable of such navigational feats [7, 8], but this remains contentious, with some arguing that demonstrations of true navigation can still be explained through associative learning [9]. In contrast, learning-based navigation, which will be the focus of this thesis, involves an animal exploring its environment, often over small spatial scales, and constructing a return journey based on information gathered during its outward excursion. The three most commonly used forms of learning-based navigation are trail following, landmark navigation and path integration.

1.1 Trail following and landmark-use

Trail following and landmark based navigation involve animals using previously experienced or learned routes marked by external positional information such as odours or visual features.

Trail following is the simplest form of learning-based navigation, such as when chitons follow the odour trail deposited during their outward foraging journey to find their way back to their home scar at the end of the day [2]. This simple mechanism can be used to solve seemingly complex navigation problems. Ants, for example, use positive feedback from deposited pheromone trails to organise traffic routes and quickly locate the fastest route out of the colony to a food source [10].

The use of external landmarks to learn the location of a goal relative to an origin is the most broadly studied form of learning-based navigation. It has been demonstrated in animals occupying aerial, aquatic and terrestrial ecologies from across the animal tree of life. A landmark is defined as a distinct feature of the environment, usually visual (such as a tree in an open field), that is recognisable from a distance. A landmark can be used by an animal to broadly recognise the environment it is in, establish its position and orientation within that environment, or to direct travel along a previously learned travel route. The use of landmarks to direct travel along a route can be split into two forms: 'beaconing' and 'piloting'. Beaconing involves learning the association between a single landmark and the location of a goal, allowing this landmark to be approached from any direction. Honeybees often use single landmark beacons to return to the colony after a foraging journey [11], and desert ants, hummingbirds, goldfish and salmon are just some examples of animals that have been shown to use beacons to find the location of food rewards [12–14]. Piloting involves an animal learning to follow a series of landmarks in a particular order to reach its goal. This is most strikingly seen in pigeons following stereotyped routes to return to their home loft, even using major roads and roundabouts to guide their trajectories [15]. Butterflyfishes, brown surgeon fish and blind cavefish can also learn the relative location of a series of landmarks in their aquatic environment, following

stereotyped foraging paths that are interrupted if a learned landmark is removed [16–19].

1.2 Path Integration

Trail-following, beaconing and piloting all involve animals retracing previous routes or trajectories using external positional cues. In contrast, path integration involves an animal using self-motion information to construct novel shortcuts through its environment. A path integrating animal continuously and automatically updates its current position with respect to 'home' by integrating self-movement vectors containing information on the constant distance and direction travelled during an outward journey. This allows the animal to at any time take the direct vector home, following a novel trajectory or 'shortcut' rather than retracing previous steps [20–22].

Path integration was first described by Darwin in 1873 [23] but not formally studied until 1980 in the gerbil, *Meriones unguiculatus* [24]. It was shown that a female gerbil can carry displaced pups along a direct path home even in complete darkness, and if the home nest is displaced during her outward journey she will ignore all odours emanating from the new location of the nest and instead carry her pups back along the computed vector home based on her summed outward vectors [24]. Moreover, if the female is displaced sideways during her return journey, she will continue along a path parallel to the true vector home. Later experiments with the desert ant, *Cataglyphis fortis*, found that this navigation strategy is present in both the vertebrate and invertebrate clades [25], and path integration has since been demonstrated in an array of terrestrial animal species such as hamsters, humans, dogs, pigeons, and spiders [11, 20, 21, 24, 26–28]. That path integration has evolved in both the vertebrate and invertebrate clades is indicative of its importance in evolutionary success. Animals capable of navigating using path integration do not need to rely on fixed positional information to follow a previously experienced route home. This is important for animals occupying featureless, spatially complex, or rapidly changing environments from which selecting and using reliable landmarks is difficult.

Unlike other forms of learning-based navigation, path integration in animals occu-

pying aquatic environments remains poorly understood. Path integration has only recently been demonstrated in the freely-swimming mantis shrimp [29] – the first evidence of this form of navigation being used by a fully aquatic animal. However, it remains unknown whether navigating by path integration is as ubiquitous among underwater animal species as it is on land, or whether the mechanisms underlying this form of navigation are the same as those used by terrestrial animals.

In order to path integrate, an animal must have access to two main forms of metric information: distance and direction [22, 30, 31]. To measure travel direction, invertebrates possess compasses relying on egocentric rotations relative to the earth's magnetic field [8, 32], overhead polarised light [29, 33, 34], and the direction of the sun or the moon and stars [34, 35]. Mammals, meanwhile, rely solely on rotational cues from the internal environment, such as measuring internal vestibular proprioceptive rotations [20]. To measure distance travelled, referred to as odometry, terrestrial animals have been shown to measure proprioceptive inputs from mechanical movements (stride integration) [36–39], energy use [40], internal vestibular movements [41, 42], and self-induced optic flow [43–47]. Although reliant on external visual information, optic flow is defined as idiothetic because it is a self-generated cue derived from the agent's own locomotion. Optic flow does not require the animal to extract a distinguishable object from the environment, but relies on any degree of visual structure, creating visual flow as information travels across the retina when the animal moves. Below we briefly introduce the mechanisms through which animals can measure optic flow.

1.2.1 Optic flow

Self-induced optic flow broadly refers to the speed at which visual information is perceived to pass by an animal as a result of its own movement. If this information is integrated over time it can produce a reliable indication of distance travelled. An animal can measure optic flow in two different ways: (i) by measuring the angular speed of visual features across the retina, or (ii) by measuring the spatio-temporal frequency of contrast

bands, or visual edges, in its environment. The former mechanism is often referred to as 'global' or even 'true optic flow' and computes the speed of image motion across the whole retina, requiring the integration of input from a range of motion-sensitive neurons. It depends on the animal's movement speed and its distance from a visual background, but crucially is independent of variations in environmental spatial frequency [48, 49]. Many previously studied terrestrial animals such as humans [42, 47], honeybees [43, 46], and desert ants [45] use global optic flow for odometry as it is easily translatable across a range of visual environments owing to its spatial frequency independence. The second mechanism can be referred to as 'local optic flow' and depends on the spatio-temporal frequency of the environment, or the optical edge rate. This form of image motion can be computed locally by populations of directionally sensitive neurons that respond to the speed of movement of visual edges in the environment [50, 51]. This latter mechanism is widely used to control the optomotor and optokinetic responses [48], which involve whole body and eye movements to correct for wide-field image motion as a result of unwanted translational or rotational movements of the visual field. It serves to stabilise the visual field and to ensure animals can maintain straight movement courses. The optomotor response has been demonstrated behaviourally in a wide range of aquatic and terrestrial animals, and extensive work has identified populations of directionally sensitive neurons in the retina and post-retinal brain regions of both vertebrates and invertebrates [48, 50–53].

In this thesis, using the aquatic vertebrate group – the teleost fish – as my study system, I investigate the mechanistic basis of distance estimation in aquatic animals for the first time. I provide the first direct test of the metric accuracy of the teleost odometer, and begin to test the sensory mechanisms underlying distance estimation in teleost fish. I particularly focus on the use of optic flow for odometry, and also swimming control more widely. Previous studies have provided early indications that teleost fish must be able to form a representation of their relative distances and directions travelled [19, 54], but path integration and the estimation of travel distances have never been directly demon-

strated in any freely-swimming fish. Understanding whether, and in turn how, teleost fish estimate travel distances has a two-fold importance.

First, the teleost fish form an early-branching group in the vertebrate phylogeny, diverging prior to the transition of tetrapods to land 400 million years ago [55]. Prior work indicates that tetrapods and teleosts share homologous navigation strategies at both the neural and behavioural levels [55–57]. Understanding how teleost fish map metric space therefore has fundamental implications for our understanding of the evolution of spatial cognition in the vertebrate clade as a whole.

Second, as a fully aquatic group, by studying the sensory mechanisms used by teleost fish to estimate distance travelled, we hope to further our understanding of how freely-swimming aquatic animals use self-motion information to navigate. Animals navigating underwater face different challenges and constraints compared to those navigating on land. It is therefore uncertain whether aquatic animals can use similar sensory self-motion information to terrestrial animals to measure distance and direction travelled.

Below, I review our current understanding of odometry in terrestrial vertebrates and invertebrates, and further explore the importance of understanding this behaviour in the teleost clade.

2 Odometry in terrestrial species

Odometry was first studied in the honeybee, *Apis mellifera*, in the context of understanding its dance language. When worker honeybees return to the hive, they accurately communicate the distance and direction to nearby food sources through elaborate dances [58–60]. Since these early studies, there has been an increasing effort to unravel the distance estimation abilities of other animals. Among the invertebrates, ants, spiders and fiddler crabs have also been found to possess accurate odometers [36, 44, 45, 61, 62]. The vertebrate clade is significantly less broadly studied, with our knowledge limited to the odometers of humans [42, 63–68] and, only very recently, rats [41].

At the sensory level, there are five non-mutually exclusive ways in which terrestrial animals have been proposed to collect information on distance travelled by measuring: (i) time spent travelling, (ii) energy expenditure, (iii) proprioceptive cues, requiring an internal step counter, (iv) self-induced optic flow, and (v) translational vestibular cues from the inner ear system in vertebrates. I hypothesise that use of specific mechanisms is related to an animal's specific physiological constraints and ecological niche. Examples from work with the honeybee, desert ant and two spider species illustrate this concept.

2.1 Honeybees

It was initially thought that honeybees used energy expenditure as a proxy for distance flown [58]. In experiments conducted on mountain slopes, bees foraging uphill from the hive against the pull of gravity indicated longer distances flown than those foraging downhill [43, 59, 69], and likewise bees laden with lead weights signalled longer distances [70]. However, later experiments controlling for wind velocities proved this association to be false [46, 60, 71, 72]. Relying on cues other than energy expenditure makes ecological sense for foraging honeybees needing to report accurate distances to their fellow workers. Bees returning to the hive from a foraging location will be laden with nectar and deposited pollen so will be heavier on the return journey, and in turn will signal further distances than fellow workers need to travel to find the same foraging patch when exiting the hive unburdened.

Honeybees instead rely almost exclusively on self-induced optic flow to gauge distance flown, a mechanism that is independent of wind load and energy expenditure [49, 73–75]. Distances are reported as a function of the total optic flow experienced during the return journey from a foraging location [74]. Honeybees measure global optic flow, or the angular speed at which information travels across the retina: objects further away will appear to travel slower than those closer to the retina, and faster movement speeds result in greater perceived visual load. Honeybees inhabit a spatially complex foraging environment and fly at a relatively constant height above the ground. They are therefore likely to

gain sufficient distance information from their ventral and lateral visual environment to consistently report accurate distances to foraging locations through their dance language. The results from previous mountain slope experiments can be explained through use of optic flow. Honeybees, once they have taken off, exhibit only small changes in altitude to fly horizontally through the air. This horizontal flight means that when the bees are travelling uphill they are travelling increasingly close to the ground, and so experience greater optic flow than when they are flying downhill increasingly far away from the ground [43, 74].

Srinivasan and colleagues sought to explore bees' use of optic flow further. In a series of experiments, worker bees were trained to fly through a tunnel lined with vertical black and white stripes, providing regular translational optic flow, to a feeder at a particular location. Following removal of the feeder and manipulation of the optic flow background by orienting the stripes horizontally, the search behaviour of workers at the perceived feeder location and their dance language upon return to the hive were analysed as a proxy for distance estimation [49]. In a tunnel in which the vertical striped pattern of the lateral walls is identical on either side, the bees fly equidistant to the flanking walls to balance the speed of image motion to each eye, and are in turn able to accurately report distances flown to their hivemates [74, 75]. Removing translational spatial frequency by providing horizontal instead of vertical stripes eliminated their ability to estimate distance [46]. This mechanism depends on distance from the visual background, as narrowing the tunnel to increase the speed of image motion also resulted in them indicating shorter distances [46]. However, it is independent of the spatial frequency of the environment, as the bees did not respond to a change in stripe period [46].

2.2 Desert ants

Studies looking at odometry in the desert ant, *Cataglyphis fortis*, known to use path integration as its primary mechanism for returning home after a foraging journey, have also tested the role of optic flow in estimating distance travelled. Similar to bees, loading ants

with weights of up to four times their body weight has no effect on distance travelled [45]. However, unlike bees, desert ants subjected to the same manipulations to the lateral optic flow background as in the Srinivasan experiments showed no impairment in their odometry [62]. Desert ants instead seem to rely on ventral and not lateral optic flow [62], perhaps because the lateral visual ecology of their natural sandy desert environment is relatively featureless, so they must gain information ventrally as they move over the sand. The use of ventral optic flow is aided by keeping their head at a constant height and position above the ground [45].

Desert ants, however, do not rely exclusively on optic flow, perhaps because of the reduced contrast frequency in their featureless natural environment. Manipulating leg length of desert ants by making them walk on trimmed leg stumps or on stilts led to them misgauging distance travelled [37]. They therefore appear to supplement information gained from self-induced optic flow with idiothetic information from an internal stride integrator that likely uses leg mechanoreceptors such as the companiform sensillae to provide input to an internal pedometer [38]. Other species, such as the fiddler crab, with highly modified retinas to more effectively collect similarly sparse visual information from the horizon, have also been found to use optic flow in combination with stride integration to assess distance travelled [36].

2.3 Visual and non-visual spiders

The wolf spider, *Lycosidae tarantula*, occupies a range of environments both above and below ground and unlike most arachnids has excellent vision. Temporarily blinding *Lycosidae* subjects after they had learned to walk a set distance showed complete impairment in odometry both when the lateral and ventral visual systems were affected, indicating complete reliance on visual information for odometry [44]. This is compared with the visually-poor wandering spider, *Cupenius salei* which retains perfect distance estimation even when blinded [39]. As with the desert ant, the wandering spider collects information on distance travelled through stride integration, using proprioceptive information gath-

ered by mechanosensory organs on their legs. If the lyriform slit organs on the femur and tibia on the wandering spider are destroyed then these spiders are unable to estimate distance [39, 76]. Among the invertebrates, the use of either optic flow, proprioceptive cues, or both, for odometry therefore seems to be linked to the animal's visual ecology.

2.4 Vertebrate odometry

Within the vertebrate clade, our understanding of the sensory basis of distance estimation is largely limited to humans [42, 63–68]. Humans, like some invertebrates, can switch between different sensory mechanisms depending on the information available to them, but this appears to be more flexible than in their invertebrate counterparts. Virtual reality experiments have indicated that humans can use optic flow to estimate distances, using a similar mechanism to that seen in honeybees [47, 66, 77, 78]. Distance estimates are a function of the distance from a visual background and the speed at which the subject is perceived to pass by that background, with only very slight sensitivity to the density of spatial frequency information [47, 64, 66]. However, humans retain the ability to estimate distance in the dark with no impairment. In environments lacking visual information, the estimation of path length becomes a function of walking velocity, step length and step rate [67, 68]. Unlike the previously studied invertebrates, there is also some evidence that humans can measure energy use as a proxy for distance travelled. Humans laden with heavy rucksacks and asked to walk through a virtual reality environment on a treadmill perceived themselves to have travelled further than those with no burden [40].

Metric distance estimation has only recently been demonstrated in rats [41]. Like humans, rats are able to learn and reproduce travel distances in the absence of visual cues, suggesting they may be using translational vestibular cues or an internal stride integrator for odometry [41]. However, most work exploring odometry in mammalian models has focused on understanding the underlying neural mechanisms of this behaviour in the context of path integration as a whole.

In mammals, spatial information is processed by the hippocampus in coordination

primarily with the entorhinal system to form the neural basis of a spatial map of the animal's environment [79–81]. Central to self-localisation are the hippocampal place cells, which typically fire when an animal enters a particular part of its environment, known as the 'place field' [82–84]. Place cells use two main sources of sensory information in the form of external landmarks (allothetic information) and self-motion cues (idiothetic information), which are processed via an array of neural navigational cell types, including head direction cells, speed cells, boundary cells and grid cells [81, 85, 86]. These additional cell types are found throughout the hippocampus, entorhinal and surrounding cortical and subcortical systems.

Grid cells and head direction cells are likely to underpin path integration navigation in mammals. The former are located in layers II and III of the medial entorhinal cortex (MEC) and have been proposed to constitute the 'neural odometer' [85]. Grid cells have many firing fields forming a periodic triangular array or 'grid' that tiles the entire environment, with a strong relationship between the position of a moving rat and MEC grid-cell activity [79, 85, 87–89]. As has been demonstrated behaviourally, firing is dependent mostly on self-motion cues; grid cell firing remained unchanged in terms of average firing rate and spatial information per spike when a rat was measured in total darkness compared to a visually rich environment [89, 90]. However, rats with lesions in the MEC are unable to return to their home cage based on self-motion cues alone, indicating their importance in path integration navigation [27]. In a linear distance estimation task, Jacob et al. also showed that rats with excitotoxic medial entorhinal cortex lesions could not estimate distance travelled based on self-movement information [41].

Head direction cells, meanwhile, are located in cortical (postsubiculum, restrosplenal cortex, entorhinal cortex) and subcortical (thalamus, lateral mamillary nucleus, dorsal tegmental nucleus, striatum) regions and encode directional information [86, 91, 92]. Alongside the other cell types, grid and head direction cells form efferent connections either directly or through interneurons with place cells in the hippocampus, which are thought to integrate information from these afferent cell types to form a 'spatial map-like'

representation of space [82]. This is likely a conserved navigation mechanism across the mammalian clade; place and grid cells in the hippocampus and medial entorhinal cortex have since been found in mice, bats, and monkeys, and signatures of grid cells have been discovered in humans [28].

3 Finding the fish odometer: the importance of fish as a model system

The knowledge of the fish navigation system at both the neural and behavioural levels remains far behind our understanding of terrestrial animals. The ability to path integrate, and in turn estimate distance travelled, may be advantageous for teleost fish navigating through their local home ranges. Light attenuates rapidly with increasing depth and horizontal distance in the water column, leading to reduced visual ranges and acuities to distinguish visual landmarks at a distance [29, 93]. The lateral line system in fish, made up of mechanoreceptor units called neuromasts, can be used alongside, or instead of, visual information to detect solid landmarks through distortions to stereotyped patterns of hydrodynamic flows around the fish's body [18]. However, the perceptual range of the lateral line system is smaller even than the visual system, requiring the fish to be within a few millimetres of a landmark [94]. Moreover, for fish occupying moving water bodies such as rivers and oceans, the spatial environment is unstable, undergoing sporadic and sometimes rapid change. Taken together, these factors may reduce their ability to fully rely on fixed, external positional cues to navigate via learned routes within their local environment [19]. Indeed, landmark use has been shown to be reduced in three-spined stickleback, *Gasterosteus aculeatus*, populations occupying spatially unstable environments with high flow rates such as rivers compared to populations occupying ponds with lower flow rates [95]. Path integration, meanwhile, is an automatic process relying on egocentric self-motion cues, with the global home vector constantly updated as the animal moves through its environment. A foraging animal can therefore interrupt its journey at any mo-

ment and construct a direct return trajectory, irrespective of the presence or absence of any spatially or temporally unreliable allocentric positional cues [20]. When analysing 3D swimming trajectories in their y-maze task, Holbrook and colleagues showed that sighted cavefish were able to discern the prior location of a reward even when all previously available landmark cues were removed [54]. This indicates that fish may be able to use internal distance and direction information to discern the location of a goal in the absence of other cues. Despite this, there have been no direct studies of path integration in teleost fish, nor of the underlying local area orientation and odometry mechanisms.

Directional sensing in fish has been studied, but in the context of long-range compasses in migrating teleosts. Mosquitofish, for example, are able to orient using a time-compensated sun compass, with failed orientation in overcast skies or diffuse light [96]. Juvenile sockeye salmon and the Mozambique tilapia are able to orient using magnetosensation [97, 98] and there is some evidence that rainbow trout can use polarized light from above [99]. Although studied in the context of long-distance migrations and not local area navigation, these mechanisms show some similarities with those used for path integration by previously studied terrestrial invertebrates. This suggests that some sensory cues used by animals to orient on land may also be important for animals navigating underwater.

In this thesis, I test the cognitive and sensory basis of distance estimation in teleost fish for the first time. I address two key areas: (i) Can teleost fish estimate distance travelled, and with what accuracy? (ii) What sensory mechanisms do teleost fish use to estimate distance travelled? Understanding whether, and in turn how, teleost fish estimate travel distances has implications firstly for our understanding of how freely-swimming aquatic animals use idiothetic information to navigate, and secondly for our understanding of the evolution of distance estimation and path integration in the vertebrate clade as a whole.

First, owing to the physical constraints water places on the scope of certain sensory information, the sensory mechanisms used for odometry may differ between terrestrial and aquatic animals. Freely-swimming animals have the challenge of navigating through

a dynamic fluid with no direct physical contact with a fixed benthic background and, benthic visual information that is prominent on land becomes indistinct over relatively short distances underwater, an effect that is inflated with increasing depth as light levels decline [29, 93]. Information generated from the benthic background may therefore be used in a different way from terrestrial animals, or not used at all, as a reference from which to estimate travel distances. Aquatic environments also contain additional sensory information that isn't available on land. Teleost fish have evolved specialised sensory organs to allow them to detect and use this additional information. For example, teleosts have a lateral line system to detect hydrodynamic cues from water flows [94], and a swim bladder to regulate buoyancy, which has the potential to be co-opted to detect hydrostatic pressure changes with depth [100]. Two radiations of electric fish also have modified electric organs and appendages to measure electric currents carried through the water [101]. Whether these specialised sensory systems are also used to measure travel distances remains to be found.

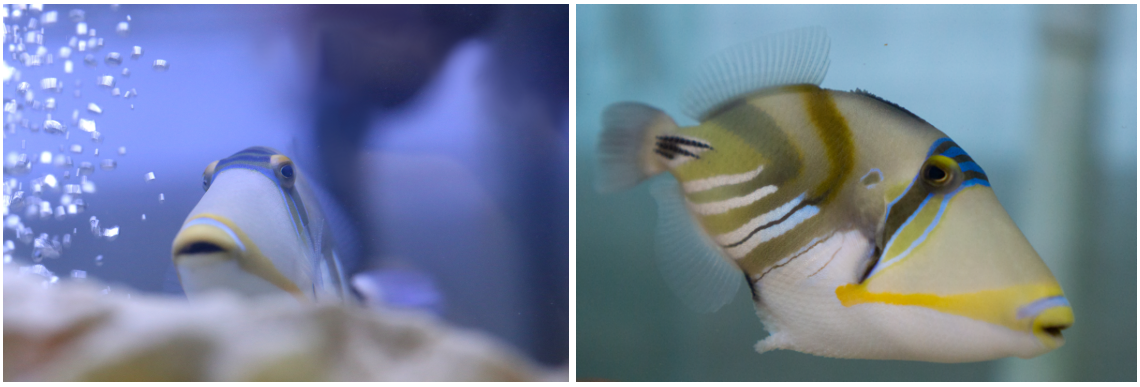
Second, the teleost fish provide a valuable study system with which to further our understanding of the evolution of spatial cognition in the vertebrate clade as a whole. The common ancestor of all extant tetrapods, or terrestrial vertebrates, was a fully aquatic animal occupying a similar ecology to many extant marine teleosts [102]. At the behavioural level, studying how teleost fish specifically collect and encode metric information will be valuable for understanding the conditions under which the vertebrate navigation system may have first evolved. At the neural level, there are also indications that brain structures underlying some navigation behaviours in teleosts and tetrapods are homologous. The lateral pallium in the goldfish forebrain is homologous and likely plays a similar role to the amniote medial pallium, or avian and mammalian hippocampus [19]. Lesions to the lateral pallium causes fish to lose the ability to find a previously learned goal [55], and goldfish trained in a spatial memory task show increased levels of protein synthesis in the lateral palium [103]. Combined with behavioural studies suggesting that both turtles and teleosts use the same strategies as mammals to solve spatial navigation tasks, it

has been proposed that the medial cortex in reptiles, the teleost lateral pallium, and the hippocampus are homologous structures [56, 57]. This suggests that a brain structure specialised for encoding spatial information evolved as many as 400 million years ago in an aquatic common ancestor [55–57]. Moreover, the optic tectum in teleosts has also been tentatively suggested to be the neural centre for multisensory integration and sensorimotor transformations, perhaps filling a functionally similar role to the medial entorhinal cortex underlying odometry in mammals [57].

In order to unequivocally demonstrate that certain neural regions and mechanisms underlie a behaviour, single-cell recordings from specific brain regions must be conducted in freely-behaving animals. Technologies are rapidly being developed to study neural activity at the cellular level in freely-swimming fish. There has been early evidence of velocity, speed and border-like cells in the lateral pallium of the goldfish brain, cell types that could be important for path integration in teleosts [104]. Finding such cell types in the goldfish brain brings us closer to understanding the anatomical and functional evolution of the vertebrate hippocampal/pallial navigation system.

However, in order to fully understand the neural mechanisms underlying navigation in mammals, birds, and fish, we must first test whether these animals share similar navigational processes and strategies at the behavioural level. Demonstrating behaviourally that teleost fish can estimate distance travelled with a similar metric accuracy to mammals is an important precursor to exploring which brain regions underlie this behaviour, and eventually whether teleost fish use a mammalian grid cell-like system to encode distance information.

In the following sections, I introduce the model species used throughout this thesis and summarise the experimental work carried out to explore the sensory and cognitive basis of distance estimation in teleost fish for the first time.



(a) (b)

Figure 1: *Rhinecanthus aculeatus* subjects used in Chapters 2-6 of this thesis (a) hiding behind tank enrichment and, (b) freely-swimming, showing different fin types including modified dorsal and ventral fins. Photos taken by J.K. Willis and Y.J. Oh.

4 Study species

I use the shallow-water marine Picasso triggerfish, *Rhinecanthus aculeatus*, as my model system to develop a behavioural task to test metric distance estimation in teleost fish, and to explore the sensory mechanisms underlying distance estimation in this species. *Rhinecanthus aculeatus* is a marine fish from the order Tetraodontiformes which typically occupies well-lit intertidal zones of the Indo-Pacific Ocean [93]. It is a highly territorial species, navigating between its home nest in the highly structured coral reef zones, and its adjacent foraging locations over indistinguishable coral rubble which has been broken up by persistent erosion from waves and the ingoing and outgoing tide. This environment is spatially complex but unstable, undergoing sporadic and sometimes rapid change. Waves and tidal movements will create irregular water currents varying in strength, direction and turbulence depending on the local structure of the coral reef, weather conditions, and the position of the moon. This will cause previously available landmarks to be regularly broken up, displaced across considerable distances, or obscured by disturbed sediment. Together, this may reduce the reliability of external landmark cues for navigation. Instead, navigating using distance and direction information derived from self-movement is likely to be central to their survival and success. The intertidal zones occupied by *Rhinecanthus*

aculeatus are usually shallow and brightly-lit, with a water depth typically below 20m. The highly visual aquatic ecology occupied by this species therefore makes it an interesting candidate to study the role of self-motion for odometry in a freely-swimming animal. Unlike teleosts that occupy deep waters in the open ocean and other dark environments such as deep river beds or caves, these fish have access to visual information, but face the challenge of extracting and using this information under the constraints and challenges of navigating through water. This species has also shown to be bold, highly trainable in complex operant conditioning tasks, and is strongly motivated for food rewards [93, 105, 106]. The operant conditioning used throughout the experiments in the following chapters relies on the precise delivery of food rewards and a strong motivation to move towards them, making this species suitable for the present study.

We started designing the behavioural task used throughout this thesis with the sighted morph of the Mexican cavefish, *Astyanax fasciatus*. This species is distributed throughout North, Central and South America and occupies the bentho-pelagic environment of slow-flowing streams and rivers. It is highly motivated for food and shoal rewards during operant conditioning tasks, both of which were used as rewards in the initial experiment design. *Astyanax fasciatus* was also used in the initial study by Holbrook and colleagues that provided the first indication that fish could remember the previous location of a reward in the absence of previously used landmark cues [54]. Work with this species was fundamental to the early design stages of our distance estimation task. However, as this species is highly sensitive to being individually housed for extended periods of time, and performing a complex behavioural task independently of conspecifics, the previously described marine fish, *Rhinecanthus aculeatus* was used for the remainder of experiments presented in this thesis.

5 Structure of Thesis

I develop a behavioural task to test the distance estimation abilities of teleost fish for the first time. Using this task, I aimed to understand first, how accurately teleost fish could estimate travel distances, and second, the sensory mechanisms used by *Rhinecanthus aculeatus* to measure travel distances. Below, I outline the experimental work answering these questions.

Chapter 2: Teleost fish can accurately estimate distance travelled

This chapter introduces the basic behavioural task used to test the teleost odometer throughout this thesis. Using the Picasso triggerfish, *Rhinecanthus aculeatus*, we show that a teleost fish can accurately learn and remember a trained distance. By analysing swimming trajectories of these distance estimates, we also begin to explore the potential mechanisms used to acquire distance information. First, by comparing the relative variance in the two metrics, we test the hypothesis that distance is represented as a measure of travel time. Second, by quantifying finbeat use across each distance estimate, we investigate whether *Rhinecanthus* may use proprioceptive inputs from a finbeat counter to measure distance travelled in a similar way to the step-counters of many walking animals.

Chapter 3: Visual odometry in a freely-swimming fish

In chapter 3, we continue exploring the sensory basis of distance estimation in *Rhinecanthus aculeatus* by testing whether optic flow information, as is widely used by terrestrial animals, can also be used by a freely-swimming animal for odometry. Using the distance estimation task presented in the previous chapter and subsequently manipulating the visual information available, we show that *Rhinecanthus* does use visual motion information to estimate distance travelled. However, the underlying mechanism differs fundamentally from that used by terrestrial animals. Humans and terrestrial invertebrates measure optic flow as the total angular motion of visual features, which does not vary with visual

density. In contrast, we show that the visual odometer used by *Rhinecanthus* is strongly dependent on the visual density of the environment. This more closely resembles the motion-detection mechanisms underlying the optomotor response, which respond to the spatio-temporal frequency of a visual scene. The optomotor response is an innate reflex resulting in head and eye movements that stabilise a visual scene upon translational or rotational displacement. We suggest that the visual odometer in *Rhinecanthus* may be underpinned by similar sensory processing mechanisms.

Chapter 4: Visual swimming control in the marine fish, *Rhinecanthus aculeatus*

Among terrestrial animals that rely on optic flow to estimate distance travelled, visual motion information is also used to manoeuvre efficiently through their environment. Flying and walking animals such as bees, birds and humans use optic flow information to maintain straight movement trajectories, navigate safely through narrow gaps, avoid collisions, and control movement speeds. Analysis of swimming trajectories from the previous chapter indicated that *Rhinecanthus* may also use optic flow to control swimming speeds. The use of optic flow information to more widely regulate movement trajectories may therefore be a universal strategy used by visually-reliant animals occupying aerial, aquatic and surface-constrained ecologies. In this chapter, we test this hypothesis by examining experimentally how the control of positioning and speed of swimming trajectories are affected by the availability and orientation of visual information in *Rhinecanthus aculeatus*. We show that *Rhinecanthus aculeatus* has evolved to control both its positioning from obstacles and swimming speed using visual motion cues. However, these processes appear to be underpinned by separate mechanisms, measuring visual expansion and translational optic flow respectively.

Chapter 5: A fish's frame of reference: distance estimation in variable flows

Teleost fish have access to two separate frames of reference from which to make navigation decisions: the fixed benthic background, and the water column through which

they swim. In chapter 5, we continued to work with *Rhinecanthus aculeatus* to examine the relative importance of sensory information from these two frames of reference for estimating distance travelled. We designed a flume system that could alter water flow within a tunnel with changeable visual information on the walls and floor. By training individuals in this flume system using the distance estimation task developed in previous chapters, we were able to test the relative importance of visual information and water flow information for odometry. Pilot results from one individual indicate that *Rhinecanthus* relies primarily on visual motion information from the fixed benthic background to estimate distance travelled. Manipulations to water flow information from the fluid medium had only small, secondary effects on odometry when visual information was present. However, when visual information was removed, the effects of altering water flows became more pronounced, indicating that *Rhinecanthus* may display hierarchical use of different sensory inputs depending on the information available to them.

Chapter 6: Developing a behavioural task for testing distance estimation in teleost fish

The behavioural task used throughout this thesis was developed gradually, with multiple iterations of design improvements prior to development of the final design. Findings from these early studies can provide a reference point from which any further modifications for studying odometry in a wider range of teleost fish species can be made. In this chapter, we outline the different stages of experiment design, testing and refinement to produce the final experiment set-up and behavioural training protocol. We present three stages of experiment design improvement. The first experiment uses the sighted morph of the Mexican cavefish, *Astyanax fasctiatus* and for the latter two experiments, we progress to using the reef dwelling Picasso triggerfish, *Rhinecanthus aculeatus*, as our study species. All experiments use a 'match-to-sample' design, in which fish are trained to a sample distance and tested in their ability to reproduce this distance. Preliminary results from the final successful experiment design provided the first indication that *Rhinecanthus aculeatus* encodes distance travelled with remarkable accuracy and precision, and requires access

to visual information to do so. Conclusions from this experiment were used to make final modifications to the behavioural task.

Finally, in chapter 7, I conclude by summarising the key findings of this thesis and indicate areas for future work, both with *Rhinecanthus aculeatus*, and teleost fish more generally. Importantly, we demonstrate the value of behavioural experiments in forming testable hypotheses about underlying neural mechanisms and processes. The work presented in this thesis provides an important baseline from which we can continue to work towards understanding how teleost fish encode metric space at the cognitive, sensory and neural mechanistic levels. This will allow us to more fully understand the evolution of spatial cognition in the vertebrate clade, and also how aquatic animals more generally have evolved to navigate efficiently in their three-dimensional aquatic world.

References

[1] Gallistel C. R. *The organization of learning*. MIT Press, 1990.

[2] Chelazzi G., Della Santina P., and Parpagnoli D. Trail following in the chiton Acanthopleura gemmata: operational and ecological problems. *Marine Biology*, 95(4): 539–545, 1987.

[3] Miller M.J., Westerberg H., Sparholt H., Wysujack K., Sorensen S.R., Marohn L., Jacobsen M.W., Freese M., Ayala D.J., Pohlmann J-D., Svendsen J.C., Watanabe S., Andersen L., Moller P.R., Tsukamoto K., Munk P., and Hanel R. Spawning by the European eel across 2000 km of the Sargasso Sea. *Biology Letters*, 15:1–5, 2019.

[4] Egevang C., Stenhouse I.J., Phillips R.A., Petersen A., Fox J.W., and Silk J.R.D. Tracking of Arctic terns Sterna paradisaea reveals longest animal migration. *Proceedings of the National Academy of Sciences (PNAS)*, 107(5):2078–81, 2010.

[5] Meier R.E., Russell B.W., Votier S.C., McMinn M., Rodríguez A., Maurice L., Emiel-van E., Loon A.R., Jonesa L., Suberg J., Arcos M., Morgang G., Josey S.A., and Guilford T. Consistent foraging areas and commuting corridors of the critically endangered Balearic shearwater Puffinus mauretanicus in the northwestern Mediterranean. *Biological Conservation*, 190:87–97, 2015.

[6] Gill R.E, Tibbitts T.L, Douglas D.C., Handel C.M, Mulcahy D.M, Gottschalck J.C, Warnock N., McCaffery B.J., Battley P.F., and Piersma T. Extreme endurance flights by landbirds crossing the Pacific Ocean: ecological corridor rather than barrier? *Proceedings of the Royal Society of London B: Biological Sciences*, 276(1656):447–457, 2009.

[7] Gagliardo A. Forty years of olfactory navigation in birds. *The Journal of Experimental Biology*, 216(Pt 12):2165–71, 2013.

[8] Lohmann K.J. and Lohmann C.M.F. Detection of magnetic field intensity by sea turtles. *Nature*, 380(6569):59–61, 1996.

[9] Guilford T. and Burt de Perera T. An associative account of avian navigation. *Journal of Avian Biology*, 48(1):191–195, 2017.

[10] Goss S., Aron S., Deneubourg J. L., and Pasteels J. M. Self-organized shortcuts in the Argentine ant. *Nature*, 76(12):579–581, 1989.

[11] Collett T.S. Insect navigation en route to the goal: multiple strategies for the use of landmarks. *Journal of Experimental Biology*, 199(1), 1996.

[12] Warburton K. The use of local landmarks by foraging goldfish. *Animal Behaviour*, 40(3):500–505, 1990.

[13] Braithwaite V.A., Armstrong J.D., McAdam H.M., and Huntingford F.A. Can juvenile Atlantic salmon use multiple cue systems in spatial learning? *Animal Behaviour*, 51(6):1409–1415, 1996.

[14] Zhao M. and Warren W.H. How You Get There From Here. *Psychological Science*, 26 (6):915–924, 2015.

[15] Biro D., Meade J., and Guilford T. Familiar route loyalty implies visual pilotage in the homing pigeon. *PNAS*, 101:17440–17443, 2004.

[16] Reese E.S. Orientation behavior of butterflyfishes (family Chaetodontidae) on coral reefs: spatial learning of route specific landmarks and cognitive maps. *Environmental Biology of Fishes*, 25(1-3):79–86, 1989.

[17] Mazeroll A.I. and Montgomery W.L. Daily Migrations of a Coral Reef Fish in the Red Sea (Gulf of Aqaba, Israel): Initiation and Orientation. *Copeia*, 4:893–905, 1998.

[18] Burt de Perera T. Fish can encode order in their spatial map. *Proceedings. Biological sciences*, 271(1553):2131–4, 2004.

[19] Braithwaite V. A. and Burt de Perera T. Short-range orientation in fish: How fish map space. *Marine and Freshwater Behaviour and Physiology*, 39(1):37–47, 2006.

[20] Etienne A.S. and Jeffery K.J. Path integration in mammals. *Hippocampus*, 14(2): 180–92, 2004.

[21] Foo P., Warren W.H., Duchon A., and Tarr M.J. Do humans integrate routes into a cognitive map? Map- versus landmark-based navigation of novel shortcuts. *Journal of Experimental Psychology*, 31(2):195–215, 2005.

[22] Etienne A.S., Maurer R., Berlie J., Reverdin B., Rowe T., Georgakopoulos J., and Séguinot V. Navigation through vector addition. *Nature*, 396(6707):161–4, 1998.

[23] Darwin C. Origin of Certain Instincts. *Nature*, 7(179):417–418, 1873.

[24] Mittelstaedt M.L. and Mittelstaedt H. Homing by path integration in a mammal. *Nature*, 67(11):566–567, 1980.

[25] Wehner R. and Srinivasan M.V. Searching behaviour of desert ants, genus-Cataglyphis (Formicidae, Hymenoptera). *Journal of Comparative Physiology A*, 142 (3):315–338, 1981.

[26] Loomis J.M., Klatzky R.L., Golledge R.G., Cicinelli J.G., Pellegrino J.W., and Fry P.A. Nonvisual navigation by blind and sighted: assessment of path integration ability. *Journal of Experimental Psychology*, 122(1):73–91, 1993.

[27] Kim S., Sapiurka M., Clark R.E., and Squire L.R. Contrasting effects on path integration after hippocampal damage in humans and rats. *Proceedings of the National Academy of Sciences of the United States of America*, 110(12):4732–7, 2013.

[28] Chen X.i, He Q., Kelly J.W., Fiete I.R., and McNamara T.P. Bias in Human Path Integration Is Predicted by Properties of Grid Cells. *Current Biology*, 25(13):1771–6, 2015.

[29] Patel R.N and Cronin T.W. Mantis Shrimp Navigate Home Using Celestial and Idiothetic Path Integration. *Current Biology*, 30:1–7, 2020.

[30] Wallace D.G., Martin M.M., and Winter S.S. Fractionating dead reckoning: role of the compass, odometer, logbook, and home base establishment in spatial orientation. *Nature*, 95(11):1011–26, 2008.

[31] Parron C. and Save E. Evidence for entorhinal and parietal cortices involvement in path integration in the rat. *Experimental Brain Research*, 159(3):349–59, 2004.

[32] Wiltschko W. and Wiltschko R. Orientation in birds. Magnetic orientation and celestial cues in migratory orientation. *EXS*, 60:16–37, 1991.

[33] Rossel S. and Wehner R. The bee's map of the e-vector pattern in the sky. *Proceedings of the National Academy of Sciences (PNAS)*, 79:4451–5, 1982.

[34] Wehner R. and Muller M. The significance of direct sunlight and polarized skylight in the ant's celestial system of navigation. *Proceedings of the National Academy of Sciences (PNAS)*, 103:12575–12579, 2006.

[35] Dacke M., Nilsson D., Scholtz C., Byrne M., and Warrant E. Insect orientation to polarized moonlight. *Nature*, 424:33–36, 2003.

[36] Walls M.L. and Layne J.E. Direct evidence for distance measurement via flexible stride integration in the fiddler crab. *Current Biology*, 19(1):25–9, 2009.

[37] Wittlinger M., Wehner R., and Wolf H. The ant odometer: stepping on stilts and stumps. *Science*, 312(5782):1965–7, 2006.

[38] Wittlinger M., Wehner R., and Wolf H. The desert ant odometer: a stride integrator that accounts for stride length and walking speed. *The Journal of Experimental biology*, 210(Pt 2):198–207, 2007.

[39] Seyfarth E.A., Hergenrider R., Ebbes H., and Barth F.G. Idiothetic orientation of a wandering spider: Compensation of detours and estimates of goal distance. *Behavioral Ecology and Sociobiology*, 11(2):139–148, 1982.

[40] Proffitt D.R., Stefanucci J., Banton T., and Epstein W. The role of effort in perceiving distance. *Psychological Science*, 14(2):106–12, 2003.

[41] Jacob P.Y., Gordillo-Salas M., Facchini J., Poucet B., Save E., and Sargolini F. Medial entorhinal cortex and medial septum contribute to self-motion-based linear distance estimation. *Brain Structure and Function*, 222(6):2727–2742, 2017.

[42] Harris L.R., Jenkin M., and Zikovitz D.C. Visual and non-visual cues in the perception of linear self-motion. *Experimental Brain Research*, 135(1):12–21, 2000.

[43] Esch H. E. and Burns J. E. Honeybees use optic flow to measure the distance of a food source. *Nature*, 82(1):38–40, 1995.

[44] Ortega-Escobar J. and Ruiz M.A. Visual odometry in the wolf spider Lycosa tarantula (Araneae: Lycosidae). *The Journal of Experimental Biology*, 217:395–401, 2014.

[45] Ronacher B. and Wehner R. Desert ants Cataglyphis fortis use self-induced optic flow to measure distances travelled. *Journal of Comparative Physiology A*, 177(1):21–27, 1995.

[46] Srinivasan M., Zhang S., and Bidwell N. Visually mediated odometry in honeybees. *Journal of Experimental Biology*, 200(19):2513–2522, 1997.

[47] Frenz H. and Lappe M. Absolute travel distance from optic flow. *Vision Research*, 45 (13):1679–92, 2005.

[48] Srinivasan M. V., Zhang S. W., and Chandrashekara K. Evidence for two distinct movement-detecting mechanisms in insect vision. *Naturwissenschaften*, 80:38–41, 1993.

[49] Srinivasan M.V. Honeybees as a model for the study of visually guided flight, navigation, and biologically inspired robotics. *Physiological Reviews*, 91(2):413–60, 2011.

[50] Kubo F., Hablitzel B., Dal Maschio M., Driever W., Baier H., and Arrenberg A.B. Functional Architecture of an Optic Flow-Responsive Area that Drives Horizontal Eye Movements in Zebrafish. *Neuron*, 81:1344–1359, 2014.

[51] Kretschmer F., Tariq M., Chatila W., Wu B., and Badea T.C. Comparison of optomotor and optokinetic reflexes in mice. *Journal of Neurophysiology*, 118:300–316, 2017.

[52] Maaswinkel H. and Li L. Spatio-temporal frequency characteristics of the optomotor response in zebrafish. *Vision Research*, 43:21–30, 2003.

[53] Dubois M. F.W. and Collewijn H. Optokinetic reactions in man elicited by localized retinal motion stimuli. *Vision Research*, 19:1105–1115, 1979.

[54] Holbrook R.I. and Burt de Perera T. Three-dimensional spatial cognition: freely swimming fish accurately learn and remember metric information in a volume. *Animal Behaviour*, 86(5):1077–1083, 2013.

[55] Rodríguez F., López J.C., Vargas J.P., Broglio C., Gómez Y., and Salas C. Spatial memory and hippocampal pallium through vertebrate evolution: insights from reptiles and teleost fish. *Brain research bulletin*, 57(3-4):499–503, 2002.

[56] Salas C., Broglio C., Durá E., Gómez A., Ocaña F.M., Jiménez-Moya F., and Rodríguez F. Neuropsychology of Learning and Memory in Teleost Fish. *Zebrafish*, 3(2):157–171, 2006.

[57] Broglio C., Rodriguez F., and Salas C. Spatial cognition and its neural basis in teleost fishes. *Fish and Fisheries*, 4(3):247–255, 2003.

[58] von. Frisch K. *Dance Language and Orientation of Bees*. HUP, 1967.

[59] Heran H. Ein Beitrag zur Frage der Wahrnehmung Grundlage der Entfernungsweisung der Bienen. *Z Vergl Physiol*, 38:168–218, 1956.

[60] Goller F. and Esch H. E. Waggle dances of honey bees. *Nature*, 77(12):594–595, 1990.

[61] Pfeffer S. E. and Wittlinger M. Optic flow odometry operates independently of stride integration in carried ants. *Science*, 353(6304), 2016.

[62] Ronacher B., Gallizzi K., Wohlgemuth S., and Wehner R. Lateral optic flow does not influence distance estimation in the desert ant Cataglyphis fortis. *The Journal of Experimental Biology*, 203(Pt 7):1113–21, 2000.

[63] Köppen J.R., Winter S.S., Loda E.L., Apger B.P., Grimelli D., Hamilton D.A., and Wallace D.G. Analysis of movement kinematics on analogous spatial learning tasks demonstrates conservation of direction and distance estimation across humans (Homo sapiens) and rats (Rattus norvegicus). *Journal of Comparative Psychology*, 127(2):179–93, 2013.

[64] Mossio M., Vidal M., and Berthoz A. Traveled distances: new insights into the role of optic flow. *Vision Research*, 48(2):289–303, 2008.

[65] Sun H.J., Campos J.L., and Chan G.S.W. Multisensory integration in the estimation of relative path length. *Experimental Brain Research*, 154(2):246–254, 2004.

[66] Redlick F.P, Jenkin M.H., and Laurence R. Humans can use optic flow to estimate distance of travel. *Vision Research*, 41(2):213–219, 2001.

[67] Mittelstaedt M.L. and Mittelstaedt H. Idiothetic navigation in humans: estimation of path length. *Experimental Brain Research*, 139(3):318–332, 2001.

[68] Durgin F.H., Akagi M., Gallistel C.R., and Haiken W. The precision of locomotor odometry in humans. *Experimental Brain Research*, 193(3):429–36, 2009.

[69] Esch H., Goller F., and Burns J. E. Honeybee waggle dances: the energy hypothesis and thermoregulatory behavior of foragers. *Journal of Comparative Physiology B*, 163 (8):621–625, 1994.

[70] Scholze E., Pichler H., and Heran H. Zur Entfernungsschaatzung der Bienen nach dem Kraftaufwand. *Naturwissenshaften*, 51:69–70, 1964.

[71] Neese V. *The Flying Honeybee; Aspects of Energetics, Biona Report 6*. Stuttgart: Gustav Fisher., 1988.

[72] Esch H. and Burns J.E. Distance estimation by foraging honeybees. *The Journal of Experimental Biology*, 199(Pt 1):155–62, 1996.

[73] Shafir S. and Barron A.B. Optic flow informs distance but not profitability for honeybees. *Proceedings of the Royal Society B: Biological sciences*, 277(1685):1241–5, 2010.

[74] Esch H.E., Zhang S., Srinivasan M.V., and Tautz J. Honeybee dances communicate distances measured by optic flow. *Nature*, 411(6837):581–3, 2001.

[75] Srinivasan M., Zhang S., Lehrer M., and Collett T. Honeybee navigation en route to the goal: visual flight control and odometry. *The Journal of Experimental Biology*, 199 (Pt 1):237–44, 1996.

[76] Seyfarth E.A. and Barth F.G. Compound slit sense organs on the spider leg: Mechanoreceptors involved in kinesthetic orientation. *Journal of Comparative Physiology*, 78(2):176–191, 1972.

[77] Baumberger B. and Flückiger M. The development of distance estimation in optic flow. *Perception*, 33(9):1081–99, 2004.

[78] Frenz H., Bremmer F., and Lappe M. Discrimination of travel distances from 'situated' optic flow. *Vision research*, 43(20):2173–83, 2003.

[79] Moser E.I. and Moser M.B. A metric for space. *Hippocampus*, 18(12):1142–56, 2008.

[80] O'Keefe J. An allocentric spatial model for the hippocampal cognitive map. *Hippocampus*, 1(3):230–5, 1991.

[81] Poucet B., Chaillan F., Truchet B., Save E., Sargolini F., and Hok V. Is there a pilot in the brain? Contribution of the self-positioning system to spatial navigation. *Frontiers in Behavioral Neuroscience*, 9(292):1–10, 2015.

[82] O'Keefe J. and Dostrovsky J. The hippocampus as a spatial map. Preliminary evidence from unit activity in the freely-moving rat. *Brain Research*, 34(1):171–5, 1971.

[83] O'Keefe J. A review of the hippocampal place cells. *Progress in Neurobiology*, 13(4): 419–39, 1979.

[84] Jeffery K.J., Wilson J.J., Casali G., and Hayman R.M. Neural encoding of large-scale three-dimensional space-properties and constraints. *Frontiers in Psychology*, 6:1–12, 2015.

[85] Sanders H., Rennó-Costa C., Idiart M., and Lisman J. Grid Cells and Place Cells: An Integrated View of their Navigational and Memory Function. *Trends in Neurosciences*, 38(12):763–775, 2015.

[86] Igarashi K.M. and Moser E.I. The entorhinal map of space. *Brain research*, 1637: 177–187, 2015.

[87] Fiete I.R., Burak Y., and Brookings T. What grid cells convey about rat location. *The Journal of Neuroscience*, 28(27):6858–71, 2008.

[88] Hardcastle K., Ganguli S., and Giocomo L.M. Environmental boundaries as an error correction mechanism for grid cells. *Neuron*, 86(3):827–39, 2015.

[89] Hafting T., Fyhn M., Molden S., Moser M.B., and Moser E.I. Microstructure of a spatial map in the entorhinal cortex. *Nature*, 436(7052):801–6, 2005.

[90] Fyhn M., Hafting T., Treves A., Moser M.B., and Moser E.I. Hippocampal remapping and grid realignment in entorhinal cortex. *Nature*, 446(7132):190–4, 2007.

[91] du Lac S. and Knudsen E. I. Neural maps of head movement vector and speed in the optic tectum of the barn owl. *Journal of Neurophysiology*, 63(1):131–46, 1990.

[92] Muller R.U., Ranck J.B., and Taube J.S. Head direction cells: properties and functional significance. *Current Opinion in Neurobiology*, 6(2):196–206, 1996.

[93] Champ C., Wallis G., Vorobyev M., Siebeck U., and Marshall J. Visual Acuity in a Species of Coral Reef Fish: *Rhinecanthus aculeatus*. *Brain, Behavior and Evolution*, 83: 31–42, 2014.

[94] Bleckmann H. and Zelick R. Lateral line system of fish. *Integrative Zoology*, 4:13–25, 2009.

[95] Odling-Smee L. and Braithwaite V.A. The influence of habitat stability on landmark use during spatial learning in the three-spined stickleback. *Animal Behaviour*, 65(4): 701–707, 2003.

[96] Goodyear C.P. and Ferguson D.E. Sun-compass orientation in the mosquitofish, Gambusia affinis. *Animal Behaviour*, 17(4):636–640, 1969.

[97] Shcherbakov D., Winklhofer M., Petersen N., Steidle J., Hilbig R., and Blum M. Magnetosensation in zebrafish. *Current Biology*, 15(5):R161–R162, 2005.

[98] Quinn T.P. and Brannon E.L. The use of celestial and magnetic cues by orienting sockeye salmon smolts. *Journal of Comparative Physiology A*, 147(4):547–552, 1982.

[99] Hawryshyn C.W., Arnold M.G., Bowering E., and Cole R.L. Spatial orientation of rainbow trout to plane-polarized light: The ontogeny of E-vector discrimination and spectral sensitivity characteristics. *Journal of Comparative Physiology A*, 166(4): 565–574, 1990.

[100] Taylor G.K., Holbrook R.I., and Burt de Perera T. Fractional rate of change of swim-bladder volume is reliably related to absolute depth during vertical displacements in teleost fish. *Journal of the Royal Society, Interface*, 7:1379–82, 2010.

[101] von der Emde G. Active electrolocation of objects in weakly electric fish. *Journal of Experimental Biology*, 202:1205–15, 1999.

[102] Near T.J., Eytan R.I., Dornburg A., Kuhn K.L., Moore J.A., Davis M.P., Wainwright P.C., Friedman M., and Smith W.L. Resolution of ray-finned fish phylogeny and

timing of diversification. *Proceedings of the National Academy of Sciences (PNAS)*, 109: 13698–703, 2012.

[103] Vargas J.P., Rodriguez F., Lopez J.C., Arias J.L., and Salas C. Spatial learning-induced increase in the argyrophilic nucleolar organizer region of dorsolateral telencephalic neurons in goldfish. *Brain research*, 865(1):77–84, 2000.

[104] Vinepinsky E., Donchin O., and Segev R. Wireless electrophysiology of the brain of freely swimming goldfish. *Journal of Neuroscience Methods*, 278:76–86, 2017.

[105] Cheney K.L., Newport C., McClure E.C., and Marshall J. Colour vision and response bias in a coral reef fish. *The Journal of experimental biology*, 216:2967–73, 2013.

[106] Pignatelli V., Champ C., Marshall J., and Vorobyev M. Double cones are used for colour discrimination in the reef fish, *Rhinecanthus aculeatus*. *Biology letters*, 6:537–9, 2010.

$\sim$ Page left blank intentionally $\sim$

Chapter 2

Teleost fish can accurately estimate distance travelled.

Teleost fish can accurately estimate distance travelled

C. Karlsson[1], J.K. Willis[1], M. Patel[1], and T. Burt de Perera[1]

[1]Department of Zoology, Research and Administration Building, 11a Mansfield Road, Oxford, OX1 3SZ

Abstract

Terrestrial animals can compute shortcuts through their environment by integrating self-motion vectors containing distance and direction information. The sensory and neural mechanisms underlying this navigational feat have been extensively documented, but their evolutionary origins remain unexplored. The teleost fish make up one of the most diverse and earliest-branching vertebrate groups, and provide a powerful system to study the origins of vertebrate spatial processing. However, it is unknown how freely-swimming teleost fish collect and compute metric spatial information underwater. Using the Picasso triggerfish, *Rhinecanthus aculeatus*, we develop a behavioural task to test distance estimation in teleost fish for the first time. We show that teleost fish can learn and remember a trained distance with remarkable accuracy, and they do so independently of external landmark information. This operant conditioning task can be used to explore the functional and mechanistic basis of distance estimation at both the sensory and neural levels. Here, using post-hoc video analysis of the distance estimates produced by our *Rhinecanthus* subjects, we explore how this distance information is represented, and the potential sensory mechanisms used to acquire distance information. First, by comparing the relative variance in the two metrics, we test the hypothesis that distance is represented as a measure of travel time. Second, by quantifying finbeat use we investigate whether *Rhinecanthus* may use proprioceptive inputs from a finbeat counter to measure distance travelled in a similar way to the step-counters of many walking animals. The results from this study provide an important baseline from which to continue to study the mechanisms underlying odometry in *Rhinecanthus* and other species of teleost fish.

1 Introduction

Path integration is a powerful way for an animal to navigate through its environment. Self-movement vectors containing distance and direction information are constantly and automatically summated throughout any journey, providing the animal with an internal store of a vector taking it directly back to a starting position [1, 2]. The result is a dramatic increase in navigation efficiency - shortcuts can be constructed through entirely unexplored terrain, avoiding the need to use external information to retrace previous steps.

To achieve this navigational feat, an animal must have dedicated sensory mechanisms and neural structures to collect and process distance and direction information from self-motion cues. Such mechanisms have been extensively studied in flying and walking terrestrial animals ranging from mammals such as humans [3] and rats [4, 5], to invertebrates such as spiders [6], ants [7], and bees [8, 9]. In contrast, how underwater species collect, process, and use metric spatial information to accurately navigate through their environment is largely unknown. An aquatic habitat is a fascinating environment to navigate through from a sensory and computational point of view. It contains sensory information not available on land, such as hydrodynamic cues from water flow, hydrostatic pressure from above, and electric currents carried through the water. Freely-swimming animals also have six degrees of freedom of movement (3 translational: forwards/backwards, left/right, up/down; 3 rotational: roll, pitch, yaw), compared to just three in surface-constrained animals (two translational: forwards/backwards, left/right; one rotational: yaw), which requires sensing and processing of spatial information in three-dimensions [10–12].

Among the animals facing these navigational challenges are the teleost fish, which display huge ecological diversity, inhabiting almost every aquatic niche on earth [13]. This makes the teleost fish a valuable study system to shed light on how animals occupying aquatic environments have evolved to solve similar navigation problems to their terrestrial counterparts. Moreover, as the most diverse and species-rich vertebrate group,

located in the sister clade to the tetrapods and lobe finned fish, studying how teleost fish encode metric spatial information is important for understanding the origins of the metric representation of space in the vertebrate clade as a whole. There is increasing evidence to suggest that the teleost pallium is not only structurally equivalent, but homologous to the mammalian and avian hippocampus, placing the origin of a brain structure used for spatial memory as far back as 400 million years ago [14–17]. However, to fully support this hypothesis, it must be demonstrated at the behavioural level that the teleost fish possess similar navigation strategies to other vertebrates.

Early evidence from analysing swimming trajectories of fish trained to swim to a specific location to gain a food reward suggests that fish can store an internal representation of the previous location of a food reward relative to home [11], and compute such information in both horizontal and vertical space [10, 18]. However, the distance and direction metrics underlying this behaviour have never been directly quantified.

The estimation of travel direction has only been studied in the context of long-range compasses in migrating fish species, indicating some analogy with terrestrial and aerial species. Mosquitofish are able to orient using a time-compensated sun compass [19], while juvenile sockeye salmon and the Mozambique tilapia orient using magneto-sensation [20, 21], and there is some evidence that rainbow trout use polarised light from above [22].

How fish encode metric distance is even more poorly understood. It is entirely unknown whether teleost fish can measure distance travelled, which sensory mechanisms may support this behaviour, and the potential neural architecture that may underlie it.

In this paper, we develop an operant conditioning task to assess whether fish can estimate travel distances. The animal is trained to a given distance using a landmark cue as the conditioned stimulus, and during testing we assess how accurately the animal can reproduce this distance when the conditioned stimulus is moved to a novel position. We use the Picasso triggerfish (*Rhinecanthus aculeatus*) as our study species, typically found defending discrete territories on shallow reef-flats throughout the Indo-Pacific Ocean. Learning and remembering territory boundaries and navigating efficiently within them

is central to their survival and success. However, coastal reef environments are often subject to rapid and sporadic change, reducing the reliability of external landmarks for marking out navigation routes. Being able to navigate using an internal reference of distance and direction travelled is therefore likely to be advantageous. Moreover, *Rhinecanthus* has proven to be trainable in complex behavioural tasks [23, 24], and owing to its natural territoriality can be housed and trained individually whilst maintaining natural behaviours, making it a suitable species for developing our behavioural task.

This behavioural paradigm can be used to explore the functional and mechanistic basis of distance estimation in teleost fish at both the sensory and neural levels. Using post-hoc video analysis of the distance estimates produced by the fish in this experiment, we proceed to explore two potential mechanisms underlying the acquisition of distance information in teleost fish.

First, it has been proposed that animals may represent distance travelled as a measure of elapsed travel time [9]. We use our distance estimate data to test this hypothesis by exploring whether travel time is a good predictor of the variation seen across individual distance estimates. If travel time is used as a measure of distance travelled, the relative variation, described by the coefficients of variance, of the time taken and distance metrics would be equivalent.

Second, previously studied invertebrates such as the desert ant, fiddler crab, and wandering spider partially or fully rely on an internal stride integrator as a measure of distance travelled through summation of inputs from leg mechanoreceptors [25–28]. Humans are similarly able to estimate distance as a function of walking speed, step length and step rate [29, 30]. Whether *Rhinecanthus aculeatus* uses a similar mechanism under the constraints of navigating in their aquatic world is unknown. The functionally equivalent mechanism for forward propulsion in a teleost fish would be the use of mechanosensory inputs from finbeat movements. *Rhinecanthus* uses three sets of fins for propulsion either in combination or in isolation: pectoral fins; undulating dorsal and anal fin pairs; and, the caudal fin. Using video analysis to quantify fin movements, we investigate whether

this species could count individual caudal finbeats (tailbeats), which provide the majority of rapid forward propulsion, or summate mechanosensory inputs across all finbeat combinations to measure distance travelled.

Overall, we design and test a behavioural paradigm that can be used to answer three key questions: (1) Can teleost fish learn and remember distance information? (2) What sensory information do teleost fish use to collect distance information? (3) How might distance information be encoded in the teleost brain? In this paper, we provide the first direct test of odometry in a teleost fish, and a baseline from which we can continue to explore the sensory mechanisms underlying odometry in *Rhinecanthus aculeatus* and other species of teleost fish.

2 Methods

2.1 Subjects

Test subjects were five wild-caught experimentally naive Picasso triggerfish, *Rhinecanthus aculeatus*, originating from coastal reefs on the Maldives. Individuals ranged from 10-14cm, standard length, and were housed in the laboratory for the duration of the experiment in tanks measuring 0.45m x 0.30m x 0.75m (width x height x length) under a 12h/12h automated day/night fluorescent light cycle. Tank enrichment was designed following a period of fieldwork tracking Picasso triggerfish in the wild. All tanks were subsequently provided with coral gravel and sand to encourage nest-building, and large rocks and caves to provide refuges. Salinity was kept constant at 35ppt using reverse osmosis water with added aquarium salts (Tropic Marine Centre Classic Sea Salt). Marine pellets (Ocean Nutrition Formula One Marine Pellet) and krill (Gamma Krill Pacifica) were provided as food rewards during training. Lance fish or cockles (Gamma) were fed as a supplement at the end of each training day. The experiment tank and home tanks were cleaned and water quality tested twice weekly (ammonia and nitrite were kept at 0ppm and nitrate was maintained below 15ppm). See supplementary information (Appendix A) for more detailed information on animals and husbandry.

2.2 Behavioural Task

Fish were trained using an operant conditioning protocol to learn a travel distance of 0.80m. A landmark cue in the form of an overhead infrared detector controlling surrounding aquarium lights was used as the conditioned stimulus for learning to travel 0.80m from a start area. During testing we then assessed whether and how accurately the fish could reproduce this distance when the conditioned stimulus was moved to a novel position.

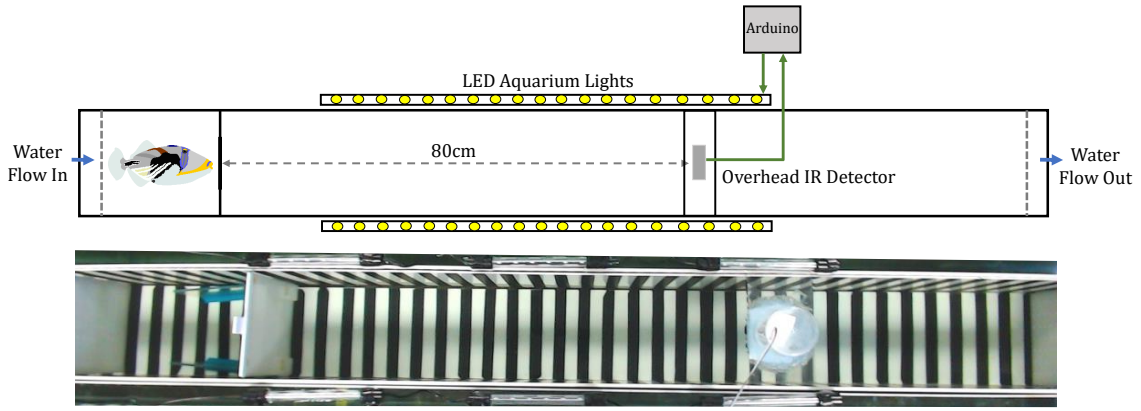


Figure 1: Overhead schematic view and photo of distance estimation task training set-up. A linear maze was constructed inside a flow-through tank, with water flow in behind the start area (blue inlet arrow) and passive water flow out at the opposite end of the tank (blue outlet arrow). Perforated white screens separated the fish from the inlet and outlet pipes and water flow was switched off during all training and testing sessions. The walls and floor of the maze were lined with alternating black and white stripes of width 0.02m to provide constant optic flow information whilst blocking visual access to external information. During training, the fish was placed in a movable start area and an overhead infrared detector controlling surrounding aquarium lights was placed 0.8m from the start area as the conditioned stimulus for learning the sample distance. When the fish swam beneath the detector a voltage change caused by reflections of infrared light from the fish's body was processed via an Arduino microprocessor and caused the aquarium lights to switch on. The fish was trained to turn around and return to the start area for a food reward once the lights had switched on. During testing, the infrared detector controlling the lights would be moved to a novel decoy position to test whether the fish could reproduce the learned distance. An overhead camera recorded distance estimates during the testing phase.

2.2.1 Experimental Set-up

A linear Perspex maze measuring 0.25m high x 0.16m wide x 1.80m long was built within a flow-through tank connected to the home water system via a pump moving water at 3 litres per minute to maintain constant water parameters (fig. 1 and supplementary information, Appendix A fig.1). This water flow was switched off during training and testing sessions. The walls and floor were patterned with regular black and white stripes of width 0.02m to provide basic visual contrast information, as many species have been shown to have impaired distance estimation in the absence of optic flow [8, 31], whilst also blocking

access to visual information external to the tank. A perforated white screen was placed at either end to permit water flow through the experiment tank, and also to block the visual stimuli provided by cues external to the tank or the inlet and outlet pipes themselves. A moveable start area of dimensions 0.25m high x 0.16m wide x 0.30m long could be placed in one of three start area positions, all 0.1m apart (fig. 2). An infrared detector (SHARP 2Y0A21 proximity sensor) was then placed at water level overhead, 0.80m from the start area doorway. This was attached to an Arduino microprocessor, which through a Matlab (Mathworks Inc.) program controlled aquarium lights (Interpret Triple LED Lighting System, 0.75m) running along the top of the lateral maze walls. The voltage of the infrared (IR) detector varied between 0V and 3.5V depending on the strength of the reflection from objects which passed in front of it. We tested the response of the detector to objects in water and after this we set a threshold of 1.7V. As the fish passed beneath the detector, a voltage change was registered and when this exceeded 1.7V, the aquarium lights switched on. A Point Grey Grasshopper 3M camera (FLIR Machine Vision Cameras) was placed 1.1m above the water level to record testing trials.

2.2.2 Training

Training was split into four main phases: quarantine, pre-training, habituation, and full training.

Upon arriving from the wild, the fish were placed in a 2-week mandatory quarantine. Each individual tank was isolated from the main flow-through home system and fish health was monitored daily for signs of imported infection. Full tank enrichment was provided and tanks were cleaned daily to maintain water quality in the absence of flow and filtration. This also accustomed the fish to the presence of the experimenter. During this time, the fish were fed a full diet delivered using tweezers. This required the fish to approach the experimenter at the front of the tank to receive food. Following a full health check at the end of the quarantine period, the tank was connected to the main water system. At this stage, if the fish consistently accepted food from the tweezers with

no hesitation or hiding between food portions, it proceeded to pre-training.

Pre-training involved the fish learning to voluntarily swim into a 2 litre transport container. Fish were gradually trained to swim into the transport container and be lifted fully out of the tank to receive a high quality food reward (krill or chopped fish) prior to being returned to their home tank. This training stage continued until fish could be captured in the container, lifted out, and placed back into their home tank across two daily feeds for three consecutive days with no visible stress responses. Monitored stress responses included gasping, extension of the dorsal and ventral trigger fins, striking at the sides of the container with their jaws or tail, or thrashing their fins.

Fish were subsequently habituated to being moved between their home tank and the experiment tank. During a habituation training session, fish were captured in the transport container and provided with a high quality food reward before being moved to the start area of the experiment tank. The fish was immediately provided with an additional food reward upon entering the start area and monitored for 2 minutes for any stress responses (gasping at the surface, attempting to jump out of the tank, raising of the dorsal and ventral trigger fins, rapid swimming along the surface). At the end of the two minutes, the start area door was opened and the fish was given 10 minutes to explore the experiment tank. During this time, food was regularly provided in the start area to encourage the fish to repeatedly return through the doorway. At the end of 10 minutes, the start area door was closed and the fish was once more captured in the transport container and returned to its home tank. This was repeated once per day until the fish could complete a habituation session with no visible stress responses.

Following completion of the habituation period, the fish began full training. The experiment tank was arranged as described in fig. 1, with the start area in one of three positions (fig. 2) and the overhead infrared detector controlling the lights placed 0.80m from the start area doorway. The fish was captured as before in the transport container and provided with a food reward prior to being placed in the start area. The fish was then given 1 minute to settle and monitored for stress responses prior to starting the session.

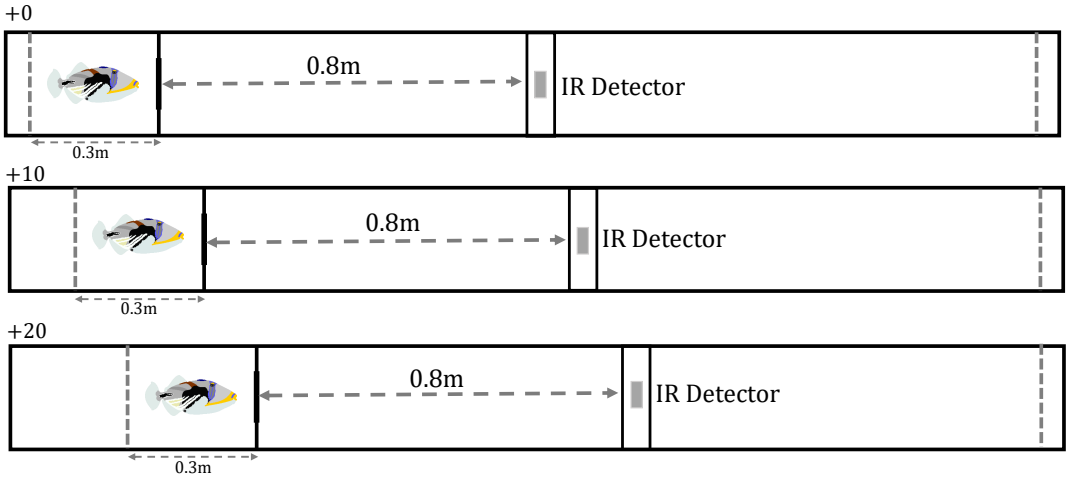


Figure 2: Schematic of the three start area positions. Each position is located increasingly distally through the tunnel by 0.10m increments (labelled +0, +10 and +20 to signify this). The rear perforated white screen moves accordingly to ensure the start area length is kept at 0.30m. The infrared detector also moves accordingly to maintain the target distance of 0.80m.

If the fish showed no visible signs of stress, the start area door was opened and the fish was permitted to enter the main experiment arena and swim uninterrupted until it passed beneath the infrared detector. Passing beneath the detector caused the aquarium lights to switch on. During early training stages, a food reward was presented using tweezers at the infrared detector as soon as the light had been switched on. Upon receipt of this first reward, food was also immediately presented in the start area. This was to teach the fish to return to the start area when the light stimulus was turned on. As they learned the association between the light and food, the reward was presented only in the start area once the light was switched on. Food was subsequently presented increasingly later during the return journey, such that by the end of training the fish had to swim to the infrared detector to turn on the lights, immediately return to the start area and have the door closed behind them before the food reward was provided. A food reward was never provided in the start area if the fish swam further than the infrared detector before turning home. Training sessions lasted 10 minutes or until 10 correct trials were complete, whichever came first. To control for use of external cues or landmarks, each session the start area was

moved randomly between three positions, located increasingly distally through the tank by 0.10m increments (fig. 2). The infrared detector was moved accordingly to maintain the correct distance of 0.80m. Distance travelled using self-motion information therefore becomes the only reliable spatial information for learning the position of the infrared detector. Training was considered complete when the fish swam directly out to the light flash and back on 80 percent of trials, with a minimum of 10 correct trials required within the 10-minute session time limit, across three consecutive sessions.

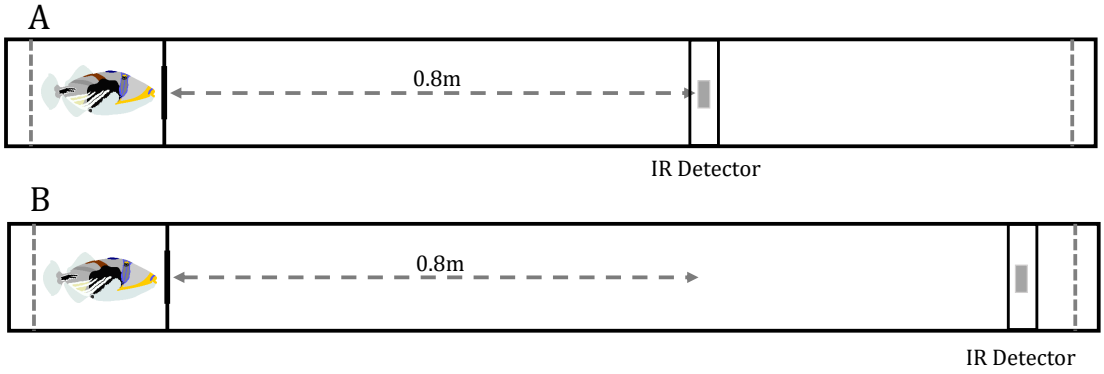


Figure 3: Distance estimation task training and testing set-up. (A) Training - the fish was trained to swim 0.8m to the infrared detector which when the fish passed beneath it, detected a voltage change and via the Arduino computer caused the aquarium lights to switch on, signalling to the fish to return to the start area for a food reward. (B) Testing - during testing trials, the infrared detector was moved distally to a decoy position 1.3m from the start area entrance. This was to test whether the fish had learned the correct distance, or to swim to the infrared detector landmark to encounter the light stimulus.

2.2.3 Testing: can teleost fish estimate distance?

Fish were tested in their ability to reproduce the learned distance when the infrared detector controlling the overhead lights was placed in a new decoy position. Test sessions were of variable length according to individual differences in motivation (5-10 testing trials), with a pseudo-randomly alternating training + testing trial structure (sessions always began with a testing trial and varied randomly thereafter). During training trials (fig. 3A), the IR detector was placed 0.8m from the start area as before and the fish was rewarded

in the start area if it was correct. During testing trials (fig. 3B), the infrared detector was moved to a decoy position 1.3m from the start area. Moving the detector distally tested whether the fish had learned to swim the correct distance, or if it had learned to beacon to the infrared detector landmark. 15 testing trials were completed at each start area position, resulting in a total of 45 distance estimates per fish. To control for use of external fixed positional information, each testing session the start area was once again moved between the three starting positions whilst keeping the distance to the infrared detector constant.

2.3 Behavioural Analysis

Testing sessions were recorded using an overhead camera (Point Grey Grasshopper 3M) at 50 frames per second and saved as Audio Video Interleave (avi) files using the Streampix 7 video capture software (Image Width: 2448 pixels; Image Height: 350 pixels). Each testing trial was then extracted into a series of jpeg images using the Streampix 7 program making them compatible for analysis in a Matlab video tracking program.

2.3.1 Extracting distance estimates

A distance estimate was considered the maximum point of the fish's nose within a successful trial prior to turning home. A Matlab program was used to track the pixel coordinate position of the fish's nose upon exiting the start area and the maximum point of the nose prior to turning home. Using the program R (The R Project, version 3.6.1) the total pixel distance travelled was calculated as the difference between the exit position and turning position, and estimates were converted to metric distances using the following conversion: 14.4 pixels = 0.01m.

2.3.2 Extracting travel time

The frame number of the fish's exit from the start area and the maximum point of the nose prior to turning home was recorded. The time taken was calculated as the difference

between the exit and turning frame, and the frame rate of the video (50fps) was used to convert this to seconds per distance estimate.

2.3.3 Finbeat analysis

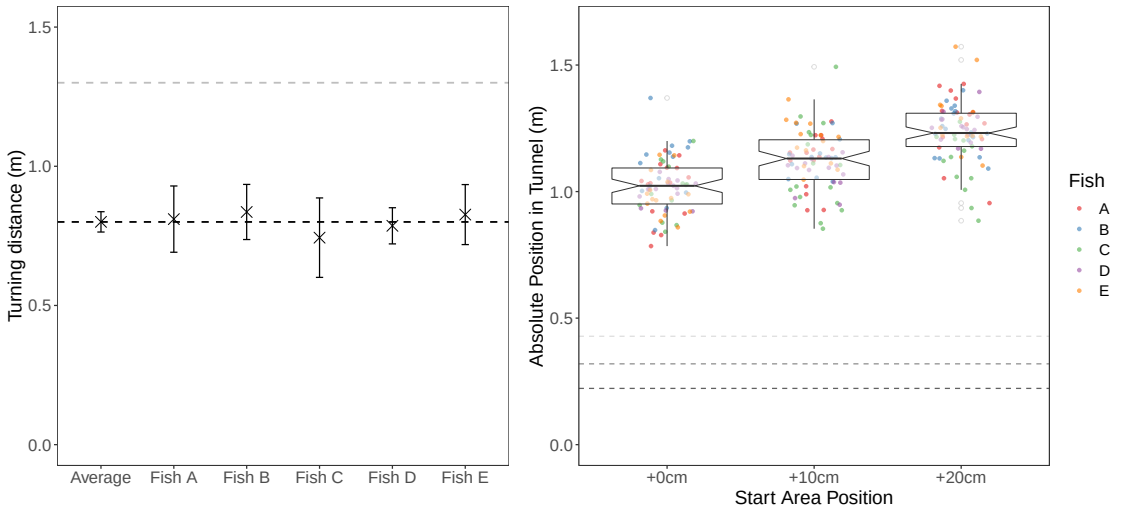
Video recordings of the distance estimates were used to test whether the Picasso triggerfish uses proprioceptive inputs from finbeats to estimate distance. The Picasso triggerfish uses three sets of fins for propulsion either in combination or in isolation: pectoral fins; undulating dorsal and anal fin pairs, and the caudal fin. The analysis was split into two levels. First, caudal finbeats, or tailbeats, account for rapid directed forward propulsion and discrete tailbeats were counted throughout each distance estimate. This data were used to test whether *Rhinecanthus* uses a tailbeat couter for odometer. Second, undulating finbeats from the pectoral and dorsal/anal fin pairs account for finer-scale propulsion and steering. The total distance per testing trial dedicated to each finbeat type and combination was measured. Combinations included: caudal only; dorsal/anal pairs only; pectoral only; all finbeats; none (gliding); caudal and dorsal/anal; caudal and pectoral; dorsal/anal and pectoral. Information was first extracted as the total pixel distance for each finbeat type, and converted into a metric distance using the previous conversion (14.4 pixels = 0.01m). This was used to explore whether *Rhinecanthus* measures distance travelled as the total mechanosensory inputs to all finbeat types.

3 Results

3.1 Teleost fish do have an internal representation of distance travelled

The five fish learned at varying rates (Fish A - 51 sessions; Fish B - 38 sessions; Fish C - 36 sessions; Fish D - 61 sessions; Fish E - 92 sessions) but all fish completed training within 6 months of their arrival in the laboratory (see supplementary information fig. 2a-f for individual fish learning curves). Figure 4a shows the average distance estimates for individual fish and the sample population (see also supplementary fig. 3 and table 1 in Appendix A for individual distance estimate distributions). There were no trials in which the fish swam to the novel position of the infrared detector to turn on the aquarium lights. The average population level distance estimate was 0.803m with a standard deviation of 0.0365m, which was not significantly different from the target distance of 0.80m - one-sample t-test, $t_{4,0.05} = 0.0232$, $p = 0.983$ (all values are given to three significant figures here and throughout all reported results).

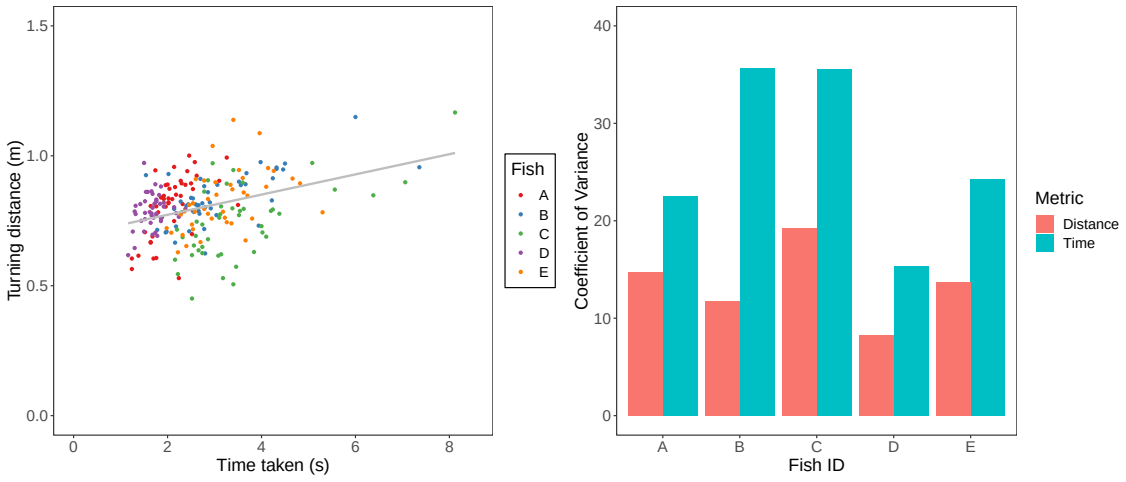
Throughout training and testing, the start area was moved between three positions (identified as +0, +10, and +20) in order to shift the absolute position of the correct turning point in the tunnel while keeping the correct distance constant. The purpose of this was to control for use of positional landmark cues internal and external to the maze and ensure only self-motion information could be used to determine the turning point. If fish were generalising across positions or using a fixed positional cue rather than an internal representation of distance, we would expect no difference in absolute turning point across the three start area positions. A linear mixed effects model (Absolute Estimate Point = Start Area Position (fixed effect) + Fish (random effect)) revealed start area position to be a good predictor of the absolute estimate point within the tunnel across fish (fig. 4b): $F_{215,2} = 69.8$, $p<0.001$, with absolute turning position for all three start area positions significantly different from each other (Tukey HSD pairwise comparison: 0:10 - $t_{215} = 5.81$, $p<0.001$; 10:20 - $t_{215} = 6.00$, $p<0.001$; 0:20 - $t_{215} = 11.8$, $p<0.001$). Individual fish identity explained some of the residual variation in distance estimates (Likelihood Ratio Test with



(a) (b)

Figure 4: (a) Mean distance estimates produced by the population and individual fish. Error bars indicate +/- 1 std dev. The black dashed line indicates the target distance (0.80m), and the grey dashed line indicates the decoy testing position of the overhead infrared detector controlling the lights. (b) Absolute distance estimate position within the tunnel maze according to start area position. The start area moved between three positions - the dashed lines indicate the position of the start area doorway from the back of the tunnel (+0cm: dark grey, +10cm: mid-grey, and +20cm: light grey). Box plots indicate the lower quartile (lower hinge), median, and upper quartile (upper hinge) of absolute turning positions. Outliers are indicated by light grey points. Coloured points correspond to fish identity - all fish performed 15 distance estimates per start area position.

and without random effect of fish = 7.63, p = 0.00575, supplementary fig. 4, Appendix A). It is possible that the fish were able to learn three separate stimulus-action-reward associations using external positional information. However, this is unlikely owing to the height of the opaque maze walls blocking access to visual cues external to the maze other than those located on the ceiling of the experiment room. The ceiling directly above the tank was white and featureless other than the presence of the overhead camera. Moreover, the three error distributions associated with each start area show similar narrow profiles with little overlap in turning position across all fish identities, which are more indicative of use of an internal distance metric than three separate positional reference points. If three discrete reference points are used, we would expect errors in reporting to produce jumps in turning positions associated with incorrect pairing of a start-area:landmark association. However, the distance estimate distributions produced by each fish show a narrow, normally distributed error profile either side of the mean distance estimate with few outliers. Taken together, our results therefore suggest that our fish are not using external positional information but an internal metric representation of distance travelled based on self-motion information. Future work directly manipulating use of self-motion information will be able to fully test this.



(a) (b)

Figure 5: (a) Variation of travel time with distance travelled - coloured points represent individual fish identity. (b) Coefficients of variance (measured as (standard deviation/average) x 100) for travel time (s) - blue, and distance estimate (m) - red, for each fish, indicating that the coefficient of variance for travel time is consistently higher than the absolute distance estimates produced.

3.2 Distance is not likely to be represented as a measure of travel time

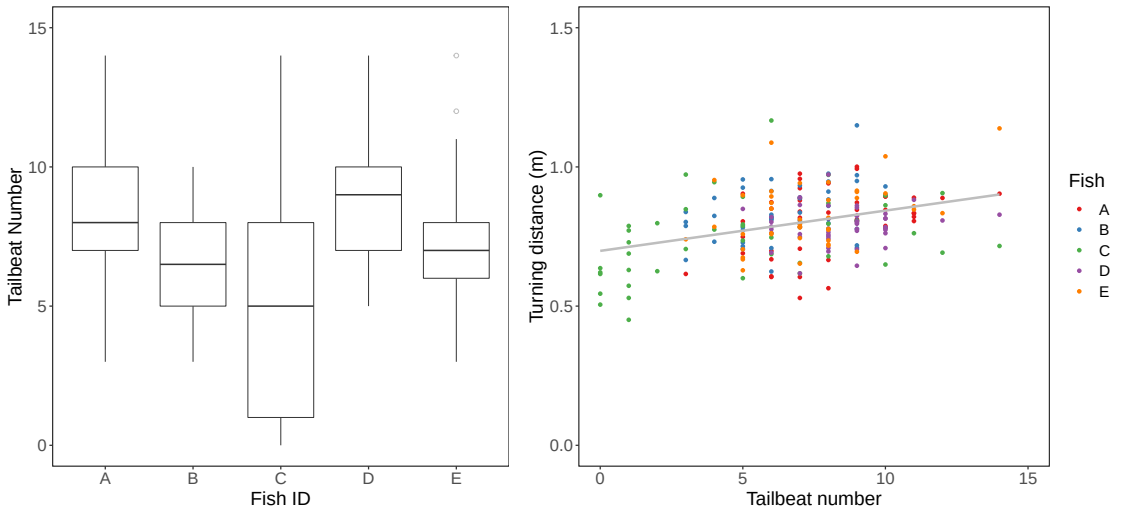
It has been proposed that instead of representing distance as its own metric, animals could measure travel time as a proxy for distance travelled [9]. While there is no evidence that any species does represent distance as a measure of travel time, we tested this hypothesis by comparing the relative variation of travel time and turning distance as described by their coefficients of variance.

Although travel time does increase with distance travelled (fig. 5a, Linear Mixed Effects Model - Distance Estimate = Time Taken (fixed effect) + Fish Identity (random effect): t_{219} = 9.16, $p<0.001$, Likelihood Ratio Test (model with and without the random effect of fish) = 43.9, $p<0.001$), the relative variation in travel time is consistently greater than the relative variation in turning distance. For all five fish the ratio of the coefficients of variance (measured as (standard deviation/average)x100) was between 1.5 and 3, with a greater error for travel time than for the distance estimates produced (paired t-test: t_4 = -4.18, p = 0.0139, fig. 5b, table 1). We therefore propose that *Rhinecanthus* is unlikely

Fish	Distance Estimate Coefficient of Variance	Time Taken Coefficient of Variance	Ratio of Coefficients
A	14.7	22.5	1.53
B	11.8	35.7	3.01
C	19.2	35.6	1.86
D	8.23	15.3	1.85
E	13.7	24.3	1.77

Table 1: Comparing coefficients of variance for distance estimates and time taken. Coefficients were calculated for all five tested fish separately, calculated using the equation: (sample standard deviation/sample mean)x100. The ratio of coefficients was calculated using the equation: Time Taken Coefficient of Variance/Distance Estimate Coefficient of Variance.

to be measuring distance as an integration of travel time, although this will require an additional direct manipulation of travel time to fully conclude.



(a) (b)

Figure 6: (a) Boxplot showing the range of tailbeat numbers for distance estimates for each fish (Fish A, 3-14; Fish B, 3-10; Fish C, 0-14; Fish D, 5-14; Fish E, 3-14). (b) Relationship between tailbeat number against corresponding distance estimate for each fish, based on a mixed effects model of tailbeat number and fish identity. Coloured points indicate individual fish identity.

3.3 *Rhinecanthus aculeatus* does not use finbeats to measure distance travelled

Video recordings of testing trials were used to explore whether the Picasso triggerfish uses mechanosensory inputs from finbeats as a sensory mechanism to collect information on distance travelled. The Picasso triggerfish uses the caudal fin, pectoral fins and undulating dorsal and ventral fins together or in isolation for propulsion and steering.

Among these, caudal finbeats (here-on tailbeats) are accountable for the majority of rapid, directed propulsion. They come in discrete units and could be counted from the video recordings. A linear mixed effects model was constructed to test whether tailbeat number varied with distance estimate: Distance Estimate = Tailbeat Number (fixed effect) + Fish Identity (random effect). There was a positive relationship between tailbeat number and distance estimate, fig. 6b (t_{202} = 5.52, $p<0.001$), with a significant degree of residual variation explained by the random effect of fish identity (Likelihood Ratio Test (model with and without the random effect of fish) = 6.96, p = 0.00835). However, there was a

Fish	Distance Estimate Coefficient of Variance	Tailbeats Coefficient of Variance	Ratio of Coefficients
A	14.7	27.7	1.88
B	11.8	29.8	2.52
C	19.2	81.2	4.23
D	8.23	20.7	2.51
E	13.7	30.9	2.25

Table 2: Comparing coefficients of variance for distance estimates and tailbeat number. Coefficients were calculated for all five tested fish separately, calculated using the equation: (sample standard deviation/sample mean)x100. The ratio of coefficients was calculated usign the equation: Tailbeats Coefficient of Variance/Distance Estimate Coefficient of Variance. Values reported to three significant figures.

large variance in tailbeat number for each fish (fig. 6a, Range: Fish A, 3-14; Fish B, 3-10; Fish C, 0-14; Fish D, 5-14; Fish E, 3-14). Comparing the ratios of the coefficients of variance between distance estimates produced and the associated tailbeat number found the ratios varied from 1.88 (Fish A) to 4.23 (Fish C), table 2. The sensory information gathered from tailbeat number is therefore unlikely to provide the metric precision we see in the distance estimation data.

To explore whether *Rhinecanthus* may instead be summating the mechanosensory inputs across finbeat types, the distance travelled per swimming modality combination was quantified for each distance estimate. Fin-use combination categories were as follows: All fin types, caudal only, pectoral only, dorsal/ventral only, dorsal/ventral and pectoral, pectoral and caudal, dorsal/ventral and caudal, none (gliding). Results can be seen in fig. 7, revealing no consistency in fin type use per trial, and how far the fish travel using each fin type and combination. This is seen across trials both within and between individual fish.

Some trials also have periods where the fish is gliding and no fins are moving. We hypothesised that if mechanosensory inputs from finbeats are used to measure distance travelled, (i) trials with periods of no fin movements should lead to longer travel distances

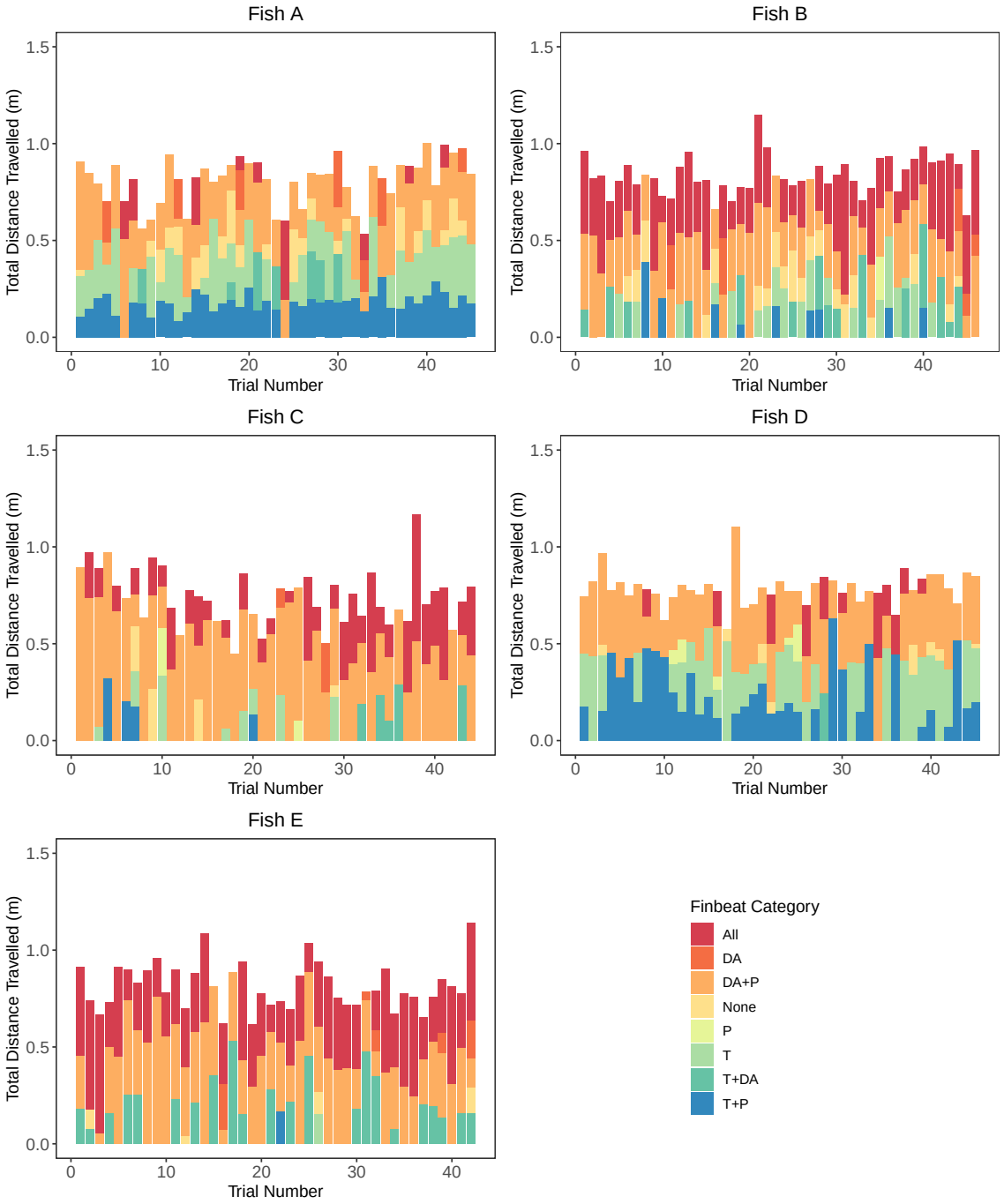


Figure 7: Bar plots showing the distance travelled using each finbeat type for each testing trial. Categories are as follows. All: All finbeat types used in combination, DA: Dorsal and Anal fins, DA+P: Dorsal, Anal and Pectoral fins, None: gliding - no fins used, P: Pectoral, T: Tail/caudal fin, T+DA: Caudal, Dorsal/Anal, T+P: Caudal + Pectoral.

than trials with continuous fin movements, and (ii) of trials where gliding is exhibited, those with longer periods of gliding should have larger overall distance estimates.

First, we split trials according to whether they had periods of no fin movements or whether fin movements were continuous. A mixed effects model of distance travelled was then constructed with the presence or absence of gliding as a fixed effect, and fish identity as a random effect. There was an increase in the total distance travelled in trials with periods of no fin movements compared to those without ($F_{1,208}$ = 12.8, $p<0.001$, fig. 8a), with some residual variance explained by the random effect of fish identity (Likelihood Ratio Test (model with and without the random effect of fish) = 4.22, p = 0.0399).

However, amongst these trials with no fin movements, there was no relationship between the distance spent gliding and the total distance travelled (mixed effects model: distance travelled = gliding distance (fixed effect) + fish identity (random effect), t_{56} = 0.327, p = 0.745, fig. 8b). The same was true when we modelled distance travelled as the proportion of the total distance in each trial spent gliding (mixed effects model: distance travelled = proportion of trial distance spent gliding (fixed effect) + fish identity (random effect), t_{56} = -1.41, p = 0.164, fig. 8c).

We therefore conclude that under the testing conditions of this experiment, mechanosensory inputs from finbeats do not provide *Rhinecanthus* with additive information on distance travelled to support the precision of distance estimates observed.

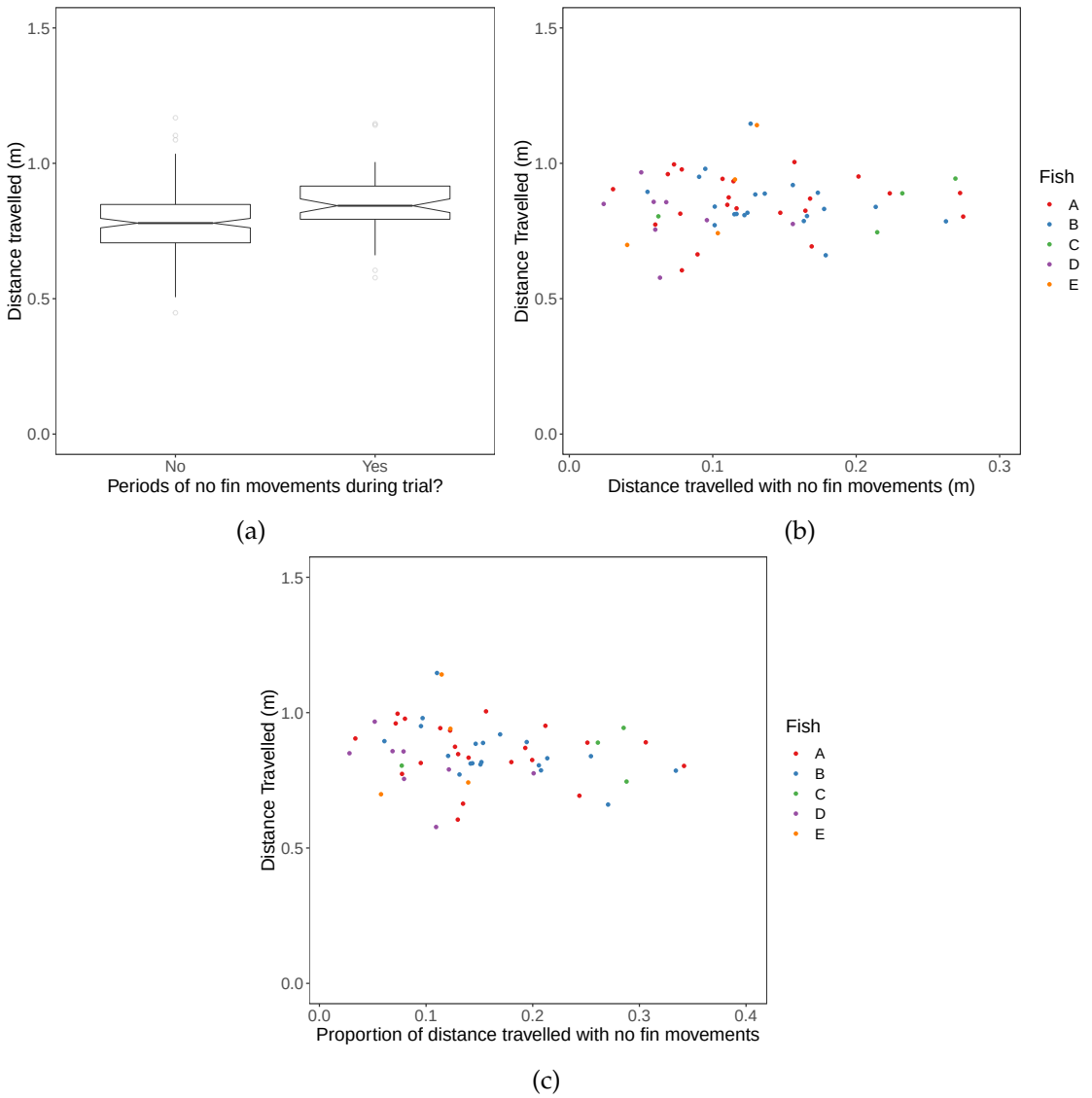


Figure 8: (a) Boxplots comparing the total distance travelled during testing trials where fish do or do not exhibit periods of gliding, defined as periods of no fin movements. Travel distance was significantly longer in trials with periods of gliding ($F_{1,208}$ = 12.8, p<0.001). (b) Plot of total gliding distance in each trial against the total distance travelled. There was no relationship between the distance travelled with no fin movements and the distance estimates produced (t_{56} = 0.327, p = 0.745). (c) Plot of the proportion of each trial distance with no fin movements against the total distance travelled. There was no significant relationship between these two variables (t_{56} = -1.41, p = 0.164). Values reported to three significant figures.

4 Discussion

We have shown, for the first time, that teleost fish can estimate distance travelled with remarkable accuracy (fig. 4a). We subsequently explored how this distance information may be encoded, and conclude that distance is not represented as a measure of travel time (fig. 5a). We also analysed video recordings of the distance estimates to test whether *Rhinecanthus aculeatus* uses mechanosensory inputs from finbeats to measure distance travelled. This would be functionally equivalent to using a step counter - a mechanism used by many vertebrate and invertebrate species walking on land. Based on the variation in finbeat types and number used, we conclude that the Picasso triggerfish is unlikely to use this mechanism to estimate distance (fig. 6a, fig. 7, fig. 8).

We used an operant conditioning task to test the teleost odometer. Fish were trained to swim a distance of 0.80m to an overhead infrared detector - the conditioned stimulus for learning the sample distance. Passing beneath the detector switched on surrounding aquarium lights, which provided the cue to return to the start area for a food reward. During testing, this infrared detector was moved to a decoy position in the tunnel. The fish were therefore presented with a conflict: whether to favour the previously learned distance information and turn around at the previous position of the landmark cue, or to ignore the distance information and swim further to the new position of the landmark. Our fish consistently chose to ignore the novel position of the landmark cue in favour of returning to the start area once they had travelled the learned distance. We observed little deviation between individuals, producing a population average of 0.803m (3sf), (fig. 4a, supplementary information: Appendix A fig. 3 and table 1). Each training and testing session, the start area moved systematically between three positions within the maze to control for use of absolute positional information. The fish were not using any absolute positional cues internal or external to the maze, as they did not generalise their turning point across these positions (fig. 4a). We therefore conclude that the fish must be using a distance metric based on self-motion information. As the fish ignored the overhead land-

mark as well as other external cues, use of metric information acquired from self-motion may be prioritised by teleost fish when making navigation decisions. In an aquatic environment, landmarks may be scarce, hard to discern at a distance, or temporally unreliable. It may therefore be advantageous to prioritise use of internal metric information when making navigation decisions. Indeed, it has been demonstrated in the three-spined stickleback, *Gasterosteus aculeatus*, that reliance on external visual information declines for populations occupying environments with turbulent or variable flow [32].

Overall, these results indicate that a teleost's mental representation of distance travelled is highly accurate. The brain regions and neural pathways underpining this representation of metric distance in teleost fish remain unknown. In mammals, the most likely candidates for encoding distance are the grid cells located in the medial entorhinal cortex. Rats with lesions to their MEC are unable to return to their home cage based on self-motion cues [4], and rats with medial entorhinal cortex lesions cannot estimate distance based on self-movement information [5]. Artificial agents trained to self-localise within a virtual environment using self-movement information spontaneously produced grid-like representations, convergent with the grid network found in mammals [33]. The authors argued that a grid cell-like network provides the most parsimonious Euclidian map of space that enables vector based navigation. Whether a grid cell-like system also exists in the teleost fish, and if this would be a result of convergence or common ancestry is unknown. As neural manipulation and recording technologies have been developed for use in fish [34], our behavioural distance task provides a valuable tool that can be used into the future alongside single cell recordings and lesioning studies to begin searching for brain regions and eventually cell types directly associated with distance estimation in teleost fish.

In the second part of our study, we proceeded to explore the mechanisms through which the *Rhinecanthus* subjects in this experiment could aquire information on distance travelled. First, by extracting the time taken for each distance estimate from video recordings of test sessions, we tested the hypothesis that distance is represented as a time metric.

Although distance estimates did increase with time taken (fig. 5a), the variability in travel time consistently surpassed the variability in distance estimates produced across all test subjects (fig. 5a and table 1). We therefore reject the null hypothesis that *Rhinecanthus* estimate distance as an integration of travel time. This is consistent with results from previously studied vertebrate and invertebrate species. Among the invertebrates, honeybees show no evidence of using travel time to estimate distance. Bees tested in a headwind underestimated distance travelled despite flights taking longer, and vice versa in a tailwind [35]. Data from humans analysed in a similar way to our fish also indicate a greater error in time measurements compared to the distance estimates produced [30].

For animals navigating in realistic, complex environments travel time is sensitive to disruption which reduces its reliability. For example, a Picasso triggerfish navigating through its coral reef habitat will have variable swimming speeds during any journey depending on whether it is in open sandy areas or enclosed reef areas, or whether it is alone or interacting with another animal. Time will therefore be progressing linearly, but distance travelled is likely to be non-linear and highly variable. The result is that travel time may not be a useful or reliable measure of distance travelled.

Finally, we used video analysis of our distance estimates to begin to explore the sensory basis of distance estimation in our test species. We explored whether the Picasso triggerfish could use mechanosensory inputs from fin beats to measure distance travelled. Many terrestrial species use idiothetic information from a step counter for odometry. Humans are able to estimate distance travelled based on a function of walking speed, step length and step rate [29, 30]. Terrestrial invertebrates such as the desert ant, wandering spider and fiddler crab use proprioceptive inputs from slit sense organs on their legs internal stride integrators to measure distance [26–28, 36]. We proposed that the functionally equivalent proprioceptive mechanism in fish would be the use of an internal finbeat counter. By quantifying finbeat use during our distance estimates, we investigated whether such a mechanism would be plausible using the highly specialised swimming modalities exhibited by the Picasso triggerfish. The Picasso triggerfish exhibits three

swimming modes using lateral beats of the caudal fin, rotational and translational movements of the pectoral fins and undulating movements of the dorsal and anal fins together or in isolation for propulsion and steering. We first tested the role of discrete tailbeat numbers for odometry, revealing a high variability in the number of tailbeats across distance estimates (fig. 6a). Comparing the coefficients of variance between tailbeat number and distance estimates show that tailbeats alone are unlikely to provide the information needed to produce the precision seen in our distance estimate data (table 2). Moreover, trials with low tailbeat numbers are associated with increased use of other swimming modes, and during some trials fish use all three fin sets (fig. 7). There are also extended stretches during some, but not all, distance estimates where the fish glide through the water with no fin movements. However, although trials with no fin movements led to overall overestimates of travel distance compared to trials with continuous fin movements, there was no correlation between the distance spent gliding and the overall reported distance. We therefore suggest that even if the Picasso triggerfish is capable of summing and integrating the total mechanosensory inputs from the different fin types, they are not using this information to measure distance travelled. To further test this hypothesis, finbeats can be manipulated experimentally during testing sessions by exposing the fish to variable flows, known to affect the frequency of tailbeats in salmonids [37]. Moreover, although our analysis suggests it is unlikely, if *Rhinecanthus* has a hierarchy of preferentially used sensory information, mechanosensory inputs from finbeats could be used as a secondary mechanism for odometry in the complete absence of visual self-motion information. Training and testing this species in darkness can be used to test this.

However, unlike for walking terrestrial species, where there is minimal ground movement as they walk across the surface, for fish swimming through variably moving water there is less likely to be a reliable directly proportional relationship between distance travelled relative to absolute space and the finbeat number used. This is especially true in rapidly moving bodies of water such as intertidal zones or fast-flowing rivers, where fin movements are often required to keep the fish stationary relative to the background [37].

The reliance on finbeats for odometry may therefore vary across fish species. Fish that occupy entirely motionless environments, and are therefore not moving against or with currents, may be more likely to experience a linear relationship between finbeat movements and distance travelled. Between-species variation in the sensory mechanisms used for odometry is observed among terrestrial animals. For example, while a step-counter is widely used by both vertebrate and invertebrate animals, flying honeybees which experience variable wind load instead rely almost fully on self-induced optic flow (the speed of visual motion across the retina) [8], and other species show varying reliance on energy use [38] and internal vestibular cues [5].

Future work should focus on unravelling species and habitat specific sensory mechanisms used for measuring distance travelled across the teleost clade. Different teleost species are likely to show a similar variation in sensory mechanisms to terrestrial animals, and this variation may be linked to their evolutionary ecology as well as their physiology. As a coral reef fish occupying well-lit, spatially complex intertidal zones, with specialised fin morphology adapted for fine scale maneuovring, the Picasso triggerfish may instead rely on visual information for odometry in a similar way to honeybees. In comparison, other less visual species such as blind cavefish may measure distance as a summation of proprioceptive inputs to their lateral line, and fish with an electric sense could measure distance using electrical currents in the water. Moreover, unlike surface-constrained terrestrial animals, teleost fish are able to move freely within a volume. If they are able to integrate information on distance travelled freely within this volume, they must be able to use sensory information from the vertical plane of movement to measure travel distances, such as by measuring pressure changes in their swim bladder according to changes in depth. Our behavioural task provides a robust paradigm through which we can continue to test these hypotheses.

5 Conclusions

Overall, we have demonstrated that teleost fish are able to estimate distance with comparable accuracy to terrestrial vertebrates, and they do so using self-motion cues alone. This distance information is not represented as a measure of travel time, but is likely to be represented as a separate metric. Our results indicate that it is unlikely that the Picasso triggerfish used in this experiment rely on idiothetic information from finbeats to collect distance information, implying that the use of a stride integrator to estimate distance may have evolved in walking land animals alone. The behavioural task developed in this paper can now be used into the future as a universal tool to explore the functional and mechanistic basis of distance estimation in fish at the neural and behavioural levels. Assessing distance estimation following neural lesioning and single cell recordings of candidate brain regions will allow us to study the neural mechanisms underlying distance estimation. By manipulating the sensory information provided during training and testing, we can also continue to explore the sensory mechanisms used in the odometers of different fish species. Gaining a more comprehensive understanding of how teleost fish encode metric space in their aquatic environment is a crucial next step in understanding the origin of metric spatial encoding in the vertebrate clade, and the navigational challenges faced by animals occupying an aquatic three-dimensional world.

6 Acknowledgements

We thank members of OxNav and in particular Tim Guilford for valuable input in the experimental design stages.

7 Funding

This work was supported in full by a Biotechnology and Biological Sciences Research Council grant (BB/M011224/1) and a St John's College Lamb and Flag studentship awarded to Cecilia Karlsson.

8 Approvals

This work did not fall under any regulated procedures outlined by ASPA, but was approved by a local ethics committee prior to starting experiments (AWERB – Animal Welfare Ethical Review Body, University of Oxford).

References

[1] Etienne AS, Maurer R, Berlie J, Reverdin B, Rowe T, Georgakopoulos J, and Séguinot V. Navigation through vector addition. *Nature*, 396(6707):161–4, 1998.

[2] Etienne AS and Jeffery KJ. Path integration in mammals. *Hippocampus*, 14(2):180–92, 2004.

[3] Loomis JM, Klatzky RL, Golledge RG, Cicinelli JG, Pellegrino JW, and Fry PA. Non-visual navigation by blind and sighted: assessment of path integration ability. *Journal of Experimental Psychology*, 122(1):73–91, 1993.

[4] Kim S, Sapiurka M, Clark RE, and Squire LR. Contrasting effects on path integration after hippocampal damage in humans and rats. *Proceedings of the National Academy of Sciences (PNAS)*, 110(12):4732–7, 2013.

[5] Jacob P-Y, Gordillo-Salas M, Facchini J, Poucet B, Save E, and Sargolini F. Medial entorhinal cortex and medial septum contribute to self-motion-based linear distance estimation. *Brain Structure and Function*, 222(6):2727–2742, 2017.

[6] Ortega-Escobar J and Ruiz MA. Visual odometry in the wolf spider *Lycosa tarantula* (Araneae: Lycosidae). *The Journal of Experimental Biology*, 217(Pt 3):395–401, 2014.

[7] Müller M and Wehner R. Path integration in desert ants, Cataglyphis fortis. *Proceedings of the National Academy of Sciences (PNAS)*, 85(14):5287–90, 1988.

[8] Srinivasan MV. Honeybees as a model for the study of visually guided flight, navigation, and biologically inspired robotics. *Physiological reviews*, 91(2):413–60, 2011.

[9] Harald W. Odometry and insect navigation. *The Journal of experimental biology*, 214 (Pt 10):1629–41, 2011.

[10] Burt de Perera T and Holbrook RI. Three-dimensional spatial representation in freely swimming fish. *Cognitive Processing*, 13 Suppl 1:S107–11, 2012.

[11] Holbrook RI and Burt de Perera T. Three-dimensional spatial cognition: freely swimming fish accurately learn and remember metric information in a volume. *Animal Behaviour*, 86(5):1077–1083, 2013.

[12] Jeffery KJ, Jovalekic A, Verriotis M, and Hayman R. Navigating in a three-dimensional world. *The Behavioral and Brain Sciences*, 36(5):523–43, 2013.

[13] Near TJ, Eytan RI, Dornburg A, Kuhn KL, Moore JA, and Davis et al. MP. Resolution of ray-finned fish phylogeny and timing of diversification. *Proceedings of the National Academy of Sciences (PNAS)*, 109(34):13698–703, 2012.

[14] Vargas JP, Rodriguez F, Lopez JC, Arias JL, and Salas C. Spatial learning-induced increase in the argyrophilic nucleolar organizer region of dorsolateral telencephalic neurons in goldfish. *Brain Research*, 865(1):77–84, 2000.

[15] Rodríguez F, López JC, Vargas JP, Broglio C, Gómez Y, and Salas C. Spatial memory and hippocampal pallium through vertebrate evolution: insights from reptiles and teleost fish. *Brain Research bulletin*, 57(3-4):499–503, 2002.

[16] Broglio C, Rodriguez F, and Salas C. Spatial cognition and its neural basis in teleost fishes. *Fish and Fisheries*, 4(3):247–255, 2003.

[17] Salas C, Broglio C, Durán E, Gómez A, Ocaña FM, and Jiménez-Moya et al. F. Neuropsychology of Learning and Memory in Teleost Fish. *Zebrafish*, 3(2):157–171, 2006.

[18] Holbrook RI and Burt de Perera T. Separate encoding of vertical and horizontal components of space during orientation in fish. *Animal Behaviour*, 78(2):241–245, 2009.

[19] Goodyear CP and Ferguson DE. Sun-compass orientation in the mosquitofish, Gambusia affinis. *Animal Behaviour*, 17(4):636–640, 1969.

[20] Quinn TP and Brannon EL. The use of celestial and magnetic cues by orienting sockeye salmon smolts. *Journal of Comparative Physiology A*, 147(4):547–552, 1982.

[21] Shcherbakov D, Winklhofer M, Petersen N, Steidle J, Hilbig R, and Blum M. Magnetosensation in zebrafish. *Current Biology*, 15(5):R161–R162, 2005.

[22] Hawryshyn CW, Arnold MG, Bowering E, and Cole RL. Spatial orientation of rainbow trout to plane-polarized light: The ontogeny of E-vector discrimination and spectral sensitivity characteristics. *Journal of Comparative Physiology A*, 166(4):565–574, 1990.

[23] Cheney KL, Newport C, McClure EC, and Marshall NJ. Colour vision and response bias in a coral reef fish. *The Journal of Experimental Biology*, 216(Pt 15):2967–73, 2013.

[24] Newport C, Green NF, McClure EC, Osorio DC, Vorobyev M, and Marshall et al. N. Fish use colour to learn compound visual signals. *Animal Behaviour*, 125:93–100, 2017.

[25] Seyfarth E-A and Barth FG. Compound slit sense organs on the spider leg: Mechanoreceptors involved in kinesthetic orientation. *Journal of Comparative Physiology*, 78(2):176–191, 1972.

[26] Wittlinger M, Wehner R, and Wolf H. The ant odometer: stepping on stilts and stumps. *Science*, 312(5782):1965–7, 2006.

[27] Wittlinger M, Wehner R, and Wolf H. The desert ant odometer: a stride integrator that accounts for stride length and walking speed. *The Journal of experimental biology*, 210(Pt 2):198–207, 2007.

[28] Walls ML, Layne JE, Altevogt R, von Hagen H-O, Zeil J, and Cannicci et al. S. Direct evidence for distance measurement via flexible stride integration in the fiddler crab. *Current Biology*, 19(1):25–9, 2009.

[29] M-L Mittelstaedt and Mittelstaedt H. Idiothetic navigation in humans: estimation of path length. *Experimental Brain Research*, 139(3):318–332, 2001.

[30] Durgin FH, Akagi M, Gallistel CR, and Haiken W. The precision of locomotor odometry in humans. *Experimental Brain Research*, 193(3):429–36, 2009.

[31] Ronacher B and Wehner R. Desert ants Cataglyphis fortis use self-induced optic flow to measure distances travelled. *Journal of Comparative Physiology A*, 177(1):21–27, 1995.

[32] Odling-Smee L and Braithwaite VA. The influence of habitat stability on landmark use during spatial learning in the three-spined stickleback. *Animal Behaviour*, 65(4): 701–707, 2003.

[33] Banino A, Barry C, Uria B, Blundell C, Lillicrap T, and Mirowski et al. P. Vector-based navigation using grid-like representations in artificial agents. *Nature*, 557(7705):429–433, 2018.

[34] Vinepinsky E, Donchin O, and Segev R. Wireless electrophysiology of the brain of freely swimming goldfish. *Journal of Neuroscience Methods*, 278:76–86, 2017.

[35] Srinivasan MV, Zhang S, and Bidwell N. Visually mediated odometry in honeybees. *Journal of Experimental Biology*, 200(19), 1997.

[36] Seyfarth E-A, Hergenrider R, Ebbes H, and FG Barth. Idiothetic orientation of a wandering spider: Compensation of detours and estimates of goal distance. *Behavioral Ecology and Sociobiology*, 11(2):139–148, 1982.

[37] Liao JC. A review of fish swimming mechanics and behaviour in altered flows. *Philosophical transactions of the Royal Society of London. Series B, Biological sciences*, 362(1487): 1973–93, 2007.

[38] Proffit D, Stefanucci J, Banton T, and Epstein W. The role of effort in perceiving distance. *Psychological Science*, 14(2):106–12, 2003.

$\sim$ Page left blank intentionally $\sim$

Chapter 3

Visual odometry in a freely-swimming fish.

Visual odometry in a freely-swimming fish

C. Karlsson[1] and T. Burt de Perera[1]

[1]Department of Zoology, Research and Administration Building, 11a Mansfield Road, Oxford, OX1 3SZ

Summary

Distance travelled is a crucial metric that underpins an animal's ability to navigate in the short-range. While there is extensive research on how terrestrial animals measure travel distance[1–8], it is entirely unknown how animals navigating in aquatic environments estimate this metric. A common method used by land animals is to measure optic flow, where the speed of self-induced visual motion is integrated over the course of a journey[1,2,8–10]. Whether freely-swimming aquatic animals also measure distance relative to a visual frame of reference is unclear. Using the marine fish *Rhinecanthus aculeatus*, we test the visual odometer of a pelagic animal for the first time. We show that *Rhinecanthus* does use visual motion information to estimate distance travelled. However, the underlying mechanism differs fundamentally from previously studied terrestrial animals. Humans and terrestrial invertebrates measure the total angular motion of visual features for odometry, a mechanism which does not vary with visual density[7,9–13]. In contrast, the visual odometer used by *Rhinecanthus acuelatus* is strongly dependent on the visual density of the environment. Odometry in fish may therefore be mediated by a movement detection mechanism akin to the system underlying the optomotor response, a separate motion-detection mechanism used by both vertebrates and invertebrates for course and gaze stabilisation.

Main

Path integration is a powerful mechanism that enables animals to find their way home efficiently. To achieve this, individuals must be able to determine the direction and distance of their travel trajectories[14]. To obtain directional information, many terrestrial animals, both vertebrate and invertebrate, possess diverse compasses based on the Earth's magnetic field[15,16], overhead polarised light[17,18], the direction of sunlight[18] or the moon and stars[19], proprioceptive inputs from body rotations[14], the position of external landmarks, and environmental geometry[20]. In order to discern travel distances, different species of terrestrial animals rely on self-induced optic flow[1,2,8–10], stride integration[21–24], energy use[6], and internal vestibular cues[25] in combination or in isolation.

While a concerted interest has been directed towards terrestrial species, virtually nothing is known of how freely-swimming aquatic animals such as the large and early-branching vertebrate group, the teleost fish, use self-motion information to navigate by path integration. This paucity of information has fundamental implications for our understanding of how universal the mechanisms of navigation are, and crucially what shapes the evolution of these mechanisms.

Here, we explore for the first time how a pelagic fish measures distance travelled. One common mechanism through which many land animals - including humans[10,26] and invertebrates such as the honeybee[1,9,12], desert ant[8], and wolf spider[2] - measure distance travelled is using self-induced optic flow. Self-induced optic flow broadly refers to the speed at which visual information is perceived to pass by an animal as a result of its own movement. This information, if integrated over time, can provide a reliable indication of distance travelled.

Animals navigating in water also have the potential to detect and use information relative to a fixed visual background. However, they would do so against the constraints of rapidly attenuating light with depth and distance, and with access to additional sensory information from the moving fluid medium through which they swim. It is there-

fore unclear if fish would have evolved to measure distance travelled in a similar way to land animals, or whether the constraints of navigating through water have resulted in use of specific sensory mechanisms adapted for reliable and robust information acquisition in water. We address this question by testing whether a shallow water marine fish, *Rhinecanthus aculeatus*, relies on optic flow information for odometry, and explore how this visual information is processed. *Rhinecantus aculeatus* is a shallow water intertidal marine fish, navigating between its home nest and foraging locations over undifferentiated coral rubble. In such an environment, prominent landmarks are scarce and temporally unreliable. Navigating using distance and direction information derived from self-movement is therefore likely to be central to their survival and success.

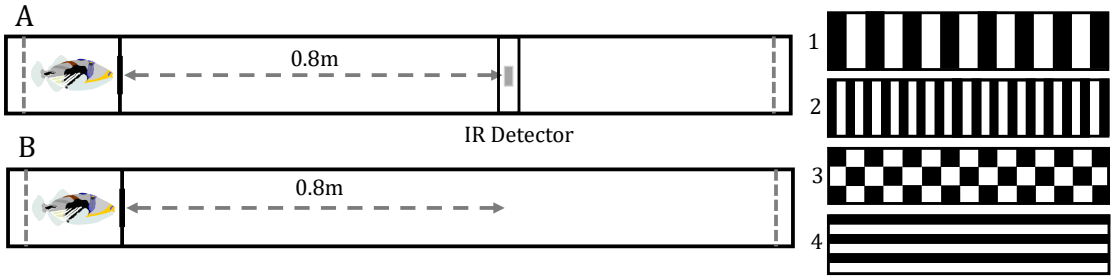


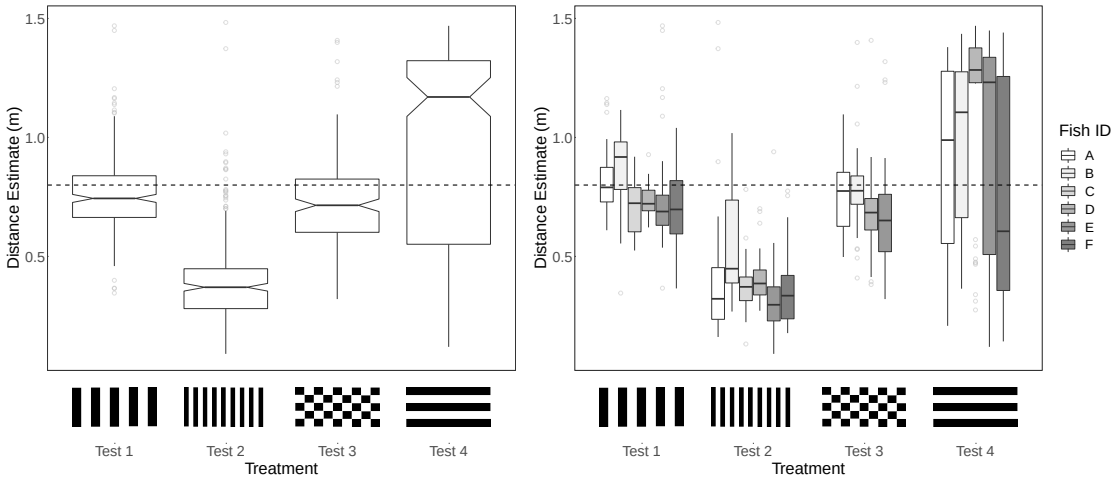
Figure 1: Testing the role of optic flow in distance estimation: training and testing set-up. (A) Training - the fish was trained to swim 0.8m to an overhead infra-red proximity sensor (IR Detector) which when the fish passed beneath it, detected a voltage change and via the Arduino computer caused the aquarium lights to switch on, signalling to the fish to return to the start area for a food reward. Training was conducted with the walls and floor patterned with alternating 0.02m-wide black and white vertical stripes (set-up 1). (B) Testing - during testing trials, the infra-red proximity sensor controlling the overhead lights was removed. The fish was therefore unable to cause the lights to turn on during testing trials. This was to test whether the fish had learned the correct distance, or to swim to the infrared detector landmark to encounter the light stimulus. The fish was tested with four different background combinations: (1) 0.02m vertical stripes; (2) 0.01m vertical stripes; (3) 0.02m wide checkerboard pattern; (4) horizontal stripes of width 0.02m.

Wild-caught *Rhinecanthus aculeatus* subjects were trained to swim a distance of 0.80m under an overhead infra-red proximity sensor controlling aquarium lights running along the top of a linear tunnel (fig. 1A). Swimming beneath this detector switched on the surrounding aquarium lights and signalled to the trained fish to return to the start area for a

food reward. Lateral and ventral walls of the tunnel were patterned with alternating black and white stripes of width, 0.02m (fig. 1, test 1). The fish were then tested in their ability to reproduce this learned distance when the infrared detector controlling the overhead lights was removed, first under the training visual condition (fig. 1B, test 1) and again following manipulations to the visual background (fig. 1, test 2-4). Visual manipulations either altered the translational spatial frequency of the visual pattern (test 2), the geometry of the visual pattern whilst keeping translational spatial frequency at the level experienced during training (test 3), or removed translational optic flow information (test 4). To ensure fish were only able to use self-motion cues and not any absolute positional cues internal or external to the tank, such as the aquarium lights or any overhead visual cues in the experiment room, the start area was shifted between three increasingly distal positions within the tunnel at the start of each training and testing session (supplementary fig. 1, Appendix B).

Figure 2 shows that odometry in *Rhinecanthus aculeatus* is visually driven and scene-dependent. Manipulating the visual background produced consistent shifts in distance estimate distributions across all tested individuals. Under the training condition, the fish reproduced the learned distance with a population average underestimate of 0.038m (fig. 2a, test 1). Distance travelled was calculated using self-motion information alone – we observed predictable systematic shifts in the absolute turning position in the tunnel according to start area position ($F_{2,262}$ = 54.2, $p<0.001$. fig. 3, test 1). Fish were therefore not using any positional landmark cues external to the maze; were not generalising across start area positions, and were not using looming stimuli internal to the maze such as learning the angle subtended by the wall to the floor at the end of the tunnel.

Removing translational optic flow by presenting horizontal stripes on the lateral and ventral walls prevented fish from being able to accurately reproduce the learned distance (fig. 2, test 4). The average distance of 0.953m was a significant overestimate compared to the baseline (χ^2_3 = 510, $p <0.001$; Tukey pairwise comparison Test 1: Test 4, z = -5.909, $p<0.001$). One out of the five tested fish in this condition swam to the end of the tunnel



(a) (b)

Figure 2: The impact of background visual patterns on estimates of distance made by *Rhinecanthus aculeatus*. (a) Overall distance estimates across visual treatments. (b) Distance estimates across visual treatments, split across fish identity. Fish were trained to a target distance of 0.80m (horizontal dashed line), and tested across four visual backgrounds. Each fish completed 45 distance estimates for each treatment. Population averages across treatments were as follows: test 1 mean = 0.762m; test 2 mean = 0.402m; test 3 mean = 0.721m; test 4 mean = 0.953m. Test 2 produced significant underestimates of distance travelled compared to all visual treatments, and test 4 produced a significant overestimates compared to all visual treatments - see table 1 in supplementary section 2.1, Appendix B, for full breakdown of analysis. Box plots indicate the median, interquartile range, and notches are used to compare medians between groups. Grey points indicate outliers.

on almost all trials before returning to the start area doorway (Fish D), but on average distance estimates had a significantly higher variance compared to the three treatments where fish had access to translational optic flow information (fig. 4 in supplementary section 2.3, Appendix B, χ^2_3 = 265, p<0.001; Tukey pairwise comparisons - Test 4: Test 1, z = -11.7, p<0.001; Test 4: Test 2, z = -10.6, p<0.001; Test 4: Test 3, z = -9.19, p<0.001).

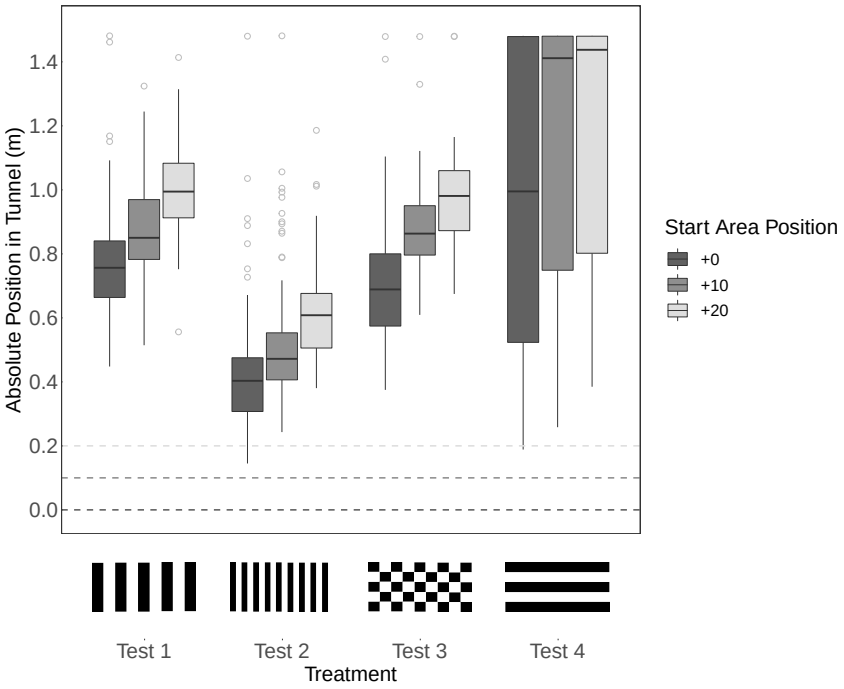


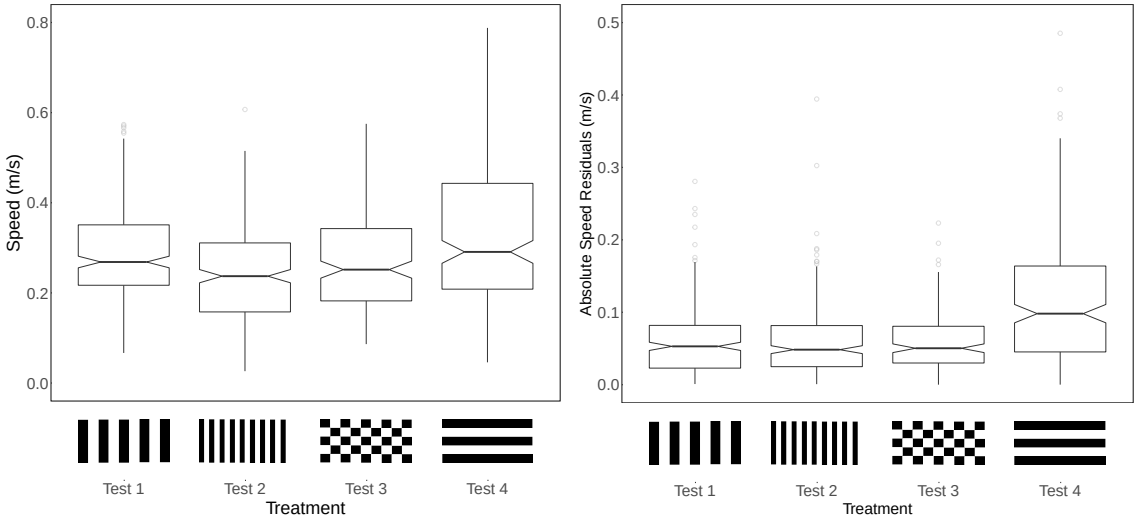
Figure 3: Absolute turning positions across treatments. Between sessions, the start area was moved across three increasingly distal positions within the tunnel to control for use of external cues and assess distance estimation abilities. Each fish completed 15 distance estimates for each start area position, producing a total of 45 distance estimates per treatment. If fish are using an internal measure of distance, there will be a systematic shift in turning position according to each start area position. This was indeed observed across treatments 1-3 where spatial frequency information was provided, indicating that fish are reporting perceived travel distance. When spatial frequency information was removed in treatment 4, there is no consistent significant shift in turning position for all start area positions. See table 2 in supplementary section 2.2, Appendix B for Tukey pairwise comparisons. Grey dashed lines indicate corresponding start area positions for the three start area positions (dark grey: +0. mid grey: +10. light grey: +20). Box plots indicate the median, interquartile range, and grey points indicate outliers.

In test 4, there was also no significant systematic shift in absolute turning position in the tunnel according to start area position. A significant pairwise difference for this

treatment was only observed between start area position +0 and +20 (whole model - χ^2_2 = 7.87, p = 0.0196; Tukey pairwise comparison +0:+20 - z = 2.69, p = 0.0198) and this was likely to have been driven by random individual responses to the removal of optic flow. Two fish (Fish D and E) swam to the end of the tunnel on some but not all trials. Trials in which fish swam to the end of the tunnel coincided with the start area in positions +10 and +20 for Fish D and +20 for Fish E (fig. 3d supplementary section 2.2, Appendix B). The three remaining fish exhibited no consistent pairwise shifts in turning position according to start area position. We therefore conclude that despite the apparent shifting trend for the summarised data in fig. 3 test 4, fish were not able to accurately resolve distance travelled when translational optic flow information was removed.

Removing optic flow information also affected both the average and variance of swimming speeds. Swimming speed on average increased compared to the training condition (Tukey pairwise comparison, Test 1: Test 4, z = -4.44, p <0.001), and the variance in swimming speed across distance estimates was greater compared to treatments where translational optic flow information was provided (fig. 4, χ^2_3 = 160, p <0.001; Tukey pairwise comparisons - Test 1: Test 4, z = 9.07, p<0.001; Test 2: Test 4, z = 8.82 , p<0.001; Test 3: Test 4, z = 7.81 , p<0.001. See table 5 in supplementary section 2.4, Appendix B for all pairwise comparisons).

When using optic flow for odometry and movement control, terrestrial animals measure the angular motion of features across the retina, a mechanism that is independent of the spatial frequency of the environment[7,9,10,12,13]. However, fig. 2 indicates that *Rhinecanthus'* visual odometer is highly sensitive to the spatial frequency of visual information. Doubling the spatial frequency (test 2) resulted in a large underestimation of travel distances compared to the training treatment (test 2 mean distance estimate = 0.402m, Tukey pairwise comparison Test 1: Test 2 - z = 18.3, p <0.001). Any generalised novelty responses were quantified by testing fish with a checkerboard pattern of equivalent spatial frequency to the training condition (test 3). In test 3, distance estimates were restored close to the level of the training condition. A population mean of 0.721m was recorded, a small



(a) (b)

Figure 4: Swimming speeds across treatments. (a) Mean swimming speeds vary with visual treatment but not proportionately with the modifications in spatial frequency. (b) The variability in swimming speed, measured as the residual swimming speeds from the treatment mean, increases with removal of translational optic flow. Each fish completed 45 distance estimates per treatment. See supplementary section 2.4, Appendix B for full analysis and all Tukey pairwise comparisons. Box plots indicate the median, interquartile range, and notches are used to compare medians between groups. Grey points indicate outliers.

underestimation compared to the training condition (Tukey pairwise comparison Test 1: Test 3 - z = -2.77, p = 0.0286). Despite this, there was a strong significant difference between test 2 and test 3 (z = 14.7, p <0.001). We can therefore conclude that the large underestimates observed in test 2, with distance estimates reduced by approximately half, were responses to the doubling of spatial frequency and not a generalised novelty response.

In contrast, swimming speeds were only partially affected by the spatial frequency of the visual background. Under the training condition (test 1), fish swam at an average speed of 0.295 m/s. If the rate of movement of visual contrast was used for speed control in the same way it is used for odometry, we would have expected the fish to reduce their speed by half. However, doubling the spatial frequency in test 2 resulted in only a small significant reduction in swimming speed compared to both tests 1 and 3 (fig. 4a). Swimming speeds on average declined by 18% compared to test 1 and 13% compared to test 3, a change that is unlikely to be biologically relevant to movement decisions by the fish (test 2 mean speed = 0.241 m/s; test 3 mean speed = 0.279 m/s. Tukey pairwise comparison, Test 1: Test 2 - z = 6.16, p <0.001; Tukey pairwise comparison, Test 2: Test 3 - z = 2.71, p = 0.0340). The visual control of swimming speed and odometry by *Rhinecanthus aculeatus* therefore appear to be underpinned by separate motion-detection mechanisms.

Overall, we have shown that teleost fish do use visual motion information to estimate distance travelled. However, the underlying mechanism differs fundamentally from previously studied terrestrial animals such as humans and honeybees. In order to estimate travel distances, terrestrial animals measure the rate of angular movement of visual features over the retina (sometimes referred to as 'true optic flow') and integrate this information over time[7,9,10,27]. This mechanism depends strongly on the distance the moving animal is from a visual background as well as its movement speed. For example, a bee passing close to a visual feature will experience a faster rate of angular change than a bee moving at the same speed but further away from the visual feature. In practice, bees use the same visual motion mechanism for odometry and flight speed control. Bees moving through cluttered environments will therefore fly at a lower speed compared to when fly-

ing through open environments[27,28]. By doing this, they ensure they experience the same rate of optic flow throughout any journey irrespective of the depth and texture of the visual scene[9,27,28]. Crucially, this mechanism is independent of the spatial frequency of the environment[7,9,12,13].

In contrast, the distance estimates produced by *Rhinecanthus aculeatus* in our tunnel experiment vary strongly with the spatial frequency of the visual background. Distance estimates are related to the number of contrast changes experienced en route to the point of interest during training. Teleost fish do not therefore appear to measure the angular rate of movement of visual features to estimate travel distances. Instead, we suggest that *Rhinecanthus'* visual odometer is mediated by a movement-detection mechanism similar to that underlying the optomotor response. The optomotor response is a reflex resulting in head and eye movements that stabilise the visual field, allowing animals to correct for any unwanted deviations such as displacements caused by water currents or gusts of wind[27,29–31]. This mechanism depends on the rate of movement of visual edges, or the spatio-temporal frequency, of the visual environment. For example, when an animal with an optomotor response is placed in a rotating drum patterned with vertical gratings, it will turn in the same direction as the movement of the visual scene, thereby stabilising its orientation relative to its surroundings[28,29]. In a similar way to the distance estimates reported in this study, this turning response is highly dependent on the spatial frequency of the rotating visual gratings, and no head or body rotations are observed in the absence of translational spatial frequency information[29].

In zebrafish, the optomotor response is mediated by direction-sensitive neurons in the pretectal area, directly ventral to the optic tectum[32]. These neurons are tuned to a restricted range of spatial frequencies and wavelengths, and are sensitive to variations in spatial contrast[29,33,34]. Whether the same neural architecture underlies sensory processing in the teleost visual odometer and the optomotor response remains to be seen. Future work quantifying the behavioural output of the teleost odometer in response to a range of visual scene changes will allow us to further compare the mechanisms underlying these

two behaviours.

An odometry mechanism that measures the spatio-temporal frequency of the visual environment is less robust to visual variability. However, *Rhinecanthus* typically forages over areas of undifferentiated coral rubble and sand, an environment that is highly structured but regular. If a fish travels through scenes with regular spatial frequencies at a near constant speed, and integrates this visual information to return to their home nest through the same environment, the underlying movement-detecting neurons will show the same pattern of responses on the outward and return journeys. In this case, using a mechanism that depends on spatial texture is therefore not likely to compromise navigation accuracy. This mechanism does, however, rely on the fish maintaining constant swimming speeds.

Previous work with zebrafish has found no evidence of visually-mediated swimming speed control in teleost fish, and it was suggested that teleost fish could instead regulate swimming speeds using hydrodynamic inputs to the lateral line[35]. However, we show that swimming speeds are visually controlled by *Rhinecanthus aculeatus*, although using a different motion-sensitive mechanism to that controlling the visual odometer. Swimming speeds in this experiment were indeed largely insensitive to variations in spatial frequency, but swimming speed control was affected when translational optic flow information was removed entirely. The visual control of swimming speed by *Rhinecanthus* appears to share similarities with a mechanism measuring the angular rate of visual features used by flying and walking terrestrial animals[10,11,27,28,30]. The increased reliance on visual information by *Rhinecanthus aculeatus* compared to zebrafish may be down to ecological differences. *Rhinecanthus'* coral-reef habitat is both highly structured and brightly-lit, which could make using visual information for navigation and swimming control more reliable than it is for zebrafish occupying waters where the range of visual information may be more limited.

To conclude, we have shown that *Rhinecanthus aculeatus* uses visual motion information for odometry and speed control. Both odometry and speed control were sensitive to the presence or absence of translational optic flow. However, the two processes appear to

be underpinned by different motion-detection mechanisms. Uncovering the neural pathways underlying these processes and how they differ from terrestrial animals will further our understanding of the evolution of visual motion controlled navigation strategies.

References

[1] Esch, H. E. & Burns, J. E. Honeybees use optic flow to measure the distance of a food source. *Nature* **82**, 38–40 (1995).

[2] Ortega-Escobar, J. & Ruiz, M. A. Visual odometry in the wolf spider Lycosa tarantula (Araneae: Lycosidae). *The Journal of Experimental Biology* **217**, 395–401 (2014).

[3] Durgin, F. H., Akagi, M., Gallistel, C. R. & Haiken, W. The precision of locomotor odometry in humans. *Experimental Brain Research* **193**, 429–36 (2009).

[4] Esch, H. E., Zhang, S., Srinivasan, M. V. & Tautz, J. Honeybee dances communicate distances measured by optic flow. *Nature* **411**, 581–3 (2001).

[5] Wolf, H., Wehner, R., Wolf, H. & Wehner, R. Odometry and insect navigation. *Journal of Experimental Biology* **214**, 1629–1641 (2011).

[6] Proffitt, D. R., Stefanucci, J., Banton, T. & Epstein, W. The role of effort in perceiving distance. *Psychological Science* **14**, 106–12 (2003).

[7] Redlick, F. P., Jenkin, M. & Harris, L. Humans can use optic flow to estimate distance of travel. *Vision Research* **41**, 213–219 (2001).

[8] Ronacher, B. & Wehner, R. Desert ants Cataglyphis fortis use self-induced optic flow to measure distances travelled. *Journal of Comparative Physiology A* **177**, 21–27 (1995).

[9] Srinivasan, M., Zhang, S. & Bidwell, N. Visually mediated odometry in honeybees. *Journal of Experimental Biology* **200** (1997).

[10] Frenz, H. & Lappe, M. Absolute travel distance from optic flow. *Vision Research* **45**, 1679–92 (2005).

[11] Mossio, M., Vidal, M. & Berthoz, A. Traveled distances: new insights into the role of optic flow. *Vision Research* **48**, 289–303 (2008).

[12] Srinivasan, M. V. & V., M. Going with the flow: a brief history of the study of the honeybee's navigational 'odometer'. *Journal of Comparative Physiology A* **200**, 563–573 (2014).

[13] Srinivasan, M., Zhang, S., Lehrer, M. & Collett, T. Honeybee navigation en route to the goal: visual flight control and odometry. *The Journal of Experimental Biology* **199**, 237–44 (1996).

[14] Etienne, A. S. & Jeffery, K. J. Path integration in mammals. *Hippocampus* **14**, 180–92 (2004).

[15] Wiltschko, W. & Wiltschko, R. Orientation in birds. Magnetic orientation and celestial cues in migratory orientation. *EXS* **60**, 16–37 (1991).

[16] Lohmann, K. J. & Lohmann, C. M. F. Detection of magnetic field intensity by sea turtles. *Nature* **380**, 59–61 (1996).

[17] Rossel, S. & Wehner, R. The bee's map of the e-vector pattern in the sky. *Proceedings of the National Academy of Sciences (PNAS)* **79**, 4451–5 (1982).

[18] Wehner, R. & Muller, M. The significance of direct sunlight and polarized skylight in the ant's celestial system of navigation. *Proceedings of the National Academy of Sciences (PNAS)* **103**, 12575–12579 (2006).

[19] Dacke, M., Nilsson, D.-E., Scholtz, C. H., Byrne, M. & Warrant, E. J. Insect orientation to polarized moonlight. *Nature* **424**, 33–33 (2003).

[20] Jeffery, K. Integration of the sensory inputs to place cells: What, where, why, and how? *Hippocampus* **17**, 775–785 (2007).

[21] Walls, M. & Layne, J. Direct evidence for distance measurement via flexible stride integration in the fiddler crab. *Current Biology* **19**, 25–9 (2009).

[22] Wittlinger, M., Wehner, R. & Wolf, H. The ant odometer: stepping on stilts and stumps. *Science* **312**, 1965–7 (2006).

[23] Wittlinger, M., Wehner, R. & Wolf, H. The desert ant odometer: a stride integrator that accounts for stride length and walking speed. *The Journal of Experimental Biology* **210**, 198–207 (2007).

[24] Seyfarth, E.-A., Hergenrider, R., Ebbes, H. & Barth, F. G. Idiothetic orientation of a wandering spider: Compensation of detours and estimates of goal distance. *Behavioral Ecology and Sociobiology* **11**, 139–148 (1982).

[25] Jacob, P.-Y. *et al.* Medial entorhinal cortex and medial septum contribute to self-motion-based linear distance estimation. *Brain Structure and Function* **222**, 2727–2742 (2017).

[26] Frenz, H., Bremmer, F. & Lappe, M. Discrimination of travel distances from 'situated' optic flow. *Vision Research* **43**, 2173–83 (2003).

[27] Srinivasan, M. V. Honeybees as a model for the study of visually guided flight, navigation, and biologically inspired robotics. *Physiological Reviews* **91**, 413–60 (2011).

[28] Srinivasan, M. & Zhang, S. Visual control of honeybee flight. *EXS* **84**, 95–113 (1997).

[29] Maaswinkel, H. & Li, L. Spatio-temporal frequency characteristics of the optomotor response in zebrafish. *Vision Research* **43**, 21–30 (2003).

[30] Srinivasan, M. V., Zhang, S. W. & Chandrashekara, K. Evidence for two distinct movement-detecting mechanisms in insect vision. *Naturwissenschaften* **80**, 38–41 (1993).

[31] Lyon, E. On rheotropism - rheotropism in fishes. *American Journal of Physiology* **12**, 149–161 (1904).

[32] Kubo, F. *et al.* Functional Architecture of an Optic Flow-Responsive Area that Drives Horizontal Eye Movements in Zebrafish. *Neuron* **81**, 1344–1359 (2014).

[33] Krauss, A. & C, N. Wavelength dependence of the optomotor response in zebrafish (Danio rerio). *Vision Research* **43**, 1275–1284 (2003).

[34] Schaerer, S. & Neumeyer, C. Motion detection in goldfish investigated with the optomotor response is 'color blind'. *Vision Research* **36**, 4025–4034 (1996).

[35] Scholtyssek, C., Dacke, M., Kröger, R. & Baird, E. Control of self-motion in dynamic fluids: fish do it differently from bees. *Biology Letters* **10**, 20140279 (2014).

Acknowledgements

We thank Tim Guildford, Ollie Padget, and members of the OxNav group for help with experimental design and data analysis, and Jay Willis for help with experiment design and construction. We also thank three anonymous reviewers for feedback that improved the manuscript considerably.

Author contributions

CK conceived the project, performed the experiments and analysis, and wrote the paper. TBdP oversaw the project, and provided feedback on the manuscript.

Competing interests

The authors declare no competing interests.

Funding

This work was supported in full by a Biotechnology and Biological Sciences Research Council grant (BB/M011224/1) and a St John's College Lamb and Flag studentship awarded to Cecilia Karlsson.

Approval

This work did not fall under any regulated procedures outlined by ASPA, but was approved by a local ethics committee prior to starting experiments (AWERB – Animal Welfare Ethical Review Body, University of Oxford.
Project code: APA/1/5/ZOO/NASPA/Burt/PathIntegration).

Methods

Behavioural apparatus

A linear Perspex maze measuring 0.25m high x 0.16m wide x 1.80m long was built within a flow-through tank connected to the home water system to maintain constant water parameters (supplementary fig. 1, Appendix B). The walls and floor were interchangeable across 4 visual patterns, created using non-toxic black vinyl adhered to white Perspex. A perforated white screen was placed at either end to create laminar water flow whilst blocking the visual stimuli provided by cues external to the tank. A moveable start area of dimensions 0.25m high x 0.16m wide x 0.30m long could be placed in one of three start area positions, all 0.1m apart. An infrared proximity sensor (SHARP 2Y0A21 proximity sensor) was placed at water level, 0.80m from the start area doorway. This was attached to an Arduino microprocessor which, through a Matlab (Mathworks Inc.) program, controlled the aquarium lights (Interpret Triple LED Lighting System, 0.75m) running along the top of the lateral maze walls. The voltage of the infrared (IR) detector varied between 0V and 3.5V depending on the strength of the reflection from objects which passed in front of it. We tested the response of the detector to objects in water and after this we set a threshold of 1.7V. As the fish passed beneath the detector, a voltage change was registered and when this exceeded 1.7V, the aquarium lights switched on. A Point Grey Grasshopper 3M camera (FLIR Machine Vision Cameras) was placed 1.1m above the water level to record testing trials.

Behavioural training

Six wild-caught Picasso triggerfish, *Rhinecanthus aculeatus*, were tested, consisting of a mixture of experimentally naive individuals and those used in a previous distance estimation experiment (4 naive, 2 experienced - see supplementary information, Appendix B for sample size, power analysis and husbandry information). Fish were trained to swim 0.80m to the overhead infrared detector to switch on the aquarium lights and return home

for a food reward. This created a learned association between active swimming of a certain distance and a food reward. Training sessions continued until 10 correct trials were complete or until 10 minutes had passed, whichever came first. To control for use of external landmarks, at the start of each session the start area was moved between three positions, located increasingly distally through the tank by 0.10m increments (supplementary fig. 2, Appendix B). The infrared proximity sensor was moved accordingly to maintain the correct distance of 0.80m. Training was considered complete when the fish swam directly out to the light flash and back on 80 percent of trials within the 10-minute session time limit, across three consecutive sessions.

Testing

Fish were tested in their ability to reproduce the learned distance following a series of manipulations to their visual background. Testing conditions were as follows. Test 1 (training condition): alternating black and white vertical stripes of width 0.02m. Test 2: Alternating black and white vertical stripes of width 0.01m, doubling the translational spatial frequency. Test 3: A checkerboard pattern of width 0.02m, restoring the translational spatial frequency to the training condition in order to test whether any distance estimate shifts in test 2 and 4 are novelty responses. Test 4: Alternating black and white horizontal stripes of width 0.02m, removing any translational optic flow. The ordering of test treatments varied between fish.

Testing sessions consisted of a 5 training + max 5 testing trial structure. The 5 training trials were conducted with a visual background of 0.02m vertical black and white stripes, and fish were rewarded if they swam out directly to the infrared detector to turn on the lights and returned home with no additional turns in the tunnel. The purpose of this block was to ensure fish were at testing criterion (80% performance) prior to each set of testing trials. If performance dropped below 80%, fish were returned to training until they achieved testing criterion once more. If fish failed to reach testing criterion again even after 10 additional training sessions, they were removed from further testing. This was to

account for any reduction in motivation between visual treatment testing blocks. All fish were motivated to complete all testing sessions for test treatments 1 and 2, but a loss of motivation and training performance resulted in one fish being removed before treatment 4 (horizontal stripes), and two fish being removed from treatment 3 (checkerboard pattern).

If the preceding 5 training trials were successful, the fish was subsequently returned to the home tank, the visual background manipulated, and then returned to the start area in the experiment tank and permitted to complete a maximum of 5 testing trials. Test trial blocks were of variable length according to individual differences in motivation, but up to a maximum of 5 consecutive trials. During these testing trials the infrared detector was removed, preventing the fish from turning on the surrounding aquarium lights at any point in the tunnel. The fish was released from the start area into the experiment arena and food rewards were randomly provided upon return to the start area to prevent extinction of learning and frustration. A distance estimate was considered the maximum position of the fish's nose prior to turning back to the start area. A total of 15 testing trials were completed at each start area position for all four treatments, producing 45 estimates per treatment for each fish.

Video analysis - extracting distance and speed data

Testing sessions were recorded using an overhead camera (Point Grey Grasshopper 3M) at 50 frames per second and saved as Audio Video Interleave (avi) files using the Streampix 7 video capture software (Image Width: 2448 pixels; Image Height: 350 pixels). A distance estimate was considered the maximum distance of the fish's nose from a position level with the start area doorway prior to returning to the same position. In some testing sessions, fish displayed stereotyped swimming behaviours indicative of disengagement with the behavioural task, and these trials were excluded from analysis if they followed a set of regular engaged trials within the same testing session. This accounted for any drop-off in motivation across the duration of a testing session. If a testing session began

with this stereotyped disengaged behaviour, these were included in analysis as long as the fish returned level with the start area doorway at the end of each trial; such trials were deemed to be representative of the reaction to the testing condition. Each successful testing trial was extracted into a series of jpeg images using the Streampix 7 program, making them compatible for analysis in a Matlab video tracking program. The Matlab program tracked the pixel coordinate position of the fish's nose upon exiting the start area and the maximum point prior to turning home. The video frame number was also recorded for each of these two points. Using the program R (The R Project, version 3.6.1) the total pixel distance travelled was calculated as the difference between the exit position and turning position, and estimates were converted to metric distances using the following conversion: 14.4 pixels = 0.01m. Swimming speed was calculated by dividing distance travelled by time taken in seconds, calculated by converting the time taken in frames to seconds using the video frame rate information.

Statistical analysis – distance estimates

General mixed effects modelling was used to analyse the effects of treatment on distance estimates. The continuous skewed data was best fitted using a gamma distribution, with the subsequent model meeting assumptions of linearity and normality of residuals. An initial model was constructed with start area position and visual treatment as fixed effects, and fish identity as a random effect. This was corrected to the most parsimonious model removing the non-significant effect of start area position. Tukey pairwise comparisons, with a correction for unbalanced designs, were then used to perform multiple pairwise comparisons between treatments.

Statistical analysis – start area position

General mixed effects modelling was used to analyse the effect of start area position on absolute turning position in the tunnel, split by treatment. The data was once more fitted with a gamma distribution, and models were constructed with start area position as a

fixed effect, and fish identity as a random effect. Tukey pairwise comparisons were then used to perform multiple comparisons across start area positions for each treatment.

Statistical analysis – swimming speed

General mixed effects models were constructed for the effect of visual treatment on average swimming speed and swimming speed residuals. Visual treatment was assigned as a fixed effect and fish identity as a random effect. The data for both models were best fitted using a gamma distribution, with models meeting assumptions of linearity and normality of residuals. Tukey comparisons subsequently performed pairwise comparisons between visual treatments.

Chapter 4

Visual swimming control in the marine fish, *Rhinecanthus aculeatus*.

Visual swimming control in the marine fish, *Rhinecanthus aculeatus*

C. Karlsson[1] and T. Burt de Perera[1]

[1]Department of Zoology, Research and Administration Building, 11a Mansfield Road, Oxford, OX1 3SZ

Abstract

For an animal to manoeuvre efficiently through its environment, it must be able to maintain straight trajectories, navigate safely through narrow gaps, avoid collisions, and control movement speeds. Flying and walking terrestrial animals are able to control these movements using visual inputs, such as by measuring the rate of translational optic flow. How freely-swimming aquatic animals control swimming trajectories remains comparatively unexplored. This has implications for our understanding of how animals occupying different ecologies and with different phylogenetic histories control navigation movements. Here, we examine experimentally how swimming trajectories of the shallow water marine fish, *Rhinecanthus aculeatus*, through a tunnel are affected by the availability and orientation of visual information. We show that, unlike many terrestrial animals, the ability to maintain straight, stable swimming trajectories is largely unaffected by manipulations to optic flow information. This ability was only lost when all visual texture information was removed, suggesting that *Rhinecanthus* is instead using visual expansion cues to move through tunnels and narrow gaps. In contrast, we show that access to translational optic flow is necessary to maintain stable and consistent swimming speeds, information that can be extracted from either the ventral or lateral visual environments. Therefore, while *Rhinecanthus* has evolved to control both its positioning from obstacles and swimming speeds using visual motion cues, these processes appear to be underpinned by separate mechanisms.

1 Introduction

For an animal to navigate successfully through its environment, it must not only be able to plan and execute a route to a goal [1], but also manoeuvre safely and efficiently along the chosen trajectory. Efficient movement is made up of several components, including: maintaining straight trajectories; navigating safely through narrow gaps by perceiving and controlling distance to nearby obstacles; and, controlling movement speeds relative to these obstacles. Extensive work with terrestrial animals indicates that these can all be controlled using visual inputs. Both flying and walking animals use the rate of translational optic flow - the pattern and speed of motion of the image of the environment – from the lateral and ventral visual fields to navigate narrow passages; control movement speed; and, by flying animals to maintain constant altitude and orchestrate smooth landings [2–6].

When navigating narrow gaps, flying invertebrates such as honeybees, bumblebees, and fruit flies, and walking and flying vertebrates such as humans and budgerigars move along a straight trajectory that balances the apparent image motion experienced by their two eyes [2, 3, 7–9]. As the magnitude of optic flow is related to the distance from a visual background, in a natural environment this often produces a centering response, with subjects moving stably down the visually-perceived midline of any gap. Experimentally manipulating optic flow by providing insects, budgeriars and humans with a corridor featuring unbalanced image motion from the two lateral walls causes them to veer away from the wall with stronger optic flow [7, 8, 10, 11]. This allows these animals to safely negotiate narrow passages and fly between obstacles without collisions [2, 12, 13]. However, work with hummingbirds suggests that an optic flow equalisation strategy to control positioning responses is not a universal strategy to maintain straight, safe flight trajectories. While hummingbird flight trajectories and hovering flight are both sensitive to even minimal image motion [14, 15], instead of measuring translational velocity to maintain straight flight paths, hummingbirds balance the rate of vertical visual expansion across

the two eyes, and will steer away from features with a greater visual extent [16]. This provides an alternative, but equally robust, mechanism to produce straight flight paths and avoid collisions, but will produce different behavioural responses in environments with unequal translational image motion across the two eyes.

Visual motion information is also widely used to control movement speeds. Flying invertebrates monitor the speed of flight by holding constant the optic flow generated from the surrounding environment. This ensures insects maintain a flying speed that is safe and appropriate to their current environment, such as flying at an efficient high speed in open environments, and then slowing down to safer speeds when entering a cluttered environment [17]. Fruit flies, bumblebees and honeybees all exhibit a continuous adjustment of flight speed when flying through narrowing or widening tunnels, and when subject to temporal increases or decreases in pattern velocity [12, 17–21]. There is even some evidence that nocturnal insects such as the sweat bee, *Megalopta genalis*, use optic flow information to control flight speed [22]. Flight speed by budgerigars also appears to be regulated by monitoring the speed of optic flow [7, 23]. However, unlike flying insects, budgerigars do not exhibit a continuous adjustment of flight speed according to the speed of perceived optic flow. When flying down a gradually narrowing tunnel, budgerigars maintain a high speed in a wide tunnel, and then switching abruptly to a slow flight speed when the tunnel reaches a threshold width [23]. It has been proposed that this strategy optimises energy usage. Birds strive to achieve the most energy efficient speed when the tunnel is wide enough to permit safe flight at this speed, and then they switch to a less energy efficient manoeuvring speed in narrow environments [23].

There are therefore subtle differences in the use of visual motion information to maintain safe movement paths between animals with different physiologies and ecologies. However, despite these mechanistic differences, using visual motion information more generally to maintain straight movement trajectories, avoid collisions when navigating narrow gaps, and controlling moving speed appears to be a universal strategy among walking and flying vertebrates and invertebrates.

Whether swimming animals use optic flow information to control movement in the same way as flying or walking terrestrial animals remains comparatively unexplored. Both flying and swimming animals navigate through fluids, providing them with two potential frames of reference from which to make movement and navigation decisions: the benthic visual background and, the pelagic air or water through which they move. Flying animals appear to use visual motion information independently of their pelagic frame of reference. Honeybees, for example, use optic flow to control flight trajectories and flight speeds independently of wind load [3, 24]. In contrast, using their lateral line, teleost fish are known to use information from their pelagic frame of reference to detect landmarks and movement speeds through distortions of hydrodynamic cues. Therefore, whether a teleost fish would use visual motion information to maintain straight trajectories, move through narrow passages avoiding collisions, and control swimming speed is unclear.

Previous experiments with the zebrafish have indicated that fish do not use visual motion cues to control swimming trajectories [25]. However, in our previous work, we have shown that the shallow water coral reef fish, *Rhinecanthus aculeatus*, relies on visual motion information for odometry, using a mechanism that measures the spatial frequency of the environment (see previous chapter). We also presented preliminary evidence to suggest that swimming speeds are also visually controlled, perhaps using a similar mechanism to that used by terrestrial animals. Differences between the zebrafish and a coral reef fish may therefore reflect adaptations to specific ecologies. *Rhinecanthus*, for example, occupies well-lit shallow coastal waters, subject to high and variable water currents. It may therefore have evolved to rely more strongly on visual motion information to navigate than the zebrafish.

In this paper, we continue work with *Rhinecanthus aculeatus* to investigate whether they use visual motion cues to manoeuvre through their environment. *Rhinecantus aculeatus* is a shallow water intertidal marine fish, manoeuvring precisely through coral reef rubble when navigating between its home nest and foraging locations. By training fish

to swim down a corridor with different visual backgrounds in a similar way to experiments conducted with flying animals, we test whether a teleost fish can use visual motion information to: (i) maintain straight swimming trajectories, (ii) move through narrow gaps, and (iii) control swimming speeds. As *Rhinecanthus* moves through a volumetric environment and could therefore use visual cues located both laterally and ventrally, by independently manipulating the ventral and lateral visual information available, we also test whether visual motion information is preferentially used by one visual field over the other, or whether visual motion information is extracted equally from both fields.

2 Methods

2.1 Subjects

Test subjects were five wild-caught Picasso triggerfish, *Rhinecanthus aculeatus*, of standard length 10-14cm, originating from coastal reefs in the Maldives. The required sample size was calculated *a priori* using the program R (the R project, version 3.6.4), and test simulations using the package 'simr' were run to assess the power of subsequent statistical analysis using mixed effects modelling, indicating adequate power (defined here as an observed power of 80% or above) would be achieved in all analyses (see supplementary information, section 1 in Appendix C for details). Subjects were housed individually in tanks measuring 0.45m width x 0.35m height x 0.75m length under a 12h/12h automated day/night Flourescent light cycle. Tank enrichment was designed following a period of fieldwork and aimed to replicate the natural observed environment of specimens in the wild. Subjects were subsequently provided with a sand and coral gravel substrate to encourage digging, and rocks and caves were provided as refuges. Marine pellets (Ocean Nutrition Formula One Marine Pellet) and krill (Gamma Krill Pacifica) were provided as food rewards during training. Lance fish or whole cockles (Gamma) were fed as a supplement at the end of each training day. The experiment tank and home tanks were cleaned and water quality tested twice weekly to keep ammonia and nitrite at 0ppm and nitrates below 15ppm. Salinity was kept constant at 35ppt using reverse osmosis water with added aquarium salts (Tropic Marine Centre Classic Sea Salt).

2.2 Experiment Set-up

A linear corridor measuring 1.8m (length) x 0.16m (width) x 0.25m (height) with changeable walls and floor was constructed inside a glass aquarium tank measuring 1.8m (length) x 0.25m (width) x 0.3m (height) (fig. 1). This was connected to the main aquarium system via an EHEIM water pump to maintain constant water parameters between the home and experiment tanks. The water pump was switched off during all training and testing ses-

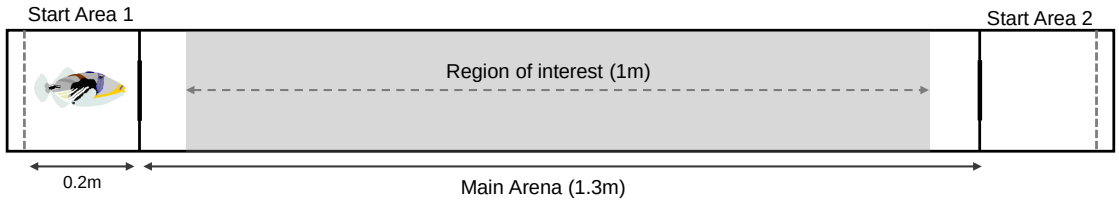


Figure 1: The linear maze was constructed inside a flow-through tank, with water flow in behind start area 1 and passive water flow out at the opposite end of the tank behind start area 2. Perforated white screens separated the fish from the inlet and outlet pipes. The maze walls and floor were lined with alternating black and white stripes of width 0.02m, oriented perpendicular to the direction of movement to provide constant optic flow information. Fish were trained to swim repeatedly between start area 1 and 2 for food rewards. To exclude any positions related to manoeuvres into and out of the start areas, only the central 1m of each trajectory was used in analysis (grey region).

sions to prevent use of hydrodynamic cues from water flow to control swimming trajectories. Start areas measuring 0.2m in length were placed at either end of the linear corridor. White screens at the back of each start area positioned 0.05m from each end of the tank separated the start area visually from the inlet and outlet pipes of the flow-through system. This created an experiment arena measuring 1.3m (length) x 0.16m (width) x 0.25m (height). A Point Grey Grasshopper 3M camera was placed overhead to record testing trials.

2.3 Training

Fish were trained to swim repeatedly between the two start areas to receive food rewards. During all training sessions, the main arena was patterned with alternate black and white stripes of width 0.02m oriented perpendicular to the direction of movement on both the ventral and lateral walls. At the start of each training session, the fish was placed in start area one and given one minute to settle. The door to the start area was then opened and the fish was permitted to enter the main experiment arena. A food reward was provided when the fish entered the opposite start area. Swimming from one start area to the next without any additional turns in the tunnel was considered a single successful training

trial. Training sessions lasted 10 minutes or until 20 trials were completed, whichever came first. Training was considered complete when the fish could swim directly from one start area to the next for 20 consecutive trials within a session, for three consecutive sessions.

2.4 Behavioural Data Collection

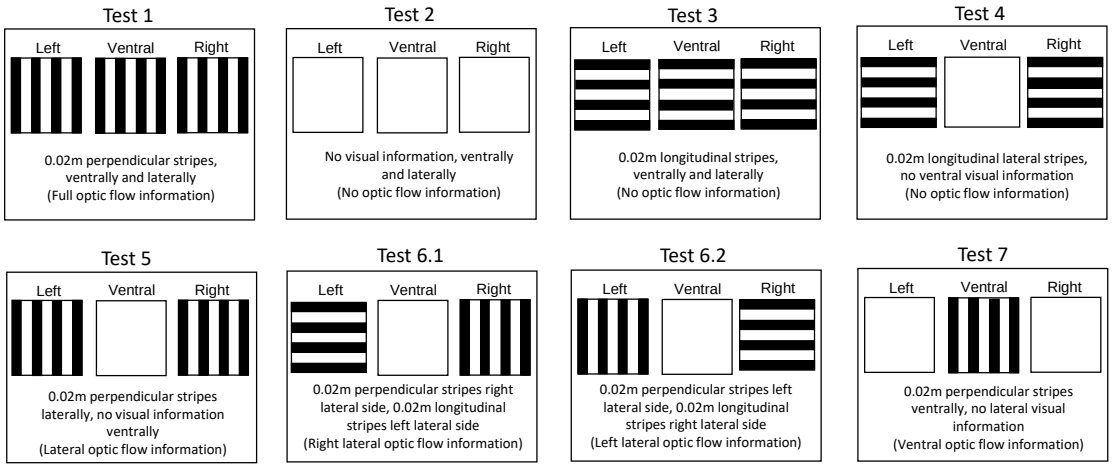


Figure 2: Visual background manipulations to test the use of visual motion information to control swimming manoeuvres. Test 1: training condition - black and white stripes of width 0.02m were oriented perpendicular to the direction of movement on both the ventral and lateral backgrounds. Test 2: no optic flow - white ventral and lateral surfaces removed all spatial contrast and frequency information. Test 3: No optic flow - black and white stripes of width 0.02m were oriented parallel to the direction of movement on both the ventral and lateral visual backgrounds (longitudinal stripes). Test 4: No optic flow - black and white stripes of width 0.02m were oriented parallel to the direction of movement on the lateral visual background, and a plain white background was provided ventrally to remove all left-right translational optic flow information. Test 5: Lateral optic flow - black and white stripes of width 0.02m were oriented perpendicular to the direction of movement, and no spatial information was provided ventrally. Test 6.1 and 6.2: Unbalanced flow - stripes perpendicular to the direction of movement were provided on one wall (right - 6.1, left - 6.2) and the other wall had stripes oriented parallel to the direction of movement. No ventral visual information was provided. Test 7: ventral optic flow - no visual information was provided laterally, while the ventral surface had black and white stripes oriented perpendicular to the direction of movement. Fish completed 30 trajectories swimming from one start area to the other for each treatment.

A series of manipulations to the visual background were performed to test whether *Rhinecanthus* uses visual motion information to control swimming manoeuvres (fig. 2). Testing sessions with novel visual backgrounds were always preceded by a single training session with the training visual background. If the fish could not produce 20 trials swimming directly between the two start areas within this session, it was returned to the

training phase prior to further testing.

30 trajectories were recorded from each fish swimming from start area one to start area two under 8 different visual manipulations (fig. 2). These 30 trajectories for each visual treatment were split across multiple testing sessions to prevent loss of motivation.

All testing trials were filmed from above at 50fps at a resolution of 2448 x 360 pixels. To extract positional data, a tracking software produced using Matlab (Mathworks Inc) was used to track the position of the fish's most anterior point for each video frame between exiting start area 1 and entering start area 2. Only points within the central 1m region of interest were analysed (fig. 1, grey region) - the first and last 0.15m of each trajectory following entry and exit from the start areas were removed as the doors of each start area were centrally positioned and hence entry and exit movements may not reflect responses to the visual background. 0.15m was chosen as the trim length as this was equal to the total length (nose to tip of the tail) of our largest specimen, and therefore ensured the fish had fully manoeuvred out of the start area doorway prior to use of the trajectory position in analysis.

2.5 Behavioural analysis

The 8 different visual treatments were used to assess multiple aspects of swimming control, including: the use of visual motion to maintain straight swimming trajectories; navigate narrow gaps; and, control swimming speeds. We also tested whether fish use information from both the ventral and lateral visual fields for swimming control. These questions were split into four separate questions, or experiments, as not all visual treatments were relevant to each question.

2.5.1 *Experiment 1*: Does *Rhinecanthus aculeatus* use visual motion to maintain straight swimming trajectories?

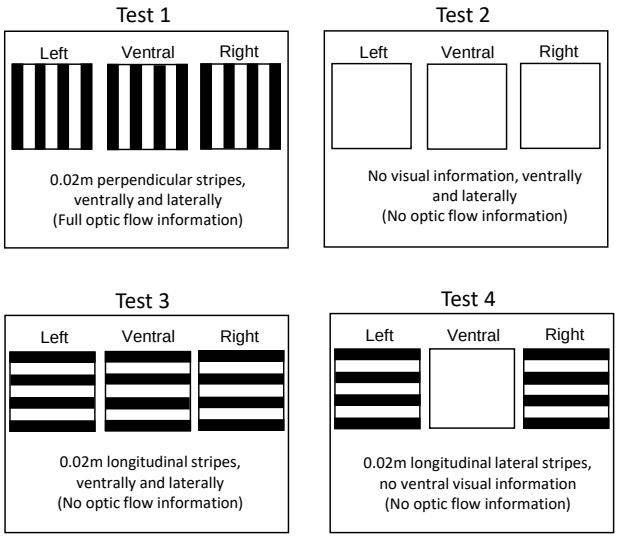


Figure 3: Visual background manipulations to test the use of visual motion information to maintain straight, central swimming trajectories. Test 1: training condition - black and white stripes of width 0.02m were oriented perpendicular to the direction of movement on both the ventral and lateral backgrounds. Test 2: no optic flow - white ventral and lateral surfaces removed all spatial contrast and frequency information. Test 3: No optic flow - black and white stripes of width 0.02m were oriented parallel to the direction of movement on both the ventral and lateral visual backgrounds. Test 4: No optic flow - black and white stripes of width 0.02m were oriented parallel to the direction of movement on the lateral visual background, and a plain white background was provided ventrally to remove all left-right translational optic flow information. Fish completed 30 trajectories from start area 1 to start area 2 for each treatment, and the average lateral position and standard deviation of each trajectory was calculated.

Many flying animals balance image velocity from their lateral visual fields across their two eyes to constantly make small adjustments to flight trajectories. This allows them to maintain straight flight courses, and increase the efficiency of any flight trajectory. By comparing the mean lateral position of each track and track standard deviations when fish have access to full lateral and ventral optic flow information (test 1) with various conditions in which translational optic flow information is removed (test 2, test 3 and test 4) we test whether translational optic flow is also used by *Rhinecanthus* to maintain straight swimming trajectories (fig. 3). Different combinations of white featureless backgrounds and backgrounds with horizontal black and white stripes tested for use of lateral visual expansion cues (test 3) or left-right optic flow information from the ventral background (test 3 compared to test 4) to maintain straight, central trajectories.

2.5.2 *Experiment 2*: Does *Rhinecanthus aculeatus* use visual motion to navigate narrow gaps?

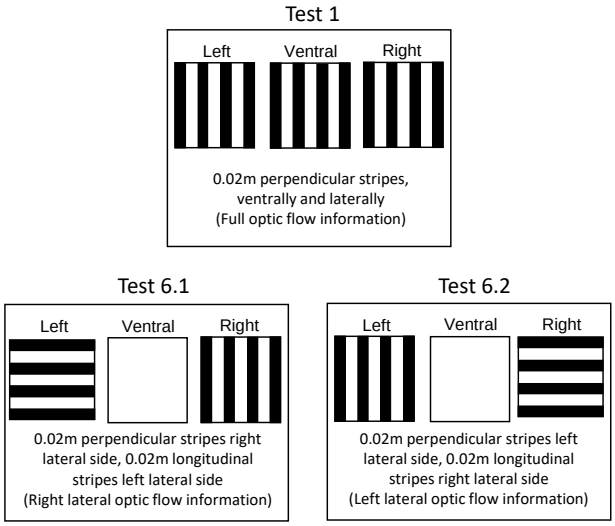


Figure 4: Visual background manipulations to test the use of visual motion information to navigate narrow gaps. Test 1: training condition - black and white stripes of width 0.02m were oriented perpendicular to the direction of movement on both the ventral and lateral background. Test 6.1: Unbalanced flow 1 - stripes perpendicular to the direction of movement were provided on the right hand wall as the fish exited start area 1, and the left-hand wall had stripes oriented parallel to the direction of movement. No ventral spatial information was provided. Test 6.2: Unbalanced flow 2 - stripes perpendicular to the direction of movement were provided on the left-hand wall as the fish exited start area 1, and the right-hand wall had stripes oriented parallel to the direction of movement. No ventral spatial information was provided. Fish completed 30 trajectories from start area 1 to start area 2, and the average lateral position for each trajectory was calculated.

Experiment 2 sought to further examine whether *Rhinecanthus* balances visual motion across its lateral visual fields to maintain central swimming trajectories. The mean lateral positions of trajectories were compared between the training condition (test 1), and when optic flow was only provided on the fish's right lateral side (test 6.1) and when optic flow was only provided on the left lateral side (test 6.2) (fig. 4). Both sides were tested to control for left/right preferences. Horizontal stripes oriented parallel to the direction of movement were provided on the lateral wall with no optic flow, vertical stripes oriented perpendicular to the direction of movement were provided on the lateral wall with optic flow information, and no visual information was provided on the ventral surface.

2.5.3 *Experiment 3*: Does *Rhinecanthus aculeatus* use visual motion to control swimming speeds?

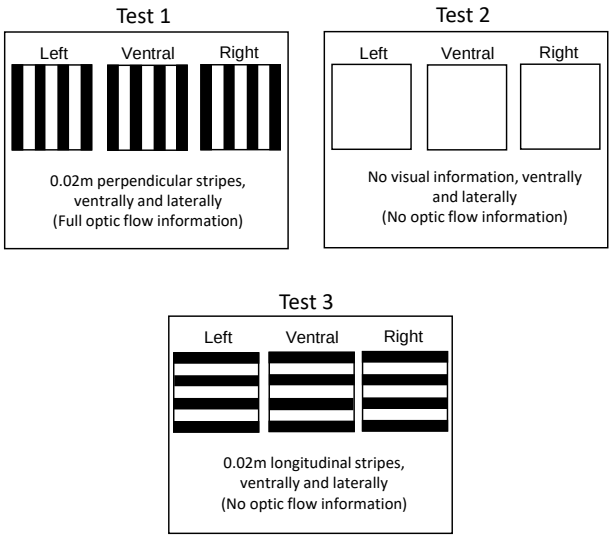


Figure 5: Visual background manipulations to test the use of visual motion information to control swimming speed. Test 1: training condition - black and white stripes of width 0.02m were oriented perpendicular to the direction of movement on both the ventral and lateral backgrounds. Test 2: No visual information on the ventral and lateral surfaces. Test 3: no optic flow - black and white stripes were oriented parallel to the direction of movement on both the ventral and lateral backgrounds. 30 trajectories were completed for each treatment, and the mean, standard deviation and jerk of swimming speeds for each trajectory were calculated.

In experiment 3, we tested the hypothesis that *Rhinecanthus* uses translational optic flow to maintain constant swimming speeds. Average swimming speeds were compared between test 1 (vertical black and white stripes - full ventral and lateral optic flow), test 2 (white backgrounds – no optic flow), and test 3 (horizontal black and white stripes - no optic flow). Test 2 and test 3 were used to assess whether any responses observed in test 2 were a novelty response to an environment with different spatial contrast. The swimming speed in metres per second was calculated between each frame by calculating the distance travelled (in metres) from one frame to the next, divided by the total frame rate (50fps). The mean, standard deviation and jerk of swimming speeds were then calculated for each of the 30 trajectories per treatment.

2.5.4 *Experiment 4*: Does *Rhinecanthus aculeatus* use visual information from both the ventral and lateral visual fields to control swimming trajectories?

In the final comparison, we explored whether *Rhinecanthus* can use optic flow information from both the ventral and lateral visual fields to control swimming speeds and navigation through narrow gaps. The training condition (test 1) was compared to treatments where visual information was removed from the ventral visual field but maintained in the lateral field (test 5) and when visual information was only provided in the ventral visual field (test 7) (fig. 6). The average and standard deviations of lateral position and swimming speed were calculated for each trajectory as previously.

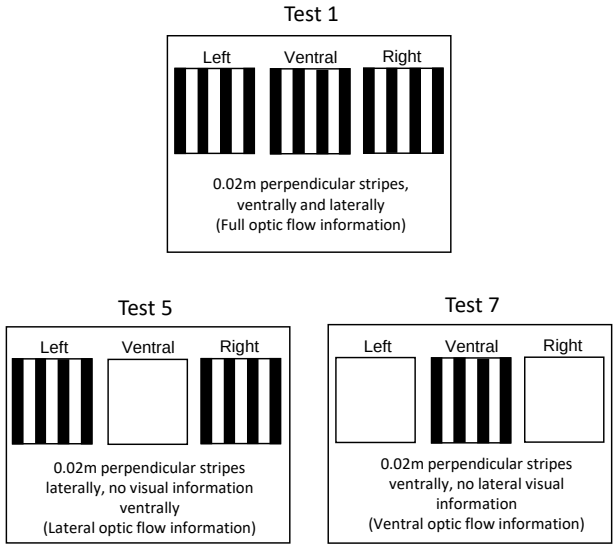


Figure 6: Visual background manipulations to test the use of visual motion information from the ventral and lateral visual fields to control lateral positioning and swimming speed. Test 1: training condition - black and white stripes of width 0.02m were oriented perpendicular to the direction of movement on both the ventral and lateral background. Test 5: Lateral optic flow - black and white stripes of width 0.02m were oriented perpendicular to the direction of movement, and no spatial information was provided ventrally. Test 7: ventral optic flow - no visual information was provided laterally, while the ventral surface had black and white stripes oriented perpendicular to the direction of movement. 30 trajectories were completed for each visual treatment, and the average lateral position was calculated for each trajectory, as well as the mean and variance of trajectory swimming speeds.

2.6 Statistical analyses

All statistical analyses were conducted in the program, R (The R Project, version 3.6.4). Using the packages 'lmer' and 'emmeans', mixed effects modelling was used to assess the fixed effects of visual treatments on the tested parameters, whilst taking into account the random effects produced by individual fish identities. Multiple pairwise comparisons, using the tukey method for adjustment of p-values, were then used to assess the specific pairwise effects of individual treatments within each of the four experiments. All models were formally inspected to ascertain that they adhered to the assumptions of linear mixed effects modelling (see supplementary information, section 3 in Appendix C).

First, to assess the effect of visual treatment on lateral position in the tunnel, models were constructed for the following: mean deviation from the central line; absolute mean deviation from the central line; residuals of average deviation from the central line from the treatment mean; and, standard deviation of track lateral position. The first two models analysed track position and quantified track biases towards the midline compared to the two lateral walls, while the latter two models gave an indication of between and within track variation. Positional data for the first two models were normally distributed and were fitted with gaussian distributions. Residual and standard deviation data displayed a positive continuous right skew so were fitted with log-linked gamma distributions, which also scales parameters with multiplicative effects (such as standard deviations) to become additive, making them suitable for linear modelling.

Second, to assess the effect of visual treatment on swimming speed, models were constructed for the following: mean swimming speed (m/s); residuals of swimming speed from the treatment mean; and, the log normalised dimensionless jerk. The first model explores whether mean speed varies across treatments, identifying differences in acceleration. The latter two models quantify swimming speed adjustment, giving an indication of active swimming speed control. By analysing residual swimming speed from the treatment means, we quantified whether fish maintained a desired target speed across multiple trips. Jerk, the second derivative of speed, meanwhile, provides a measure of track

smoothness, or the moment-to-moment adjustment of acceleration in each track. For a fish swimming through a dynamic fluid exerting drag forces, a high jerk would reflect many small-scale adjustments of acceleration and deceleration to maintain a target speed, whereas a low jerk would reflect a continuous acceleration or deceleration, producing a high within-track variance in swimming speed. As smoothness needs to be a measure of the shape of the movement signal, it must be converted into a dimensionless form that is independent of amplitude and duration prior to analysis [26]. The normalised dimensionless jerk (nd_j) is defined as the total squared jerk normalised by track length in time (t) and peak velocity (v) (eq. (1)). Taking the natural log of this measure produces a smooth variation in dimensionless jerk with track variability [26, 27].

$$nd_j = \frac{(t_2 - t_1)^3}{v_p^2} \int_{t_1}^{t_2} \left(\frac{d^2 v}{dt^2} \right)^2 dt \tag{1}$$

The mean swimming speed and log normalised dimensionless jerk were normally distributed and were fitted with a gaussian distribution. The absolute residuals of swimming speed from the treatment mean were continuous positive with a right skew and were therefore fitted with a log-linked gamma distribution.

3 Results

Overall model results across all visual treatments are summarised in sections 3.1 (lateral position models) and 3.2 (swimming speed models) of the supplementary information. Post-hoc pairwise comparisons of specific visual treatments are subsequently analysed in sections 3.1-3.4 below in the context of the four questions outlined previously.

3.1 Experiment 1: Does *Rhinecanthus aculeatus* use visual motion to maintain straight swimming trajectories?

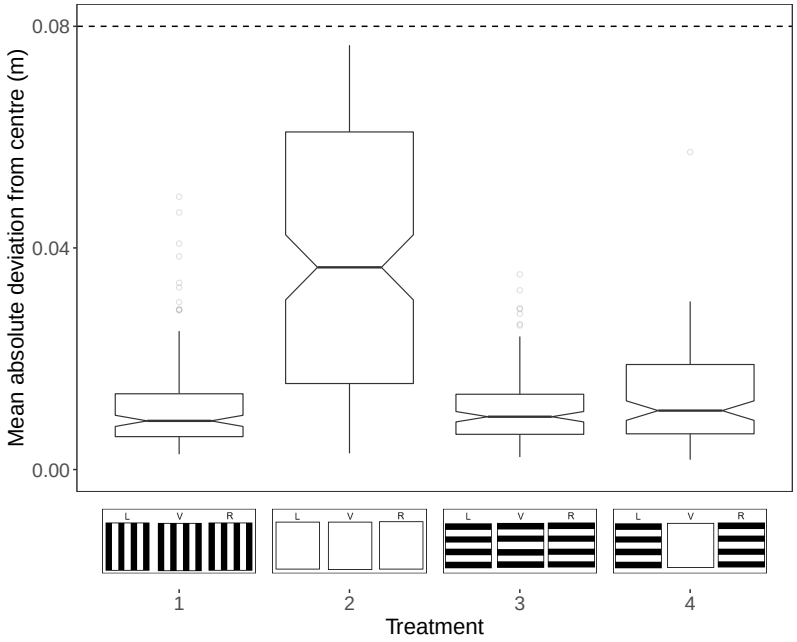


Figure 7: Mean absolute deviation from the central line across visual treatments. Fish are able to maintain central trajectories when lateral visual texture information is provided (treatment 1, 3 and 4), but not when it is removed (treatment 2). The horizontal dashed line at 0.08m deviation indicates the tunnel boundary.

To assess whether *Rhinecanthus* uses visual motion cues to navigate centrally through the tunnel, the average deviation and average absolute deviation of each track from the central line in the tunnel were compared between treatment 1, where full translational optic flow information was available; treatment 2, where no visual texture information

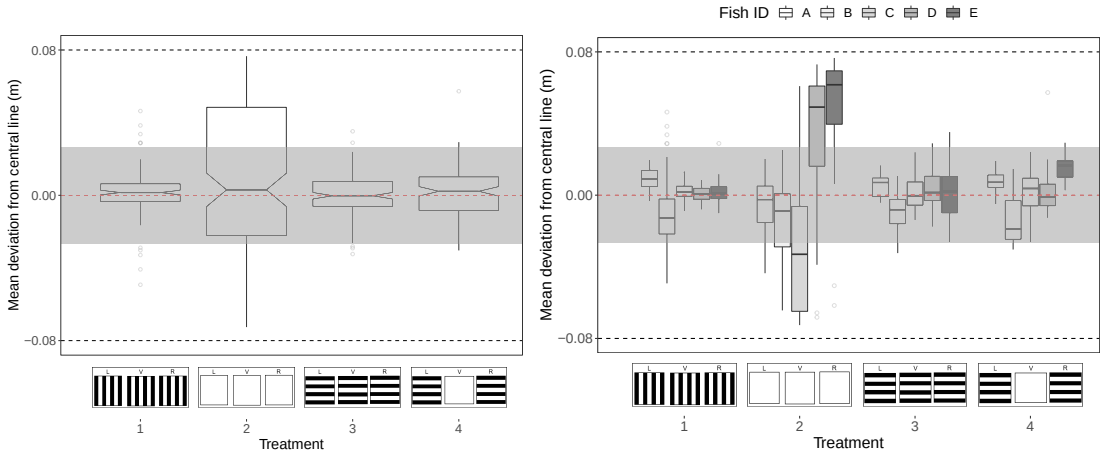


Figure 8: Overall mean deviation from the central line across visual treatments (a) and split by fish identity (b). Fish produced 30 tracks per visual treatment. The horizontal red dashed line indicates the centre of the tunnel, and the black horizontal lines indicate the tunnel edges. Fish are able to maintain central trajectories within the central third of the tunnel when lateral visual texture information is provided (treatment 1, 3 and 4), but not when it is removed (treatment 2). 95% confidence intervals for track position remain within the central third of the tunnel (grey shaded region) for treatment 1 (-0.0147m - 0.0173m), treatment 3 (-0.0159m - 0.0160m) and treatment 4 (-0.0117m - 0.0201m). Under treatment 2, Fish A, B and C steered towards the left lateral wall while Fish D and E steered towards the right lateral wall. Box plots indicate the median and interquartile range, and grey points indicate outliers.

was provided; treatment 3, where visual texture was provided ventrally and laterally but stripes were oriented to remove translational optic flow; and, treatment 4, where no texture was provided ventrally, and lateral stripes were oriented to remove translational optic flow. Visual treatment did have an effect on absolute deviation from the central line ($F_{7,1098}$ = 128, $p<0.001$) but Tukey pairwise comparisons between treatments using the Kenward-Roger method for degrees of freedom indicated that only visual treatment 2 produced absolute deviations significantly different from all other visual treatments (Tukey pairwise comparison, treatment 1: treatment 2, t_{1098} = -17.1, $p<0.001$; treatment 2: treatment 3, t_{1098} = 17.6, $p<0.001$; treatment 2: treatment 4, t_{562} = 14.3, $p<0.001$).

When all visual information was removed in treatment 2, fish were unable to maintain central swimming trajectories, with average position moving out of the central third and

towards the edges of the tunnel (fig. 8b). However, access to translational optic flow is not required for this centralisation response, with no significant difference in mean absolute deviation from the central line between treatments 1, where translational optic flow is provided, and treatments 3 and 4 where translational optic flow information is removed (Tukey pairwise comparison, treatment 1: treatment 3, t_{1098} = 0.392, p = 0.999; treatment 1: treatment 4, t_{1098} = -2.09, p = 0.419), with the 95% confidence interval of average lateral position remaining within the central third of the tunnel (fig. 8b). As there is no significant difference in deviation between treatments 3 and 4, fish are also not relying on following visual features or left-right optic flow cues from the ventral visual background to maintain these central trajectories (Tukey pairwise comparison, treatment 3: treatment 4, t_{1098} = -2.47, p = 0.208).

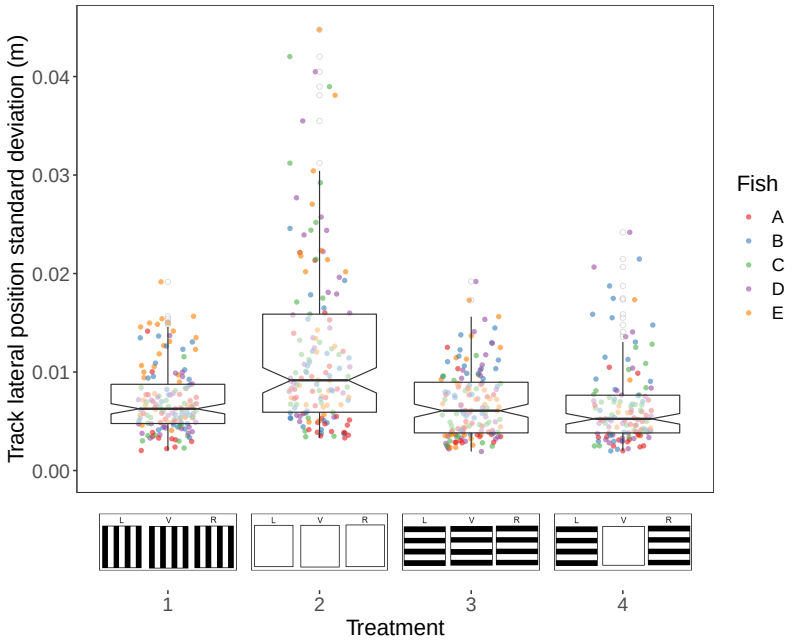


Figure 9: Individual track standard deviation across visual treatments. Coloured points identify individual fish, with fish producing 30 tracks for each visual treatment. Track standard deviation is significantly higher only when visual texture information is removed in treatment 2. Box plots indicate the median and interquartile range, and grey points indicate outliers.

The standard deviation of each track, calculated as a measure of track straightness and

lateral position stability, also varied across visual treatments (χ^2_7 = 203, p<0.001). Under treatment 2, where all visual texture was removed, there were higher lateral position standard deviations than when visual texture was provided in treatments 1, 3 and 4 (Tukey pairwise comparison, treatment 1: treatment 2, t_{1098} = -8.72, p <0.001; treatment 2: treatment 3, t_{1098} = 9.39, p <0.001; treatment 2: treatment 4, t_{1098} = 9.13, p <0.001), fig. 9. There was no difference in track stability between the three treatments where visual texture was provided (Tukey pairwise comparison, treatment 1: treatment 3, t_{1098} = 0.660, p = 0.997; treatment 3: treatment 4, t_{1098} = 0.160, p = 1.00; treatment 1: treatment 4, t_{1098} = 0.788, p = 0.993).

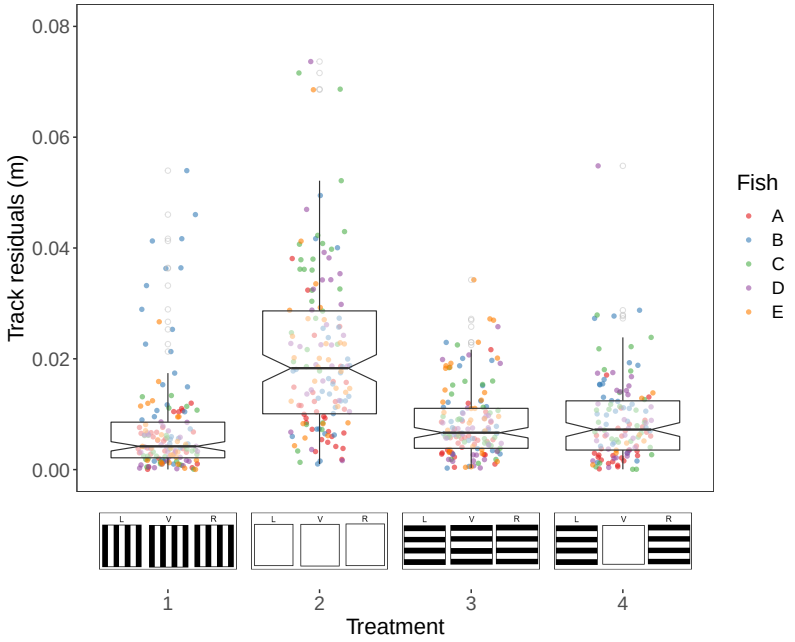


Figure 10: Track residuals from treatment means across visual treatments. Coloured points indicate individual fish data points, with 30 tracks produced per fish for each visual treatment. Residual positions are significantly higher when visual texture information is removed in treatment 2. Box plots indicate the median and interquartile range, and grey points indicate outliers.

Analysis of track residuals from the treatment mean also indicates that repeated trips are more clustered when visual texture information is provided (χ^2_7 = 357, p<0.001, fig. 10, and see also raw track data in Appendix C section 2). Removing visual contrast

information increased the dispersion of repeated trajectories throughout the width of the tunnel (Tukey pairwise comparison, treatment 1: treatment 2, t_{1098} = -11.6, p <0.001; treatment 2: treatment 3, t_{1098} = 9.83, p <0.001; treatment 2: treatment 4, t_{1098} = 9.48, p <0.001), but there was no difference between treatments where optic flow was present (treatment 1) or removed (treatment 3 and 4) - Tukey pairwise comparison, treatment 1: treatment 3, t_{1098} = -1.98, p = 0.496; treatment 1: treatment 4, t_{1098} = -1.77, p = 0.638; treatment 3: treatment 4, t_{1098} = 0.127, p = 1.00.

Access to visual texture information is therefore necessary for *Rhinecanthus* to maintain straight, central trajectories through narrow gaps or tunnels. However, access to translational optic flow information either ventrally (left-right translational optic flow) or laterally (front-back translational optic flow) is not required to achieve this, suggesting that *Rhinecanthus* may be using other visual information such as visual expansion cues to steer straight swimming trajectories.

3.2 Experiment 2: Does *Rhinecanthus aculeatus* use visual motion information to navigate narrow gaps?

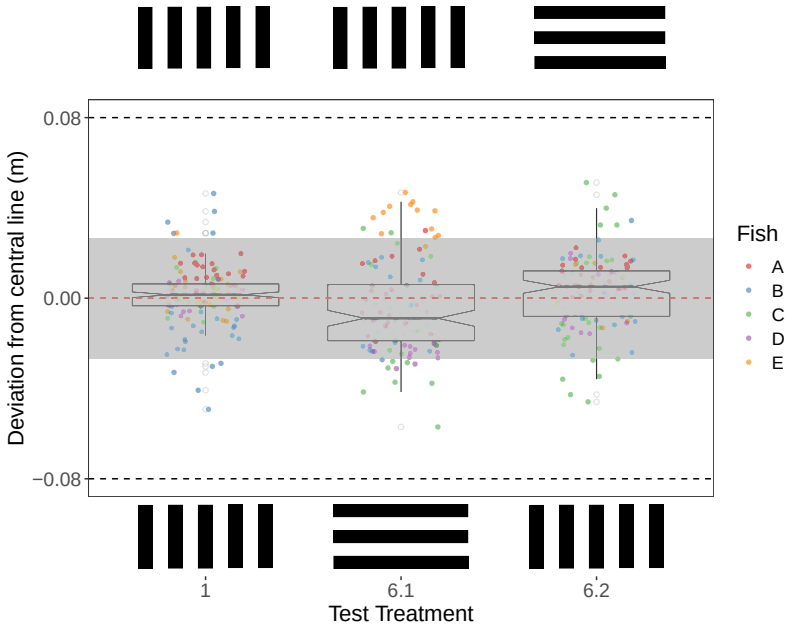


Figure 11: Mean deviation from the central line across visual treatments. Coloured points indicate individual fish identity, with 30 tracks produced per visual treatment for each fish. The horizontal red dashed line indicates the centre of the tunnel, and the black horizontal lines indicate the tunnel edges. The shaded region represents the central third of the tunnel. Positive numbers on the y-axis indicates steering towards the left lateral wall and negative numbers indicate steering towards the right lateral wall. Patterns present on the left and right lateral walls are represented by graphics above and below the plot. The 95% confidence intervals of all three treatments overlap with the central line of the tunnel and remain within the central third of the tunnel (treatment 1: -0.0147m - 0.0173m; treatment 6.1: -0.0173m - 0.0146m; treatment 6.2: -0.00927m - 0.0226m). Box plots indicate the median and interquartile range, and grey points indicate outliers.

To test whether *Rhinecanthus* uses a visual motion equalisation strategy to navigate narrow gaps, the average deviation of each track from the central line for treatment 1, where translational optic flow was equal on both walls, was compared with treatment 6, where translational optic flow was removed from either the right lateral wall (treatment 6.1) or the left lateral wall (treatment 6.2), fig. 11. While the overall model across visual treatments indicated that visual treatment did affect average lateral position ($F_{1098,7} = 3.78$,

$p<0.001$), subsequent Tukey pairwise comparisons indicate that there was no significant difference in the lateral positioning between test 1, test 6.1 and test 6.2 (Treatment 1: Treatment 6.1 - $t_{1098} = 0.924$, $p = 0.983$; treatment 1: treatment 6.2 - $t_{1098} = -1.811$, $p = 0.613$; treatment 6.1: treatment 6.2 - $t_{1098} = -2.63$, $p = 0.146$, fig. 11). The 95% confidence intervals of all three treatments overlap with the central line of the tunnel and remain within the central third of the tunnel (treatment 1: -0.0147m - 0.0173m; treatment 6.1: -0.0173m - 0.0146m; treatment 6.2: -0.00927m - 0.0226m), fig. 11. Figure 11 also indicates some between-fish variability in response to unbalanced visual patterns. For example, while Fish D trends slightly towards the wall with parallel stripes, Fish E trends slightly towards the wall with perpendicular stripes, but this effect is not equally strong between treatments 6.1 and 6.2.

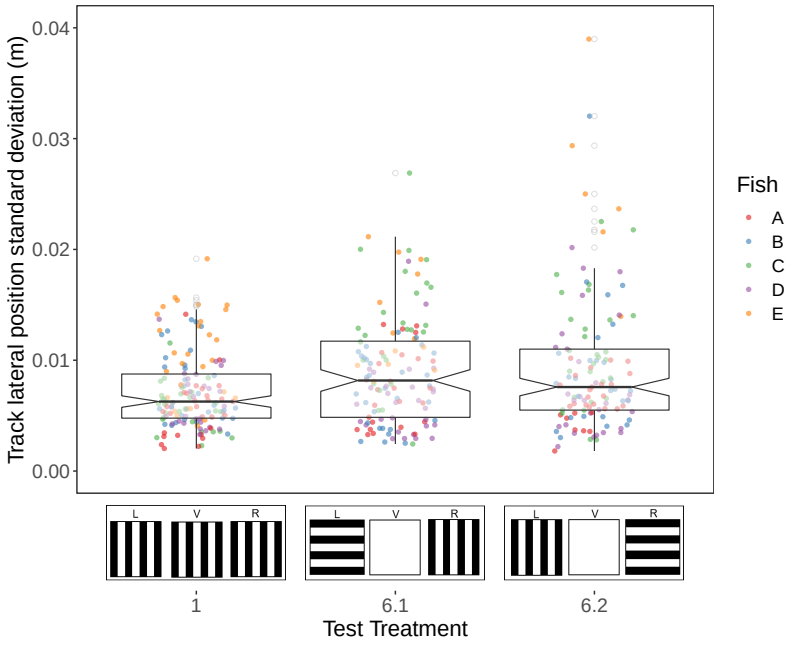


Figure 12: Individual track standard deviation across visual treatments. Coloured points identify individual fish, with 30 tracks produced per visual treatment for each fish. Track standard deviation increases in both treatments where visual motion information from the two walls is unbalanced. Box plots indicate the median and interquartile range, and grey points indicate outliers.

The mixed effects model for the standard deviation of track lateral position did, however, indicate a greater standard deviation in track lateral position when visual informa-

tion was unbalanced across the lateral walls (χ^2_2 = 38, p<0.001, Tukey pairwise comparisons, treatment 1: treatment 6.1, t_{1098} = -3.78, p = 0.00390; treatment 1: treatment 6.2, t_{1098} = -4.55, p<0.001; treatment 6.1: treatment 6.2, t_{1098} = -0.764, p = 0.995), fig. 12. This suggests that while unbalanced visual information causes only small changes in overall lateral position, when information is unbalanced fish are less able to maintain straight, stable trajectories.

3.3 Experiment 3: Does *Rhinecanthus aculeatus* use visual motion to control swimming speed?

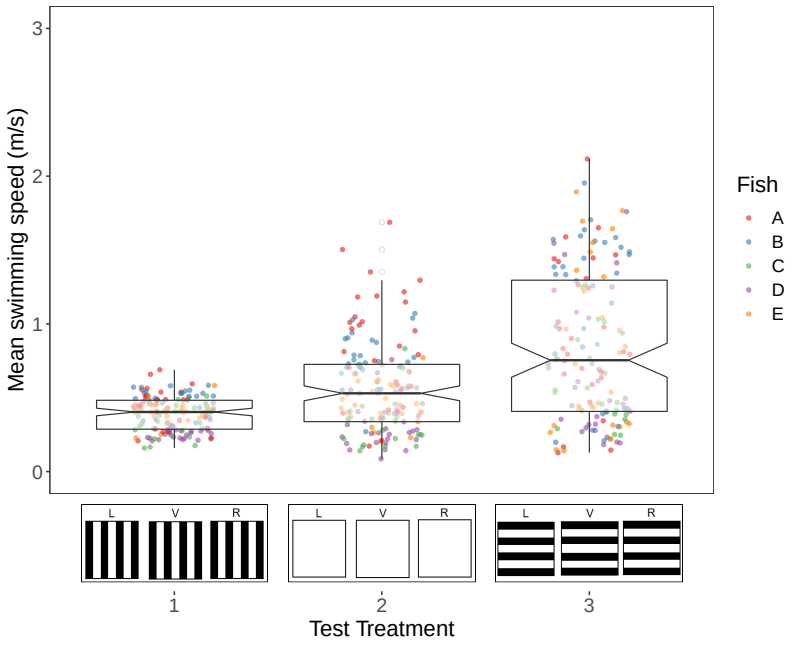
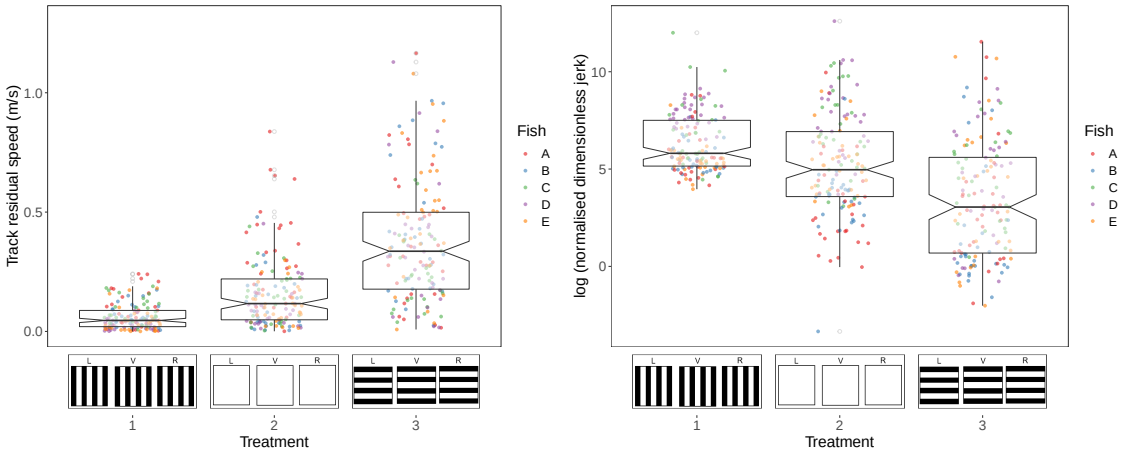


Figure 13: Mean track swimming speed across visual treatments. Coloured points identify individual fish, with 30 tracks produced per treatment by each fish. Track swimming speed increased when translational optic flow was removed in treatments 2 and 3, with treatment 3 also producing higher swimming speeds than treatment 2. Box plots indicate the median and interquartile range, and grey points indicate outliers.

Previous work indicates that *Rhinecanthus* relies on translational optic flow to control swimming speeds. To investigate this further, treatment 1, where optic flow information was provided ventrally and laterally, was compared to treatment 2, where all visual texture information was removed, and treatment 3, where stripes were oriented parallel to the direction of movement to remove all optic flow information. Swimming speed did vary with visual treatment ($F_{2,7}$ = 119, $p<0.001$), with fish reaching higher swimming speeds in treatment 2 and treatment 3 when translational spatial frequency information was removed, fig. 13 (Tukey pairwise comparisons, treatment 1: treatment 2 - t_{1098} = -5.46, $p<0.001$; treatment 1: treatment 3 - t_{437} = -14.8, $p<0.001$). Fish swimming speed was highest when stripes were oriented parallel to the direction of movement, reflecting greater



(a) (b)

Figure 14: Residual track swimming speed (a) and track jerk (b) across visual treatments. Coloured points indicate individual fish identity, with 30 tracks produced per treatment by each fish. (a) The variance, indicated by the residuals from the treatment mean, in swimming speed was lowest for treatment 1, and highest for treatment 3. (b) Track jerk was highest for treatment 1 where translational optic flow was provided, indicating finer control of swimming speed. Box plots indicate the median and interquartile range, and grey points indicate outliers.

acceleration from stationary at the start area doorway (Tukey pairwise comparison, treatment 2: treatment 3 - t_{1098} = -9.38, $p<0.001$).

The lowest mean speed was recorded for treatment 1, which was also accompanied by a low between-track variance in swimming speed (fig. 14a), indicating that fish were more able to maintain a preferred target speed when translational spatial frequency information was provided (χ^2_7 = 640, $p<0.001$, Tukey pairwise comparisons, treatment 1: treatment 2 - t_{1098} = -9.57, $p<0.001$; treatment 1: treatment 3 - t_{437} = -18.9, $p<0.001$; treatment 2: treatment 3 - t_{437} = -9.41, $p<0.001$). Treatment 3 produced the highest variance in swimming speeds compared to both treatment 1 and treatment 2.

Jerk was also highest for visual treatment 1, and lowest for visual treatment 3, fig. 14b (whole model: $F_{7,1098}$ = 90.0, $p<0.001$, Tukey pairwise comparisons, treatment 1: treatment 2 - t_{1098} = 4.75, $p = 0.001$; treatment 1: treatment 3 - t_{1098} = 12.9, $p<0.001$; treatment 2: treatment 3 - t_{1098} = 8.17, $p<0.001$). Fish in treatment 1, where they had access to translational optic flow, were therefore more able to maintain swimming speeds close to their preferred

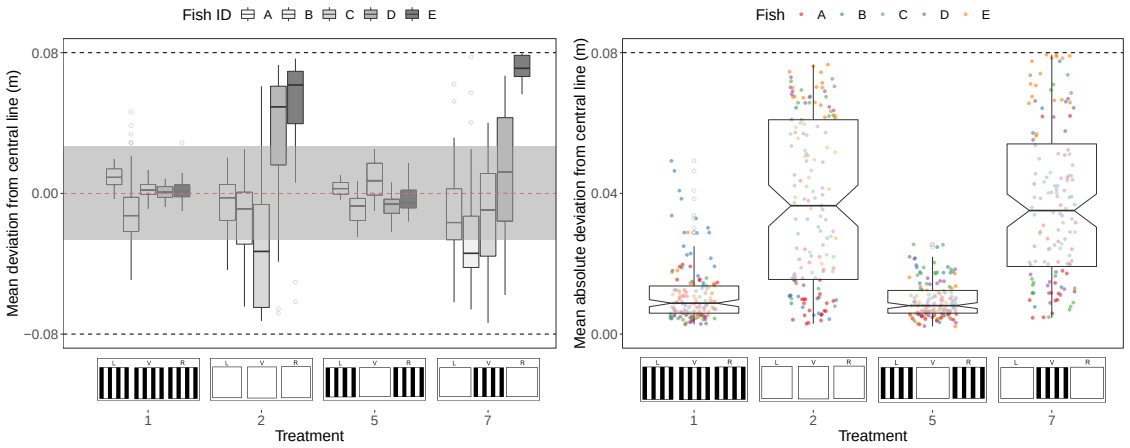
low target speed by constantly adjusting acceleration and deceleration within the tunnel, possibly using spatial frequency inputs. Fish with no access to translational optic flow exhibited smoother trajectories with a more constant acceleration to reach higher overall swimming speeds, indicating a reduction in swimming speed control.

3.4 Experiment 4: Does *Rhinecanthus aculeatus* use visual information from both the ventral and lateral visual fields to control swimming trajectories?

In experiment 4, we explored the use of visual information from the ventral and lateral visual fields separately and together to control swimming trajectories through narrow gaps and tunnels, and to regulate swimming speeds. The condition where translational optic flow was present both ventrally and laterally (treatment 1) was compared with conditions where no visual information was present both ventrally and laterally (treatment 2), and where translational optic flow was only provided on the lateral (treatment 5) or ventral (treatment 7) surfaces.

First, we assessed the effect of visual treatment on deviation from the centre of the tunnel (fig. 15). Absolute deviation from the central line increased during treatment 2 and treatment 7 where lateral visual information was removed, compared to treatments 1 and 5 where lateral translational optic flow was present (Tukey pairwise comparisons: treatment 1: treatment 2 - t_{1098} = -17.1, $p<0.001$; treatment 1: treatment 7 - t_{1098} = -19.4, $p<0.001$; treatment 2: treatment 5 - t_{1098} = 18.2, $p<0.001$; treatment 5: treatment 7 - t_{1098} = -20.5, $p<0.001$). There was no difference in track deviation from the central line between treatment 1 and treatment 5, where lateral visual information was present (Tukey pairwise comparison, treatment 1: treatment 5 - t_{1098} = 1.06, $p = 0.964$).

Individual track standard deviation, and lateral position residuals were also greater when visual information was removed laterally in both treatment 2 and 7 (Tukey pairwise comparisons - residual model: treatment 1: treatment 2 - t_{1098} = -11.6, $p<0.001$; treatment 1: treatment 7 - t_{1098} = -11.5, $p<0.001$; treatment 2: treatment 5 - t_{1098} = 13.8, $p<0.001$; treatment 5: treatment 7 - t_{1098} = -13.7, $p<0.001$. Tukey pairwise comparisons - standard deviation model: treatment 1: treatment 2 - t_{1098} = -8.72, $p<0.001$; treatment 1: treatment 7 - t_{1098} = -7.12, $p<0.001$; treatment 2: treatment 5 - t_{1098} = 9.46, $p<0.001$; treatment 5: treatment 7 - t_{1098} = -7.86, $p<0.001$.), but not when visual information was present in treatment 1 and 5 (Tukey pairwise comparison - residual model, treatment 1: treatment 5



(a) (b)

Figure 15: (a) Mean deviation from the central line across visual treatments split by fish identity (30 tracks per fish for each treatment). The horizontal red dashed line indicates the centre of the tunnel, and the black horizontal lines indicate the tunnel edges. (b) Mean absolute deviation from the central line. Fish are able to maintain central trajectories within the central third of the tunnel when lateral visual texture information is provided (treatments 1 and 5), but not when it is removed (treatments 2 and 7). 95% confidence intervals for track position remain within the central third of the tunnel in (a), (grey shaded region) for treatment 1 (-0.0147m - 0.0173m) and treatment 5 (-0.0181m - 0.0139m). Under treatments 2 and 7, fish exhibited greater absolute mean deviation from the central line, with Fish A, B and C steering towards the left lateral wall while Fish D and E steered towards the right lateral wall. Box plots indicate the median and interquartile range, and grey points indicate outliers.

- t_{1098} = 1.90, p = 0.549. Tukey pairwise comparison - standard deviation model, treatment 1: treatment 5 - t_{1098} = 0.709, p = 0.997).

This indicates that the trend seen in treatment 2 is a true signal of fish responses to the absence of visual texture information and not a novelty response to the first novel visual change from the training condition, as treatment 2 was always the first novel visual manipulation experienced by all fish and treatment 7 was always the final manipulation.

Unlike the centering response, mean track swimming speed only increased when visual information was removed *both* ventrally and laterally in treatment 2 (fig. 16a, Tukey pairwise comparisons: treatment 1: treatment 2 - t_{1098} = -5.46, $p<0.001$; treatment 2: treatment 5 - t_{1098} = 5.64, $p<0.001$; treatment 2: treatment 7 - t_{1098} = 4.59, $p<0.001$). Fish were able to use information from either the ventral or lateral surfaces to achieve mean swimming speeds close to their preferred speed (Tukey pairwise comparisons: treatment 1: treatment 5 - t_{1098} = 0.178, p = 1.00; treatment 1: treatment 7 - t_{1098} = -0.861, p = 0.989; treatment 5: treatment 7 - t_{1098} = -1.04, p = 0.968). The same trend was reported for the variability swimming speed, with residual speed from the treatment mean only increasing when visual information was removed from both the ventral and lateral surfaces (fig. 16b, Tukey pairwise comparisons: treatment 1: treatment 2 - t_{1098} = -9.57, $p<0.001$; treatment 2: treatment 5 - t_{1098} = 9.31, $p<0.001$; treatment 2: treatment 7 - t_{1098} = 5.87, $p<0.001$).

The use of visual inputs to actively control swimming speed in treatments 1, 5 and 7 was also reflected in the track jerk (fig. 16c). Log normalised dimensionless jerk only decreased in treatment 2 (Tukey pairwise comparisons: treatment 1: treatment 2 - t_{1098} = 4.75, $p<0.001$; treatment 2: treatment 5 - t_{583} = -4.77, $p<0.001$; treatment 2: treatment 7 - t_{583} =-3.12, p = 0.0381). Fish were able to continuously adjust their acceleration and deceleration to remain close to their target swimming speed in all treatments where visual information was provided, with no difference in the log normalised dimensionless jerk (Tukey pairwise comparisons: treatment 1: treatment 5 - t_{583} = -0.003, p = 0.999; treatment 1: treatment 7 - t_{583} = 1.63, p = 0.735; treatment 5: treatment 7 - t_{583} = 1.63, p = 0.731).

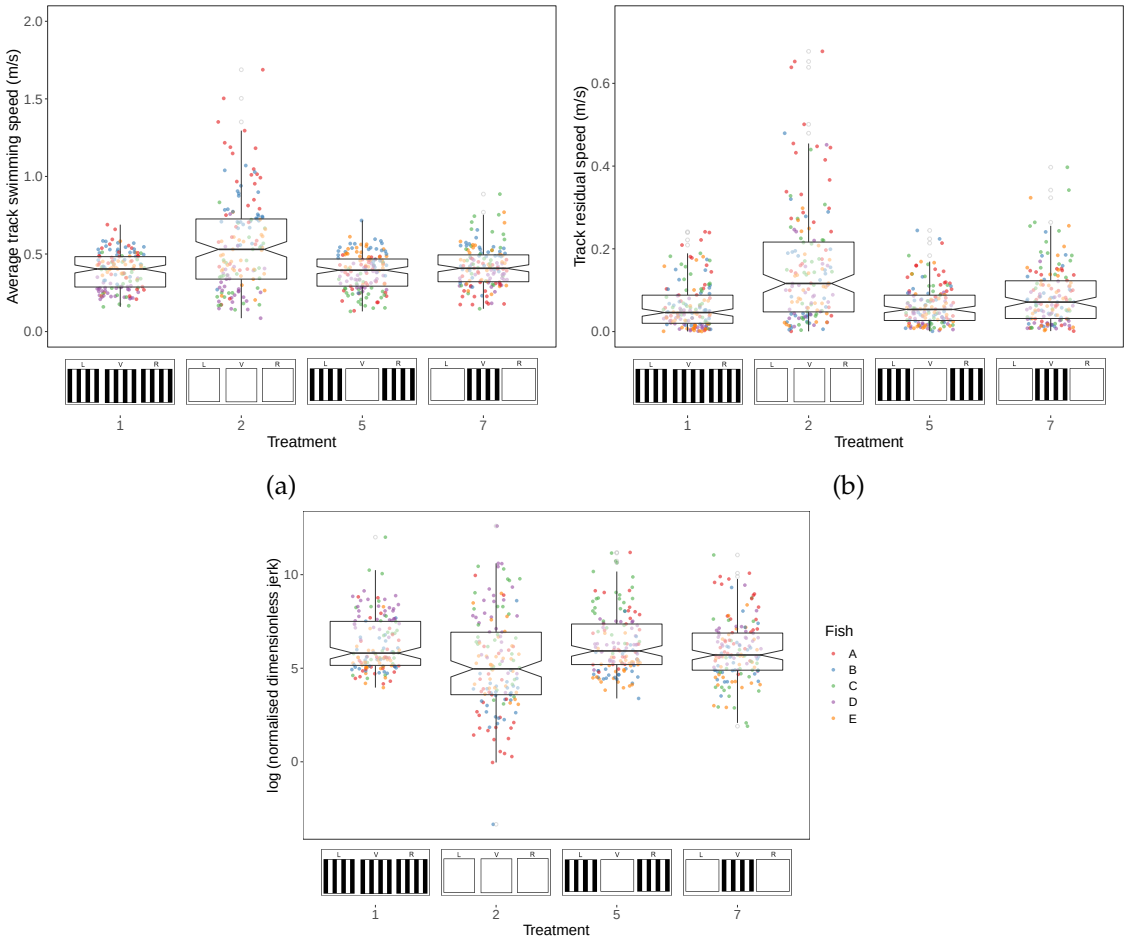


Figure 16: Mean track swimming speed (a), residual swimming speed from the treatment mean (b) and track jerk (c) across visual treatmets. In all plots, coloured points indicate fish identity according to the legend in (c), with 30 tracks produced by each fish for each visual treatment. Average track swimming speed and residual speed only increased in treatment 2, which was accompanied by a reduction in track jerk only in treatment 2. Fish were therefore able to maintain swimming speeds close to their preffered level using information from the ventral and lateral surfaces either in combination or in isolation. Box plots indicate the median and interquartile range, and grey points indicate outliers.

4 Discussion

To explore whether *Rhinecanthus aculeatus* uses visual motion information for swimming control, we examined how swimming trajectories were affected by the availability and orientation of visual textures. Fish were trained to swim repeatedly through a 1.3m tunnel between two start areas and were filmed completing swimming trajectories following a series of visual manipulations. Unlike many flying and walking vertebrates and invertebrates such as honeybees [3], budgerigars [2] and humans [9], *Rhinecanthus* does not use an optic flow equalisation strategy to swim down the midline of the tunnel. The lateral positions of swimming trajectories were unaffected by removal of optic flow information by orienting stripes parallel to the direction of movement. Moreover, when optic flow information was unbalanced across the two walls, fish still maintained central trajectories. The ability to maintain straight, stable trajectories was only lost when all visual texture information was removed. This suggests that *Rhinecanthus*, like hummingbirds [16], may instead use visual expansion cues to navigate through tunnels and narrow gaps. In contrast, access to translational optic flow is important for controlling swimming speeds. Removal of optic flow information caused fish to accelerate to higher swimming speeds, with lower levels of apparent control. *Rhinecanthus* has therefore evolved to control both its positioning from obstacles and swimming speed using visual motion cues, but these processes appear to be underpinned by separate mechanisms.

To assess the use of visual motion cues to steer straight, central courses through narrow gaps and passages, swimming trajectories when the fish had access to translational optic flow were compared to trajectories when translational optic flow was removed, and when translational optic flow was unbalanced. Overall, we show that trajectories remained within the central third of the tunnel and did not deviate significantly from the midline provided that some visual texture information was present, irrespective of whether this texture was oriented parallel or perpendicular to the direction of movement. This suggests that lateral translational optic flow is not necessary to maintain straight,

central trajectories. This is unlike many flying and walking invertebrates and vertebrates that move down the midline of a tunnel by balancing the apparent rate of translational image motion generated by the two walls. Such animals are unable to maintain straight, stable trajectories when translational optic flow is removed, and if information is unbalanced will strongly veer away from surfaces with greater image velocity [2, 3, 7, 9, 12, 25]. Honeybees also use optic flow cues from the ventral left-right direction as well as lateral front-back direction to minimise lateral deviations [28]. However, we demonstrate no difference in *Rhinecanthus'* ability to maintain straight trajectories when the ventral background is either white or patterned with parallel black and white stripes, indicating that they are not following ventral linear features or using left-right translational optic flow inputs to steer straight courses.

Trajectories only became less stable when all visual texture information was removed from both lateral walls in treatments 2 and 7. Fish swam closer to the edges of the tunnel and exhibited an increased within and between track variance. By swimming closer to one of the lateral walls, the fish could instead be seeking positional mechanosensory inputs from the lateral line, which has a lower perceptual range than the visual system. Visual information is therefore preferentially used over hydrodynamic inputs by *Rhinecanthus* for manoeuvring through its aquatic environment. Honeybees demonstrate a similar preference for use of visual inputs over mechanosensory inputs from the dynamic fluid medium through which they fly - the speeds and lateral positions of worker bees flying in a wind tunnel remain unchanged regardless of wind load [24].

As the presence of visual texture information is required to steer straight courses, irrespective of whether this information is oriented parallel or perpendicular to the direction of movement, this suggests that *Rhinecanthus* could instead be using a visual expansion equalisation strategy. A visual expansion strategy relies on the change in image size being a function of the change in distance from a surface. In a uniform environment where background features have a consistent size, the rate of image expansion can be a reliable cue informing the animal of time to collision. For *Rhinecanthus*, navigating over relatively

featureless coral rubble where prominent landmarks are scarce and temporally unreliable, measuring the rate of visual expansion would provide a reliable mechanism for measuring the time to collision with the background. Hummingbirds use this strategy instead of equalising translational optic flow to fly centrally through tunnels and gaps, with subjects steering away from features that have a greater vertical extent, and not those with greater pattern velocity [16]. Hummingbirds are able to maintain straight flight trajectories down the midline of a tunnel even when optic flow information is unbalanced, with only slight shifts towards the wall patterned with horizontal stripes. The fish in our experiment similarly only exhibited very small shifts in lateral position when visual information was unbalanced, with trajectories still remaining within the central third of the tunnel. There was, however, a small increase in track lateral position standard deviation when visual motion information was unbalanced. This error could be consistent with a visual expansion equalisation strategy, as the rate of change of visual expansion of larger objects is greater than that of smaller objects. Therefore, the rate of vertical visual expansion will be greater from the wall with horizontally oriented stripes, while the rate of horizontal visual expansion will be greater from the wall with vertically oriented stripes. This could make measuring and maintaining a consistent rate of visual expansion across the two walls computationally more complex, leading to greater track instability. Analysing trajectories of fish in a tunnel with dynamically changing visual expansion from the two walls throughout the length of the tunnel could be used to test the visual expansion hypothesis further. If a visual expansion strategy is used, fish should consistently shift their lateral position away from the wall with greater apparent visual expansion.

In contrast to the centering response, *Rhincenathus* does rely on translational optic flow information to control its swimming speed. In treatments where fish had access to translational optic flow, they were able to more accurately regulate swimming speeds close to a preferred target. Removing optic flow information by providing stripes oriented parallel to the direction of movement and by removing all visual texture information caused fish to accelerate to reach higher swimming speeds, with lower levels of regulatory control.

These results are in accordance with those previously observed in *Rhinecanthus* completing a distance estimation task – in conditions where optic flow information was removed, fish displayed a higher average swimming speed and a greater variance in swimming speed (see previous thesis chapter). Interestingly, we show that *Rhinecanthus* is also able to flexibly use information from either the ventral or lateral environment to control swimming speeds, stably maintaining them close to their preferred speed. For a fish navigating in a fluid volumetric environment, light will attenuate with both depth and lateral distance from the visual benthic background, making a flexible strategy using visual motion information from either the ventral or lateral environment advantageous.

The use of translational optic flow to control swimming speeds therefore appears to be widely used among walking, flying and swimming animals. However, the underlying mechanism differs between animals with differing ecologies and physiologies. Flying insects such as the honeybee, bumblebees, fruit flies, and even nocturnal insects, are able to continuously adjust their flight speed according to the velocity of apparent image motion to maintain a constant velocity of image motion on the retina, slowing down in a narrowing tunnel and when the velocity of lateral walls is experimentally increased, but independently of any spatial frequency changes [5, 17, 18, 20, 22, 24]. Humans similarly control their walking speed by measuring the velocity of image motion as a function distance from a flanking wall [9]. However, walking speeds also show very slight, additive sensitivity to the spatial frequency of the environment [29, 30]. Flying budgerigars appear to adjust flight speed as a function of the apparent rate of image motion from flanking walls, and is once more fully independent of spatial frequency, as is observed for flying insects [7]. However, their adjustment of flight speed is not continuous, with birds adopting a high flight speed in a wide tunnel with low levels of apparent image motion, switching to a low flight speed in a narrowing tunnel with a threshold increase in apparent image motion [8, 23].

In our experiment, swimming speeds were highest and accompanied with the lowest levels of apparent control in treatment 3 where fish were provided with parallel stripes.

The difference between treatment 2 (white background) and treatment 3, both of which completely remove optic flow information, could be a result of the increased tortuosity of tracks in treatment 2 – an increased tortuosity, reflecting fin movements leading to body turning, would impede constant acceleration to reach higher swimming speeds than when fish are following straight trajectories. However, this continuous variance in swimming speeds exhibited between treatments 1, 2 and 3 implies that *Rhinecanthus* is comparatively free from physiological energy constraints to the adjustment of swimming speed, suggesting they may be able to continuously adjust their swimming speed in accordance with the speed of apparent image motion.

The mechanism used to regulate swimming speeds therefore appears to more closely resemble the mechanism used by terrestrial animals such as humans and flying insects. This mechanism involves continuously holding constant the angular rate of movement of the visual environment, and relies on the presence of some translational visual texture, but is largely independent of the spatial frequency of this texture. Previous work indicates that visual speed control by *Rhinecanthus* is also largely insensitive to the spatial frequency of the environment, but as with humans some very small variations are still seen (see previous thesis chapter). Further experiments to more extensively explore adjustments to swimming speed in a tunnel with a variety of spatial frequencies, and in a tunnel with tapering width will be required to fully quantify their perception of swimming velocity as a function of both distance from their visual background and the spatial frequency of their environment.

5 Conclusion

Taken together, our results indicate that *Rhinecanthus* does rely on access to visual motion information to control swimming trajectories, and only in the absence of all visual information are proprioceptive inputs to the lateral line used to maintain safe swimming courses and avoid collisions. However, unlike many terrestrial animals that rely almost exclusively on translational optic flow, *Rhinecanthus* appears to use separate visual mechanisms to control positioning and swimming speed. Our results suggest that visual expansion cues may be used to maintain straight trajectories and steer centrally through gaps, but translational optic flow cues are used to maintain constant swimming speeds close to a target level. These results also indicate a divergence from the visual strategy used by the previously tested zebrafish, which appear to be largely insensitive to manipulations to their visual environment [25]. These differences could reflect adaptations to different visual ecologies. *Rhinecanthus* is a highly visual species navigating through brightly lit shallow intertidal waters, strongly relying on visual information to find food, communicate with conspecifics, and for navigation tasks such as estimating distance travelled. Use of visual information to also manoeuvre safely through its environment could therefore reflect a specific adaptation for navigating through its brightly lit, highly structured reef environment. Work with additional teleost fish species from a range of visual ecologies and phylogenetic positions will allow us to fully understand how universal visual manoeuvring mechanisms in teleost fish are, and how these mechanisms compare to flying and walking terrestrial animals.

6 Acknowledgements

We thank members of the OxNav group for help with experimental design and Matishalin Patel for help with data analysis.

7 Author contributions

CK conceived the project, performed the experiments and analysis, and wrote the paper. TBdP oversaw the project, and provided feedback on the manuscript.

8 Competing interests

The authors declare no competing interests.

9 Funding

This work was supported in full by a Biotechnology and Biological Sciences Research Council grant (BB/M011224/1) and a St John's College Lamb and Flag studentship awarded to Cecilia Karlsson.

10 Approval

This work did not fall under any regulated procedures outlined by ASPA, but was approved by a local ethics committee prior to starting experiments (AWERB – Animal Welfare Ethical Review Body, University of Oxford.
Project code: APA/1/5/ZOO/NASPA/Burt/PathIntegration).

References

[1] Gallistel C. R. *The organization of learning*. MIT Press, 1990.

[2] Altshuler D.L. and Srinivasan M.V. Comparison of Visually Guided Flight in Insects and Birds. *Frontiers in Neuroscience*, 12(157):1–11, 2018.

[3] Srinivasan M.V. Honeybees as a model for the study of visually guided flight, navigation, and biologically inspired robotics. *Physiological Reviews*, 91(2):413–60, 2011.

[4] Srinivasan M.V., Zhang S.W., and Bidwell N. Visually mediated odometry in honeybees. *Journal of Experimental Biology*, 200(19):2513–2522, 1997.

[5] Srinivasan M. V. and Zhang S.W. Visual control of honeybee flight. *Orientation and Communication in Arthropods*, 84:95–113, 1997.

[6] Srinivasan M. V., Zhang S.W., Chahl J.S., Barth E., and Venkatesh S. How honeybees make grazing landings on flat surfaces. *Biological Cybernetics*, 83(3):171–183, 2000.

[7] Bhagavatula P.S., Claudianos C., Ibbotson M.R., and Srinivasan M.V. Optic Flow Cues Guide Flight in Birds. *Current Biology*, 21(21):1794–1799, 2011.

[8] Schiffner I. and Srinivasan M.V. Direct evidence for vision-based control of flight speed in budgerigars. *Scientific Reports*, 5(10992), 2015.

[9] Duchon A.P. and Warren W.H. A Visual Equalization Strategy for Locomotor Control: Of Honeybees, Robots, and Humans. *Psychological Science*, 13(3):272–278, 2002.

[10] Dyhr J. P. and Higgins C. M. The spatial frequency tuning of optic-flow-dependent behaviors in the bumblebee Bombus impatiens. *Journal of Experimental Biology*, 213 (10):1643–1650, 2010.

[11] Srinivasan M.V., Lehrer M., Kirchner W.H., and Zhang S.W. Range perception through apparent image speed in freely flying honeybees. *Visual Neuroscience*, 6(5): 519–35, 1991.

[12] Srinivasan M.V, Zhang S.W., Lehrer M., and Collett T. Honeybee navigation en route to the goal: visual flight control and odometry. *The Journal of Experimental Biology*, 199(Pt 1):237–44, 1996.

[13] Muijres F.T., Elzings M.J., Melis J.M., and Dickinson M.H. Flies Evade Looming Targets by Executing Rapid Visually Directed Banked Turns. *Science*, 344(6180):172–177, 2014.

[14] Goller B. and Altshuler D.L. Hummingbirds control hovering flight by stabilizing visual motion. *Proceedings of the National Academy of Sciences (PNAS)*, 111(51):18375–18380, 2014.

[15] Ros I.G. and Biewener A. Optic flow stabilizes flight in ruby-throated hummingbirds. *Journal of Experimental Biology*, 219(16):2443–2448, 2016.

[16] Dakin R., Fellows T.K., and Altshuler D.L. Visual guidance of forward flight in hummingbirds reveals control based on image features instead of pattern velocity. *Proceedings of the National Academy of Sciences (PNAS)*, 113(31):8849–8854, 2016.

[17] Baird E., Srinivasan M.V., Zhang S.W., and Cowling A. Visual control of flight speed in honeybees. *Journal of Experimental Biology*, 208(20):3895–3905, 2005.

[18] David C. T. Compensation for height in the control of groundspeed by Drosophila in a new, barber's pole wind tunnel. *Journal of Comparative Physiology A*, 147(4):485–493, 1982.

[19] Fry S.N., Rohrseitz N., Straw A.D., and Dickinson M. H. Visual control of flight speed in Drosophila melanogaster. *Journal of Experimental Biology*, 212(8):1120–1130, 2009.

[20] Baird E., Kornfeldt T., and Dacke M. Minimum viewing angle for visually guided ground speed control in bumblebees. *Journal of Experimental Biology*, 213(10):1625–1632, 2010.

[21] Baird E., Srinivasan M.V., Zhang S.W., Lamont R., and Cowling A. Visual control of flight speed and height in the honeybee. *In: Nolfi S. et al. (eds) From Animals to Animats 9. SAB 2006. Lecture Notes in Computer Science*, 4095:40–51, 2006.

[22] Baird E., Kreiss E., Wcislo W., Warrant E., and Dacke M. Nocturnal insects use optic flow for flight control. 7(4):499–501, 2011.

[23] Schiffner I. and Srinivasan M.V. Budgerigar flight in a varying environment: flight at distinct speeds? *Biology Letters*, 12(20160221), 2016.

[24] Barron A. and Srinivasan M.V. Visual regulation of ground speed and headwind compensation in freely flying honey bees (Apis mellifera L.). *Journal of Experimental Biology*, 209(5):978–984, 2006.

[25] Scholtyssek C., Dacke M., Kroger R., and Baird E. Control of self-motion in dynamic fluids: fish do it differently from bees. *Biology Letters*, 10(5):20140279, 2014.

[26] Balasubramanian S., Melendez-Calderon A., and Burdet E. A robust and sensitive metric for quantifying movement smoothness. *IEEE Transactions on Biomedical Engineering*, 59(8):2126–2136, 2012.

[27] Hogan N. and Sternad D. Sensitivity of smoothness measures to movement duration, amplitude, and arrests. *Journal of Motor Behavior*, 41(6):529–534, 2009.

[28] Linander N., Baird E., and Dacke M. How bumblebees use lateral and ventral optic flow cues for position control in environments of different proximity. *Journal of Comparative Physiology A*, 203(5):343–351, 2017.

[29] Ludwig C.J.H., Alexander N., Howard K.L., Jedrzejewska A.A, Mundkur I., and Redmill D. The influence of visual flow and perceptual load on locomotion speed. *Attention, Perception, and Psychophysics*, 80(1):69–81, 2018.

[30] Denton G.G. The influence of visual pattern on perceived speed. *Perception*, 9(4): 393–402, 1980.

$\sim$ Page left blank intentionally $\sim$

Chapter 5

A fish's frame of reference: distance estimation in variable flows.

A fish's frame of reference: distance estimation in variable flows

C. Karlsson[1], J.K. Willis[1], and T. Burt de Perera[1]

[1]Department of Zoology, Research and Administration Building, 11a Mansfield Road, Oxford, OX1 3SZ

Abstract

Teleost fish have access to two separate frames of reference from which to make navigation decisions: the fixed benthic background, and the water column through which they swim. Using the marine fish, *Rhinecanthus aculeatus*, we examined the relative importance of sensory information from these two frames of reference for estimating distance travelled. We designed a flume system that could alter water flow within a tunnel with changeable visual backgrounds. By training fish using a distance estimation task developed in previous chapters with one combination of visual and water flow inputs, and testing following manipulations to the water and visual flow information, we examined the relative importance of visual information and water flow information for odometry. Pilot results from one individual indicate that *Rhinecanthus aculeatus* relies primarily on visual motion information from the fixed benthic background to estimate distance travelled. Manipulations to water flow information from the fluid medium had only small, secondary effects on odometry when visual information was present. However, when visual information was removed, the effects of altering water flows became more pronounced, indicating that *Rhinecanthus* may display hierarchical use of different sensory inputs depending on the information available.

1 Introduction

For decades, research has focused on elucidating the sensory mechanisms underlying odometry in terrestrial animals. Flying and walking vertebrates and invertebrates have been shown to estimate distances using measurements of self-induced optic flow [1–6], proprioceptive inputs from mechanical leg movements [7–11], energy expenditure [12], or internal vestibular motion [13].

Until recently, nothing was known about how freely-swimming aquatic animals estimate distance travelled in order to navigate through their local environment. Unlike flying and surface-constrained terrestrial animals, freely-swimming aquatic animals navigate without direct physical contact with the benthic background. The water medium through which they swim also places physical constraints on the scope of certain sensory information, while simulatenaously providing additional sensory information not available on land. For example, underwater, the ability to use visual information declines rapidly with both depth and horizontal distance from a visual background [14], but the water itself provides additional hydrodynamic cues that could be useful for distance estimation. Fully aquatic animals are therefore said to have access to two frames of reference which they can use to perform navigation calculations: the fixed benthic background, and the dynamic fluid through which they swim. It therefore remains unclear to what extent the mechanisms used by terrestrial animals are also used by their aquatic counterparts.

Our previous work with the shallow water marine fish, *Rhinecanthus aculeatus*, indicates that teleost fish, much like terrestrial animals such as honeybees [1–3], desert ants [4], spiders [6], and humans [5, 15], are able to use optic flow information from the benthic visual background for odometry ([16], in review). However, the underlying mechanism differs from that used by terrestrial animals. Humans and honeybees estimate distances as the total optic flow experienced across the retina during a journey, using a mechanism that is dependent on moving speed and distance from the visual background, but largely independent of the density, or spatial frequency, of that visual background [2, 3, 5, 15, 17].

In contrast, we have shown that although *Rhinecanthus* also relies on optic flow information to estimate distance travelled, the mechanism used strongly depends on the spatial frequency of the visual background.

Except for the honeybee, that appears to rely solely on information from self-induced optic flow for odometry, many terrestrial animals use multiple sources of sensory information depending on the information available to them. Humans, for example, can use optic flow to estimate distance travelled, but in complete darkness or in environments otherwise lacking visual information they show no impairment in distance estimation ability. In such environments, humans can instead use idiothetic information from stride integration to estimate path length [11, 18].

For teleost fish, visual information provides just one potential source of sensory information which they can use for navigation. Teleost fish may be able to estimate distance travelled either with respect to the benthic background, such as using visual motion cues, or with respect to the water column itself, such as using information from the water flows encountered during a journey.

Water flow cues could be measured as a function of the energy expended during a journey, although a distance mechanism relying on measuring energy use has limited support in both flying and walking terrestrial animals. Bees and desert ants show no difference in distance estimation abilities when laden with weights [19], or when moving against gravity or increased wind load [1, 3, 20, 21]. Some evidence in humans suggests that subjects encumbered with heavy weights perceived themselves to have travelled further than those free from extra weights [12], although there have been difficulties reproducing this result [22].

However, unlike terrestrial animals, teleost fish have a dedicated sensory system to detect hydrodynamic stimuli - the lateral line system. The lateral line system detects movements and pressure gradients in the water column, using functional mechanoreceptor units called neuromasts organised along the length of the fish and clustered around the head [23, 24]. Hydrodynamic inputs to the lateral line are already known to control

an array of teleost behaviours such as schooling [25], predation [26], and landmark-based navigation [27]. The lateral line system could also be co-opted to measure travel distances as a function of the mechanical inputs to the neuromasts from water flows.

In this chapter, we design a flume system to test the use of hydrodynamic inputs from water flows to measure travel distances in teleost fish. Using the marine fish, *Rhinecanthus aculeatus*, we seek to quantify the relative importance of hydrodynamic cues from the fluid frame of reference and visual motion cues from the benthic visual frame of reference to estimate travel distances. *Rhinecanthus* is a highly visually-reliant shallow water intertidal marine fish, that we have previously shown to use visual motion information for odometry. Its natural intertidal environment is also subject to high water flows, which may provide additional information on distance travelled. Here, we present pilot results from one individual providing preliminary indications that while visual information is the primary source of sensory inputs used by *Rhinecanthus* to measure distance travelled, hydrodynamic cues from water flows may offer a secondary level of distance information, particularly under circumstances where visual information is absent.

2 Methods

2.1 Subjects

The test subject was one adult wild-caught Picasso triggerfish, *Rhinecanthus aculeatus*, of standard length 14cm, sourced from coral reefs in the Maldives through a local supplier. A total of six test subjects started behavioural training and testing following *a-priori* power analysis, all of standard length 10-14cm, but were unable to complete training owing to an infectious disease outbreak in the population causing extensive morbidity and mortality (see Appendix D for details). Subjects were housed individually, as in previous experiments, in tanks measuring 0.45m width x 0.35m height x 0.75m length with tank enrichment including coral gravel and sand as a substrate, and rocks and caves for refuges. A 12h/12h automated day/night flourescent light cycle was maintained throughout. A diet of formulated marine pellets (Ocean Nutrition Formula One Marine Pellet) were provided as food rewards during training. Lance fish, krill, and whole cockles (Gamma) were fed as a supplement at the end of each training day. The experiment tank and home tanks were cleaned and water quality tested twice weekly to keep ammonia and nitrite at 0ppm and nitrates below 15ppm. Salinity was kept constant at 35ppt using reverse osmosis water with added aquarium salts (Tropic Marine Centre Classic Sea Salt).

2.2 Experiment set-up

A flume was constructed to create variable flow through a main experiment arena (fig. 1, and Appendix D fig. 1-3). The experiment arena consisted of a 1.5m long channel of width 0.16m and height 0.25m with changeable walls and floor, with inlet pipes at the distal end (fig. 1 - region A) from two pumps located in a lower sump tank.

Water was pumped from the home aquarium system into the upper tank containing the experiment arena, and this was allowed to passively flow into the sump tank beneath, which was in turn passively connected to the home aquarium system (fig. 1 - region C). This created a continuous flow of water between the experiment flume and the home

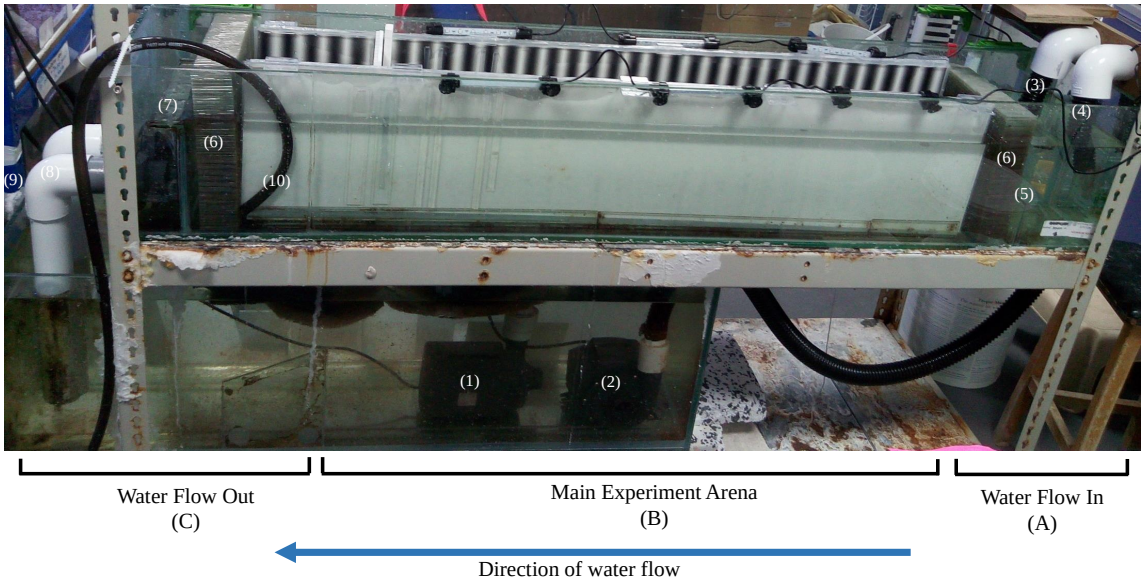


Figure 1: Flume system constructed to assess the use of water flow for distance estimation. Two pumps are located in a lower sump tank beneath the main experiment tank: (1) and (2), each capable of moving 150l/minute into the distal end of the main experiment arena via two inlet pipes: (3) and (4). A glass weir at either end of the main experiment tank: (5) and (7) maintain a minimum water depth even in the absence of water flow. Flow straighteners: (6) ensure constant laminar flow through the main experiment arena, whilst also acting as screens from any looming stimuli from each end of the tank. Two large outlet pipes: (8) ensure a closed system of water flow into the flume system sump, and an additional outlet pipe from the flume sump to the home aquarium system sump: (9) creates a closed system of water flow with the home aquariums. Water is in turn pumped from the home aquarium system sump back into the flume system via an eheim pump moving 15l/minute into the experiment tank: (10).

aquarium system, to ensure water parameters (most importantly salinity and temperature) were kept constant.

Flow through the main experiment arena could be adjusted by switching on and off two pumps located in the flume system sump - (1) and (2) in fig. 1, feeding into the experiment channel via two inlet pipes at the distal end (fig. 1 - region A). Each pump displaced 150l per minute from the sump into the experiment system channel. Weirs at either end of the experiment channel ensured that the water depth was maintained at a minimum level, and flow straighteners were placed at either end to ensure consistent laminar flow throughout the tunnel. The walls and floor of the experiment channel were interchange-

able between two patterns: (i) black and white pattern spatial contrast changing according to a sinusoidal function oriented perpendicular to the direction of movement, or (ii) a plain grey background with no spatial contrast.

A moveable start area of dimensions 0.25m high x 0.16m wide x 0.30m long could be placed in one of three start area positions spaced 0.1m apart at the proximal end in region C. An infrared detector (SHARP 2Y0A21 proximity sensor) was then placed at water level overhead, 0.60m from the start area doorway (Appendix D, fig. 2). This was attached to an Arduino microprocessor, which through a Matlab (Mathworks Inc.) program controlled aquarium lights (Interpret Triple LED Lighting System, 0.75m) running along the top of the lateral maze walls. The voltage of the infrared (IR) detector varied between 0V and 3.5V depending on the strength of the reflection from objects which passed in front of it. We tested the response of the detector to objects in water and after this we set a threshold of 1.7V. As the fish passed beneath the detector, a voltage change was registered and when this exceeded 1.7V, the aquarium lights switched on. A Point Grey Grasshopper 3M camera (FLIR Machine Vision Cameras) was placed 1.1m above the water level to record testing trials.

2.3 Training

Fish were trained according to the training protocol developed in previous chapters of this thesis. However, the trained distance was shortened to 0.60m owing to the shorter available experiment arena (1.5m) as a result of inlet and outlet systems of the flume.

Training sessions were always conducted at a medium level of flow, with the experiment channel supplied by water flow from Pump 1, moving 150l of water per minute through the channel. The walls and floor were patterned with black and white spatial contrast changing according to a sinusoidal function oriented perpendicular to the direction of movement (fig. 2, test 1). Fish were trained to swim 0.60m to the overhead infrared detector against the direction of flow. Upon passing beneath the infrared detector, the aquarium lights switched on and signalled the need to return to the start area for a food

reward. Fish were initially presented with a food reward in the start area at the same time as the light flash. As performance improved, food was presented increasingly late during the return journey until a reward was only provided once the fish had fully returned to the start area.

Training sessions lasted 10 minutes, or until 10 correct trials were complete, whichever came first. A correct trial was considered a straight trajectory from the start area to turn on the light followed by a straight trajectory back to the start area with no additional turns or pauses in the tunnel. To control for use of external landmarks, each session the start area was moved randomly between the three possible positions, located increasingly distally through the tank by 0.10m increments (here-on referred to as +0, +10 and +20). The infrared detector was moved accordingly to maintain the correct distance of 0.60m. Training was considered complete when the fish swam directly out to the light flash and back on 80 percent of trials within the 10-minute session time limit, across three consecutive sessions.

Only one out of the 6 fish completed training to progress onto the testing phase. The remaining fish were removed from the experiment in various stages of training due to a novel parasite emerging in the population, causing severe morbidity and eventual mortality (see Appendix D for details).

2.4 Testing

Testing sessions consisted of a 5 training + 5 testing trial structure to ensure fish were at testing criterion (80% performance) prior to each set of testing trials. Within a testing session block, fish were placed in the experiment start area in one of the three possible start area positions and completed five training trials prior to being returned to the home tank. The 5 training trials were conducted with the visual background provided during training accompanied by a medium level of flow (150l/minute), supplied by pump 1. Fish were rewarded if they swam out directly to the infrared detector to turn on the light and returned home with no additional turns in the tunnel. If performance dropped below 80%

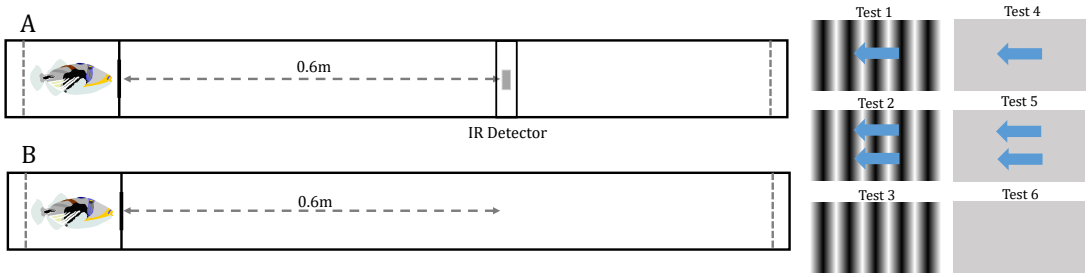


Figure 2: Testing for an interaction between visual flow and water for fish odometry: training and testing set-up. (A) Training - the fish was trained to swim 0.6m to an overhead infra-red proximity sensor (IR Detector) which when the fish passed beneath it, detected a voltage change and via the Arduino computer caused the aquarium lights to switch on, signalling to the fish to return to the start area for a food reward. Training was conducted with a visual background with a sinusoidal change from black to white and a medium level of flow supplied by a single pump. The distance between black and white was 0.02m. (B) Testing - during testing trials, the infra-red proximity sensor was removed. This was to test whether the fish had learned the correct distance, or to swim to the infrared detector landmark to encounter the light stimulus. The fish was tested with six different visual and water flow combinations: (1) 0.02m sinusoidal stripes, medium flow; (2) 0.02m sinusoidal stripes, high flow (2 pumps); (3) 0.02m sinusoidal stripes, no flow (both pumps turned off); (4) Grey visual background, medium flow; (5) Grey visual background, high flow; (6) Grey visual background, no flow.

in this training block, fish were returned to training until they achieved testing criterion once more. The experiment set-up was subsequently manipulated for the required test condition before the fish was returned to the start area (which had been moved to a new position), and completed five testing trials with the infrared detector removed and the aquarium lights disabled. 15 trials split across three separate sessions were completed at each start area position for all six treatments, producing 45 estimates per treatment.

Testing conditions were as follows, fig. 2 : Test 1 (training condition) - medium water flow (pump 1 - 150l/minute) + black and white pattern spatial contrast changing according to a sinusoidal function oriented perpendicular to the direction of movement; Test 2 (high water flow, optic flow present) - high water flow (pump 1 and 2 - 300l/minute) + black and white pattern spatial contrast changing according to a sinusoidal function oriented perpendicular to the direction of movement; Test 3 (no water flow, optic flow

present) - no water flow + black and white pattern spatial contrast changing according to a sinusoidal function oriented perpendicular to the direction of movement; Test 4 (medium water flow, no optic flow) - medium water flow (pump 1 - 150l/minute) + grey background with no spatial contrast; Test 5 (high water flow, no optic flow) - high water flow (pump 1 and 2 - 300l/minute) + grey background with no spatial contrast; Test 6 (no water flow, no optic flow) - no water flow + grey background with no spatial contrast. A sinusoidal change in colour was used in the optic flow condition to provide a more continuous and gradual change in translational spatial contrast compared to previous experiments. The purpose of these test treatments was to primarily explore the role of measuring water flow for odometry, but also its relative importance to use of visual information. We predicted that if water flow and visual flow information were both used for odometry, then *Rhinecanthus* would underestimate travel distances when water flow was increased in treatments 2 and 5, and would show a greater error in distance estimates or overestimate travel distance when water flow was removed in treatments 3 and 6, even in the presence of visual information. However, if *Rhinecanthus aculeatus* preferentially relies on visual information for odometry and water flow is used as secondary source of distance information, the effects of increasing and removing water flow may only become apparent when visual information is also removed in treatments 4-6. This would be evidence of *Rhinecanthus* having a hierarchy of sensory information for odometry.

2.5 Statistical analysis

For a full sample size, mixed effects models would have been constructed to assess the fixed effects of start area position and treatment, and the random effect of fish identity on the following measures: (i) Distance estimates; (ii) Absolute distance estimate error; (iii) Absolute distance estimate residuals, to assess the direction of distance estimate change under varying levels of water and optic flow, as well as the accuracy and precision of distance estimates.

Only one fish (Fish ID: Fish B) completed training and all testing sessions out of a

possible sample size of 6. However, to gain an early indication of the effect of various treatments on distance estimates produced to inform future refinements and hypotheses, models were constructed as intended using the 45 replicated distance estimates for each treatment, with the caveat that these constituted pseudoreplicates from the same individual. The following models were constructed: (i) Distance estimate = Start Area Position + Treatment; (ii) Absolute distance estimate error = Treatment; (iii) Distance estimate residuals = Treatment. In the model on distance estimates, start area position was included as an effect to ascertain that start area position had no effect on distance estimates produced, and that external cues were not used. To probe this further for individual treatments, an additional model was constructed: Absolute turning position = Start Area Position + Treatment + Start Area Position*Treatment (interaction) to assess whether there was a predictable shift in absolute turning position in the tunnel according to start area position across treatments, as would be expected if fish were estimating distance travelled and not using external cues or turning randomly in the tunnel.

3 Results

3.1 The effect of visual and water flow treatment on distance estimates

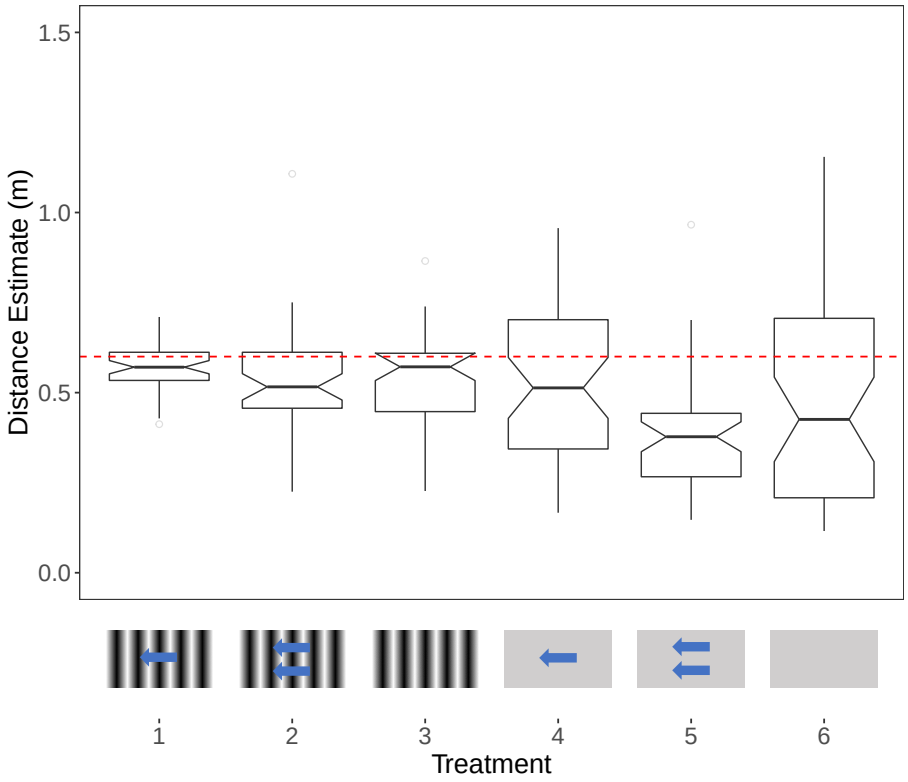


Figure 3: Distance estimates across visual and water flow treatments for Fish B only (45 distance estimates per treatment). The red horizontal dashed line indicates the target distance of 0.60m. All treatments produced distance estimates with bootstrapped 95% confidence intervals below the target distance. Only treatment 5 produced distance estimates significantly different from the baseline training treatment (treatment 1).

Figure 3 shows the distance estimates produced by Fish B across the six different visual and water flow treatments. The bootstrap means and 95% confidence intervals (with 1000 re-samples) indicate that all treatments produced average distance estimates that are significant underestimates of the target distance of 0.60m (table 1).

The model of start area position and test treatment on distance estimates revealed that treatment did have a significant effect on distance estimates produced ($F_{5,262}$ = 5.67, $p<0.001$). Subsequent pairwise comparisons using the tukey method for p-value adjust-

Treatment	Bootstrap mean distance estimate (m)	Lower 95% Confidence Interval (m)	Upper 95% Confidence Interval (m)
1	0.569	0.549	0.587
2	0.532	0.483	0.578
3	0.538	0.503	0.574
4	0.523	0.459	0.595
5	0.382	0.341	0.440
6	0.484	0.411	0.565

Table 1: Bootstrap distance estimate means and confidence intervals for Fish B across visual and water flow treatments. Bootstrap values were calculated with 1000 re-samples.

ments indicated that only treatment 5 produced a mean distance estimate significantly different from treatment 1, the baseline training condition (tukey pairwise comparisons, Treatment 1: Treatment 2 95% CI_{diff} = -0.149m - 0.0734m, p = 0.924; Treatment 1: Treatment 3 95% CI_{diff} = -0.143m - 0.0801m, p = 0.966; Treatment 1: Treatment 4 95% CI_{diff} = -0.156m - 0.0665m, p = 0.856; Treatment 1: Treatment 5 95% CI_{diff} = -0.297m - -0.0739m, $p < 0.001$; Treatment 1: Treatment 6 95% CI_{diff} = -0.197m - 0.0263m, p = 0.244). However, trends in fig. 3 and table 1 indicate that there is some underestimation compared to the baseline in treatment 2, where water flow is increased. Trends of underestimation were also observed in all of treatments where optic flow information was removed (treatment 4, 5 and 6), but the effect was most pronounced in treatment 5 where water flow was also increased. Replication with a full experimental sample size is necessary to fully test and quantify these trends.

To ascertain that fish were measuring distance travelled and not turning at an approximate position in the tunnel, start area position was included in the main model. Start area position did not have a significant effect on distance estimates produced, implying that fish are indeed estimating travel distances ($F_{2,262} = 1.42$, p = 0.243). To investigate this further, a model for the effect of start area position, test treatment, and the interaction of those two parameters was constructed for the absolute turning position in the tunnel. If

Treatment	Pairwise Comparison	Difference Lower 95% Confidence Interval	Difference Upper 95% Confidence Interval	t-statistic	p-value
1	**+ 0 : +10**	**-0.117**	**-0.0228**	**-3.11**	**0.00580**
1	**+10 : +20**	**-0.160**	**-0.0515**	**-4.01**	**<0.001**
1	**+ 0 : +20**	**-0.214**	**-0.137**	**-9.53**	**<0.001**
2	+ 0 : +10	-0.151	0.0962	-0.456	0.652
2	**+10 : +20**	**-0.255**	**-0.0612**	**-3.35**	**0.00247**
2	**+ 0 : +20**	**-0.299**	**-0.0721**	**-3.38**	**0.00256**
3	+ 0 : +10	-0.129	0.0349	-1.18	0.249
3	+10 : +20	-0.0983	0.0589	-0.516	0.611
3	+ 0 : +20	-0.159	0.0252	-1.49	0.148
4	**+ 0 : +10**	**-0.432**	**-0.104**	**-3.35**	**0.00240**
4	**+10 : +20**	**-0.322**	**0.0151**	**-1.87**	**0.00728**
4	**+ 0 : +20**	**-0.570**	**-0.272**	**-5.79**	**<0.001**
5	+ 0 : +10	-0.196	0.0654	-1.03	0.313
5	**+10 : +20**	**-0.236**	**-0.0109**	**-2.25**	**0.0326**
5	**+ 0 : +20**	**-0.326**	**-0.0509**	**-2.81**	**0.00912**
6	+ 0 : +10	-0.120	0.314	0.918	0.367
6	+10 : +20	-0.196	0.159	-0.212	0.834
6	+ 0 : +20	-0.120	0.278	0.816	0.422

Table 2: Pairwise comparisons between the absolute turning position in the tunnel across start area positions within each treatment. p-values were adjusted using the Bonferroni correction for 18 pairwise comparissons. Significant differences are highlighted in bold. All values are given to 3 significant figures.

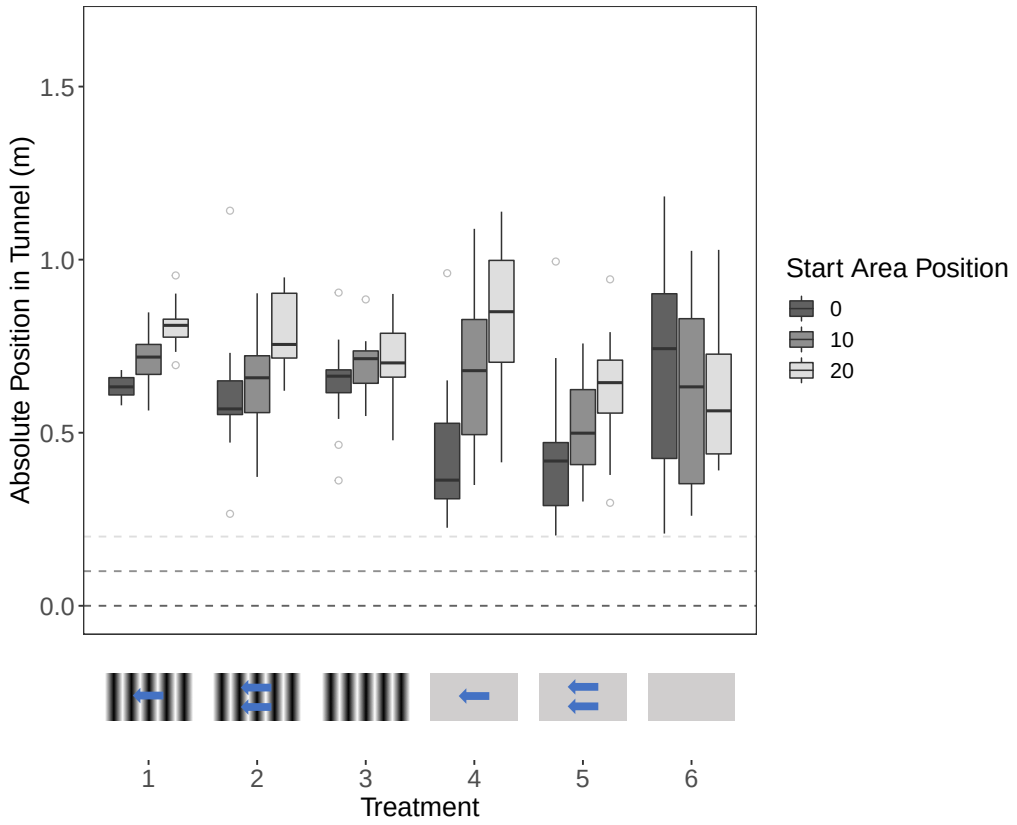


Figure 4: Absolute turning position in the tank across start area positions for each visual and water flow treatement. Horizontal dashed lines indicate shifts in start area position (dark grey = +0, mid grey = +10, light greay = +20), and box plots of absolute turning position are colour coded by corresponding start area position. The fish produced 15 distance estimates per start area position, split across 3 sessions.

the fish is estimating distance travelled and not generalising across start area positions or using external absolute position cues, then there should be a sequential shift in turning position according to the start area position from +0 to +10 to +20. All three parameters in the model had significant effects on the absolute turning position (Start Area Position: $F_{2,252} = 19.1$, $p<0.001$; Treatment: $F_{5,252} = 6.84$, $p<0.001$; Start Area Position*Treatment: $F_{10,252} = 3.68$, $p<0.001$).

Absolute turning positions according to start area position can be seen in fig. 4, indicating that trends of the expected sequential shift can be observed in all treatments except for treatment 6 where both water flow and optic flow were removed.

Testing of specific pairwise comparisons of turning position according to start area position were subsequently performed within each treatment to explore these trends further, using the Bonferroni p-value correction for multiple comparisons (see table 2 - significant differences between start area positions are indicated in bold). Significant pairwise shifts in absolute turning positions across all three start area positions are seen for treatment 1 and treatment 4, both of which have the training level of water flow of 150l/minute, but all optic flow and spatial contrast information is removed in treatment 4. Treatments where water flow is increased show pairwise shifts in some comparisons but not others, but the expected trends are maintained, indicating fish are still able to estimate perceived distance under these treatments. Overall, this implies that the fish is able to extract some distance information from hydrodynamic cues, in both the presence and absence of visual information. This hypothesis is further supported by the loss of systematic pairwise shifts in treatment 6 where both water flow and optic flow are removed - there is no significant pairwise difference in absolute turning position across start area positions, and the expected trend cannot be seen in fig. 4.

3.2 The effect of visual and water flow treatment on the magnitude of distance estimate error

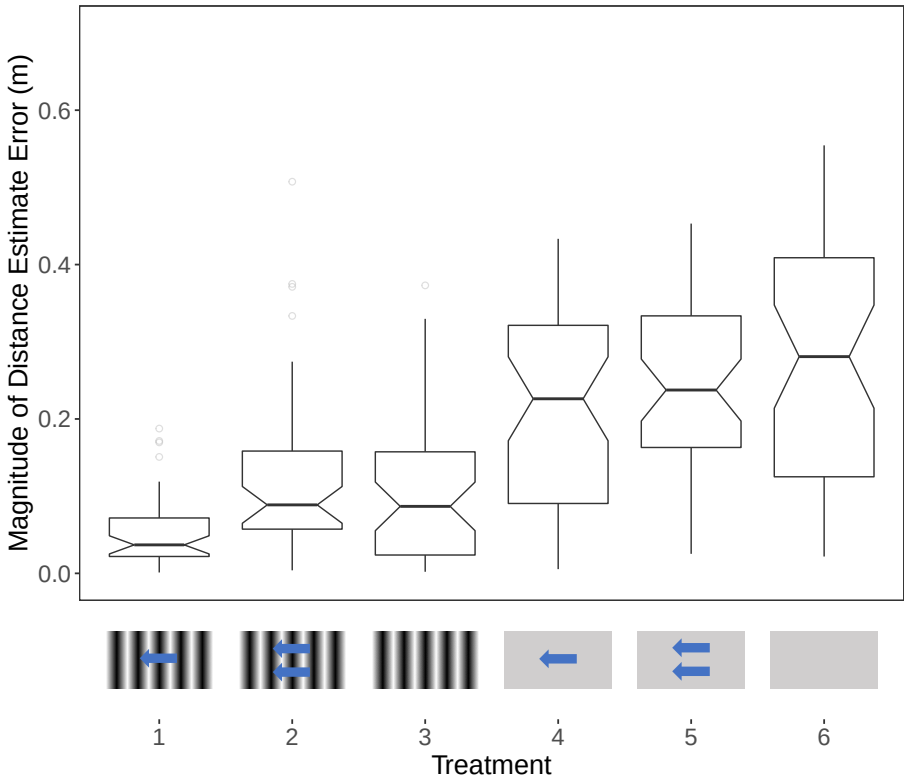


Figure 5: Absolute distance estimate error from the target distance of 0.60m across visual and water flow treatments. The model of water and visual treatment on distance estimate error was significant, with distance estimate error increasing significantly for treatments 2, 4, 5 and 6 when compared to the training condition (treatment 1).

To further explore the effect of visual and water flow treatment on distance estimates, we compared the effect of visual and water flow treatment on the magnitude of distance estimate error. The absolute value of the difference between the distance estimate produced and the target distance of 0.60m was calculated for each distance estimate across the six treatments (fig. 5), and the model of visual and water flow treatment on this distance estimate error was significant ($F_{5,262} = 25.7$, $p<0.001$).

Compared to the training condition with optic flow present and a medium level of water flow (treatment 1), increasing water flow but keeping optic flow conditions the same

(treatment 2) led to an increase in distance estimate error (tukey pairwise comparison, Treatment 1: Treatment 2 95% CI_{diff} = 0.00370m - 0.139m, p = 0.0321), but removing water flow entirely had no effect on distance estimate error if optic flow information was provided (tukey pairwise comparison, Treatment 1: Treatment 3 95% CI_{diff} = -0.0182m - 0.118m, p = 0.289).

In contrast, when optic flow information was removed, distance estimate error increased under all flow conditions compared to the baseline training condition (Treatment 1: Treatment 4 95% CI_{diff} = 0.0847m - 0.220m, $p<0.001$; Treatment 1: Treatment 5 95% CI_{diff} = 0.120m - 0.256m, $p<0.001$; Treatment 1: Treatment 6 95% CI_{diff} = 0.146m - 0.282m, $p<0.001$). Distance estimate error also increased between equivalent water flow treatments when optic flow was removed (Treatment 2: Treatment 5 95% CI_{diff} = 0.0489m - 0.185m, $p<0.001$; Treatment 3: Treatment 6 95% CI_{diff} = 0.0.0962m - 0.232m, $p<0.001$). There was no difference in absolute distance estimate error between treatments of variable water flow when optic flow was removed (Treatment 4: Treatment 5 95% CI_{diff} = -0.0321m - 0.207m, p = 0.656; Treatment 4: Treatment 6 95% CI_{diff} = -0.00666m - 0.129m, p = 0.103; Treatment 5: Treatment 6 95% CI_{diff} = -0.0424m - 0.0933m, p = 0.891).

This suggests that the availability of translational optic flow has a larger effect on the ability to reproduce previously learned distances than the magnitude, or presence or absence of water flow information. However, there is some evidence to suggest that the strength of water flow does have a small effect on the accuracy of distance estimates even when optic flow information is present.

3.3 The effect of visual and water flow treatment on the variability of distance estimates

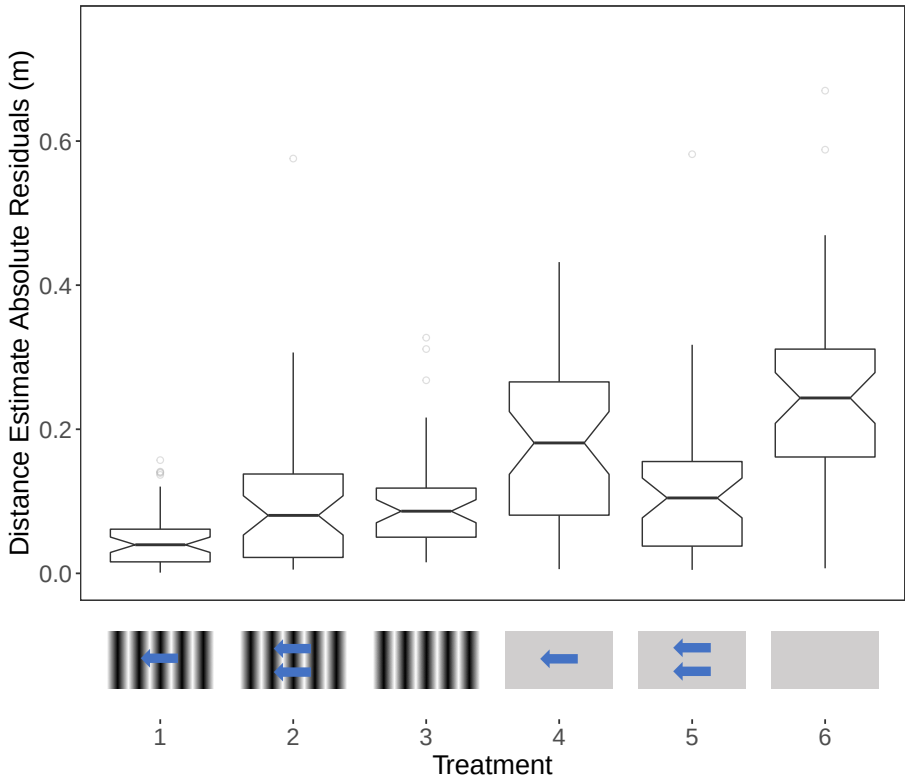


Figure 6: Absolute residuals of distance estimates from the treatment mean across visual and water flow treatments. The model of visual and water flow treatment on distance estimate residuals was significant, with an increase in absolute residuals when visual information was removed. A significant secondary effect of water flow treatment is only observed when visual information is also removed in treatments 4, 5 and 6.

Finally, to assess the variability in distance estimates produced, reflecting the precision of distance estimation, the residuals of individual distance estimates were taken from the treatment mean across all treatments. Visual and water flow treatment was found to have a significant effect on distance estimate residuals ($F_{5,264}$ = 21.7, $p<0.001$). Distance estimate residuals only showed a small, non-significant increase under variable water flows when optic flow was present (Treatment 1: Treatment 2 95% CI_{diff} = -0.00575m - 0.120m, p = 0.0987; Treatment 1: Treatment 3 95% CI_{diff} = -0.0106m - 0.115m, p = 0.164). In

contrast, when optic flow information was removed, distance estimate residuals increased for all levels of water flow compared to the baseline (Treatment 1: Treatment 4 95% CI_{diff} = 0.0773m - 0.203m, $p<0.001$; Treatment 1: Treatment 5 95% CI_{diff} = 0.00602m - 0.132m, p = 0.0225; Treatment 1: Treatment 6 95% CI_{diff} = 0.139m - 0.266m, $p<0.001$). Interestingly, for treatments where optic flow information was removed, distance estimate residuals increased in accordance with the strength of water flow. Residuals were highest when no flow was present, and lowest in the condition with the highest flow (Treatment 4: Treatment 5 95% CI_{diff} = -0.134m - -0.00826m, p = 0.0.0164; Treatment 4: Treatment 6 95% CI_{diff} = -0.000757m - 0.125m, p = 0.0493; Treatment 5: Treatment 6 95% CI_{diff} = 0.0705m - 0.196m, $p <0.001$).

This provides further evidence that while the availability of visual information has the greatest effect on distance estimation abilities, there may be a secondary effect from altering water flow information, which is further inflated when visual information is also removed.

Taken together, although our results remain preliminary (being the trends observed from just one individual), they provide the first indication that *Rhinecanthus* is able to estimate distance travelled, albeit with reduced accuracy and precision, when visual information is removed if hydrodynamic cues from water flows remain available. Moreover, they indicate that the effects of altered water flows are larger in the absence of visual information, suggesting that *Rhinecanthus* has a hierarchy of sensory information use for odometry. Replication with a full sample size will be required to robustly test these hypotheses.

4 Discussion and Future Directions

Teleost fish have the potential to use sensory information from two frames of reference to estimate distance travelled: the fixed benthic background, and the water column through which they swim. Using the marine fish, *Rhinecanthus aculeatus*, we examined the relative importance of two forms of sensory information from these different frames of reference: visual motion information and water flow. Although further testing with a full sample size is required to form robust conclusions, pilot results from one individual indicate that *Rhinecanthus* relies primarily on visual motion information from the fixed benthic background to estimate distance travelled. Manipulations to water flow information had only small effects on odometry when visual information was present. However, when visual information was removed, the effects of altering water flows became more pronounced, indicating that *Rhinecanthus* may display hierarchical use of different sensory inputs depending on the information available from the benthic and fluid backgrounds.

We designed a flume system that allowed us to adjust water flow through a main experiment tunnel. The experiment tunnel itself had changeable walls to manipulate the visual background by providing or removing translational optic flow. Six fish were trained using the distance estimation task developed in previous chapters of this thesis, and were provided with full optic flow information on both the ventral and lateral surfaces and a water flow of 150l per minute. The fish were trained to swim to a target distance of 0.60m to an overhead infrared detector controlling surrounding aquarium lights. During testing, the overhead infrared detector was removed, and fish were assessed in their ability to reproduce the learned distance in the absence of the light cue following a series of manipulations to visual and water flow.

Owing to an infectious disease outbreak in the population, only one fish (Fish B) completed all training and testing stages (Appendix D, section 2). Fish B was able to reproduce the learned distance with a high level of accuracy and precision under the training conditions of water and visual flow. *Rhinecanthus* is therefore able to manoeuvre precisely even

under considerable levels of water flow to reproduce learned distances.

When optic flow information was removed, the distance estimate error and the variability in distance estimates produced increased considerably. This is in accordance with our previous experiment in Chapter 3 indicating that *Rhinecanthus*, like many aerial and surface-constrained animals [3, 4, 15], strongly relies on access to visual motion information for odometry [16].

In contrast to the effect of altering the visual background, doubling the water flow experienced or removing it entirely when optic flow information was present had only small effects on odometry. There was only a small and non-significant decrease in distance estimates, and increase in distance estimate variability when water flow was increased. However, the absolute error in distance estimates from the target did significantly increase when compared to the training condition, indicating a reduction in accuracy following a water flow manipulation. Although further testing is required to quantify and fully test these small effect sizes, *Rhinecanthus* therefore appears to preferentially rely on visual information for estimating distance travelled.

In the absence of translational optic flow information, however, *Rhinecanthus* does appear to rely more strongly on sensory inputs from water flow information. When visual contrast information was removed and water flow was doubled, the average distance estimate significantly decreased, as would be predicted if the strength of water flow was used as a measure of distance travelled. Further evidence for the use of water flows to obtain distance information was seen in the analysis of absolute turning positions in the tunnel. During both training and testing, the start area was moved between three increasingly distal locations within the tunnel. A signal of distance estimation rather than random turns in the tunnel or use of external landmark cues would be reflected in a sequential shift in absolute turning position in the tunnel according to start area position. In our previous study exploring the use of optic flow for distance estimation, this sequential shift was lost when optic flow information was removed, indicating an inability to estimate distance in the absence of translational optic flow (see Chapter 3). However, results from

Fish B indicate that this pairwise shift is maintained even in the absence of optic flow in treatments where water flow is at, or increased beyond, the training level. The pairwise shift is only lost when both visual and water flow information are removed.

Therefore, although visual information is required for accurate distance information, in the absence of visual information *Rhinecanthus* seems to be able to use sensory inputs from water flow to gain an indication of distance travelled. That *Rhinecanthus* appears to rely more strongly on sensory inputs from water flow information when visual contrast information is removed entirely, suggests that there is also a hierarchy of preferred sensory information for estimating travel distances. In their intertidal habitat, water flows will be spatially and temporarily variable in strength and structure. Preferentially using information from the fixed visual background is therefore likely to be more reliable than using information from a variably moving background. However, when navigating through areas of increased turbidity, lower light levels, or at a greater distance from visual backgrounds, having access to a secondary source of sensory information would allow the fish to continue to estimate relative travel distances.

This result presents another key difference from previously tested aerial animals, such as the honeybee, that also navigate through a dynamic fluid. Honeybees measure distance travelled as the total visual motion experienced throughout a journey [2, 3], and do so entirely independently of wind load [3, 20, 21]. This may be a reflection of the differences in visual ecology between an aquatic and aerial environment, and specific physiological differences between teleosts and honeybees. Underwater, freely-swimming animals move without direct physical contact with the benthic backgorund, and visual information may be less reliable owing to the rapid attenuation of light with depth and distance. The ability to flexibly rely on sensory information from two alternative frames of reference according to the richness and reliability of information in each will therefore be advantageous. Unlike many flying animals, teleost fish also have a dedicated sensory system - the lateral line - to measure water flows, which is already known to be used for other spatial tasks such as finding prey [26], schooling [25] and landmark based navigation [27]. This system

could, in theory, be co-opted to also measure travel distances.

Our preliminary results from one fish can now be used to inform future refinements to sample size based on measured effect sizes, and also expand the scope of the experiment to explore underlying mechanisms. Our results indicate the potential of a small effect of altering water flows on odometry even under conditions where optic flow is present. A larger sample size will therefore be required in future experiments to gain adequate power in detecting this small effect size. When measuring water flow, *Rhinecanthus* could be summating hydrodynamic inputs to its lateral line as mentioned above, or the energy expended during its journey. In order to study the mechanism underlying the use of water flow for odometry, future studies could compare populations of *Rhinecanthus* with the lateral line either experimentally ablated or intact. If hydrodynamic inputs to the lateral line are used to learn and remember travel distances, individuals with an ablated lateral line should display no shifts in distance estimates if water flows are manipulated, and should be unable to discriminate distances in the absence of optic flow information.

Work with additional teleost fish species occupying a wider range of ecologies can also be used to test the hypothesis that the relative reliance on visual vs hydrodynamic inputs varies with eco-evolutionary history and the accompanying physiological differences in the visual and lateral line system. For example, while highly visual coral reef fish (such as *Rhinecanthus aculeatus*) may strongly rely on visual information for odometry, less visual species or those without vision at all, but with a highly developed lateral line (such as many cavefish) may instead preferentially use hydrodynamic cues for odometry.

References

[1] Esch H. E. and Burns J. E. Honeybees use optic flow to measure the distance of a food source. *Nature*, 82(1):38–40, 1995.

[2] Esch H.E., Zhang S., Srinivasan M.V., and Tautz J. Honeybee dances communicate distances measured by optic flow. *Nature*, 411(6837):581–3, 2001.

[3] Srinivasan M., Zhang S., and Bidwell N. Visually mediated odometry in honeybees. *Journal of Experimental Biology*, 200(19):2513–2522, 1997.

[4] Ronacher B. and Wehner R. Desert ants Cataglyphis fortis use self-induced optic flow to measure distances travelled. *Journal of Comparative Physiology A*, 177(1):21–27, 1995.

[5] Frenz H. and Lappe M. Absolute travel distance from optic flow. *Vision research*, 45 (13):1679–92, 2005.

[6] Ortega-Escobar J. and Ruiz M.A. Visual odometry in the wolf spider Lycosa tarantula (Araneae: Lycosidae). *The Journal of Experimental Biology*, 217(Pt 3):395–401, 2014.

[7] Wittlinger M., Wehner R., and Wolf H. The ant odometer: stepping on stilts and stumps. *Science*, 312(5782):1965–7, 2006.

[8] Wittlinger M., Wehner R., and Wolf H. The desert ant odometer: a stride integrator that accounts for stride length and walking speed. *The Journal of Experimental Biology*, 210(Pt 2):198–207, 2007.

[9] Walls M.L. and Layne J.E. Direct evidence for distance measurement via flexible stride integration in the fiddler crab. *Current biology*, 19(1):25–9, 2009.

[10] Seyfarth E.A., Hergenrider R., Ebbes H., and Barth F.G. Idiothetic orientation of a wandering spider: Compensation of detours and estimates of goal distance. *Behavioral Ecology and Sociobiology*, 11(2):139–148, 1982.

[11] Mittelstaedt M.L. and Mittelstaedt H. Idiothetic navigation in humans: estimation of path length. *Experimental Brain Research*, 139(3):318–332, 2001.

[12] Proffitt D.R., Stefanucci J., Banton T., and Epstein W. The role of effort in perceiving distance. *Psychological Science*, 14(2):106–12, 2003.

[13] Jacob P-Y., Gordillo-Salas M., Facchini J., Poucet B., Save E., and Sargolini F. Medial entorhinal cortex and medial septum contribute to self-motion-based linear distance estimation. *Brain Structure and Function*, 222(6):2727–2742, 2017.

[14] Champ C., Wallis G., Vorobyev M., Siebeck U., and Marshall J. Visual Acuity in a Species of Coral Reef Fish: *Rhinecanthus aculeatus*. *Brain, Behavior and Evolution*, 83(1): 31–42, 2014.

[15] Redlick F.P, Jenkin M.H., and Laurence R. Humans can use optic flow to estimate distance of travel. *Vision Research*, 41(2):213–219, 2001.

[16] Karlsson C. and Burt de Perera T. Visual odometry in a freely-swimming fish. *In Prep (Nature Communications Biology)*, 2020.

[17] Mossio M., Vidal M., and Berthoz A. Traveled distances: new insights into the role of optic flow. *Vision Research*, 48(2):289–303, 2008.

[18] Durgin F.H., Akagi M., Gallistel C.R., and Haiken W. The precision of locomotor odometry in humans. *Experimental Brain Research*, 193(3):429–36, 2009.

[19] Wehner R. *Arthropods*. Springer Netherlands, 1992.

[20] Goller F. and Esch H. E. Waggle dances of honey bees. *Nature*, 77(12):594–595, 1990.

[21] Esch H., Goller F., and Burns J. E. Honeybee waggle dances: the energy hypothesis and thermoregulatory behavior of foragers. *Journal of Comparative Physiology B*, 163 (8):621–625, 1994.

[22] Woods A.J., Philbeck J.W., and Danoff J.V. The various perceptions of distance: an alternative view of how effort affects distance judgments. *Journal of Experimental Psychology*, 35(4):1104–17, 2009.

[23] Bleckmann H. and Zelick R. Lateral line system of fish. *Integrative Zoology*, 4(1):13–25, 2009.

[24] Coomb S. and Van Netten S. The Hydrodynamics and Structural Mechanics of the Lateral Line System. *Fish Physiology*, 23:103–139, 2005.

[25] Mekdara P.J., Schwalbe M.A.B., Coughlin L.L., and Tytell E.D. The effects of lateral line ablation and regeneration in schooling giant danios. *Journal of Experimental Biology*, 221(8):1–12, 2018.

[26] Jiang Y., Fu J., Zhang D., and Zhao Y. Investigation on the Lateral Line Systems of Two Cavefish: Sinocyclocheilus Macrophthalmus and S. Microphthalmus (Cypriniformes: Cyprinidae). *Journal of Bionic Engineering*, 13(1):108–114, 2016.

[27] Burt de Perera T. Fish can encode order in their spatial map. *Proceedings. Biological Sciences*, 271(1553):2131–4, 2004.

Chapter 6

Development of methods: designing and testing a behavioural task for studying distance estimation in teleost fish.

Development of methods: designing and testing a behavioural task for studying distance estimation in teleost fish

C. Karlsson, J.K. Willis, and T. Burt de Perera

In this chapter, we present a series of pilot experiments that were instrumental in developing the behavioural task used to test the functional and mechanistic basis of the teleost odometer throughout this thesis.

1 Background

Understanding how teleost fish learn and remember metric spatial information such as distance travelled has important implications for our understanding of the evolution of spatial cognition in the vertebrate clade as a whole, and the mechanisms underlying odometry in freely-swimming aquatic animals more generally. Prior to the work presented throughout this thesis, distance estimation had been studied in a range of terrestrial animals, including mammals such as humans and rats [1, 2], as well as invertebrates such as bees, ants, fiddler crabs, and spiders [3, 4, 5, 6, 7, 8], but never before in a freely-swimming aquatic animal. We designed and tested a series of behavioural tasks in order to develop a suitable paradigm to assess distance estimation in freely-swimming teleost fish for the first time. This final design was subsequently used in Chapter 2, 4 and 5 of this thesis, and provides a powerful tool for testing the sensory and neural mechanisms underlying odometry in teleost fish.

Testing the odometers of human and honeybee test subjects presents a comparatively simple challenge as humans are able to verbally communicate perceived distances [1, 9], and foraging honeybees will communicate flown distances and directions to their hivemates upon return from a foraging location through their waggle dance language [6]. For example, throughout their studies looking at the role of optic flow in distance estimation in honeybees, Srinivasan and colleagues placed a food source at the end of a tunnel connected to the test subjects' hive, and assessed the output of their dance language. Subsequent manipulations to the optic flow background revealed that the duration of the waggle dance was directly proportional to the total amount of visual motion experienced en route to the feeder, and the direction of the waggle relative to the sun communicates the direction of the visual environment that the bee must fly through relative to the hive [10, 11].

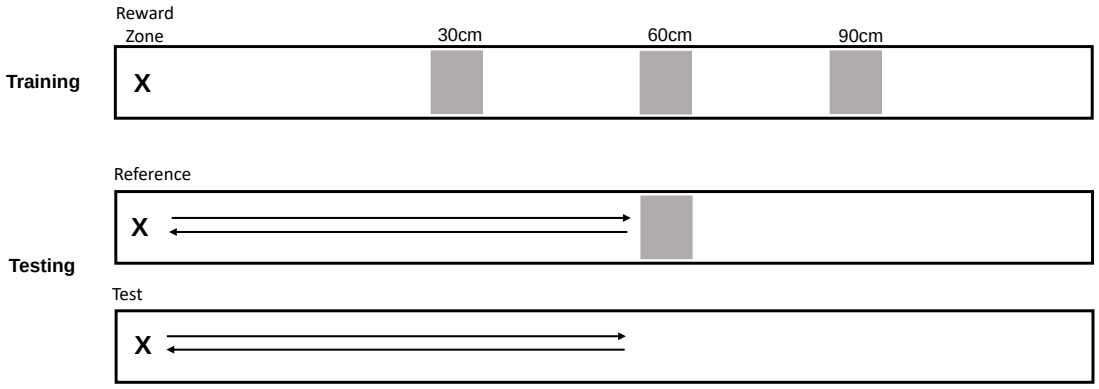


Figure 1: The behavioural task designed to assess linear distance estimation in rats based on self-motion cues. Rats were trained to three separate distances (A), and then during testing were assessed in session pairs (B): In session one they were given one of the three distances as a reference, and during testing the tile was removed and their ability to reproduce the reference distance in the absence of external cues was assessed. Figure from Jacob et al., Brain Struct Funct (2017) 222:2727–2742. DOI 10.1007/s00429-017-1368-4

One way to test the odometers of animals lacking a language that humans can interpret is to develop a 'match-to-sample' behavioural task to assess distance estimation abilities. The subject is trained to a sample distance, and during testing we assess how ac-

curately the animal can match this trained distance. For example, in a study by Jacob and colleagues exploring the neural basis of distance estimation in rats, subjects were trained to run one of three distances to a textured tile and return for a reward, fig. 1A. During testing, this tile was removed to assess their ability to reproduce the reference distance, fig. 1B [2]. Comparing the performance of control rats to those with hippocampal or medial entorhinal cortex (MEC) regions revealed the importance of the MEC and grid cells in linear distance estimation in mammals.

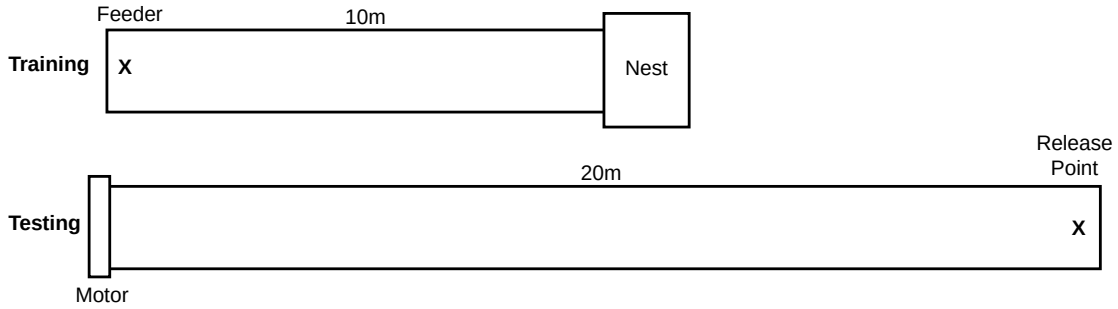


Figure 2: The behavioural task used to assess distance estimation in the desert ant, *Cataglyphis fortis*. During training, the ants were placed in a 10m long Perspex tunnel with their nest located at one end and a feeder providing crushed biscuits at the other. During testing, the ants were translated to a parallel testing tunnel of 20m length and their undisrupted straight line trajectories were analysed. A distance estimate was considered complete when the ant turned through 180°, indicating 'search behaviour'. The ventral optic flow could then be altered using a motorised belt of black and white stripes that could be moved at different speeds and in directions. Figure from Ronacher and Wehner, J Comp Physiol A (1995) 177:21 27. DOI 10.1007/BF00243395

In another variation of a match-to-sample distance task, when testing distance estimation in the desert ant, Ronacher and Wehner placed an ants' nest at one end of a 10m long Perspex tunnel and a feeder at the other end. During training, the ants were allowed to freely move between the feeder and the nest. During testing, the ant was translated from the feeder location to another tunnel of length 20m (fig. 2). The homing distances were then recorded as the points at which the animal turned around by 180°, indicating the start of 'search behaviour'. Subsequent alterations to the visual background showed that desert ants partially rely on optic flow to estimate linear distance travelled [4].

In this chapter, we develop a similar operant conditioning behavioural task to assess the distance estimation abilities of teleost fish. Fish are trained to a position a set distance from a start area using a conditioned stimulus which is then remove to test if incidental learning of travel distance has occured. We present three iterations of experiment design improvement. The first experiment uses the sighted morph of the Mexican cavefish, *Astyanax fasciatus* and for the latter two experiments, we progress to using the reef dwelling Picasso triggerfish, *Rhinecanthus aculeatus*, as our study species, which occupies well-lit intertidal zones of the Indo-Pacific Ocean. The final experiment design formed the basis of the distance estimation tasked used throughout this thesis exploring the sensory basis of distance estimation in *Rhinecanthus aculeatus*.

2 Experiment 1: Odometry in *Astyanax fasciatus*

The sighted Mexican cavefish, *Astyanax fasciatus*, was selected for the first iteration of this experiment. This species is highly motivated for food and shoal rewards during behavioural training, and has been shown in previous experiments to form strong associations between particular spatial locations and food rewards [12, 13, 14]. Work with *Astyanax fasciatus* also provided the first indication that a teleost fish could remember the previous location of a food reward in the absence of previously available landmark cues, suggesting they do have an internal representation of the distance and direction to previously visited locations [13].

2.1 Methods

2.1.1 Subjects

Test subjects were 10 experimentally naïve *Astyanax fasciatus* bred in the laboratory. They were housed in shoals of a maximum of 20 individuals prior to experiments, and individually throughout behavioural training. Individually housed fish were given visual and olfactory access to neighbours. Tanks measured 0.35m (width) x 0.3m (height) x 0.6m (length) and enrichment in the form of caves, tubes and artificial plants was provided. The tanks were cleaned and water quality tested weekly. kH was kept at 10 using reverse osmosis water with added minerals (Tropic Marin Re-mineraliser), measured using an API test kit. Nitrates were kept below 15ppm, and ammonia and nitrites were kept at 0ppm. Fish were fed Gamma mini bloodworms during experiments, and supplemented with TetraMin flake at the end of each training day. An automated 12h/12h day/night light cycle was maintained throughout.

2.1.2 Experimental Set-up

A linear Perspex maze measuring 1.5m (length) x 0.15m (height) x 0.14m (width) was constructed in a glass tank. The walls and floor were patterned with 0.02m-wide alternating

black and white vertical stripes to provide optic flow information, as many animals are unable to estimate travel distances in visually impoverished environments [11, 4, 5]. A white screen was placed at either end to prevent access to external visual cues. A movable start area of dimensions 0.15m x 0.14m x 0.15m was placed at one end of the tank, and a clear Perspex barrier was positioned 0.6m from the start area doorway, with a 0.2m holding area for a shoal reward behind it (fig. 3A). The start area and position of the clear barrier and holding area could be moved distally within the tunnel between training and testing sessions to prevent fish from using fixed external reference cues (fig. 4).

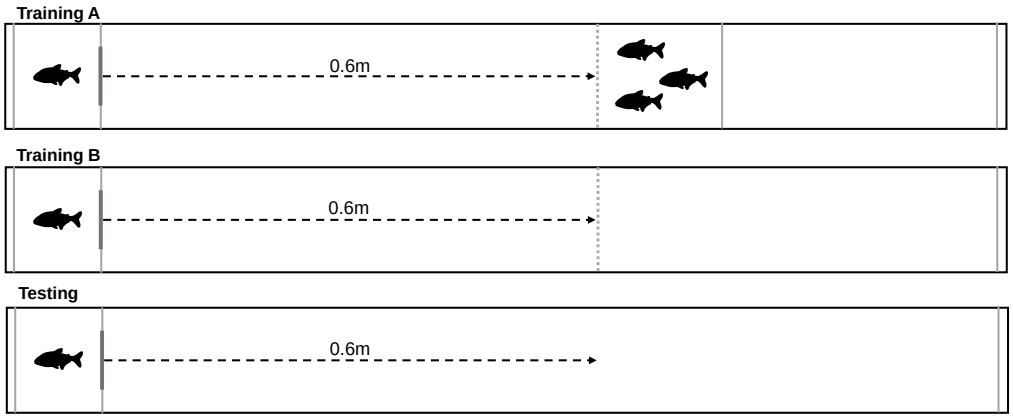


Figure 3: Experimental set-up to test the *Astyanax* odometer. A linear Perspex maze measuring 1.5m in length was constructed in a glass tank. A moveable start area was placed at one end, and fish were trained to swim 0.6m first to a clear Perspex barrier through which they could see three shoal companions (Training A), and as training progressed the shoal reward was removed and fish were trained to swim to the clear Perspex barrier and back to the start area for a food reward (Training B). Testing involved removing the Perspex barrier and measuring the maximum distance of the fish's nose prior to returning fully to the start area. Testing sessions were filmed from above at 30fps using a Point Grey Grasshopper 3M camera.

2.1.3 Training

Test subjects were split into two groups (group 1: Fish A-E, group 2: Fish F-J), and each group was trained on alternate days, with a maximum of three training sessions on each training day. This was to prevent overfeeding and loss of motivation. At the start of

each session, fish were randomly assigned one of three start area positions (fig. 4). Fish were trained to swim 0.6m from the start area doorway to a clear Perspex barrier and return home for a food reward. As this is a schooling species, during the first training stage a shoal reward of three fish was placed on the other side of the Perspex barrier in a compartment measuring 0.2 m in length (Training A). This was to encourage the fish to exit the start area and explore as far as the barrier early in training. When the fish could complete three consecutive sessions with at least 20 trials in 5 minutes, the shoal reward was no longer used (Training B).

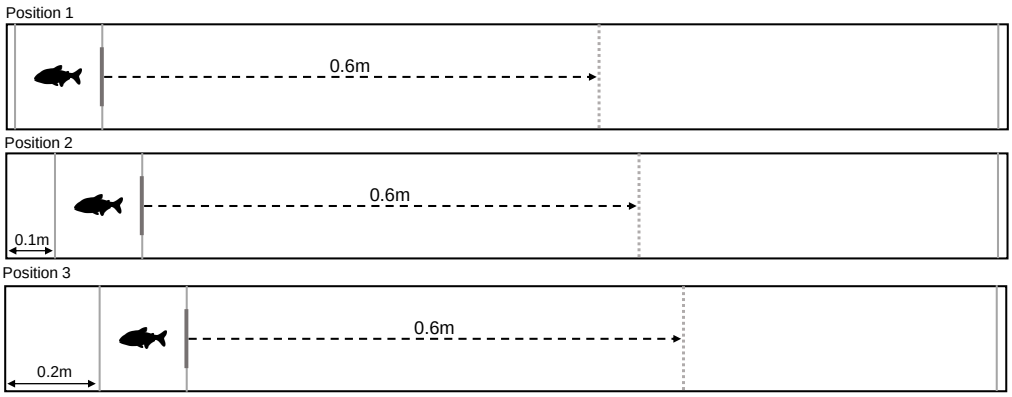


Figure 4: Three positions of the start area, shifting increasingly distally in the tunnel by 0.1m increments to control for use of external positional cues. The distance from the start area doorway to the Perspex barrier was always maintained at 0.60m.

During the first training stage, fish were rewarded with Gamma mini bloodworms upon arrival at the Perspex barrier, and food was concurrently presented in the start area to encourage them to return to the start area to begin another trial (Phase I). The fish exiting and returning to the start area was considered to be one trial. Sessions initially lasted 20 minutes but were shortened to 10 minutes and eventually 5 minutes as fish exceeded the threshold of 30 trials in one session. When fish performed at 80% proficiency on three consecutive 5-minute sessions, food was randomly not presented at the barrier, but instead only in the start area doorway (Phase II). The next training stages involved presenting the food in the start area once they were halfway home and not at the barrier

(Phase III) and finally only once fully in the start area (Phase IV). Fish were required to complete three consecutive training sessions consisting of at least 10 trials at 80% proficiency in Phase IV prior to testing. 80% proficiency was set as our training criterion following previous successful spatial memory training protocols with *Astyanax fasciatus* using this training threshold [15, 13]. We set the additional criterion of needing to complete three consecutive training sessions at this level of performance or higher. This was to ensure fish could consistently repeat previous performance levels as testing would be split across multiple sessions. A trial was considered successful when the fish exited the start area, swam directly to the Perspex barrier and then directly back to the start area to claim a food reward with no additional turns or pauses in the tunnel.

2.1.4 Testing

Upon initial design of the experiment, once fish had reached the criterion of 80% proficiency in the final training stage across three consecutive sessions, they were to be tested in their ability to reproduce the 0.6m distance with the barrier removed. The fish would have had to produce 30 distance estimates split across three testing sessions. In this experiment, no fish reached the final training stage. However, a sample of the best performing fish underwent diagnostic pilot testing to inform any future improvements to experimental design. The fish was placed in the start area in one of three randomly selected positions in the tunnel (fig. 4) and the Perspex barrier was removed (fig. 3, testing). Fish were released from the start area and were permitted to perform 10 distance estimates prior to being shut back in the start area. A distance estimate was considered the maximum distance of the fish's nose prior to turning back to the start area with no additional turns in the tunnel. Testing sessions were filmed from above at 30 frames per second using a Point Grey Grasshopper 3M camera controlled using Streampix 7 video capture software.

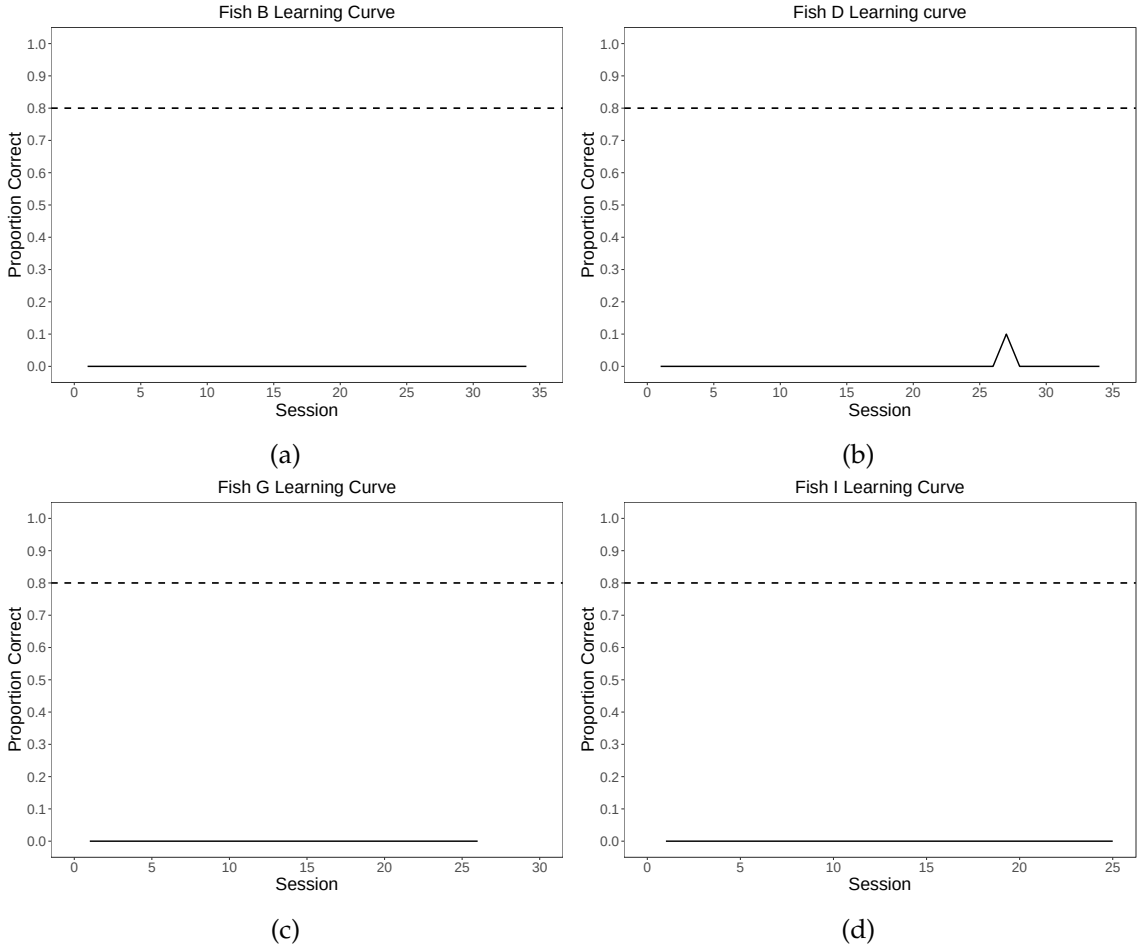


Figure 5: Learning curves for Fish B, D, G and I, indicating no learning taking place. Except for on one occasion (fish D), these fish did not leave the start area throughout training and were removed early from experiments.

2.2 Results

2.2.1 Training data

The number of training sessions completed by individual fish varied substantially (A: 69, B: 34, C: 60, D: 34, E: 60, F: 48, G: 29, H: 51, I: 26, J: 44). No fish reached the end of training by the experiment end-point. Four fish (Fish B, D, G and I) were entirely unresponsive to training, and did not leave the start area throughout training (fig. 5). These individuals were removed from further training at an early stage.

All remaining fish did display a gradual improvement in experiment proficiency over

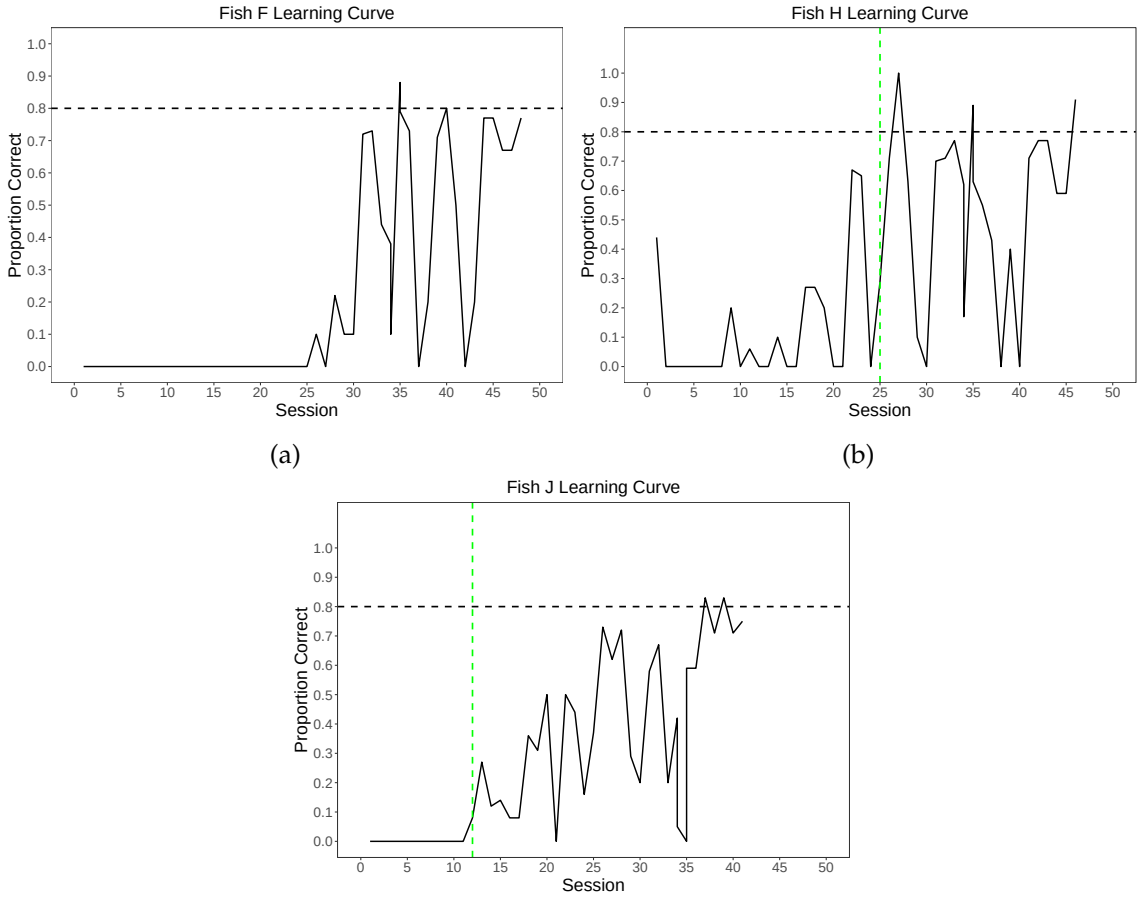


Figure 6: Learning curves for fish F (a), fish H (b) and fish J (c), indicating slow and variable experiment performance. Fish F failed to reach the criterion trial number to remove the shoal reward in part A of training. Both fish H and J progressed beyond needing the shoal reward (green vertical line), but performance was too variable to progress through any additional training phases. These fish were not included in pilot testing. Big fluctuations in performance could be largely attributed to construction work noise, especially drilling, before and during training sessions.

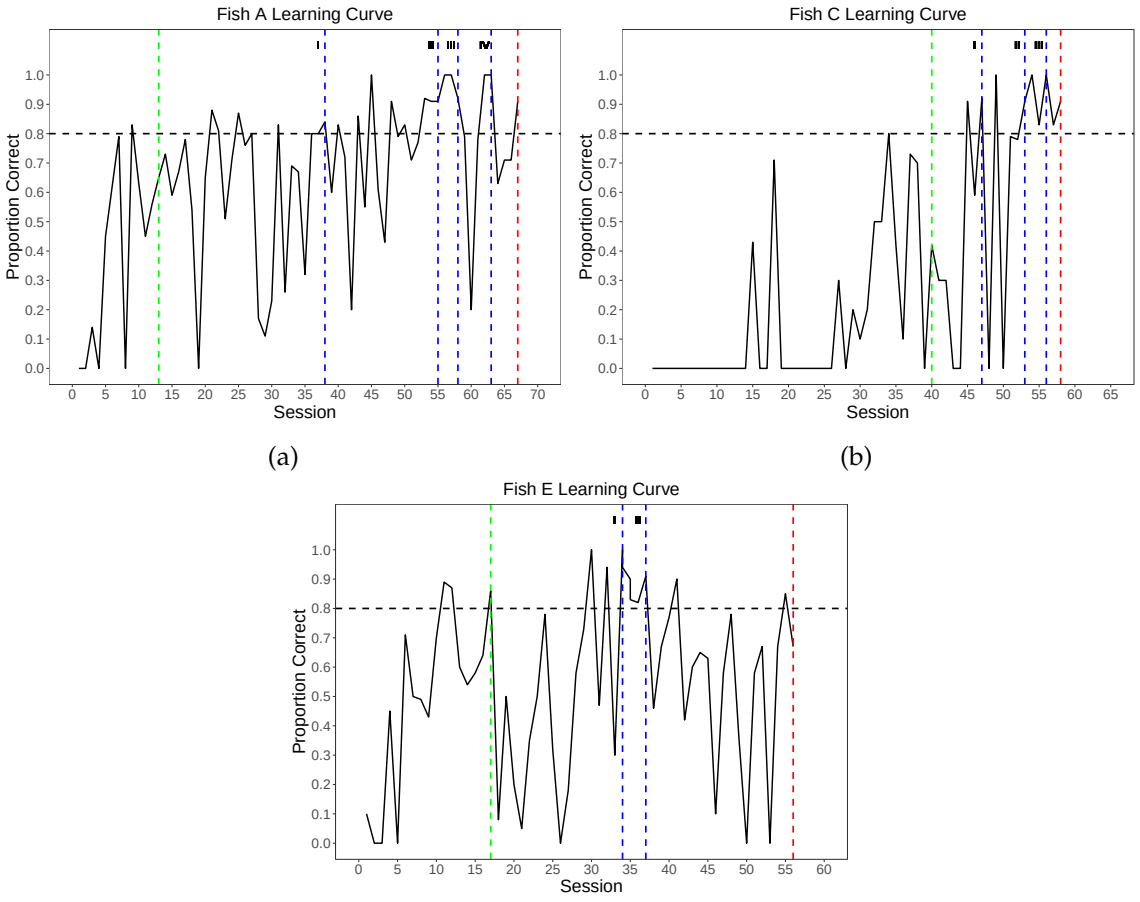


Figure 7: Learning curves for Fish A, C and E, all subsequently used for pilot testing. All three fish progressed beyond needing a shoal reward in part A of training (green vertical line). Fish A progressed the furthest in training, completing training phase I-III (blue vertical lines), and was being trained under phase IV prior to pilot testing. Fish C was at training phase III by pilot testing, and Fish E was at training phase II. Big fluctuations in performance could be largely attributed to construction work noise, especially drilling, before and during training sessions. A decline in performance as a result of construction noise is most apparent in Fish E. These three fish were selected for pilot testing at the point where it was decided to change study species, indicated by the red vertical dashed line.

time (fig. 6, fig. 7). However, there were large variations in performance. Fish F did not reach the point of shoal removal, with too few trials completed in each session. Fish H and J did progress past shoal removal, but did not consistently learn to swim as far as the barrier and back to progress past any training stages beyond Phase I where food was presented upon reaching the barrier and concurrently in the start area (fig. 6).

The best performing fish did progress through the planned training stages. Of these, Fish A was the most proficient, reaching training Phase IV after 63 sessions (fig. 7a). Fish C reached training Phase III after 56 sessions (fig. 7b), and Fish E reached Phase II after 57 sessions (fig. 7c), but no further improvements were made.

Of the fish making progress in experiment performance, large fluctuations in the proportion of correct trials could be attributed to external factors. This was particularly the case towards the end of training. Loud and prolonged construction work was taking place adjacent to the laboratory. Loud drilling before or during training regularly resulted in performance dropping to 0, with fish displaying freezing behaviours when frightened.

Further developments to experimental design would therefore need to be done with a more robust species that could be housed individually under compromised conditions without affecting natural behaviours.

2.2.2 Pilot testing

To inform any refinements to experiment design, the three best performing fish (Fish A, C and E) were chosen for pilot testing. On a day with no planned construction work, each fish completed 10 testing trials according to the initial design, with the start area placed in position 2. A distance estimate was considered the maximum point of the fish's nose in the tunnel prior to turning home. A Matlab program was used to track the pixel coordinate position of the fish's nose upon exiting the start area and the maximum point of the nose prior to turning home. Using the program R (The R Project, version 3.6.1) the total pixel distance travelled was calculated as the difference between the exit position and turning position, and estimates were converted to metric distances using the following

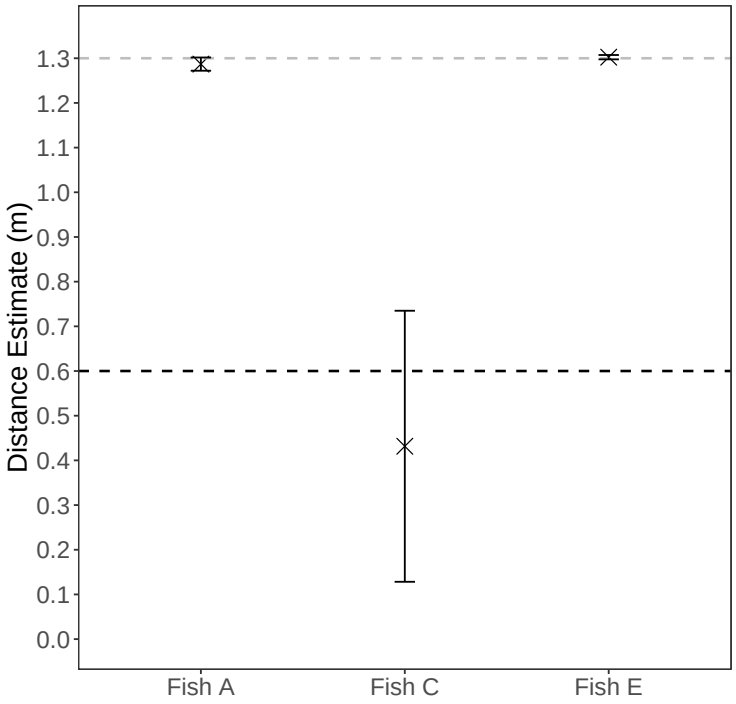


Figure 8: Average distance estimates from three fish during pilot testing. Error bars indicate +/- 1 standard deviation. No fish show evidence of distance estimation. The black horizontal line indicates the target distance of 0.6m, and the grey dashed line indicates the end of the tunnel.

conversion: 14.4 pixels = 0.01m. Fish A and E both swam to the end of the tunnel before turning home, indicating they had not learned the distance, but to swim to a solid barrier before turning home. The mean distance swum by fish A was 1.29m (3sf), with a narrow 95% confidence interval (1.28m - 1.30m), despite having progressed the furthest in training. The mean distance swum by fish E was 1.30m, also with a narrow 95% confidence interval (1.30m-1.31m).

Unlike the other two fish, fish C did not swim to the end of the tank, and the 95% confidence interval of its distance estimates does overlap with the training distance of 0.60m (0.215 - 0.649m). However, this confidence interval is very wide indicating that the result is unlikely to reflect the individual reporting upon perceived distance travelled. The average distance estimate of this individual is 0.432m, which amounts to a 0.168m

underestimation of the target distance.

2.3 Conclusions and Next Steps

Under the present set-up, we were unable to reliably assess the distance estimation abilities of the sighted mexican cavefish, *Astyanax fasciatus*. The experiment lasted for a duration of five months, after which six out of an initial ten experimental individuals had progressed in training. However, performance by all experimental subjects was highly variable and reflected compromised working conditions external to the laboratory in which the fish were housed. As a schooling species, *Astyanax fasciatus* relies on conspecifics for safety and security, but for the duration of the experiment, subjects were individually housed and trained, making the experiment vulnerable to external interference. Major building works to the foundations of the building outside of the behaviour laboratories spooked fish before and during training sessions resulting in regular fluctuations in training performance. We were informed that these building works would continue and worsen in magnitude and duration prior to our lab relocation. As a result of these severely compromised working conditions, it was deemed appropriate to temporarily stop using the sensitive *Astyanax fasciatus* as a model system for studying distance estimation in teleost fish.

The more robust Picasso triggerfish, *Rhinecanthus aculeatus* was selected as the new study species. This is a territorial coral reef fish that has a 'fight' rather than 'flight' response to compromised conditions, making it a useful species when developing the behavioural task in the current location. Moreover, although the time taken to learn the behavioural task could in part be attributed to the compromised laboratory conditions, evidence from this first experiment with *Astyanax fasciatus* implies that accurate learning of distance in fish is likely to be slow. To prevent overfeeding and maintain high motivation levels, the *Astyanax* were only trained every other day, and a maximum of three sessions per training day. The Picasso triggerfish has a higher metabolic rate and can instead be trained every day and training sessions can last longer. Owing to their territorial

nature these individuals are also required to be individually housed and as such present no ethical limit to the duration of the experiment.

Pilot testing with the best performing individuals in the current set-up also identified that the experimental design needed to be altered. A solid barrier was used to teach the distance of 0.6m, but when we tested three subjects in their ability to reproduce this distance, two out of the three fish consistently swam to the end of the tunnel instead of to the correct distance when the barrier was removed. Previous experiments with *Astyanax fasciatus* suggests that fish can store an internal representation of distance and direction to a food reward relative to home with a high degree of accuracy in both horizontal and vertical space [15, 13]. We therefore propose that the results observed here are not necessarily an indication that teleost fish do not form an internal representation of distance travelled, but rather that use of a barrier landmark was not appropriate to teach fish a certain distance, and a different landmark cue will need to be used when working with *Rhinecanthus aculeatus*.

3 Experiment 2: Odometry in *Rhinecanthus aculeatus*

The Picasso triggerfish, *Rhinecanthus aculeatus* is a territorial visual predator occupying the intertidal reefs of the Indo-Pacific. They are highly exploratory with large territories extending up to 50m in diameter. In the lab, they have proven to be robust fish that are easy to work with on operant conditioning tasks [16, 17, 18, 19]. Unlike the sighted Mexican cavefish, triggerfish also defend solitary territories so can live in isolation in tanks with no ethical limit to experiment time. This is important if behavioural training in a distance estimation task takes a long time, as indicated in experiment 1.

In the wild, Picasso triggerfish will continually forage for small fish and crustaceans, cracking open shells and turning over rocks to find food using their sharp teeth and powerful jaws. This behaviour can easily be co-opted in a laboratory setting to assess choices, such as in previous experiments looking at the triggerfish visual system. Such experiments have co-opted pecking and stone turning behaviours to peck at a stimulus [17] or to turn over a cup [18, 19] to make a choice regarding colour discrimination. Here, we present a variation of the distance task tested in experiment 1 that harnesses the stimulus choice behaviour of the Picasso triggerfish by teaching the fish to discriminate between stimuli placed at a trained and a decoy distance. Results from previous choice experiments exploring the visual acuity and colour vision of Picasso triggerfish have also informed us that *Rhinecanthus aculeatus* has a high visual acuity and trichromatic vision, similar to that seen in humans [18, 19]. We used these results to select the colour and size of landmark stimuli used for distance training.

3.1 Methods

3.1.1 Subjects

Subjects were six wild-caught Picasso triggerfish originating from the Maldives, purchased through a local supplier. They were housed individually in tanks measuring 0.35m (width) x 0.30m (height) x 0.60m (length), and provided with coral gravel, tubes, and pots

for enrichment. A diet of Formula One Marine Pellets and Lance fish was fed once daily when not in experiments. During experiments, pellets were provided as food rewards during training and fish was fed as a supplement at the end of each training day. A 12h/12h automated day/night light cycle was maintained throughout. Water changes were conducted twice weekly, with salinity kept at 35ppm, Nitrates below 15ppm and Ammonia and Nitrites at 0ppm.

3.1.2 Experimental Set-up

In order to keep salinity and water parameters constant between home tanks and the main experiment tank, a flow through system was built to connect the experiment tank to the main system. A linear tunnel measuring 0.25m (height) x 0.16m (width) x 1.8m (length) with walls and floor of black and white stripes of frequency 0.02m were built inside this flow through tank. White perforated screens were placed inside in front of the inlet and outlet pipes to prevent the fish from seeing outside the tank and to block the potential looming stimuli provided by the pipes. The basic set-up of the task is shown in fig. 9 below. The barrier in the previous experiment was replaced with a grey cup landmark of diameter 0.05m. Grey was chosen as it is a neutral colour, that is not naturally associated with foods or toxins [19]. This controls for prior experience in the wild with potential preferred foods or learned aversions associated with colour. The fish were trained to swim to the target cup 0.8m from the start area door. Fish had to peck at the cup and return to the start area to gain a food reward. Testing would introduce a second decoy cup at an incorrect distance and the fish would have to ignore the decoy and peck at the target cup to make the correct choice.

3.1.3 Training

Phase I: Pre-training and acclimatisation

Fish were first pre-trained to associate the grey cup with a food reward in their home tanks. The cup was presented and a food pellet reward was given as soon as the fish

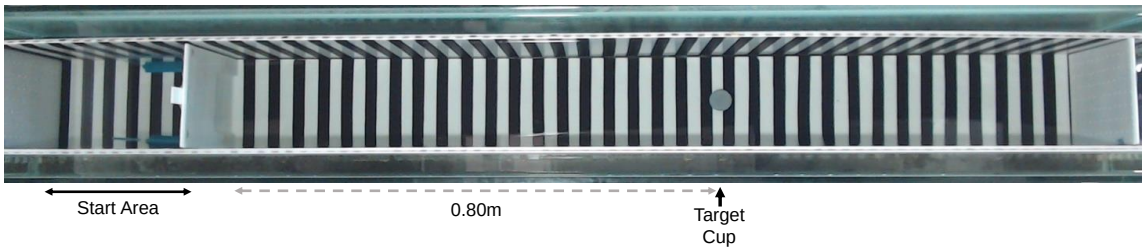


Figure 9: Linear odometry maze, with black and white striped walls of 0.02m frequency to provide consistent visual motion information (optic flow). The start area with manually operated doorway is on the left-hand side, and boundaries of the training arena are marked by white perforated screens. These block the looming visual stimulus provided by the inlet and outlet piping. A training cup has been placed at the correct distance 0.8m from the doorway of the start area.

pecked it. This training stage was complete once there was less than a 2s delay between cup presentation and pecking for 10 pellets, across three consecutive feeding sessions. Such a short delay was used as triggerfish in the wild will move quickly between potential sources of prey, rapidly striking with their powerful jaws at suitable prey items.

The fish subsequently underwent a phase of acclimatisation to being moved out of their home tank and into the experiment tank. They were trained to swim into a 2l container and placed in the start area prior to release into the main experiment arena. They were rewarded with food pellets each time they exited and returned to the start area, with the door closed behind them each time. This was continued until the fish could swim in and out of the start area with no hesitation or stress responses. Typical stress responses include raising of the dorsal and ventral trigger fins, a common sign of aggression in this species, gasping at the water surface, or erratic swimming near to the water's surface.

Phase II: Single cup training

In the first main training phase, the fish had to learn to swim to the grey cup placed 0.8m from the start area, peck at it and return to the start area to gain a food reward (fig. 10A). At first, a food pellet reward was presented in the start area as soon as the fish pecked the cup. As proficiency increased, the pellet reward was presented as the fish was

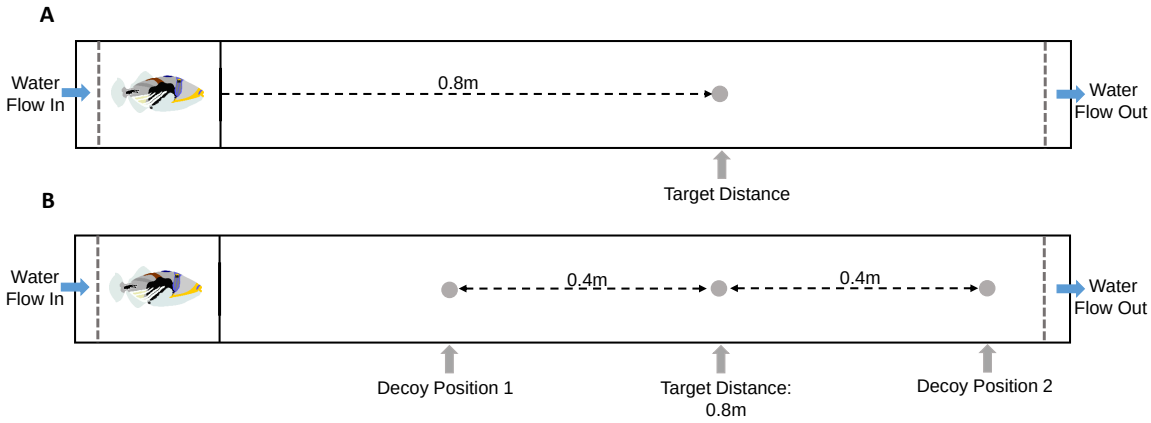


Figure 10: (A) A schematic representation of the first stage of training in the linear maze task set-up, with water flow highlighted. Fish were trained to swim out to a single cup located 0.8m from the start area doorway. If the fish pecked at this cup, a food reward was provided in the start area. (B) Schematic set-up for decoy training, with the target cup still at 0.8m from the start area, and a decoy cup placed in either position 1 (proximal) or position 2 (distal), 0.4m either side of the target.

increasingly close to returning home. At the final training stage, the pellet was only presented once the fish had fully returned to the start area. Training sessions consisted of 10 trials or until 10 minutes had passed, whichever came first. This stage was complete when fish were 80% proficient within three consecutive sessions. A trial was considered successful when the fish swam out directly to peck the cup and immediately returned to the start area for a food reward with no hesitation or additional turns in the tunnel.

Phase III: Decoy cup training

In the second main training phase, a decoy cup was introduced. Each trial, this was randomly placed either 0.4m in front of or behind the target cup as the fish approached it from the start area (fig. 10B). Each training session consisted of 10 trials, with 5 trials in position 1 and 5 trials in position 2. These positions randomly alternated throughout each session, with the order determined using a random number generator. The fish had to peck the target cup 0.8m from the start area to gain a food reward, and ignore the decoy. To prevent use of specific cup features or odours, each trial the cups were removed from the tunnel, rinsed and randomly allocated as the target or the decoy. To complete this training stage, the fish had to be correct on 4 out of 5 training trials for both decoy positions. A simple criteria of 80% overall proficiency across the 10 trials, as used in the previous experiment and training stages according to results from previous spatial training tasks [15, 14, 12, 13], could permit a choice bias strategy, such as choosing the first cup encountered in the tunnel on the majority of trials.

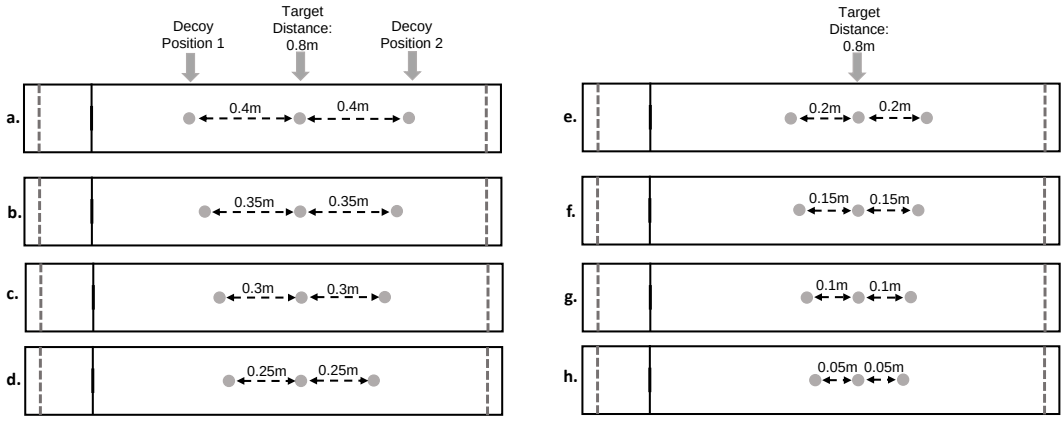


Figure 11: 8 testing stages for the main distance estimation task (a-h). Each stage the decoy cup is placed 0.05m closer to the target cup than the previous stage. Each trial, the decoy was randomly placed in either position 1 or position 2.

3.1.4 Testing

To assess the accuracy of distance estimation, there were 8 testing stages in which the decoy cup would be moved gradually closer to the target cup to assess when distance discrimination broke down. The distance between the target and decoy cups would be titrated down in stages of 0.05m from a distance of 0.40m from the target (fig. 11a) to 0.05m from the target (fig. 11h). Test sessions would have a 10 training + 5 testing trial structure. Fish would be trained with the decoy cup 0.4m from the target cup, randomly placed in position 1 or 2 each trial, for 10 trials (5 trials for each decoy position). The fish would be rewarded in the start area if it was correct. The fish would subsequently undergo 5 testing trials if performance on the ten preceding training trials was at criterion. During testing, the decoy would be randomly placed in position 1 or position 2 and the fish would choose one cup prior to returning to the start area. The fish would not be rewarded at this stage. 30 testing trials, equating to 6 testing sessions, would be conducted at each discrimination distance (a-h).

3.2 Results

3.2.1 Training Phase I: Single cup training

During single cup training, fish had to swim directly out of the start area, peck at the cup and return to the start area for a food reward with no hesitation or additional turns in the tunnel. Fish completed this training stage when they could complete 8/10 correct trials across three consecutive training sessions.

Five out of the six fish progressed past this training stage (Fish ID: A, B, C, E, F), fig. 12. This training stage took longer than expected. It was designed to harness a natural foraging behaviour - Picasso triggerfish will naturally turn over rocks and peck at hard crustaceans when hunting for food. However, due to the delay between a foraging behaviour usually associated with finding food in situ (pecking the cup) and getting a food reward (here requiring the additional behaviour of swimming away from the cup and to a displaced location not associated with the foraging behaviour), this training step took longer than expected, with one fish (Fish A) taking over 40 sessions to learn this step.

3.2.2 Training Phase II: Decoy Training

During decoy training, fish had to select the cup at the previously learned distance, 0.8m from the start area doorway, ignoring a decoy cup placed either 0.4m prior to encountering the target cup (position 1) or 0.4m after encountering the target cup (position 2).

Figure 13 shows the performance of Fish A, B, C, E and F during this training phase, with the left figure for each fish indicating overall performance. No fish reached criterion of 80% performance (4/5 correct choices) for both position 1 and 2 of the decoy cup. Although Fish B (fig. 13b) did reach the 80% proficiency across three consecutive sessions, motivation was lost before these sessions were complete with the fish unable to complete the required 10 trials in these sessions.

The right hand figure in fig. 13a-e indicates the proportion of trials that were correct when the decoy was in position 1, before encountering the target (red bar) and position 2,

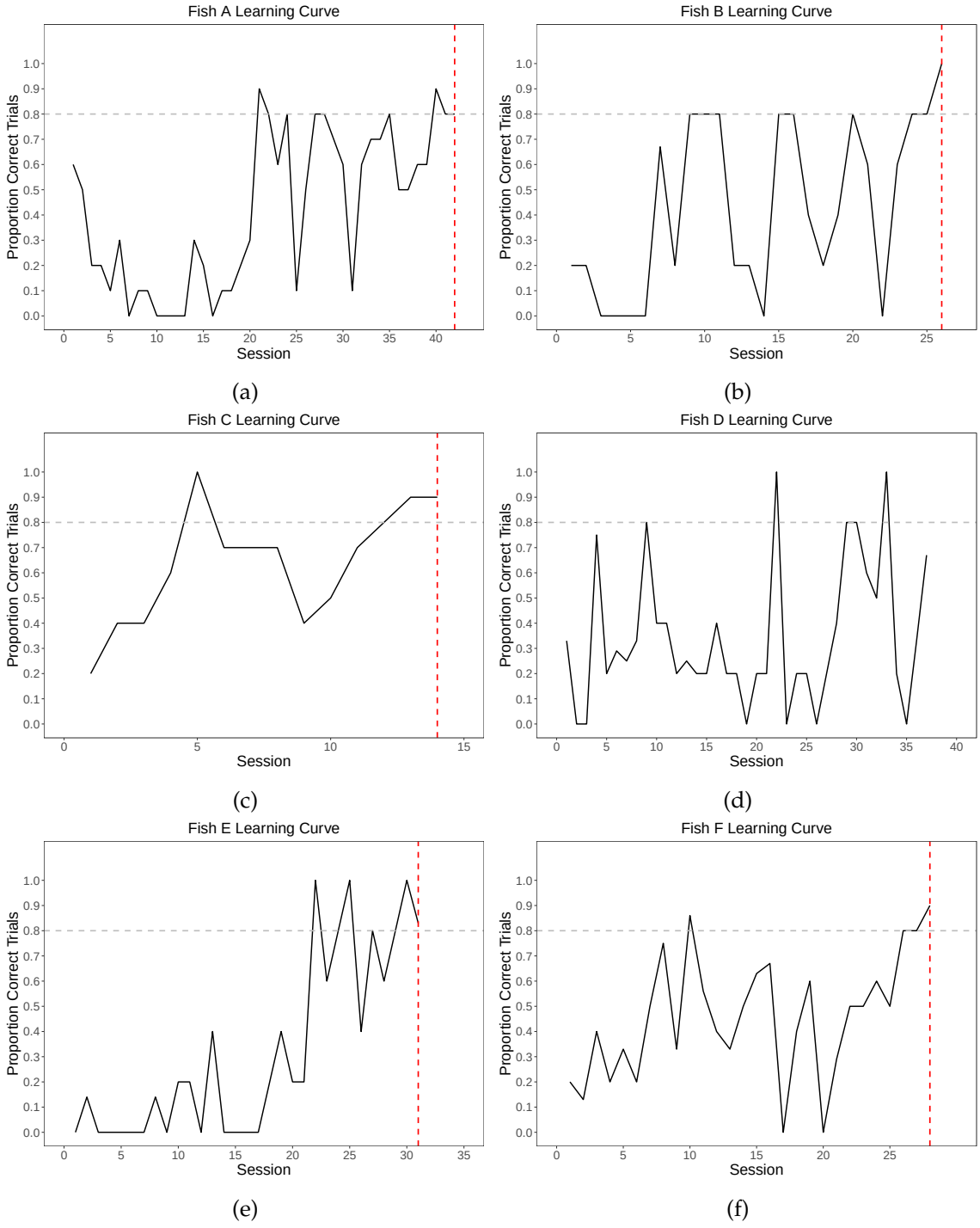
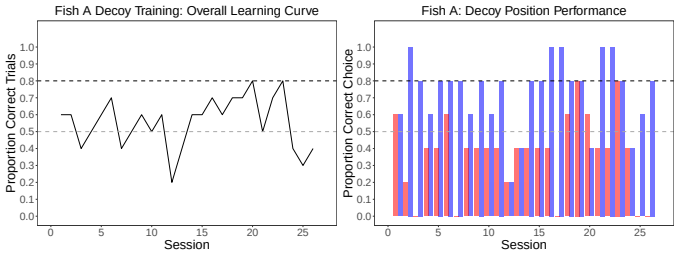


Figure 12: Single cup learning curves for Fish A-F. All fish except for Fish D progressed past this training phase, indicated by the red vertical line. The criterion for progressing through successive training phases was 80% performance across three consecutive sessions.

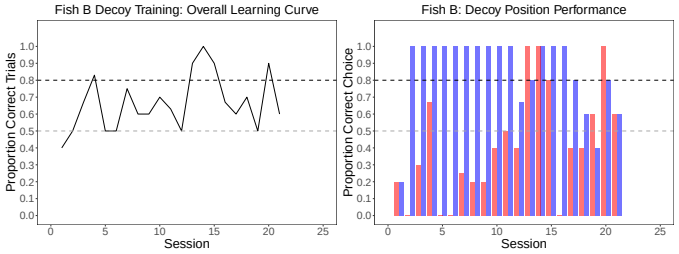
after encountering the target (blue bar). This indicates that performance when the decoy is located further from the start area than the target, position 2 - blue, rapidly goes beyond criterion up to 100% performance. However, when the decoy is encountered before the target cup, position 1 - red, performance is often below chance, and in two out of the five fish drops to 0 for the final three sessions. This was most strikingly seen in Fish E, which rapidly started performing at 100% accuracy when the decoy was further away from the start area than the target, and 0% accuracy when the decoy cup was encountered first. The fish therefore seem to learn to swim out and select the first cup they encounter. As all sessions had a standard set-up of 5 trials with the decoy in position 1 and 5 trials in position 2, this strategy was reinforced 50% of the time and can lead to fixation of this behaviour. Indeed, while a partial reinforcement regime leads to slower learning, it can also result in slower extinction of a learned behaviour.

Moreover, during training, fish often displayed stereotypical exploratory behaviour when presented with two identical stimuli that when pecked the fish assumed would produce food. Trigger fish will naturally move rapidly between different food sources, turning over rocks to search for food and rapidly striking at any cockles, small fish and crustaceans they encounter. In this experiment even if the correct choice was initially made, when pecking this cup did not immediately produce food, the fish often pecked the second decoy cup as well. Only when pecking the second cup also did not immediately produce food, did the fish swim back to the start area. Due to the shape of the maze, this was especially problematic during trials when the decoy was in front of the target; even if the decoy was ignored on the outward journey, it was often pecked on the return journey. Even though the correct cup was pecked first, this trial could not be rewarded. This resulted in slower learning and increased expression of frustration-related behaviours.

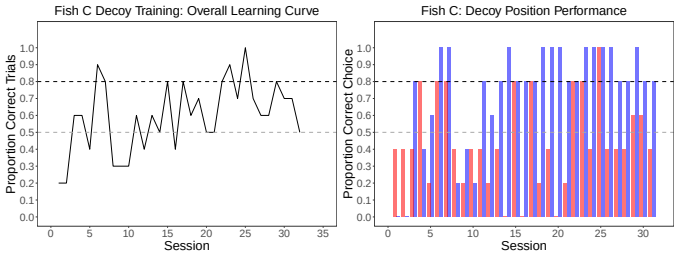
At this stage, it was therefore decided that a new training paradigm needed to be designed to ensure fish were learning the appropriate metric, in this case distance travelled.



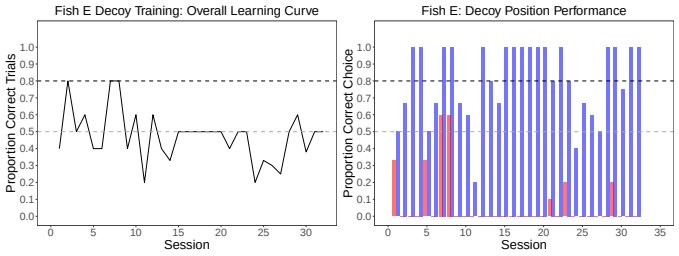
(a)



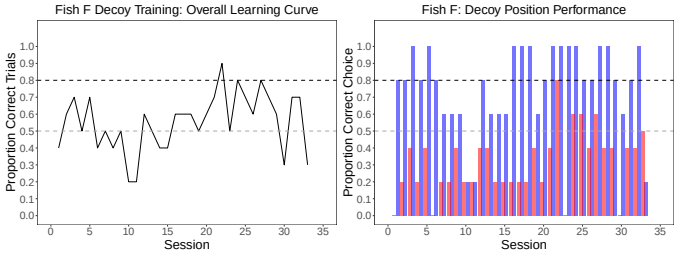
(b)



(c)



(d)



(e)

Figure 13: Decoy cup learning curves for Fish A, B, C, E and F. No fish progressed beyond this training stage, with all fish ending training at or near chance performance (50%, grey horizontal line). The black horizontal line indicates target performance of 80%. The right hand bar charts indicate performance when the decoy was in position 1 (red) and position 2 (blue).

3.3 Conclusion and Next Steps

To conclude, in this design none of the test subjects completed all training stages, even after 4 months of training with 2 training sessions daily. As these fish are known to be rapid learners in appropriate operant conditioning tasks, it was decided that a refinement to the experiment design had to be made. Two key changes were required: (i) owing to the unavoidable time and distance delay between the operant task and the food reward, the operant task had to be distinct from a natural foraging behaviour to prevent expression of frustration or exploratory behaviours, and (ii) it could not be a two-way choice task owing to the fixation of a behaviour yielding a food reward 50% of the time.

4 Experiment 3: Continuous distance estimation task with *Rhinecanthus aculeatus*.

The previous experiments were refined to replace the target cup and clear barrier landmarks with an intermediate design. In the weeks prior to a lab re-location from the original facility, a single experimentally naive Picasso triggerfish was trained in this new distance estimation task, housed in identical conditions to the six Picasso triggerfish used in the previous choice experiment. The fish was trained to swim a set distance to turn on surrounding aquarium lights to receive a food reward in the start area. This refinement meant that the rewarded behaviour would be the travelling aspect of swimming and not a goal-oriented foraging behaviour. In this pilot, we tested first how accurately the fish could recall a learned distance, and second whether visual motion information needed to be provided. The purpose of this was to pilot and refine this new experiment design so that training could begin with a new wild-caught population of Picasso triggerfish in the new facility.

4.1 Methods

4.1.1 Experimental Set-up

The same flow-through tank system constructed for the choice experiment was used in this set-up. A linear maze with changeable walls and floor was built within this tank, measuring 0.25m high x 0.16m wide x 1.80m long (fig. 14). Throughout training, the walls and floor were patterned with regular black and white stripes of width 0.02m. A perforated white screen was placed at either end to allow water flow through whilst blocking the stimuli provided by cues external to the tank or the inlet and outlet pipes themselves. A moveable start area of dimensions 0.25m high x 0.16m wide x 0.30m long could be placed in one of four start area positions, two at either end of the tank, 0.1m apart (fig. 14).

The target cup at 0.8m from the start area was replaced with an overhead infra-red proximity sensor (SHARP 2Y0A21 proximity sensor) connected to an Arduino microprocessor which through a Matlab program controlled lights surrounding the top of the maze walls (Interpret Triple LED Lighting System, 0.75m). The Arduino set-up is described in Appendix E. The voltage of the infrared detector varied depending on the strength of reflections from objects passing in front of it. With no objects between the detector and the floor of the maze, the reflection produced a voltage of 1.2-1.4V. A threshold of 1.7V was set during a period of acclimatisation to the maze with the experiment fish. During this time, the fish was permitted to repeatedly pass beneath the overhead infrared detector, indicating that 1.7V ensured the fish's nose turned on the overhead lights irrespective of swimming depth in the tunnel. A Point Grey Grasshopper 3M camera used in the previous experiment designs was placed overhead to film testing sessions.

4.1.2 Training

The fish first underwent a period of acclimatisation. In the home tank, it was trained to swim into a 2l container used to transfer it to the experiment tank. The fish was then given three sessions of 20 minutes to freely explore the experiment tank. Pellet food was

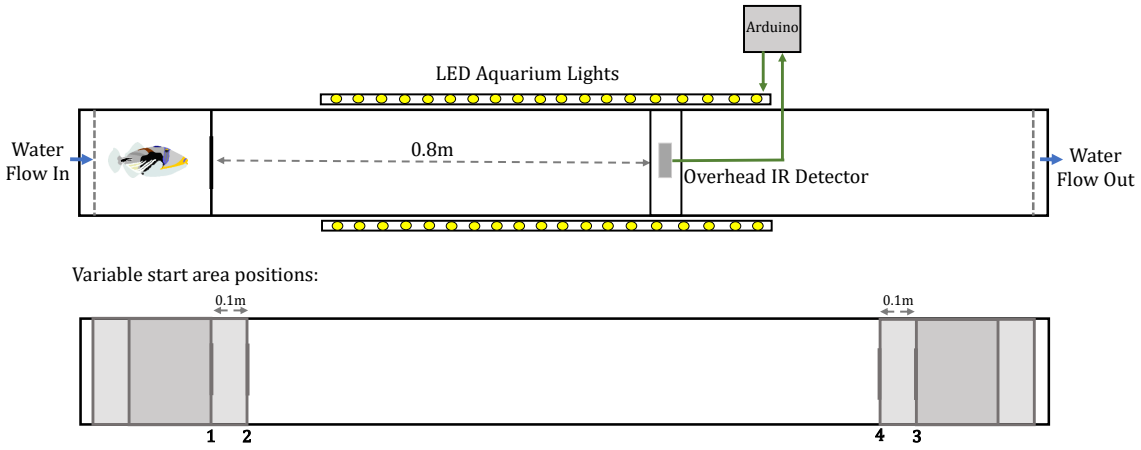


Figure 14: Main set-up for continuous distance estimation task with *Rhinecanthus aculeatus*. A low level of water flow, displacing 3l of water per minute, connected the main experiment tank to the home aquarium system to ensure water parameters remained constant. The fish was placed in a moveable start area in one of four positions at either end of the tunnel, either with or against the low water flow. An overhead infrared detector connected to surrounding aquarium lights controlled using an Arduino microprocessor provided the conditioned stimulus for teaching the sample distance.

scattered inside the start area and along the length of the experiment tunnel to encourage the fish to swim repeatedly in and out of the start area. Additional high-quality food rewards (chopped fish and krill) were dropped into the tank each time it passed beneath the infrared detector to turn on the aquarium lights.

Following the acclimatisation phase, the fish began full training. All training was done with a 0.02m frequency black and white striped pattern on the ventral and lateral maze surfaces, with stripes oriented perpendicular to the direction of movement. At the start of each training session, the fish was randomly assigned one of four start area positions according to the schematic in fig. 14. This was to control for use of external positional cues independently of distance travelled. Training sessions lasted 10 minutes, or until 10 correct trials were completed, whichever came first.

In the first stage of training, the fish was released from the start area and food was presented using tweezers at the infrared detector. Upon taking this food and turning on the lights, a second reward was immediately presented in the start area doorway. As

the fish learned the association between turning on the lights and getting food in the start area, food was randomly presented at the infrared detector 50% of the time, and always in the start area concurrently with the light flash. Finally, food was no longer given at the infrared detector, and presented increasingly later in the start area during the return journey. Eventually, the fish had to swim out to the infrared detector to turn on the lights and return fully to the start area before a food reward was provided. Training was considered complete when the fish swam directly out to the light and back on 80% of trials within the 10-minute session time limit, across three consecutive sessions.

4.1.3 Testing

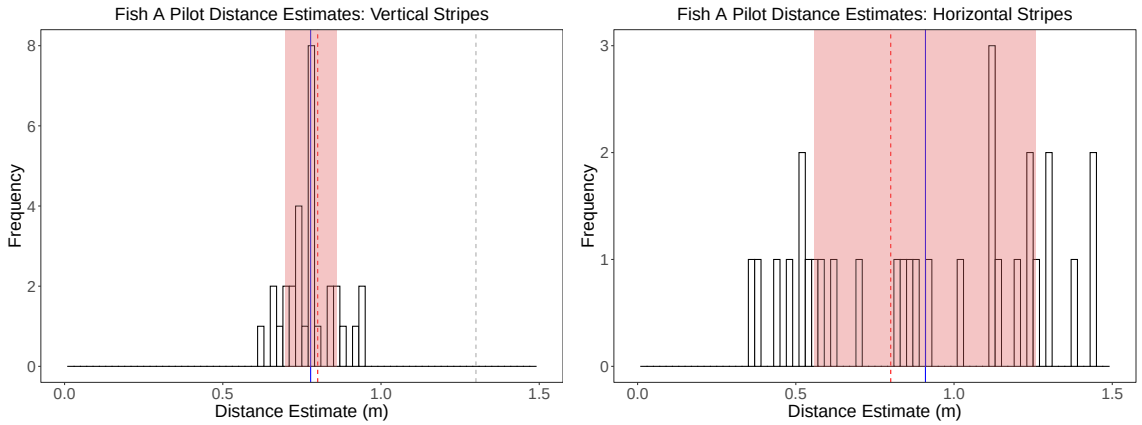
Part 1: Can a fish estimate distance?

First, we wanted to test whether a fish could estimate distance travelled under this set-up. The maze walls and floor were kept at the training treatment with 0.02m wide vertical black and white stripes. Each session, the fish was randomly assigned one of the four start area positions. Testing sessions were 10 trials in length and consisted of 5 randomly alternating training and testing trials. During training trials, the overhead infrared detector was placed 0.8m from the start area doorway as before, and the fish was rewarded if it swam directly out to turn on the lights and returned to the start area with no hesitation or additional turns in the tunnel. During testing trials, the infrared detector was placed in a decoy position 1.3m from the start area doorway and the fish was not rewarded upon returning home to the start area. A distance estimate was considered the maximum distance of the fish's nose from the start area doorway prior to returning to the start area. If the fish swam the 1.3m to the infrared detector to turn on the lights during testing trials, this was not considered to be a distance estimate. The fish completed 30 distance estimates, across 6 sessions. The infrared detector was positioned in a decoy position instead of removed to ascertain (i) that the fish was estimating distance travelled instead of beaconing to a landmark cue, and (ii) to test the relative importance of a previously learned landmark cue and an internal memory of distance travelled for making navigation decisions.

Part 2: Do Picasso triggerfish use optic flow to estimate distance travelled?

Part two aimed to explore whether provision of optic flow information was important to assess the accuracy of distance estimation in the Picasso triggerfish. We only had time for very early pilot testing prior to a building closure and lab relocation. Distance estimation accuracy was therefore compared between only two maze conditions: (1) 0.02m vertical black and white stripes which provide constant optic flow information, (2) 0.02m horizontal black and white stripes, providing no optic flow information.

For this pilot experiment, the distance estimates produced under testing part 1 were used as the dataset for treatment 1. For treatment 2, where no optic flow information was provided, testing was conducted under a 5 training trials + 5 test trials structure. As before, the fish was randomly allocated one of four start area positions for each testing session. Training trials were conducted as before with lateral and ventral maze walls with 0.02m vertical stripes, with the fish provided with a food reward in the start area if it swam directly to the light flash and back with no hesitation or additional turns in the tunnel. The fish was then moved to a holding tank while the infrared detector was removed and the maze walls and floor were changed to remove the optic flow by providing horizontal black and white stripes. The infrared detector was not placed in a decoy position during these trials as we were no longer assessing the relative importance of landmark vs distance cues, but were interested in the change in distance estimate distribution. The fish was then returned to the start area and after 1 minute of acclimatisation to the new visual pattern was released and permitted to produce five repeated distance estimates. A distance estimate was once more considered to be the maximum distance of the fish's nose from the start area doorway prior to returning to the start area. A food reward was not provided. This was continued over 6 testing sessions.



(a) (b)

Figure 15: Distance estimates for Pilot Fish A in the continuous distance estimation task. (a) Distance estimate distribution for 30 trials with the training visual background (0.02m vertical black and white stripes, (b) Distance estimate distribution for 30 trials with no optic flow information (0.02m horizontal black and white stripes). The blue line indicates the average distance estimate for that treatment, the red dash line indicates the target distance of 0.8m, and the grey line indicates the decoy position of the overhead infrared detector. +/- 1 standard deviation from the mean is indicated by the red shading. The infrared detector was removed for the second treatment with horizontal stripes.

4.2 Results

Part 1: Can a fish estimate distance travelled?

Our pilot data indicate that fish are able to represent distance travelled with remarkable accuracy. On all 30 testing trials, our test fish, Fish A, ignored the decoy position of the overhead infrared detector controlling the overhead lights, in favour of turning at the perceived correct distance travelled. Fish A produced an average distance estimate of 0.778m, which was not significantly different from the target trained distance of 0.8m (t_{29} = -1.51, p = 0.141), fig. 15a. Distance estimates were very precise, with a standard deviation of 0.0811m (red shading in fig. 15a). These results therefore validate continued use of the present pilot set-up and training protocol to test distance estimation in a larger population of *Rhinecanthus aculeatus*.

In the current experimental set-up, the start area was placed in one of four positions, two with the direction of water flow, and two against the direction of water flow through

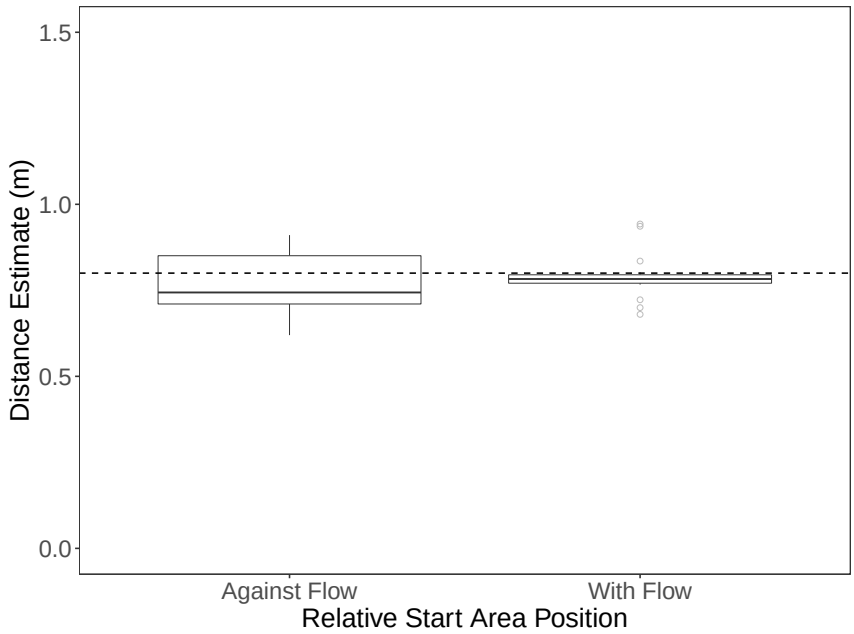


Figure 16: Distance estimates produced in two relative start area positions, with or against the direction of water flow in the experiment tank. There was no significant difference in distance estimate produced, with both being an underestimate of the target distance. However, the distance estimate error was larger in the orientation against water flow.

the tank (see fig. 14). The speed of water flow was kept very low whilst ensuring the water circulated between the home aquarium system to maintain constant water parameters. However, we do not know whether water flow is a cue used to learn travel distances by this species, or indeed if distance estimation performance was different across two positions oriented 180 degrees from each other. To inform whether further change would be needed to refine the distance estimation set-up, we tested whether the average distance estimate and distance estimate error differed across the two orientations (with or against flow). Figure 16 indicates that while average distance estimate was the same (Mann-Whitney-Wilcoxon test: W = 137, p = 0.325 (3sf)), the variance in distance estimates produced was higher in one relative orientation than the other (Levene's test: $F_{2,57}$ = 31.5, $p<0.001$), with greater distance estimate error when the fish was estimating distance against the direction of water flow. This implies that the fish was either using water flow as a cue to learn distance travelled, or that there was something about one orienta-

tion that distracted the fish from the task or interfered with reproduction of the learned distance. For the full experiment in the new facility, the set-up was therefore refined such that the start area position only shifted with respect to one direction and not both. This made different sessions with changes in start area positions more directly comparable. The water flow was also be switched off during training and testing sessions, which are short enough so as not to have an effect on water quality. The role of water flow for odometry would instead be tested separately in a fully controlled experiment (see chapter 5).

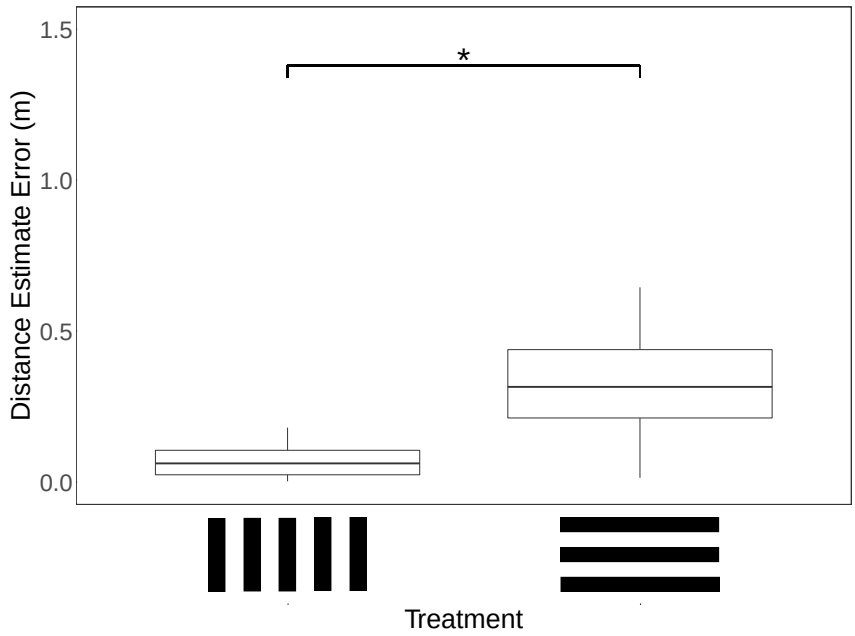


Figure 17: Absolute distance estimate error for the two visual treatments. Removing optic flow (horizontal stripes, right) led to a significant increase in absolute distance estimate error. Mann-Whitney-Wilxocon test: W = 85, $p<0.001$.

Part 2: Do Picasso triggerfish use optic flow to estimate distance travelled?

In part 1 of testing, Fish A was provided with the training visual background of vertical 0.02m black and white stripes. However, in part 2 of pilot testing, the fish produced 30 individual distance estimates with horizontally-oriented stripes. Orienting the black and white stripes horizontally removes optic flow information. Figure 15b shows the distance estimates produced by Fish A under this treatment, indicating a reduction in distance

estimation accuracy compared to the target distance (mean = 0.910m (3sf)). The Fish produced a more uniform distance travelled distribution, with a large standard deviation (standard deviation = 0.349m), implying that the fish is no longer capable of estimating distance travelled when spatial contrast information is removed.

Comparing the absolute distance estimate error (calculated as the difference between the absolute value of distance estimate and the target distance) between the two treatments indicates that the increase in error when spatial contrast information is removed is significant (Mann-Whitney-Wilcoxon test: W = 85, $p<0.001$).

4.3 Conclusion

This pilot experiment provided the first indication that a teleost fish can learn and remember distance travelled with remarkable accuracy and precision. We also provided the first indication that the Picasso triggerfish requires access to visual motion information to estimate distance travelled. When the tunnel was lined with regular translational spatial frequency information in the form of vertical alternating black and white stripes, they were able to accurately recall the learned distance. However, when this information was removed by replacing the vertical stripes with horizontally-oriented stripes they were no longer able to estimate distance travelled.

This experiment set-up therefore provides a robust method for testing various mechanisms underlying odometry in teleost fish, and it formed the baseline for the experiments in chapters 2, 3 and 5 investigating the sensory basis of odometry in *Rhinecanthus aculeatus*.

5 Discussion and Implications

In this chapter, we have summarised a series of pilot experiments used to develop the behavioural task to assess distance estimation abilities in teleost fish. The first experiment worked with the sighted Mexican cavefish, *Astyanax fasciatus*, and involved training the fish to swim through a linear tunnel to a clear solid barrier and return to a start area for a food reward. Due to severely compromised conditions in the behavioural laboratories owing to extensive construction work, learning in this schooling species was slow and irregular. It was therefore deemed necessary to work with a less flighty species to develop the behavioural task for use in a new behavioural facility. Pilot testing indicated that a solid barrier provided too salient a landmark cue for the fish to beacon towards, resulting in a preference to swim to this landmark cue over the trained distance when the barrier was removed.

Rhinecanthus aculeatus, or the Picasso triggerfish, a territorial coral reef fish that aggressively defends individual territories, was selected as our new study species. The visual discrimination abilities of this fish species have been extensively documented, co-opting stone turning, shell breaking and similar foraging behaviours to assess choices. In the second experiment, we used a similar training protocol to visual discrimination experiments, by training fish to swim to and peck at a target landmark and return to the start area for a food reward. During testing, the fish would have to discriminate between the learned distance of the target cup and the incorrect distance of a second decoy cup. Titrating down the distance between the target and the decoy during testing would then assess at what stage the fish was unable to discriminate between the correct and incorrect distance. However, owing to the task being in a linear tunnel, with the decoy placed either in front of or behind the target cup as the fish approached it from the start area, the fish was unable to learn the desired distance metric. In all trained individuals, choice accuracy remained near 50%, with most individuals learning to peck the first encountered cup and then return to the start area. As the cup was placed in front of the target 50% of the time,

and behind the target 50% of the time, this resulted in 50% reinforcement with a food reward, and in some cases resulted in fixation of this behaviour.

The final, successful, experiment design was an intermediate between the two previous experiments, and continued to use the Picasso triggerfish as the study species. A single fish was trained to swim to an overhead infrared detector which controlled overhead aquarium lights, causing them to turn on as the fish passed beneath the detector. The fish was trained to return to the start area for a food reward when the aquarium lights switched on. During testing, the infrared detector controlling the lights was moved to a decoy position and the turning position of the fish within the tunnel was filmed from above. The pilot individual in this experiment consistently ignored the new position of the infrared detector during testing trials, in favour of turning at the perceived correct distance. The fish reproduced the target distance with remarkable accuracy and precision. Moreover, preliminary evidence suggests a key role for visual motion information for learning and remembering travel distances. Final modifications to this experiment design provided the baseline for the experiments on odometry presented throughout this thesis.

Overall, this distance estimation task provides a valuable tool to study the neuroethology of distance estimation in teleost fish. By continuing to study the neural and sensory mechanisms underlying distance estimation in teleost fish, we will further our understanding of when vertebrate navigation systems evolved, and the differences between animals navigating through different ecologies.

References

[1] Durgin F.H., Akagi M., Gallistel C.R., and Haiken W. The precision of locomotor odometry in humans. *Experimental Brain Research*, 193(3):429–36, 2009.

[2] Jacob P-Y., Gordillo-Salas M., Facchini J., Poucet B., Save E., and Sargolini F. Medial entorhinal cortex and medial septum contribute to self-motion-based linear distance estimation. *Brain Structure and Function*, 222(6):2727–2742, 2017.

[3] Ronacher B., Gallizzi K., Wohlgemuth S., and Wehner R. Lateral optic flow does not influence distance estimation in the desert ant Cataglyphis fortis. *The Journal of Experimental Biology*, 203(Pt 7):1113–21, 2000.

[4] Ronacher B. and Wehner R. Desert ants Cataglyphis fortis use self-induced optic flow to measure distances travelled. *Journal of Comparative Physiology A*, 177(1):21–27, 1995.

[5] Ortega-Escobar J. and Ruiz M.A. Visual odometry in the wolf spider Lycosa tarantula (Araneae: Lycosidae). *The Journal of Experimental Biology*, 217(Pt 3):395–401, 2014.

[6] von. Frisch K. *Dance Language and Orientation of Bees*. HUP, 1967. ISBN 9780674418776.

[7] Goller F. and Esch H. E. Waggle dances of honey bees. *Nature*, 77(12):594–595, 1990.

[8] Walls M.L. and Layne J.E. Direct evidence for distance measurement via flexible stride integration in the fiddler crab. *Current Biology*, 19(1):25–9, 2009.

[9] Frenz H. and Lappe M. Absolute travel distance from optic flow. *Vision Research*, 45 (13):1679–92, 2005.

[10] Esch H.E., Zhang S., Srinivasan M.V., and Tautz J. Honeybee dances communicate distances measured by optic flow. *Nature*, 411(6837):581–3, 2001.

[11] Srinivasan M.V. Honeybees as a model for the study of visually guided flight, navigation, and biologically inspired robotics. *Physiological Reviews*, 91(2):413–60, 2011.

[12] Burt de Perera T. and Holbrook R. Three-dimensional spatial representation in freely swimming fish. *Cognitive Processing*, 13:S107–11, 2012.

[13] Holbrook R.I. and Burt de Perera T. Three-dimensional spatial cognition: freely swimming fish accurately learn and remember metric information in a volume. *Animal Behaviour*, 86(5):1077–1083, 2013.

[14] Burt de Perera T. Fish can encode order in their spatial map. *Proceedings of the Royal Society B*, 271:2131–4, 2012.

[15] Holbrook R.I. and Burt de Perera T. Separate encoding of vertical and horizontal components of space during orientation in fish. *Animal Behaviour*, 78(2):241–245, 2009.

[16] Newport C., Green N.F., McClure E.C., Osorio D.C., Vorobyev M., Marshall N..J., and Cheney K.L. Fish use colour to learn compound visual signals. *Animal Behaviour*, 125: 93–100, 2012.

[17] Champ C., Wallis G., Vorobyev M., Siebeck U., and Marshall J. Visual Acuity in a Species of Coral Reef Fish: Rhinecanthus aculeatus. *Brain, Behavior and Evolution*, 83 (1):31–42, 2014.

[18] Cheney K.L., Newport C., McClure E.C., and Marshall N.J. Colour vision and response bias in a coral reef fish. *The Journal of Experimental Biology*, 216(Pt 15):2967–73, 2013.

[19] Pignatelli V., Champ C., Marshall J., and Vorobyev M. Double cones are used for colour discrimination in the reef fish, Rhinecanthus aculeatus. *Biology Letters*, 6(4): 537–9, 2010.

$\sim$ Page left blank intentionally $\sim$

Chapter 7

General Discussion

General Discussion

1 Summary

How animals collect and compute information on distance travelled as part of a navigation strategy called path integration has been studied for many decades. However, such studies remain limited to animals navigating on land, either through the air or across surfaces. Whether freely-swimming aquatic animals can measure travel distances, and the mechanisms underlying this ability, have remained unknown.

In this thesis, I studied the behavioural basis of distance estimation in the aquatic vertebrate group, the teleost fish, for the first time. I aimed to answer three key questions: (i) Can teleost fish learn and remember travel distances? (ii) What sensory mechanisms do teleost fish use to measure distance travelled?, and as part of this (iii) How do fish regulate straight-line swimming? Understanding odometry in teleost fish and also more broadly how they organise and maintain optimal navigation trajectories to a fixed, unmarked point in space has important implications for our understanding of the evolution of vertebrate spatial cognition from an aquatic common ancestor, and also how aquatic animals more generally have evolved to collect and encode metric spatial information under the constraints and challenges of navigating underwater.

Using an operant conditioning protocol, I showed that teleost fish can learn and remember travel distances with remarkable accuracy, and appear do so independenly of external fixed positional cues. I subsequently explored the sensory self-motion mechanisms underlying distance estimation in the shallow-water marine fish, *Rhinecanthus ac-*

uleatus. Using this highly visual teleost fish, I tested whether mechanisms used by visual terrestrial animals – travel time, proprioceptive cues from a step counter, and optic flow – are also used by a fully aquatic animal. I particularly focused on exploring the use of self-induced visual motion information for distance estimation and also for the efficient control of navigation trajectories. Finally, I began to explore whether teleost fish can use additional sensory cues not available on land, such as hydrodynamic cues from water flows.

In this chapter, I discuss the key findings of my experimental work, the questions this work has generated, and highlight key areas for future study.

2 Key findings and future directions

2.1 Distance estimation in a teleost fish

I developed a novel distance estimation task to explore whether a teleost fish could learn and remember travel distances using self-motion cues alone. Fish were trained using an operant conditioning protocol to a sample distance, and then tested in their ability to reproduce this distance. I demonstrated that teleost fish are able to learn and remember travel distances with a high degree of accuracy, and they do this independently of external positional cues. The fish in this experiment even ignored a previously used landmark cue (the conditioned stimulus for learning the sample distance) in favour of using an internal reference of distance travelled when the landmark was placed in a novel position. By analysing videos of these distance estimates, I also provide evidence that elapsed time is unlikely to be as a proxy for measuring metric distance travelled. This implies that teleost fish do have an internal representation of travel distance, which is used independently of other metric measures.

The ability to estimate distance travelled is central to navigating by path integration. A path integrating animal uses measures of the constant distance and direction travelled to compute a continuously updated home vector to a starting position independently of

external information [1, 2]. However, whether the ability to estimate travel distance is part of a teleost path integrator remains unknown. Previous work with fish trained to swim to a specific location within a three-dimensional y-maze for a food reward, and released during testing trials in the absence of the maze and previously available landmark cues, has shown that they are still able to reach a previous goal [3]. Therefore, in the absence of landmark cues teleost fish are able to rely on an internal frame of reference to compute navigation trajectories. Together with my work demonstrating that teleost fish do have an internal representation of metric distance travelled, this suggests that teleost fish may be able to path integrate in a similar way to many terrestrial animals.

However, in order to unequivocally demonstrate path integration in teleost fish, future work should design and test a displacement task similar to those used to test the path integrators of the gerbil [4] and the desert ant [5]. Path integration is most easily demonstrated in central place foragers. Central place foragers typically occupy a home nest or area, returning to this location after foraging trips or territory patrols. *Rhinecanthus aculeatus* is one such central place forager, leaving its home area on the coral reefs to forage for small fish and crustaceans amongst the adjacent coral rubble. Another group that can be used to test teleost path integration is the freshwater African radiation of shell-dwelling cichlids. Both male and female shell-dwelling cichlids aggressively defend a single main shell and additional sub-shells from heterospecific and conspecific intruders [6]. These fish will leave their shell for foraging journeys and to chase away competitors, returning home rapidly between each journey. However, the lake and river floors are littered with visually indistinguishable shells, from which they must be able to rapidly determine the location of their own shell. Having an internal vector containing information on the direct distance and direction back to their home shell is therefore likely to be advantageous. Using a pilot study with the shell-dwelling cichlid *Lamprologus ocellatus* I have designed an operant conditioning protocol with which to comprehensively test path integration in this teleost species (see Appendix F).

2.2 Sensory mechanisms underlying distance estimation in *Rhinecanthus aculeatus*

Throughout the rest of this thesis, I worked with *Rhinecanthus aculeatus* to explore the sensory mechanisms underlying distance estimation in this species. The roles of optic flow, water flows, and proprioceptive inputs from finbeats for measuring travel distances were tested. I aimed to compare the sensory mechanisms underlying odometry in an animal navigating in water with animals navigating on land. *Rhinecanthus aculeatus* has high visual acuities alongside full colour vision, and typically occupies brightly-lit intertidal coral reef zones in the Indo-Pacific Ocean [7]. In such an environment, these fish have access to visual information in a similar way to many diurnal terrestrial animals, but they need to extract this information under the constraints of navigating underwater. Pelagic fish also navigate without direct physical contact with the fixed benthic background, and with access to additional sensory information from the dynamic fluid medium they swim through.

Optic flow: specific mechanistic adaptations for a life underwater?

In chapter 3, I explored whether *Rhinecanthus aculeatus* uses self-induced optic flow for odometry. I showed that, like many terrestrial animals occupying highly visual ecologies, *Rhinecanthus aculeatus* strongly relies on access to self-induced visual motion information to measure travel distances. However, unlike previously studied terrestrial animals, *Rhinecanthus aculeatus* does not appear to measure 'true optic flow' to achieve this. True optic flow refers to the angular rate of movement of visual features over the retina, and this depends on the depth of the visual scene and the speed of the moving animal, but crucially not on the spatial structure of the environment (see Chapter 1, section 1.2.1 for overview). I have shown that *Rhinecanthus'* visual odometer is strongly tuned to the spatial frequency of the environment and proposed that it may therefore instead be underpinned by a mechanism similar to that underlying the optomotor response. The opto-

motor response is used to stabilise the visual field and correct for unwanted rotational and translational displacements. In zebrafish, the optomotor response is underpinned by directionally-sensitive pretectal neurons that similarly respond to the spatio-temporal frequency (rate of movement of visual edges) of the visual environment [8].

In order to conclusively rule out a global optic flow mechanism measuring angular motion, further experiments will be required to assess the effect of varying tunnel width in combination with the temporal frequency of the visual background. Narrowing the tunnel whilst keeping spatial frequency constant will increase the angular rate of movement of visual features for a set swimming speed. This will lead to underestimates of a previously learned travel distance if a mechanism measuring the angular rate of movement of the visual field is used. In contrast, if fish are measuring the rate of movement of visual edges, narrowing the tunnel will have no effect on the distance estimates produced.

If these experiments provide additional evidence against use of a mechanism measuring angular motion, then further work should focus on the neural architecture underlying visual processing in the teleost odometer. It is possible that the same directionally-sensitive neurons in the pretectal area underlying the optomotor response are also involved in the processing of visual motion information for odometry, and that this information is later integrated to give an indication of distance travelled. Neural lesioning and single cell recording studies similar to those conducted to determine the neural architecture involved in the optomotor response will be required to investigate this [8]. Additionally, optomotor behaviour in zebrafish and goldfish has been shown to be sensitive to variations in spatial contrast, and is tuned to particular wavelengths of light [9–11]. Future work quantifying similarities between the behavioural output of the optomotor response and visual odometer in response to a range of visual scene changes will allow us to further compare the mechanisms underlying these two behaviours.

In the following chapter, I sought to further explore *Rhinecanthus'* use of visual motion information to organise optimal navigation to a fixed, unmarked point in space. For an animal to navigate successfully through its environment, it must not only be able to

plan and execute a route to a goal using navigation mechanisms such as path integration, but also manoeuvre safely and efficiently along the chosen trajectory. To efficiently navigate through its environment, an animal must be able to maintain straight movement trajectories, regulate movement speeds, navigate safely through narrow gaps, and avoid collisions with obstacles. In chapter 4, I explored whether *Rhinecanthus aculeatus* uses visual motion information to control its swimming trajectories. By altering the orientation and availability of spatial frequency information, I showed that as well as being central to odometry, *Rhinecanthus* has evolved to control both its lateral positioning and swimming speed using visual motion cues. However, these processes appear to be underpinned by separate mechanisms.

In order to maintain straight trajectories and to navigate centrally through tunnels and narrow gaps, I have proposed that *Rhinecanthus* may rely on visual expansion cues. A visual expansion equalisation strategy is also used by hummingbirds to avoid collisions with obstacles. This is hypothesised to be due to their extensive use of hovering flight, and translational optic flow is reliant on continuous forward motion to obtain sensory inputs [12–14]. All other previously tested flying and walking animals use translational optic flow to maintain straight courses and avoid collisions [15–19]. Underwater, where visual acuities decline more rapidly with distance, use of visual expansion information to avoid collisions could be preferable to relying on continuous inputs from translational optic flow. If visual expansion cues are used, visual inputs can be acted upon as a background is approached and enters the fish's perceptual range. Further experiments exploring the centering response of *Rhinecanthus* in a tunnel with dynamically changing visual expansion information will be required to fully test this hypothesis.

Unlike the centering response, translational optic flow is used by *Rhinecanthus* to maintain constant swimming speeds. This result was also shown in chapter 3, where post-hoc analysis of distance trajectories indicated that swimming speeds are sensitive to the presence or absence of optic flow information. Interestingly, this was not observed in a similar experiment with zebrafish, which appear to control swimming speeds independently of

visual information [20]. Whether this behaviour is unique to *Rhinecanthus aculeatus* or to fish occupying more highly structured and brightly lit environments remains to be found. However, by repeating this tunnel experiment with walls that can move the visual background either with or against the direction of swimming at varying speeds, this behaviour in *Rhinecanthus* can be fully quantified (fig. 1). This will allow us to assess to what extent swimming speeds are visually controlled. For example, if the visual pattern on the lateral walls moves in the same direction as the fish, we would expect faster swimming speeds than if the visual pattern moves against the direction of swimming (fig. 1b).

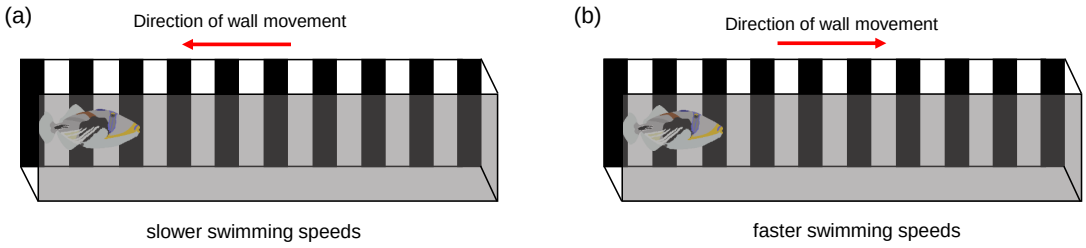


Figure 1: Possible experiment set-up exploring the sensitivity of swimming speeds to visual motion information. We would expect slower swimming speeds for fish swimming in the opposite direction to the moving wall (a). Fish would swim faster when travelling in the same direction as a moving wall (b).

Trajectories of *Rhinecanthus* subjects swimming down a tunnel of varying width can also be used to compare the mechanism underlying speed control with terrestrial animals. In chapter 3, I showed that swimming speeds are largely insensitive to variations in spatial frequency. It is therefore possible that *Rhinecanthus* is measuring true optic flow to control swimming speeds. If an angular motion mechanism is used, swimming speeds should decrease as the tunnel narrows. This is because the fish will be forced to swim closer to the visual background, thereby increasing the angular rate of movement of visual features, and giving the perception of faster movement for a set swimming speed. In the wild, using such a mechanism to control swimming speeds could serve to avoid dangerous collisions with surrounding coral by slowing swimming speeds in cluttered environments to permit safer and more efficient maneouvring. This is also observed in

flying budgeriars and honeybees when flying through clutter, and has similarly been proposed to be a mechanism to avoid dangerous collisions with trees and vegetation during flight [15, 19].

Finally, I explored the relative importance of visual motion cues from the ventral and lateral visual environments. I showed that *Rhinecanthus* can flexibly use information from the lateral and ventral fields to control swimming speeds, and does not use visual information from the ventral visual background to maintain straight trajectories. This information can be used as evidence that ventral information can be removed from the distance estimation set-up with no effect on the ability to learn and remember travel distances. This will allow us to conduct the above suggested experiments by varying optic flow information in the lateral environment, such as altering tunnel width or the speed of movement of the lateral walls, without having to account for use of visual information from the ventral background.

Overall, my experiments provide the foundation upon which to continue to study the mechanisms underlying visual odometry and swimming control in *Rhinecanthus aculeatus*. This will give us a greater understanding of the similarities and differences between *Rhinecanthus* and terrestrial animals such as honeybees and humans. Neuroanatomical work will be instrumental for understanding the retinal and post-retinal processing of visual motion cues in these animals, allowing us to make direct mechanistic comparisons. The functional visual acuity of *Rhinecanthus* is also at the same level as other freshwater teleost species occupying less brightly lit or visually structured ecologies, such as the goldfish [21, 22] and the bluegill [23]. Testing the role of visual motion cues for odometry and swimming control in such freshwater teleosts will indicate whether the mechanisms used by *Rhinecanthus* are used across the teleost clade, or if they reflect specific adaptations to navigating through an intertidal coral reef environment.

Water flow – evidence of a hierarchy of sensory processing?

A teleost fish using visual information underwater does so in the presence of additional sensory information from the fluid medium through which they swim. The water column can be said to provide the fish with a second frame of reference from which to make navigation decisions and movement calculations. In previous experiments, *Rhinecanthus* subjects performed distance estimation tasks and swimming manoeuvres in the absence of any water flows. In chapter 5, I therefore constructed a flume system to explore the relative importance of visual information from the benthic background and water flows from the dynamic fluid medium to estimate travel distances. While I was unable to complete this experiment, pilot results from one individual indicate that *Rhinecanthus* relies primarily on visual motion information from the fixed benthic background to estimate distance travelled. Only when visual information was absent did the distance estimates vary with the strength of water flows. This indicates that *Rhinecanthus* may display hierarchical use of different sensory inputs depending on the information available. Completion of this experiment with a full sample size will be able to fully quantify these effects.

Preferential use of visual information for odometry may be advantageous for a teleost fish occupying highly-structured coral-reefs in the intertidal zones. In these environments, water flows will be temporally variable in strength and structure, and will be heavily shaped by the benthic structure of the environment. In the absence of visual information, water flows may be able to provide some indication of the relative distance travelled. However, water flows alone are unlikely to provide sufficiently reliable or accurate information on distance travelled. In contrast, for teleost species navigating under different ecological and physiological constraints, hydrodynamic information from water flows may play a greater role in estimating travel distances. For example, the water column may be used as the frame of reference for fish navigating with little or no access to visual information, or in environments with lower and more constant water flows. Future work should test the relative importance of sensory cues from the water column itself in teleosts occupying a range of visual and water flow ecologies.

If water flows are used for odometry, experiments will be required to untangle the underlying mechanism. To measure water flows, a teleost fish could either measure total energy expenditure or hydrodynamic inputs using their lateral line. The lateral line is made of functional units called neuromasts, present on the surface of the fish's skin or embedded in canals beneath the skin's surface [24]. By training individuals with an intact lateral line, and temporarily ablating the lateral line using chemical or mechanical means, we can test whether sensory inputs to the lateral line are required for using water flows as a source of information on distance travelled. If hydrodynamic inputs to the lateral line are used, fish with ablated lateral lines should be unable to estimate distance travelled in the absence of visual information. There should also be no effect of varying water flows on the magnitude of the distance estimates produced. However, if teleosts measure energy expenditure, then the effects of water flow treatments will be observed even when the lateral line is ablated.

Proprioceptive cues from finbeats – relevant in an aquatic world?

For many surface-constrained animals, distance travelled is measured as an integration of step length and frequency, a mechanism known as stride integration [25, 26]. When walking across a solid surface, there is likely to be a directly proportional relationship between the number of steps of a fixed length and distance travelled. This is observed in humans, ants, and fiddler crabs – disruption of this relationship by experimentally altering leg length or modifying the surface to increase backwards slippage leads to predictable disruptions to the distance estimates produced [25–29]. For a teleost fish, the equivalent mechanism would be to use a finbeat integrator. However, for many freely-swimming fish, there is less likely to be a reliable, directly proportional relationship between finbeat number and distance travelled. The amount of forward motion generated from a finbeat depends on the strength, direction and type of water flow experienced, and the proximity of any nearby obstacles affecting the forward thrust obtained against the water [30].

Rhinecanthus aculeatus occupies an environment with variable flows. Moreover, it has

evolved a series of fin adaptations for the purpose of communication and manoeuvrability. The front dorsal and ventral fins have been modified to create two 'triggers', used in displays of aggression towards predators and conspecifics, and to anchor themselves inside crevices in the coral reef to avoid predation, particularly at night. The rear dorsal and anal fins have been extended across the length of the posterior end, and slow but precise forward and backward propulsion is achieved through undulations of these fin pairs. The caudal fin provides rapid, directed forward propulsion and together with the pectoral fins is responsible for steering. During forward swimming, *Rhinecanthus* will use these fin pairs in isolation or in combination, interspersed with periods of gliding movements where no fin movements are used. In chapter 2, using post-hoc video analysis, I quantified fin use during testing trials in our distance estimation task. I found that finbeat type and number used, and the distance travelled using each swimming modality varied beyond the variation in distance estimates produced. I therefore proposed that *Rhinecanthus* subjects were not summating mechanical inputs from finbeat movements to estimate travel distances. However, as demonstrated in chapter 5, *Rhinecanthus* may display a hierarchy of sensory information use for odometry, favouring inputs from visual motion cues. The experiment testing the accuracy of the teleost odometer in chapter 2 was conducted in the presence of visual motion cues, as pilot testing during the experiment design stages had indicated that *Rhinecanthus* requires access to visual motion information to learn and remember travel distances (see chapter 6). Therefore, in the absence of visual information, *Rhinecanthus* may begin to rely on a finbeat integrator for odometry. A repeat of the video analysis on distance estimates conducted in the dark will be able to test this. However, I predict that owing to the highly specialised swimming modalities exhibited by *Rhinecanthus aculeatus*, mechanical inputs from finbeats are unlikely to provide reliable information on distance travelled. *Rhinecanthus aculeatus* is also a diurnal species, which exhibits a strong motivation to hide, and a strong aversion to forage, explore or eat in the absence of light. Other species of teleost with less specialised morphologies may be more likely to use finbeats for odometry. For example, the freshwater goldfish

inhabits mostly still pond and slow moving river habitats and relies primarily on regular caudal finbeats for propulsion. For such species, there may be a more reliable relationship between tailbeat number and travel distance.

2.3 Navigating in three dimensions

Throughout this thesis, I have focused on the sensory and cognitive basis of distance estimation in the horizontal x,y-plane. However, unlike terrestrial surface-constrained animals, teleost fish are free to move unrestricted into the vertical z-plane. Freely-swimming animals therefore move with six degrees of freedom, with three types of translational movement - forwards/backwards, left/right, up/down - and three types of rotational movement - roll, pitch and yaw (fig. 2b). This is compared to just three degrees of freedom in surface-constrained animals, two translational - forwards/backwards, left/right - and one rotational - yaw (fig. 2a) [3, 31, 32].

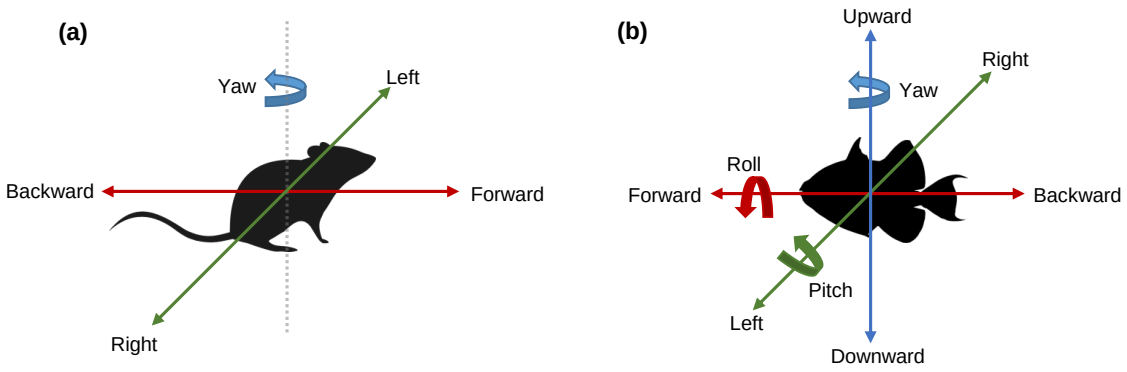


Figure 2: Degrees of freedom of movement for surface-constrained (a) and freely-swimming animals (b).

Among vertebrates, there is evidence that surface-constrained animals such as rats encode vertical space with less accuracy than horizontal space. For example, rats exploring a cubic lattice maze adopt a layer-like foraging strategy, spending more time moving in the horizontal plane than the vertical [33], and are better at finding a goal in horizontal

than vertical space [34]. At the neural level, this is accompanied by a relative insensitivity of grid and place cell firing to changes in height above the ground [35, 36]. It has been proposed that surface-bound animals have a bi-coded representation of space, with horizontal information represented with metric accuracy, and vertical space represented contextually as a series of layers [37]. However, for animals moving freely through volumetric space, the same computations for representing horizontal space are also likely to be important in vertical space, necessitating a fully-integrated three-dimensional representation of space [38].

Behavioural and neural evidence from hummingbirds, bats and fishes suggests that volumetric animals differ from surface bound animals in the representation and use of three dimensional space. Bats and birds, which fly with six degrees of freedom of movement, show evidence of a volumetric representation of space. For example, hummingbirds foraging in a cubic lattice maze will move in all three dimensions equally and are able to use this strategy to accurately find the location of a goal in three-dimensional space [34]. Neural recordings from freely-flying Egyptian fruit bats also indicate that bats have isotropic movement patterns through three-dimensional space, and this is accompanied by isotropic spherical hippocampal place fields and three-dimensional sensitivity of head-direction cells [39–41]. Recent behavioural experiments also indicate that teleost fish may have a volumetric representation of space. Fish trained in volumetric maze tasks are able to learn vertical and horizontal movement components at equal rates and accuracies [3, 31, 42], and this is true even for fish that preferentially occupy benthic zones [43]. Moreover, when previously learned information from the vertical and horizontal planes are put in conflict, fish will preferentially use information from the vertical plane [31, 42, 44]. This suggests not only that teleost fish have an accurate representation of volumetric space, but also that there are particularly salient cues relevant for navigation in the vertical dimension.

This therefore raises three key questions with regards to the cognitive and sensory basis of metric distance estimation in freely-swimming teleost fish. First, how accurately do

teleost fish encode distance information in horizontal vs vertical space? Second, what sensory information do teleosts use to extract information on vertical distance travelled? Finally, how do teleost fish integrate metric movements diagonally through a volume, with components of both horizontal and vertical travel? By extending my distance estimation task first into assessing vertical distance estimation only, and second in an environment involving both horizontal and vertical movement, we can test how vertical distance is represented and integrated with horizontal displacements to compute volumetric movements.

The distance estimation task can also be used to investigate the sensory mechanisms underlying odometry in the vertical plane. Possible mechanisms include measurements of temperature or light intensity changes with increasing depth, or directly sensing depth using the swim bladder. The swim bladder is used primarily to regulate buoyancy, and the fractional rate of change of swim bladder volume varies in direct proportion with increasing depth [45]. Changes in swim bladder volume with depth could, in theory, be detected by sensing stretching of the swim bladder wall [31, 45, 46], and this could, in turn, be used as a measure of metric vertical distance travelled.

Finally, in order to fully understand how teleost fish represent volumetric space, we must study how distance information is encoded at the neural level, and whether neural cell types encoding spatial information are able to fully represent volumetric travel.

2.4 The neural basis of odometry in teleost fish

There is increasing evidence to suggest that the teleost pallium, underlying many spatially-relevant behaviours, is homologous with the mammalian and avian hippocampus [47–49]. Therefore, a brain structure involved in vertebrate spatial memory may have evolved over 400 million years ago in an aquatic common ancestor of extant vertebrate groups. Such studies have involved indirectly implicating brain regions through impairments in spatial memory tasks following experimental brain lesioning [50], or through recording increased protein synthesis in specific brain regions following training in spatial memory

tasks [51].

In mammals, metric distance information is represented by grid cells in the medial entorhinal cortex, receiving multiple sensory afferents from cortical brain regions [52–55]. This information is then integrated with information from other afferent spatial cell types including speed cells, head direction cells and boundary cells by the place cells in the hippocampus to form a neural representation of space [52, 56, 57]. Whether teleost fish share this mechanism through common ancestry, or if they have evolved a separate architecture to represent spatial information is unknown.

Results from my behavioural experiment revealing that teleost fish possess a highly accurate internal representation of travel distance provides further evidence that teleosts have similar spatial mapping abilities to those observed in mammals. As neural manipulation and recording technologies have been developed for use in freely-behaving fish [58], my behavioural distance task now provides a valuable tool that can be used to test whether these spatial mapping abilities are also based on homologous neural mechanisms. Completion of the distance estimation task alongside single cell recordings and brain lesion studies will allow us to begin testing candidate brain regions, such as the teleost lateral pallium and optic tectum, and eventually cell types directly associated with distance estimation in teleost fish. Simultaneous study of the behaviour and underlying neural activity will be instrumental in allowing us to form robust conclusions on the representation of volumetric space in teleost fish, and also the neural mechanisms responsible for integrating information from multiple sensory inputs. This information will be central to understand when, and under what selective pressures the neural representation of space evolved in the vertebrate clade.

3 Concluding remarks

To conclude, in this thesis I have shown that teleost fish can estimate distance travelled with remarkable accuracy using self-motion cues alone. This is the first time the metric accuracy of spatial cognition has been directly studied in the teleost clade, and provides the first indication that teleost fish encode horizontal space with comparable metric accuracy to tetrapods. Whether this ability is underpinned by homologous neural architecture that evolved in an aquatic common ancestor remains unknown. However, understanding the behavioural output of a process is a crucial pre-cursor to understanding its underlying neural mechanisms and evolutionary origins. The behavioural task developed and tested throughout this thesis can now be used as a universal tool to explore the functional and mechanistic basis of distance estimation in freely-behaving fish at the neural and behavioural levels.

Throughout this thesis, I used this distance estimation task to explore the sensory mechanisms underlying odometry in the visual shallow-water marine fish, *Rhinecanthus aculeatus*. Aquatic animals occupy a unique spatial ecology, such that the way spatial information is collected and encoded may differ substantially from their terrestrial counterparts. I show that, like many terrestrial animals, a visually reliant teleost fish can use visual motion cues to estimate distance travelled, but the underlying mechanisms reflect adaptations to solving the problem of navigating underwater. Moreover, mechanisms such as use of a stride integrator, that are central to odometry in many walking animals, show limited reliability for teleost fish navigating through variable flows. Instead, teleosts are likely to have evolved distinct sensory mechanisms for extracting distance information underwater, such as hydrodynamic inputs detected using their lateral line or vertical displacements through detections of changes in pressure in their swim bladder. Further work with *Rhinecanthus aculeatus* and other fish from across the teleost clade will continue to inform us of the sensory mechanisms used by teleost fish to estimate travel distances in their volumetric world. Continued efforts to gain a comprehensive understanding of

how teleost fish encode metric space are central to understanding the origin of metric spatial encoding in the vertebrate clade, and the navigational challenges faced by animals occupying an aquatic three-dimensional world.

References

[1] Etienne A.S. and Jeffery K.J. Path integration in mammals. *Hippocampus*, 14(2):180–92, 2004.

[2] Etienne A.S., Maurer R., Berlie J., Reverdin B., Rowe T., Georgakopoulos J., and Séguinot V. Navigation through vector addition. *Nature*, 396(6707):161–4, 1998.

[3] Holbrook R.I. and Burt de Perera T. Three-dimensional spatial cognition: freely swimming fish accurately learn and remember metric information in a volume. *Animal Behaviour*, 86(5):1077–1083, 2013.

[4] Mittelstaedt M-L. and Mittelstaedt H. Homing by path integration in a mammal. *Nature*, 67(11):566–567, 1980.

[5] Müller M. and Wehner R. Path integration in desert ants, Cataglyphis fortis. *Proceedings of the National Academy of Sciences (PNAS)*, 85(14):5287–90, 1988.

[6] Bills I.R. *Eco-ethology of shell-dwelling cichlids in Lake Tanganyika*. PhD thesis, Rhodes University, 1996.

[7] Champ C., Wallis G., Vorobyev M., Siebeck U., and Marshall J. Visual Acuity in a Species of Coral Reef Fish: *Rhinecanthus aculeatus*. *Brain, Behavior and Evolution*, 83(1): 31–42, 2014.

[8] F Kubo, B Hablitzel, M Dal Maschio, W Driever, H Baier, and A B Arrenberg. Functional Architecture of an Optic Flow-Responsive Area that Drives Horizontal Eye Movements in Zebrafish. *Neuron*, 81:1344–1359, 2014.

[9] H Maaswinkel and L Li. Spatio-temporal frequency characteristics of the optomotor response in zebrafish. *Vision Research*, 43:21–30, 2003.

[10] A Krauss and Neumeyer C. Wavelength dependence of the optomotor response in zebrafish (Danio rerio). *Vision Research*, 43:1275–1284, 2003.

[11] S Schaerer and C Neumeyer. Motion detection in goldfish investigated with the optomotor response is 'color blind'. *Vision Research*, 36:4025–4034, 1996.

[12] Goller B. and Altshuler D.L. Hummingbirds control hovering flight by stabilizing visual motion. *Proceedings of the National Academy of Sciences (PNAS)*, 111(51):18375–18380, 2014.

[13] Ros I.G. and Biewener A.A. Optic flow stabilizes flight in ruby-throated hummingbirds. *Journal of Experimental Biology*, 219(16):2443–2448, 2016.

[14] Dakin R., Fellows T.K., and Altshuler D.L. Visual guidance of forward flight in hummingbirds reveals control based on image features instead of pattern velocity. *Proceedings of the National Academy of Sciences (PNAS)*, 113(31):8849–54, 2016.

[15] Srinivasan M.V. Honeybees as a model for the study of visually guided flight, navigation, and biologically inspired robotics. *Physiological reviews*, 91(2):413–60, 2011.

[16] Bhagavatula P.S., Claudianos C., Ibbotson M.R., and Srinivasan M.V. Optic Flow Cues Guide Flight in Birds. *Current Biology*, 21(21):1794–1799, 2011.

[17] Schiffner I. and Srinivasan M.V. Direct Evidence for Vision-based Control of Flight Speed in Budgerigars. *Scientific Reports*, 5(1):10992, 2015.

[18] Duchon A.P. and Warren W.H. A visual equalization strategy for locomotor control: of honeybees, robots, and humans. *Psychological Science*, 13(3):272–8, 2002.

[19] Altshuler D.L. and Srinivasan M.V. Comparison of visually guided flight in insects and birds. *Frontiers in Neuroscience*, 12(157):1–11, 2018.

[20] C Scholtyssek, M Dacke, R Kröger, and E Baird. Control of self-motion in dynamic fluids: fish do it differently from bees. *Biology Letters*, 10:20140279, 2014.

[21] Hester F.J. Visual contrast thresholds of the goldfish (*Carassius auratus*). *Vision Research*, 8(10):1315–1336, 1968.

[22] Neumeyer C. Wavelength dependence of visual acuity in goldfish. *Journal of Comparative Physiology A: Neuroethology, Sensory, Neural, and Behavioral Physiology*, 189(11): 811–821, 2003.

[23] Breck J.E. and Gitter M.J. Effect of Fish Size on the Reactive Distance of Bluegill (*Lepomis macrochirus*) Sunfish. *Canadian Journal of Fisheries and Aquatic Sciences*, 40(2): 162–167, 1983.

[24] Bleckmann H. and Zelick R. Lateral line system of fish. *Integrative Zoology*, 4(1):13–25, 2009.

[25] Walls M.L. and Layne J.E. Direct evidence for distance measurement via flexible stride integration in the fiddler crab. *Current biology*, 19(1):25–9, 2009.

[26] Mittelstaedt M-L. and Mittelstaedt H. Idiothetic navigation in humans: estimation of path length. *Experimental Brain Research*, 139(3):318–332, 2001.

[27] Durgin F.H., Akagi M., Gallistel C.R., and Haiken W. The precision of locomotor odometry in humans. *Experimental Brain Research*, 193(3):429–36, 2009.

[28] Wittlinger M., Wehner R., and Wolf H. The ant odometer: stepping on stilts and stumps. *Science*, 312(5782):1965–7, 2006.

[29] Wittlinger M., Wehner R., and Wolf H. The desert ant odometer: a stride integrator that accounts for stride length and walking speed. *The Journal of Experimental Biology*, 210(Pt 2):198–207, 2007.

[30] Liao J.C. A review of fish swimming mechanics and behaviour in altered flows. *Philosophical Transactions of the Royal Society of London. Series B, Biological Sciences*, 362 (1487):1973–93, 2007.

[31] Burt de Perera T. and Holbrook R.I. Three-dimensional spatial representation in freely swimming fish. *Cognitive Processing*, 13:S107–11, 2012.

[32] Jeffery K.J., Jovalekic A., Verriotis M., and Hayman R. Navigating in a three-dimensional world. *The Behavioral and Brain Sciences*, 36(5):523–43, 2013.

[33] Jovalekic A., Hayman R., Becares N., Reid H., Thomas G., Wilson J., and K. Jeffery. Horizontal biases in rats' use of three-dimensional space. *Behavioural Brain Research*, 222(2):279–88, 2011.

[34] Flores-Abreu I.N., Hurly T.A., Ainge J.A., and Healy S.D. Three-dimensional space: locomotory style explains memory differences in rats and hummingbirds. *Proceedings of the Royal Society of London B: Biological Sciences*, 281(1784), 2014.

[35] Hayman R., Verriotis M.A., Jovalekic A., Fenton A.A., and Jeffery K.J. Anisotropic encoding of three-dimensional space by place cells and grid cells. *Nature Neuroscience*, 14(9):1182–8, 2011.

[36] Jeffery K.J. Distorting the metric fabric of the cognitive map. *Trends in Cognitive Sciences*, 19(6):300–1, 2015.

[37] Jeffery K.J., Wilson J.J., Casali G., and Hayman R.M. Neural encoding of large-scale three-dimensional space-properties and constraints. *Frontiers in Psychology*, 6(927): 1–12, 2015.

[38] Burt de Perera T., Holbrook R., Davis V., Kacelnik A., and Guilford T. Navigating in a volumetric world: metric encoding in the vertical axis of space. *The Behavioral and Brain Sciences*, 36(5):546–7, 2013.

[39] Ulanovsky N. Neuroscience: How Is Three-Dimensional Space Encoded in the Brain? *Current Biology*, 21(21):R886–R888, 2011.

[40] Yartsev M. M. and N. Ulanovsky. Representation of Three-Dimensional Space in the Hippocampus of Flying Bats. *Science*, 340(6130):367–372, 2013.

[41] Finkelstein A., Derdikman D., Rubin A., Foerster J.N., Las L., and Ulanovsky N. Three-dimensional head-direction coding in the bat brain. *Nature*, 517:159–164, 2015.

[42] Holbrook R.I. and Burt de Perera T. Separate encoding of vertical and horizontal components of space during orientation in fish. *Animal Behaviour*, 78(2):241–245, 2009.

[43] Davis V. A., Holbrook R. I., Schumacher S., Guilford T., and Burt de Perera T. Three-dimensional spatial cognition in a benthic fish, corydoras aeneus. *Behavioural Processes*, 109(PB):151–156, 2014.

[44] Holbrook R.I. and Burt de Perera T. Three-dimensional spatial cognition: information in the vertical dimension overrides information from the horizontal. *Animal Cognition*, 14(4):613–9, 2011.

[45] Taylor G.K., Holbrook R.I., and Burt de Perera T. Fractional rate of change of swimbladder volume is reliably related to absolute depth during vertical displacements in teleost fish. *Journal of the Royal Society, Interface / the Royal Society*, 7(50):1379–82, 2010.

[46] Holbrook R.I. and Burt de Perera T. Fish navigation in the vertical dimension: can fish use hydrostatic pressure to determine depth? *Fish and Fisheries*, 12(4):370–379, 2011.

[47] Rodríguez F., López J.C., Vargas J.P., Broglio C., Gómez Y., and Salas C. Spatial memory and hippocampal pallium through vertebrate evolution: insights from reptiles and teleost fish. *Brain Research Bulletin*, 57(3-4):499–503, 2002.

[48] Salas C., Broglio C., Durán E., Gómez A., Ocaña F.M., Jiménez-Moya F., and Rodríguez F. Neuropsychology of Learning and Memory in Teleost Fish. *Zebrafish*, 3 (2):157–171, 2006.

[49] Broglio C., Rodriguez F., and Salas C. Spatial cognition and its neural basis in teleost fishes. *Fish and Fisheries*, 4(3):247–255, 2003.

[50] Salas C., Rodríguez F., Vargas J.P., Durán E., and Torres B. Spatial learning and mem-

ory deficits after telencephalic ablation in goldfish trained in place and turn maze procedures. *Behavioral Neuroscience*, 110(5):965–80, 1996.

[51] Vargas J.P., Rodriguez F., Lopez J.C., Arias J.L., and Salas C. Spatial learning-induced increase in the argyrophilic nucleolar organizer region of dorsolateral telencephalic neurons in goldfish. *Brain Research*, 865(1):77–84, 2000.

[52] Moser E.I. and Moser M-B. A metric for space. *Hippocampus*, 18(12):1142–56, 2008.

[53] Moser E.I., Kropff E., and Moser M-B. Place cells, grid cells, and the brain's spatial representation system. *Annual Review of Neuroscience*, 31:69–89, 2008.

[54] McNaughton B.L., Battaglia F.P., Jensen O., Moser E.I., and Moser M-B. Path integration and the neural basis of the 'cognitive map'. *Nature Reviews. Neuroscience*, 7(8): 663–78, 2006.

[55] Jacob P-Y., Gordillo-Salas M., Facchini J., Poucet B., Save E., and Sargolini F. Medial entorhinal cortex and medial septum contribute to self-motion-based linear distance estimation. *Brain Structure and Function*, 222(6):2727–2742, 2017.

[56] O'Keefe J. and Dostrovsky J. The hippocampus as a spatial map. Preliminary evidence from unit activity in the freely-moving rat. *Brain Research*, 34(1):171–5, 1971.

[57] Fiete I.R., Burak Y., and Brookings T. What grid cells convey about rat location. *The Journal of neuroscience : the official journal of the Society for Neuroscience*, 28(27):6858–71, 2008.

[58] Vinepinsky E., Donchin O., and Segev R. Wireless electrophysiology of the brain of freely swimming goldfish. *Journal of Neuroscience Methods*, 278:76–86, 2017.

Appendices

$\sim$ Page left blank intentionally $\sim$

Appendix A

Supplementary Information: Teleost fish can accurately estimate distance travelled.

Supplementary Information: Teleost fish can accurately estimate distance travelled

C. Karlsson[1], J.K. Willis[1], M. Patel[1], and T. Burt de Perera[1]

[1]Department of Zoology, Research and Administration Building, 11a Mansfield Road, Oxford, OX1 3SZ

Contents

1 Methods: additional information **i**

1.1 Animals and husbandry details i

1.2 Detailed set-up iii

2 Individual fish learning curves **v**

3 Individual fish distance estimates **vii**

4 Testing assumptions **ix**

4.1 t-test ix

4.2 Linear mixed effects models x

5 Use of external cues for distance estimation **xi**

1 Methods: additional information

1.1 Animals and husbandry details

Rhinecanthus aculeatus is a marine fish from the order Tetraodontiformes which typically occupies well-lit intertidal zones of the Indo-Pacific Ocean. Such an environment is spatially complex and unstable, undergoing sporadic and sometimes rapid change. This may reduce reliance on external landmark cues for navigation purposes, making distance estimation and path integration important navigation mechanisms.

Five experimentally naive individuals were sourced from coastal reefs on the Maldives through a local supplier. The age of these wild-caught individuals could not be ascertained, but a standard size of 10 to 14cm (standard length) was used. Fish were individually housed in large aquaria measuring 0.45m wide x 0.30m high x 0.75m long as both males and females are known to defend individual territories. Individual housing prevented stress and injury to subordinate individuals.

Tank enrichment and feeding protocols were designed following a period of field work tracking individual Picasso triggerfish as they explored their territories on coastal reefs in Australia (Lizard Island), work led by Cait Newport, Department of Zoology, University of Oxford. Tanks were filled with a base mixture of sand and coral gravel to encourage digging and nest building behaviours, and large coral rocks and caves provided hiding refuges. All tested individuals were observed to nest build and use these hiding places.

Fish were fed a varied seafood diet alongside a complete pellet food. Pellet food was provided as standardised rewards during experiments. At the end of each experiment day, they were provided with krill, lance fish, squid, and mussels fed from tweezers and as scatter feeds as enrichment to encourage foraging. Once weekly individuals were provided with whole cockles, and empty shells were left in the tanks as additional enrichment. This diet was designed following observations of feeding habits in the wild, and in consultation with the university vets and aquarium specialists.

Tanks were aerated through individual airlines to ensure enough oxygen was sup-

plied, and all tanks were connected through a communal recirculation system to ensure standardised water parameters and constant water flow through the tanks.

Tanks were cleaned twice weekly and water quality tested on a weekly basis. Ammonia and Nitrite were kept at 0ppm and Nitrate was kept below 15ppm. Salinity varies between 32 and 37 parts per thousand (ppt) in the Indian Ocean, so was maintained at 35ppt.

These procedures ensured fish were kept as naturally as possible in the laboratory to ensure we were assessing natural behaviours.

1.2 Detailed set-up

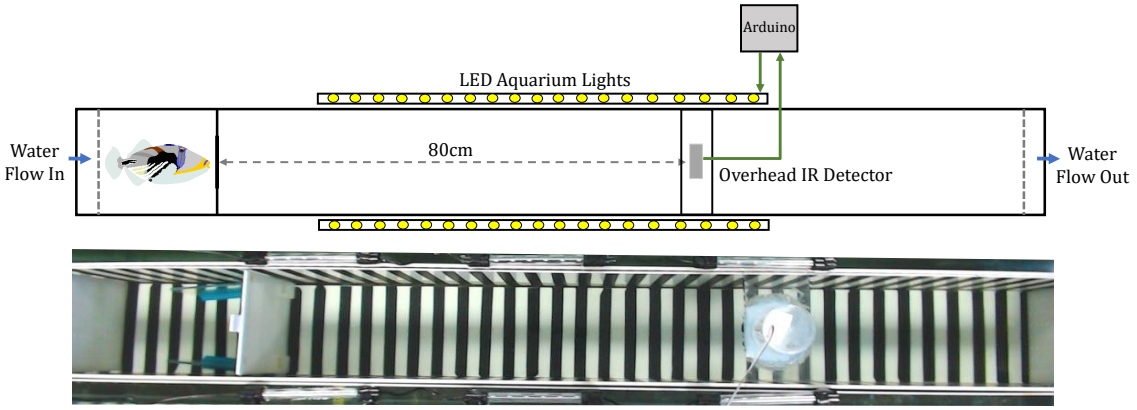


Figure 1: Top: Distance estimation task basic training set-up. The linear maze was constructed inside a flow-through tank, with water flow in behind the start area (blue inlet arrow) and passive water flow out at the opposite end of the tank (blue outlet arrow). Perforated white screens separated the fish from the inlet and outlet pipes and ensured laminar flow. The maze walls and floor were lined with alternating black and white stripes of width 0.02m to provide constant optic flow information. The fish was placed in a movable start area and was trained to swim to an overhead infrared detector, which via an Arduino microprocessor caused the surrounding aquarium lights to switch on. The fish was trained to return to the start area for a food reward once the lights had switched on. An overhead camera recorded distance estimates during the testing phase. Bottom: Overhead photo of main set-up in position +20. Two perforated white screens either end ensure laminar flow and prevent the fish from seeing outside of the tank. The start area is 0.30m long, and the overhead infrared detector sits overhead 0.80m from the start area doorway. This in turn controls aquarium lights running along the top of the maze walls symmetrically on either side.

A linear Perspex maze measuring 0.25m high x 0.16m wide x 1.80m long was built within a flow-through tank connected to the home water system to maintain constant water parameters (fig. 1). The walls and floor were patterned with regular black and white stripes made from non-toxic waterproof black craft vinyl of width 0.02m to provide basic visual contrast information, as many species have been shown to have impaired distance estimation abilities in the absence of optic flow. A perforated white screen was placed at either end to create laminar water flow whilst blocking the visual stimuli provided by cues external to the tank or the inlet and outlet pipes themselves. A moveable start area

of dimensions 0.25m high x 0.16m wide x 0.30m long could be placed in one of three start area positions, all 0.1m apart. Figure 1, bottom, is an overhead photo of the main set-up in position +20. An infrared detector (SHARP 2Y0A21 proximity sensor) was then placed at water level overhead, 0.80m from the start area doorway. This was attached to an Arduino microprocessor, which through a Matlab (Mathworks Inc.) program controlled aquarium lights (Interpret Triple LED Lighting System, 0.75m) running along the top of the lateral maze walls. The voltage of the infrared (IR) detector varied between 0V and 3.5V depending on the strength of the reflection from objects which passed in front of it. We tested the response of the detector to objects in water and after this we set a threshold of 1.7V. As the fish passed beneath the detector, a voltage change was registered and when this exceeded 1.7V, the aquarium lights switched on. A Point Grey Grasshopper 3M camera (FLIR Machine Vision Cameras) was placed 1.1m above the water level to record testing trials.

2 Individual fish learning curves

After pre-training and habituation to the experiment set-up, full training was split into four main phases as follows:

Phase I: A food reward was presented using tweezers at the infrared detector as soon as the light had been switched on. Upon receipt of this first reward, food was also immediately presented in the start area. This was to teach the fish to return to the start area when the light stimulus was turned on.

Phase II: As fish learned the association between the light and food, the reward was presented only in the start area once the light was switched on. A food reward was never provided in the start area if the fish swam further than the infrared detector before turning home.

Phase III: Food was subsequently presented increasingly later during the return journey once the fish had turned 180 degress from switching on the light to return to the start area.

Phase IV: By the end of training the fish had to swim to the infrared detector to turn on the lights, immediately return to the start area and have the door closed behind them before the food reward was provided.

The rate of learning varied between fish (36-92 full training sessions), but all fish had completed training and testing within 6 months of being brought into the lab from the wild. Figure 2a-f below shows the learning curves for all five fish, with progression through the four training phases indicated by blue vertical lines. Fish progressed from one training phase to the next if they performed at 80% proficiency in the preceding session, whilst completing the minimum requirement of 10 successful trials (ie a minimum of 10/12 performance). Fish reached testing criterion (highlighted by the red vertical line) once they could complete three consecutive sessions in Phase IV of training at 80% proficiency, with a minimum of 10 successful trials within each session.

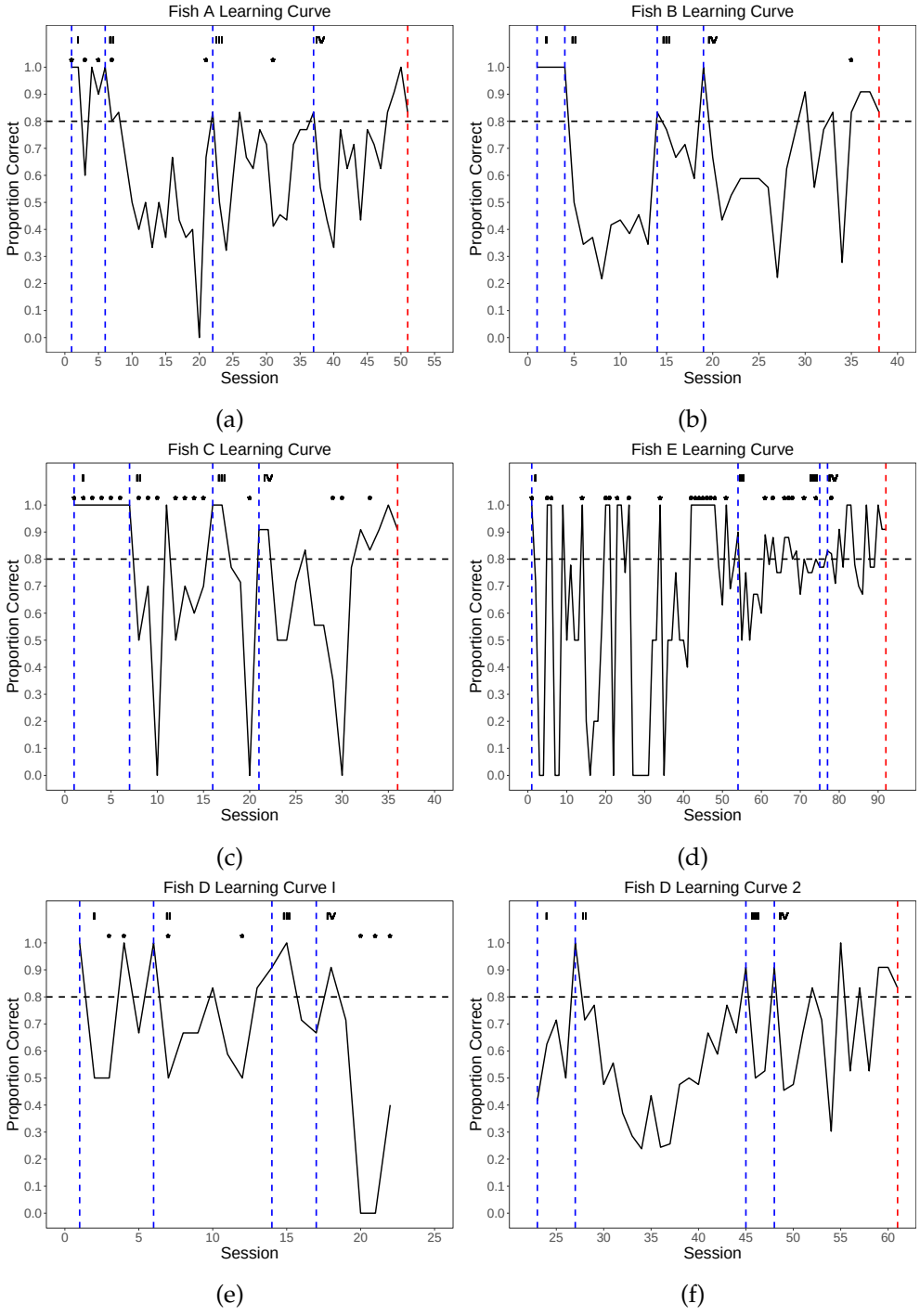


Figure 2: Learning curves for 5 fish prior to testing in a distance estimation task. Blue vertical lines indicate progression to the next training phase. The red vertical line highlights the fish reaching testing criterion. Asterixes indicate training sessions where fish failed to reach the minimum trial number to proceed to the next phase (at least 10 sucessful trials needed to be completed). The black horizontal line indicates progression criterion of 80%. Fish D (e. and f.) was split into two training blocks before and after the Christmas vacation.

Fish	Average Distance Estimate (m)	Standard Deviation
A	0.810	0.119
B	0.835	0.0990
C	0.744	0.142
D	0.786	0.0648
E	0.826	0.108

Table 1: Average distance estimates and standard deviations for fish A-E (given to 3sf).

3 Individual fish distance estimates

Values of average distance estimates and standard deviations for all tested fish are in table 1, and individual distance estimate distributions are shown in fig. 3

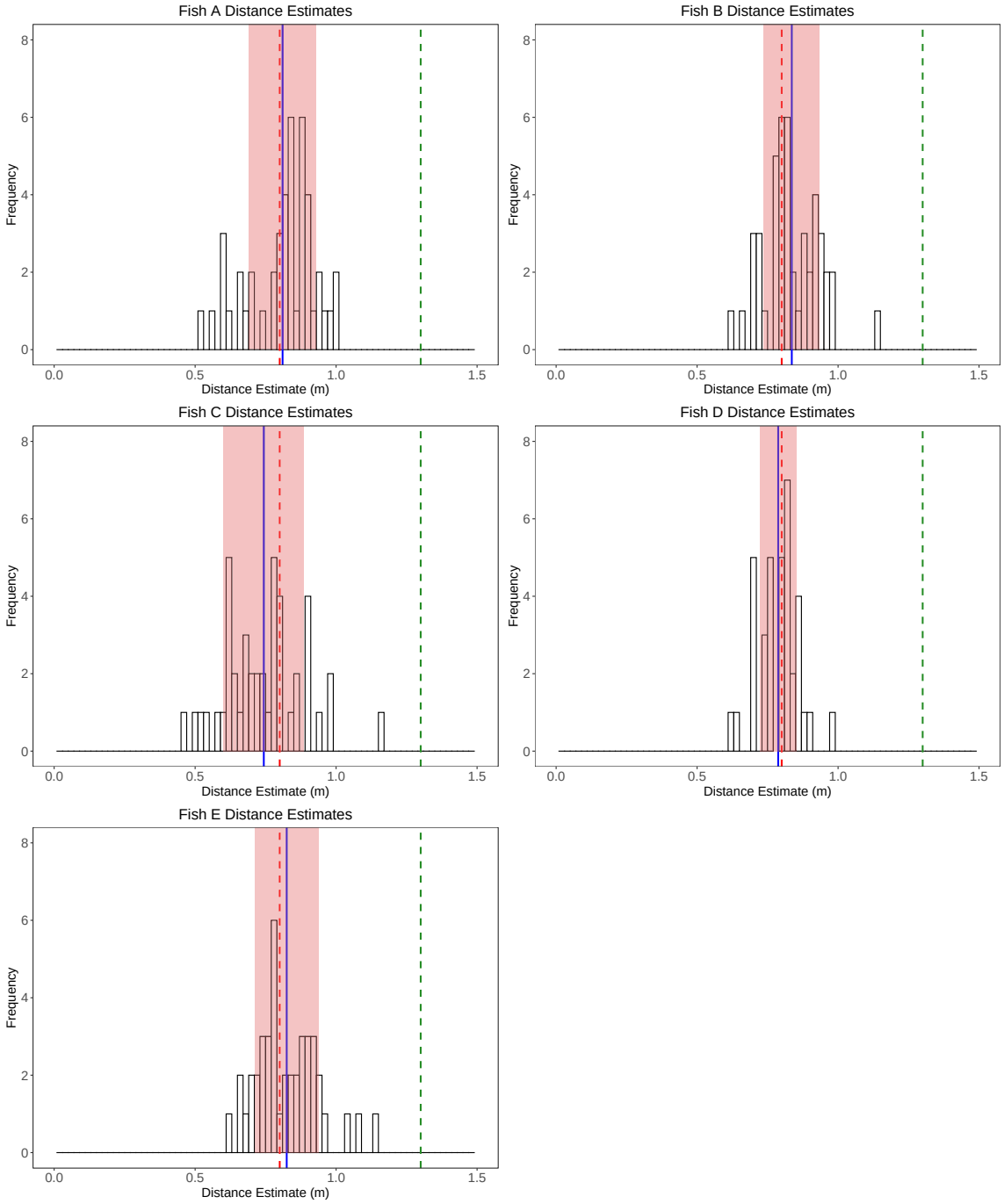


Figure 3: Distance estimate distributions for fish A-E. Average distance estimate = blue solid line, target distance (0.80m) = red dashed line, decoy position of infrared detector = green dashed line. Red shading indicates the standard deviations of the average distance estimate.

4 Testing assumptions

4.1 t-test

Data points (average distance estimates, fish A-E), were independent and distance estimates were normally distributed (Shapiro-Wilk normality test, W = 0.925 (3sf), p=0.566 (3sf)), fig. 4. Parametric tests could therefore be used to test the distance estimates against the target distance of 80cm.

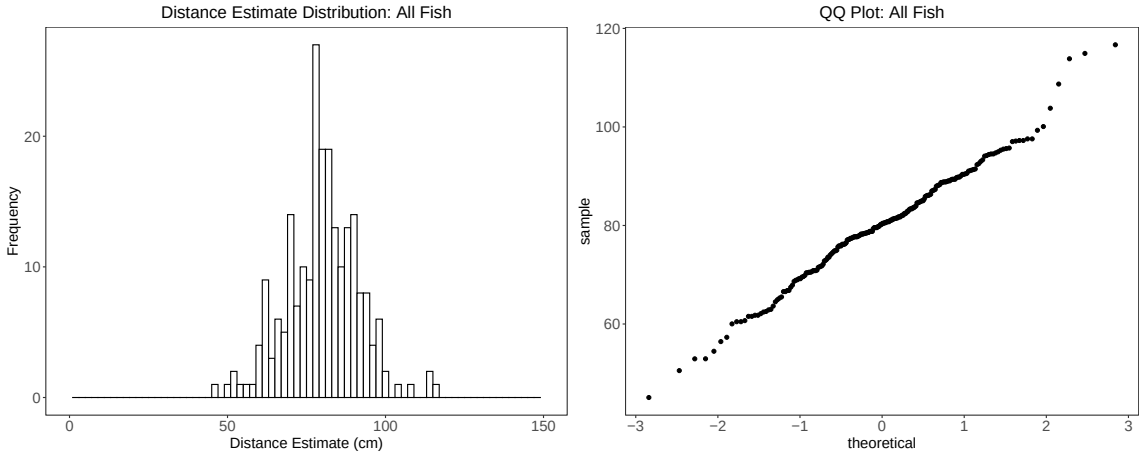


Figure 4: Normal qq plot providing an indication of the normality of distance estimates, allowing us to use parametric tests for analysis of distance estimates.

4.2 Linear mixed effects models

We ascertained that models described in the analysis adhered to the assumptions of linear mixed effects modelling. All data was inspected visually to ascertain that the data was normally distributed, and fitted accordingly using gaussian distributions. Models were subsequently tested to ensure they met three key criteria, as outlined below.

Normality of residuals

Model residuals were required to be normally distributed. Histograms of residuals and qqplots of standard normal quantiles against standardised residuals were visually inspected. Residuals were deemed to be normally distributed if the majority of points on the qqplot followed the central 1:1 straight line, but small deviations of the tails from the 1:1 line were permitted. Small deviations of tails in the same direction from the qqplot 1:1 line would indicate a slight left or a right skew, but tails deviating in opposite directions simply reflect 'fat' or 'thin' tails to the normal distribution.

Linearity

Data was required to show a linear variation with model predictors. To test this, model residuals were plotted against the model predictor, and linearity was ascertained if the points were randomly distributed and no clear linear pattern emerged.

Homogeneity of variances

Finally, variances were required to be homogeneous for all values of the predictor variable. The fitted model data was plotted against the model residuals, and points should be equally distributed above and below the 0.00 line. All models met this criterion.

5 Use of external cues for distance estimation

A linear mixed effects model was used used to assess whether fish were generalising across the three start area positions (+0, +10 and +20): Absolute Estimate Point = Start Area Position (Fixed Effect) + Fish (Random Effect). Start area position was a good predictor of the absolute estimate point within the tunnel across fish: $F_{210,2}$=58.8 (3sf), $p<0.001$, but some residual variation was explained by individual variation between fish (Likelihood Ratio Test with and without random effect = 7.63, p=0.00575 (3sf)). Figure 5 shows the absolute turning position for the three start area positions across all five fish. This confirms that our fish are not generalising across the start area positions, but are more likely to be using metric distance information.

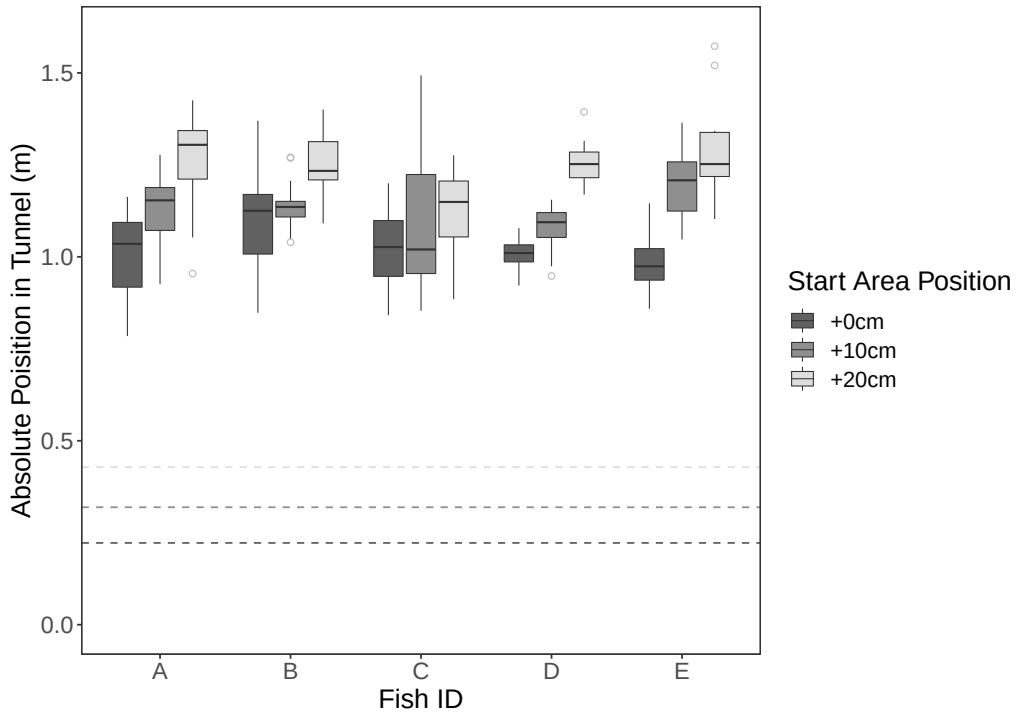


Figure 5: Absolute distance estimate position within the tunnel maze, split by start area position and fish identity. The start area moved between three positions: +0cm (dark grey), +10cm (mid-grey) and +20cm (light grey), all moving distally through the tunnel in 0.10m increments - the dashed lines indicate the position of the start area doorway from the back of the tunnel.

$\sim$ Page left blank intentionally $\sim$

Appendix B

Supplementary Information: Visual odometry in a freely swimming fish.

Supplementary Information: Visual odometry in a freely-swimming fish

C. Karlsson[1] and T. Burt de Perera[1]

[1]Department of Zoology, Research and Administration Building, 11a Mansfield Road, Oxford, OX1 3SZ

Contents

1 Methods: additional information **i**

1.1 Controlling for use of external cues i

1.2 Study species and population sampling ii

1.3 Full distance training protocol iv

2 Results: additional information **vi**

2.1 Distance estimates across visual treatments vi

2.2 Absolute turning position by starting area position across visual treatments vii

2.3 Distance estimate variability x

2.4 Swimming speed across visual treatments xi

1 Methods: additional information

1.1 Controlling for use of external cues

The start area was moved between three different positions within the tunnel to prevent the fish from being able to use positional cues internal or external to the maze. Each session the start area and infrared proximity sensory moved within the tunnel to a new position. These are as follows: +0 - the baseline positon with the rear perforated screen 0.02m from the rear of the tank; +10 - 10cm distal movement from the baseline +0 position; +20 - 20cm distal movement from the baseline +0 position. The rear perforated screen was shifted accordingly to maintain the start area length at 0.3m. This was to account for different individuals starting their distance estimates at different points within the start area. Figure 1 is a schematic of these positions.

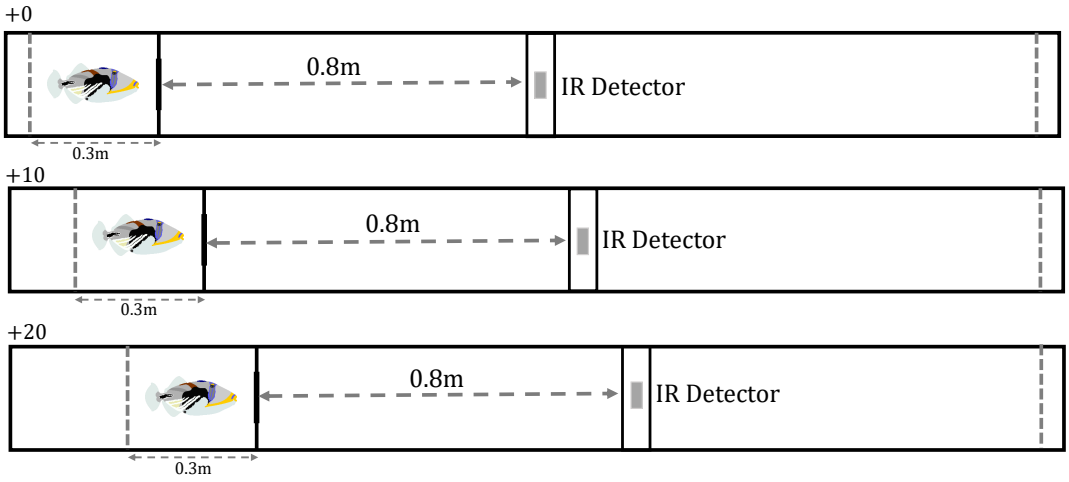


Figure 1: Schematic of the three start area positions. Each position is located increasingly distally through the tunnel by 0.10m increments (labelled +0, +10 and +20). The rear perforated white screen moves accordingly to ensure the start area length is kept at 0.30m. The infrared detector also moves accordingly to maintain the target distance of 0.80m.

1.2 Study species and population sampling

The Picasso triggerfish, *Rhinecanthus aculeatus*, was chosen as our study species as it has proven to be trainable in complicated long-term experiments, and responds well to training in operant conditioning paradigms[1,2]. Individuals are also naturally territorial, with males defending discrete territories with female harems. Within these harems, females defend their own territories within the larger male territory. This makes them amenable to individual housing without compromising welfare and altering natural behaviours.



Figure 2: An experimental subject used in experiments, hiding behind tank enrichment. Photo taken by J.K. Willis.

Tank design and enrichment was designed following a period of field work filming Picasso triggerfish in their natural environment on reefs off Lizard Island in Australia (work led by Cait Newport, 2018). Individuals were housed in tanks measuring 0.45m width x 0.35m height x 0.75m length with coral gravel, sand, rocks and caves provided for enrichment. All tanks were provided with an individual airline to ensure sufficient aeration, and were inter-connected to a communal sump system ensuring high flow and water cycling. Tanks were cleaned twice weekly, with water parameters monitored weekly (Nitrates at max 15ppm, Nitrite at 0ppm, Ammonia at 0ppm, and salinity at 35ppt). Fish were rewarded with Ocean Nutrition formula one and two pellets and krill pacifica during experiments, and supplemented with a diet of krill, lance fish and cockles at the end

of each training day. Supplement feeds were given as a combination of tweezer feeds and scatter feeds to encourage active foraging.

Power analysis was conducted prior to experiments to estimate required sample size and minimise the number of individuals used to answer the question. Initial sample size was calculated using the 'pwr' package in R (The R project, version 3.6.1). To achieve a power of 80%, with a significance level of 0.05 for a large predicted effect size (set at 0.8, using the Cohen 1988 approximation[3]), with four treatment levels, the required sample size was calculated as 5.3 individuals.

We tested 6 individuals that had previously undergone behavioural training in a distance estimation accuracy task[4]. All had been housed in captivity for under 9 months by experiment completion. All fish were of similar size (10-14cm standard length), but as they were wild-caught we could not determine sex or age. All fish underwent a standard 4-week quarantine procedure prior to inclusion in the main aquarium system to ensure only healthy individuals were used in experiments. Pre-training involved teaching the fish to associate tweezers with food, and all fish were trained to swim voluntarily into a 2l container to transfer them between their home tank and experiment tank without causing stress.

In the main experiment, fish were trained up to testing criterion (80% performance across 3 consecutive sessions), and were subsequently tested in their abilities to reproduce learned distances across four visual treatments, one after the other. Treatments were provided as follows: Test 1 (0.02m stripes), training condition; Test 2 (0.01m stripes); Test 3 (0.02m checkerboard); Test 4 (horizontal stripes). Four fish (ID: A, B, D and E) completed all four testing treatments, but Fish C and F experienced loss of motivation and were unable to continue the distance estimation task following Test 2 and Test 3 respectively. These fish were unable to reliably complete the 5 training trials at 80% accuracy that preceded each block of 5 testing trials. When this continued across over 10 consecutive sessions, fish were removed from experiments. Sample sizes across treatments were therefore as follows:

Treatment 1 (0.02m stripes, baseline): 6 fish

Treatment 2 (0.01m stripes): 6 fish

Treatment 3 (horizontal stripes): 5 fish

Treatment 4 (0.02m checkerboard): 4 fish

Post-hoc power simulation analysis using the R package, 'simr', assessed the actual observed power of the results produced, given the true effect sizes. A simulation on the generalised linear mixed effects model assessing the effect of the fixed effect of treatment and random effect of fish ID on distance estimates was carried out first with 100 iterations and again with 1000 iterations. The 95% confidence interval for observed power was 96.38-100.00 for 100 iterations and 99.30-100.00 for 1000 iterations. We therefore conclude that the desired power was achieved even under the modified sample size.

1.3 Full distance training protocol

Fish were trained according to a distance estimation accuracy task developed for use with this species[4]. Following a period of pre-training, involving fish learning the association between tweezers and food and being trained to voluntarily swim into a 2l transport container for a food reward, fish were trained to swim 0.80m to an overhead infrared detector to switch on the aquarium lights and return home for a food reward (main text, figure 1).

Initially, fish were rewarded at the infrared detector concurrently with the light flash and then immediately provided with a food reward in the start area. This was to teach fish that they had to swim out as far as the infrared detector and then return home for a food reward. As they learned the association between the light and food, a reward was then presented only in the start area as the light was switched on. Food was subsequently presented increasingly later during the return journey. By the end of training, the fish had

to return to the start area and the door closed before the food reward was provided. Training sessions lasted until 10 correct trials were complete or until 10 minutes had passed, whichever came first. Fish were deemed to have completed training when they swam directly out to the light and returned fully to the start area prior to being presented with and given a food reward on 80% of trials in three consecutive sessions.

Comparison	z-ratio	p-value
Test 1 (0.02m stripes): Test 2 (0.01m stripes)	-18.3	<0.001
Test 1 (0.02m stripes): Test 3 (0.02m check)	-2.77	0.0286
Test 1 (0.02m stripes): Test 4 (horizontal stripes)	5.91	<0.001
Test 2 (0.01m stripes): Test 3 (0.02m check)	14.7	<0.001
Test 2 (0.01m stripes): Test 4 (horizontal stripes)	22.3	<0.001
Test 3 (0.02m check): Test 4 (horizontal stripes)	8.05	<0.001

Table 1: Pairwise comparisons of visual treatments, using the Tukey method for comparing a family of four estimates. All pairwise comparisons indicate significant differences.

2 Results: additional information

All results were analysed using the program R (The R Project, version 3.6.1) and mixed effects models were constructed using the 'lmer' and 'car' packages.

2.1 Distance estimates across visual treatments

To assess the effect of visual treatment on distance estimate distributions, a generalised linear mixed effects model was fitted by maximum likelihood (Laplace approximation) with a gamma distribution family. Visual test treatment was a fixed effect and fish identity was a random effect. A type II Wald Chisquare test revealed the overall model to be significant (χ^2_3 = 510, p<0.001). Subsequent Tukey pairwise comparisons identified significant treatment effects (table 1).

Inspection of the mixed effects distance estimate model indicated that the assumptions of testing were met. Selecting a gamma distribution ensured model residuals were normally distributed, ascertained by inspecting a qq-plot and histogram of residuals which revealed a better fit than when a gaussian distribution family was used in the original model.

2.2 Absolute turning position by starting area position across visual treatments

If fish perceived themselves to be estimating distance, then there would be consistent systematic shifts in absolute turning position within the tunnel according to start area position. Data was best modelled with a gamma distribution, and generalised linear mixed effects models were constructed for each visual treatment, assessing the effect of start area position on absolute turning position (Absolute turning positon = Start Area Position (fixed effect) + Fish identity (random effect)). Type II Wald Chisquare tests revealed the overall models to be significant for all visual treatments (Test 1, χ^2_2 = 109, p$<$0.001; Test 2, χ^2_2 = 44.4, p$<$0.001; Test 3, χ^2_2 = 81.3, p $<$0.001; Test 4, χ^2_2 = 7.87, p = 0.0196).

However, Tukey pairwise comparisons identified that stepwise significant differences for all three start area positions were only observed for the three treatments where translational spatial frequency information was provided across all tested individuals (Test 1, Test 2 and Test 3), table 2 and fig. 3a-c. Removing translational spatial frequency in test 4 resulted in significant pairwise comparisons only being observed for the comparison between start area position +0 and +20. To be certain that fish are estimating distance, all pairwise treatments need to be significantly different. Inspecting individual fish responses across test treatments can explain the apparent shifting trend in test 4 (fig. 3d). Fish A, B and F exhibit no consistent pairwise shifts according to start area position. For Fish A, the median turning position increases between position +0 and +10, but declines again for position +20. A similar trend is observed for Fish F. Fish B demonstrates no shift between position +0 and +10, and only a very small shift in position +20. The significant trend is therefore likely to be driven by the random effects of Fish D and E. Fish D and E swam to the end of the tunnel on some but not all trials. Trials in which fish swam to the end of the tunnel coincided with the start area in positions +10 and +20 for Fish D and +20 for Fish E.

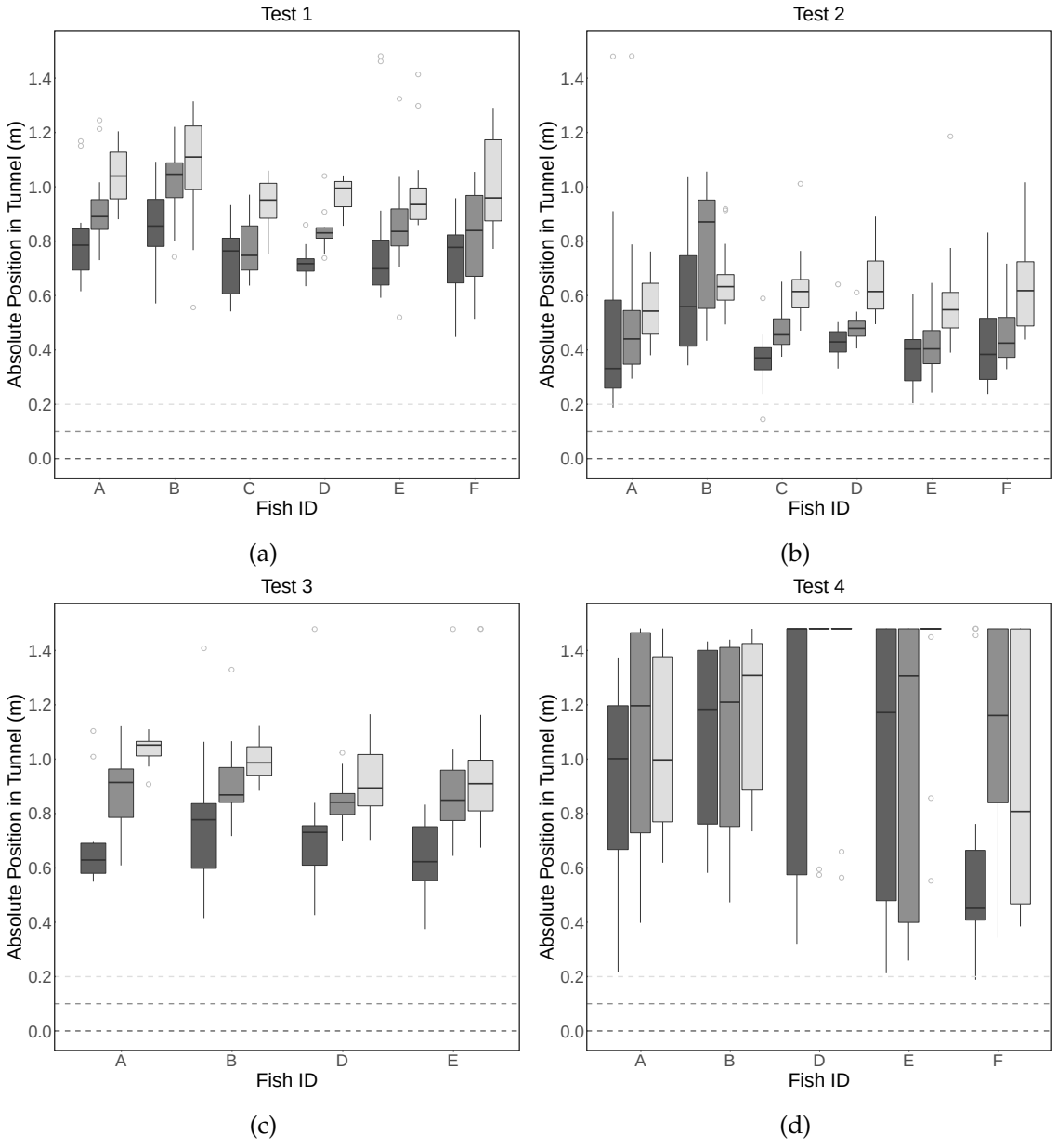


Figure 3: Absolute turning positions for individual fish across start area positions. Pairwise shifts are observed across almost all individuals for Tests 1-3 where translational optic flow information is provided (a) - (c). When translational optic flow information was removed (d), there were no consistent shifts in turning position, with a high variability in response across fish identities.

Model	Comparison	z-ratio	p-value
Test 1	+0 : +10	4.65	<**0.001**
Test 1	+10 : +20	5.79	<**0.001**
Test 1	+0 : +20	10.3	<**0.001**
Test 2	+0 : +10	3.40	**0.0019**
Test 2	+10 : +20	3.40	**0.0019**
Test 2	+0 : +20	6.55	<**0.001**
Test 3	+0 : +10	6.22	<**0.001**
Test 3	+10 : +20	2.70	**0.0193**
Test 3	+0 : +20	8.92	<**0.001**
Test 4	+0 : +10	2.22	0.0673
Test 4	+10 : +20	0.481	0.880
Test 4	+0 : +20	2.69	**0.0198**

Table 2: Pairwise comparisons of start area position by visual treatments, using the Tukey method for comparing a family of four estimates.

Inspection of the mixed effects models indicate that the assumptions of testing were met. A gamma distribution was selected, as the model residuals were closer to a normal distribution than when fitted with a gaussian distribution. Normality was ascertained by inspecting qq-plots and histograms of the model residuals.

Comparison	z-ratio	p-value
Test 1 (0.02m stripes): Test 2 (0.01m stripes)	-1.78	0.285
Test 1 (0.02m stripes): Test 3 (0.02m check)	1.59	0.385
Test 1 (0.02m stripes): Test 4 (horizontal stripes)	-11.7	<0.001
Test 2 (0.01m stripes): Test 3 (0.02m check)	-0.003	0.999
Test 2 (0.01m stripes): Test 4 (horizontal stripes)	-10.6	<0.001
Test 3 (0.02m check): Test 4 (horizontal stripes)	-9.19	<0.001

Table 3: Pairwise comparisons of absolute distance estimate error across visual treatments, using the Tukey method for comparing a family of four estimates.

2.3 Distance estimate variability

Analysing the distance estimate error profiles could be used to investigate the role of visual motion information for odometry. For each distance estimate produced across the four visual treatments, the residuals of estimates from the mean were calculated. These were then converted to absolute error values to permit a standardised comparison of absolute distance estimate variability across treatments. A generalised linear mixed effects model was constructed with a gamma family distribution to test the effect of visual treatment on absolute residuals (fig. 4). Treatment was designated as a fixed effect, and fish identity as a random effect. The overall model was found to be significant (χ^2_3 = 265, p<0.001), and subsequent Tukey pairwise comparisons revealed that only test 4, where fish had access to no spatial frequency information, was different from the other four treatments (table 3). This indicates that access to spatial frequency information is necessary for accurate distance estimation.

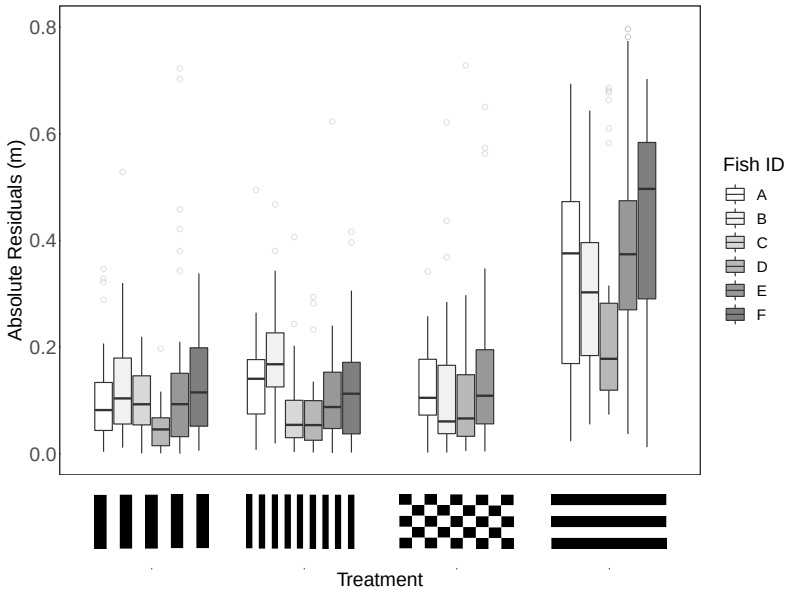
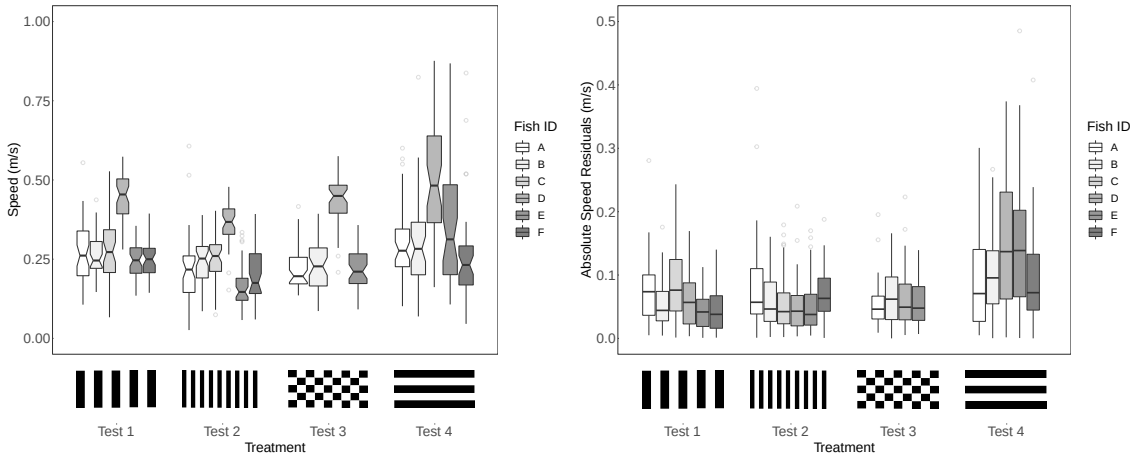


Figure 4: Absolute distance estimate error compared to treatment average. Visual treatment was a significant predictor of distance estimate error (Generalised Linear Mixed Effects model: Absolute Residual = Treatment (fixed effect) + Fish ID (random effect), Type II Wald Chisquare test: χ^2_3 = 265, p<0.001). Tukey pairwise comparisons identified that only test 4 with no spatial frequency information provided produced an absolute distance estimate error profile that was significantly different from the other test treatments (table 3). This indicates that fish rely on spatial frequency information for odometry.

2.4 Swimming speed across visual treatments

Inspecting the overall distribution for swimming speeds indicated the data to be strongly right skewed, and a gamma distribution was therefore chosen for all modelling, as it can be used for skewed continuous positive data. A generalised linear mixed effects model was selected to model swimming speed using visual treatment as a fixed effect, and fish identity as a random effect. A type II Wald Chisquare test indicated that swimming speed was found to vary with visual treatment (χ^2_3 = 116, p <0.001). Subsequent Tukey pairwise comparisons identified that swimming speeds showed small variations with spatial frequency and pattern, with high variability in responses across individuals (table 4 and fig. 5). Mean swimming speeds increased uniformly in test 4 when optic flow information was removed.



(a) (b)

Figure 5: (a) Individual swimming speeds split by treatment and fish identity. Average swimming speeds show slight sensitivity to translational spatial frequency, an effect exhibited more strongly by some individuals than others. (b) Absolute swimming speed residuals split by treatment and fish identity. Swimming speed and absolute residuals of swimming speed (a measure of swimming speed variability) increased uniformly for all fish in test 4.

To assess the effect of visual test treatment on the variance in swimming speeds, a mixed effects model with visual treatment as a fixed effect and fish identity as a random effect was constructed for the residuals of swimming speeds from the treatment means. A type II Wald Chisquare test indicated that the magnitude of swimming speed residuals varied with visual treatment (χ^2_3 = 160, p <0.001). Subsequent Tukey pairwise comparisons identified that residuals only increased in test 4 for all tested individuals, where translational optic flow information was removed (table 5).

Inspection of the mixed effects swimming speed and swimming speed residuals models indicated that the assumptions of testing were met. Selecting a gamma distribution ensured model residuals were normally distributed, ascertained by inspecting a qq-plot and histogram of residuals which revealed a better fit than when a gaussian distribution family was used in the original model.

Comparison	z-ratio	p-value
Test 1 (0.02m stripes): Test 2 (0.01m stripes)	6.16	<0.001
Test 1 (0.02m stripes): Test 3 (0.02m check)	-2.80	0.0266
Test 1 (0.02m stripes): Test 4 (horizontal stripes)	-4.44	<0.001
Test 2 (0.01m stripes): Test 3 (0.02m check)	2.71	0.0340
Test 2 (0.01m stripes): Test 4 (horizontal stripes)	-10.1	<0.001
Test 3 (0.02m check): Test 4 (horizontal stripes)	-6.75	<0.001

Table 4: Pairwise comparisons of swimming speed across visual treatments, using the Tukey method for comparing a family of four estimates. All pairwise comparisons indicate significant differences.

Comparison	z-ratio	p-value
Test 1 (0.02m stripes): Test 2 (0.01m stripes)	0.340	0.986
Test 1 (0.02m stripes): Test 3 (0.02m check)	-0.271	0.996
Test 1 (0.02m stripes): Test 4 (horizontal stripes)	9.07	<0.001
Test 2 (0.01m stripes): Test 3 (0.02m check)	-0.519	0.955
Test 2 (0.01m stripes): Test 4 (horizontal stripes)	8.82	<0.001
Test 3 (0.02m check): Test 4 (horizontal stripes)	7.81	<0.001

Table 5: Pairwise comparisons of swimming speed residuals across visual treatments, using the Tukey method for comparing a family of four estimates. Pairwise comparisons between test 4 and all other treatments indicate significant differences.

References

[1] Cheney, K. L., Newport, C., McClure, E. C. & Marshall, N. J. Colour vision and response bias in a coral reef fish. *The Journal of experimental biology* **216**, 2967–73 (2013).

[2] Newport, C. *et al.* Fish use colour to learn compound visual signals. *Animal Behaviour* **125**, 93–100 (2017).

[3] Cohen, J. *The Concepts of Power Analysis BT - Statistical Power Analysis for the Behavioral Sciences (Revised Edition)* (Hillsdale, N.J. : L. Erlbaum Associates, 1988).

[4] Karlsson, C., Willis, J., Patel, M. & Burt de Perera, T. Teleost fish can accurately estimate distance travelled. *bioRxiv* 834341 (2019).

Appendix C

Supplementary Information: Visual swimming control in the marine fish, *Rhinecanthus aculeatus*.

Supplementary Information: Visual swimming control in the marine fish, *Rhinecanthus aculeatus*

C. Karlsson[1] and T. Burt de Perera[1]

[1]Department of Zoology, Research and Administration Building, 11a Mansfield Road, Oxford, OX1 3SZ

Contents

1 Sample size and power analysis **i**

2 Individual fish tracks **iii**

3 Statistical model summaries **ix**

3.1 Model results: lateral position ix

3.2 Model results: swimming speed ix

4 Testing model assumptions **xi**

1 Sample size and power analysis

Fish were wild-caught to ensure their full evolutionary and life-history was from a natural environment. Sample size was therefore minimised to remove as few specimens from their natural habitat as possible. Based on previous experiments, the availability of visual information is known to have large effect on distance estimates (Cohen's d = 1.54, calculated from residual distance estimates from the treatment mean between treatments with optic flow and no optic flow) for *Rhinecanthus aculeatus* - see previous thesis chapter.

Observed Cohen's d values are given by:

$$\text{Cohen's d} = \frac{\bar{g_1} + \bar{g_2}}{\sigma_P}\,, \tag{1}$$

where, $\bar{g_1}$ is the mean value for treatment 1, and $\bar{g_2}$ is the mean value for treatment 2, and σ_P is the pooled standard deviation. The pooled standard deviation is calculated by:

$$\sigma_P = \sqrt{\frac{\sigma(g_1)^2 + \sigma(g_2)^2}{2}}\,, \tag{2}$$

where, $\sigma(g_1)$ is the standard deviation of treatment 1, and $\sigma(g_2)$ is the standard deviation for treatment 2. Large effect sizes are therefore hypothesised for both deviation from the central line and swimming speeds in this experiment.

A more conservative effect size estimate was then used for *a priori* power analysis in the planning stages of the experiment, using Cohen's approximation of large effect sizes at d = 0.8 [1]. Based on four way comparisons using analysis of variance, with a significance level set at 0.95 and a desired power of 0.8, 5.3 individuals would be required to achieve appropriate power (calculated using the statistics programe R, the R project, version 3.6.4). 5 individuals were therefore chosen for our experiment.

A test model on the effect of visual treatment on absolute deviation from the central line (Absolute deviation from the central line = Visual Treatment (fixed effect) + Fish ID (random effect)), was then run on data randomly generated from a normal distribution

with an average deviation of 0.010m, and standard deviation of 0.008m for the baseline treatment, and an average deviation of 0.023m (based on an effect size 1.54 times the baseline standard deviation) and accompanying standard deviation of 0.016m for three treatments where optic flow was to be removed (the standard deviation was doubled for optic flow removal treatments as this effect was observed in previous distance estimation data). The package 'simr' in the statistics program R (the R project, version 3.6.4), was subsequently used to simulate 1000 iterations of the mixed effects model to determine the observed power with the sample size of five individuals. The 95% confidence interval for the observed power for visual treatment was between 99.63% and 100.0%, indicating that five fish would be sufficient to answer this question using mixed effects modelling.

2 Individual fish tracks

Figures 1-5 below show individual tracks across visual treatments for all fish. Treatments 6.1 and 6.2 are provided on the same plot for ease of comparison, indicating high between-fish variability in lateral positioning responses to unbalanced visual information. All fish show complete datasets, with 30 trials completed for all treatments, except for Fish E which displayed strong stress responses at the end of three consecutive testing sessions for treatment 4. Testing under treatment 4 was therefore discontinued for Fish E according to ethical animal welfare practices.

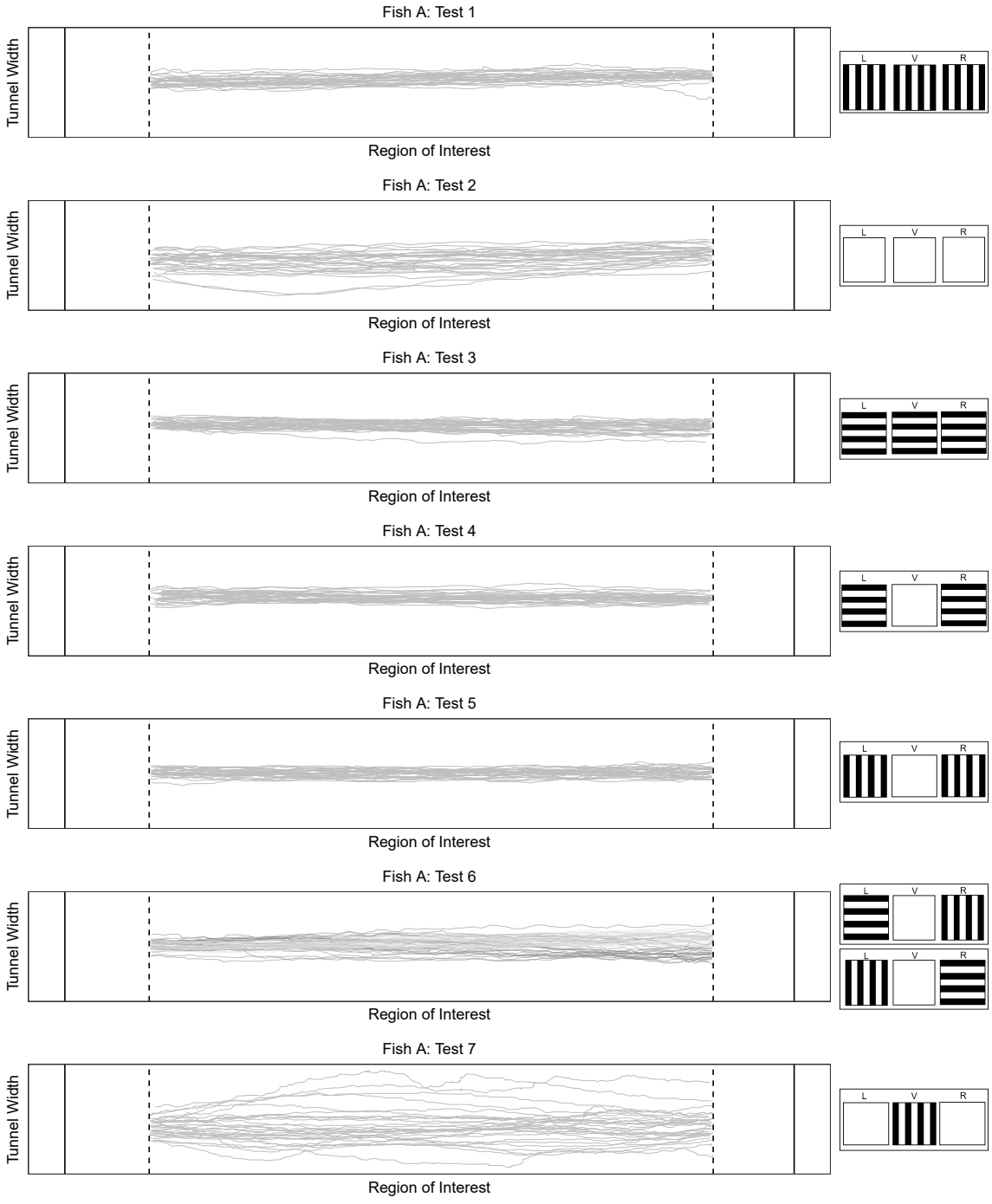


Figure 1: Individual tracks for Fish A between start areas across treatments. Tracks go from left to right. In test 6, tracks in light grey indicate test 6.1 (top image) and tracks in dark grey indicate test 6.2 (lower image). Only tracks from the region of interest, bounded by the vertical black dashed lines are shown.

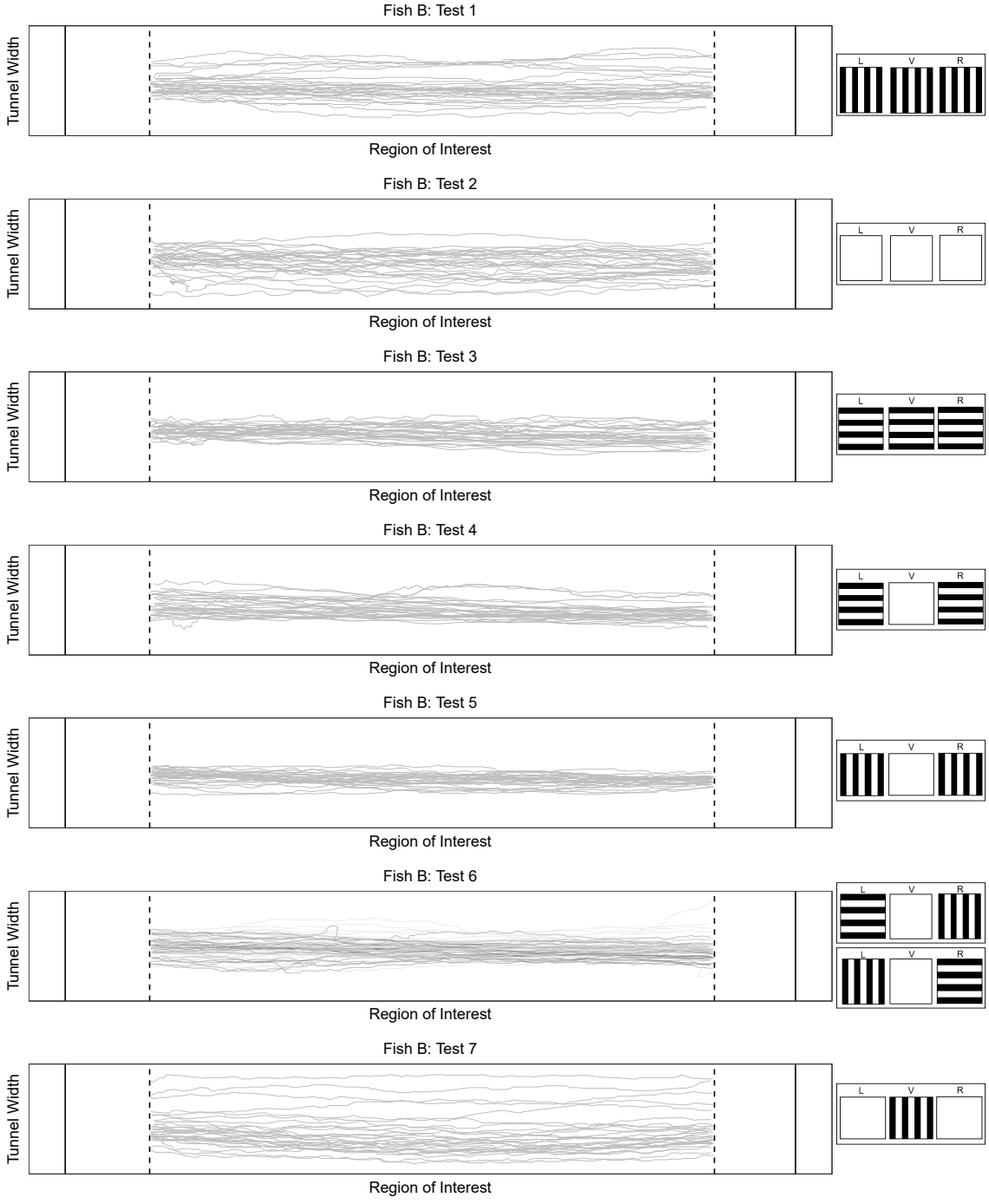


Figure 2: Individual tracks for Fish B between start areas across treatments. Tracks go from left to right. In test 6, tracks in light grey indicate test 6.1 (lower image) and tracks in dark grey indicate test 6.2 (lower image). Only tracks from the region of interest, bounded by the vertical black dashed lines are shown.

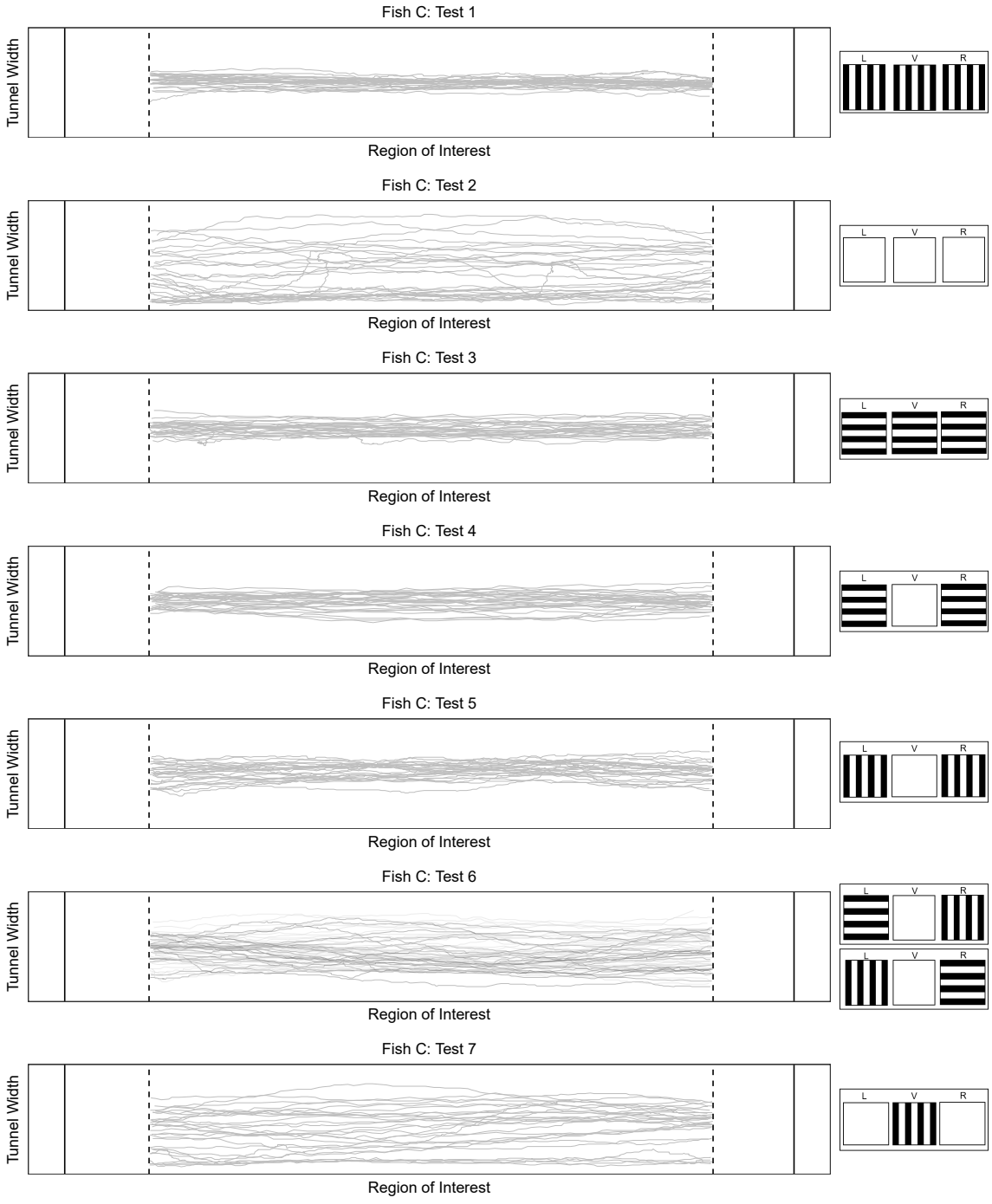


Figure 3: Individual tracks for Fish C between start areas across treatments. Tracks go from left to right. In test 6, tracks in light grey indicate test 6.1 (top image) and tracks in dark grey indicate test 6.2 (lower image). Only tracks from the region of interest, bounded by the vertical black dashed lines are shown.

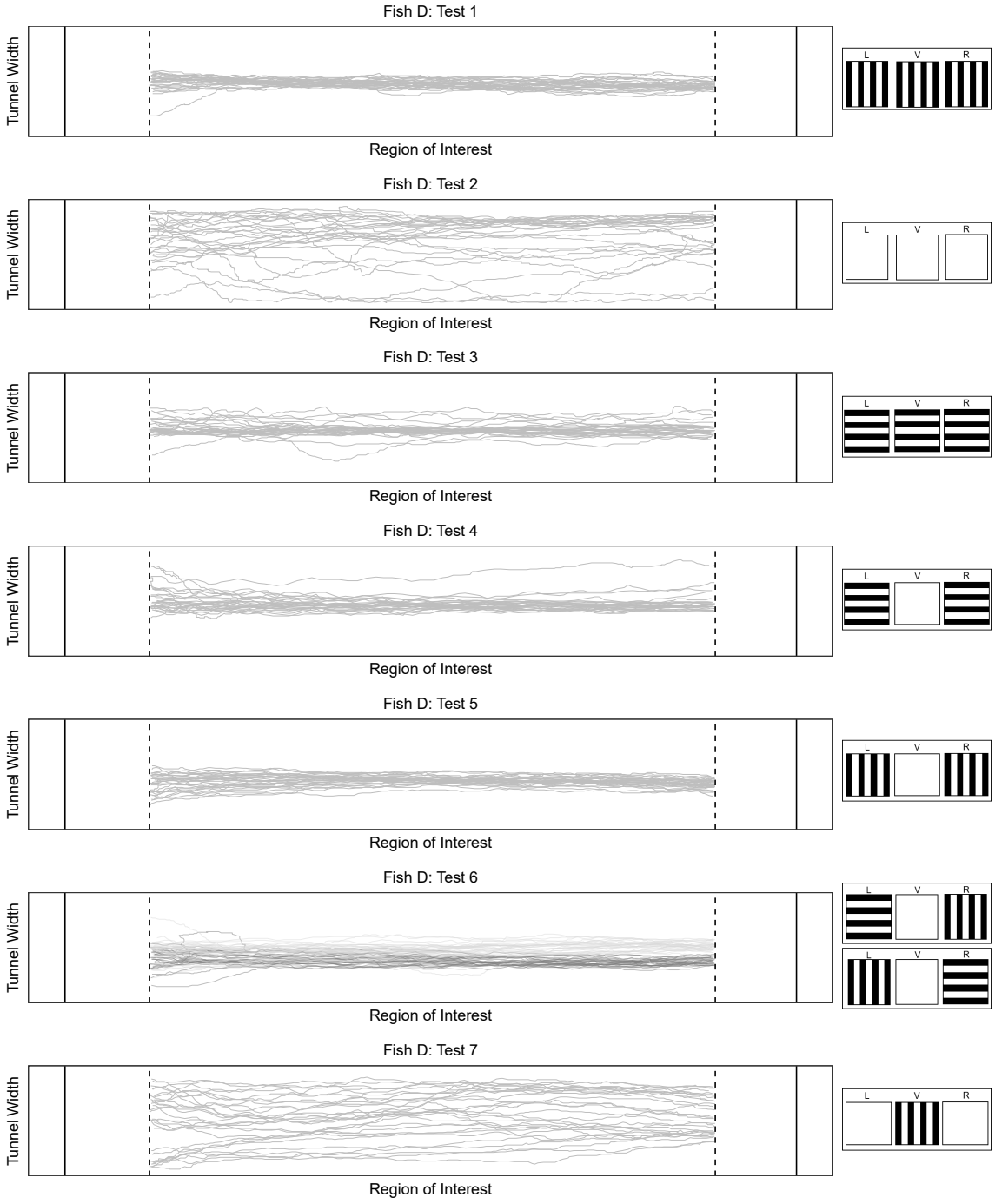


Figure 4: Individual tracks for Fish D between start areas across treatments. Tracks go from left to right. In test 6, tracks in light grey indicate test 6.1 (top image) and tracks in dark grey indicate test 6.2 (lower image). Only tracks from the region of interest, bounded by the vertical black dashed lines are shown.

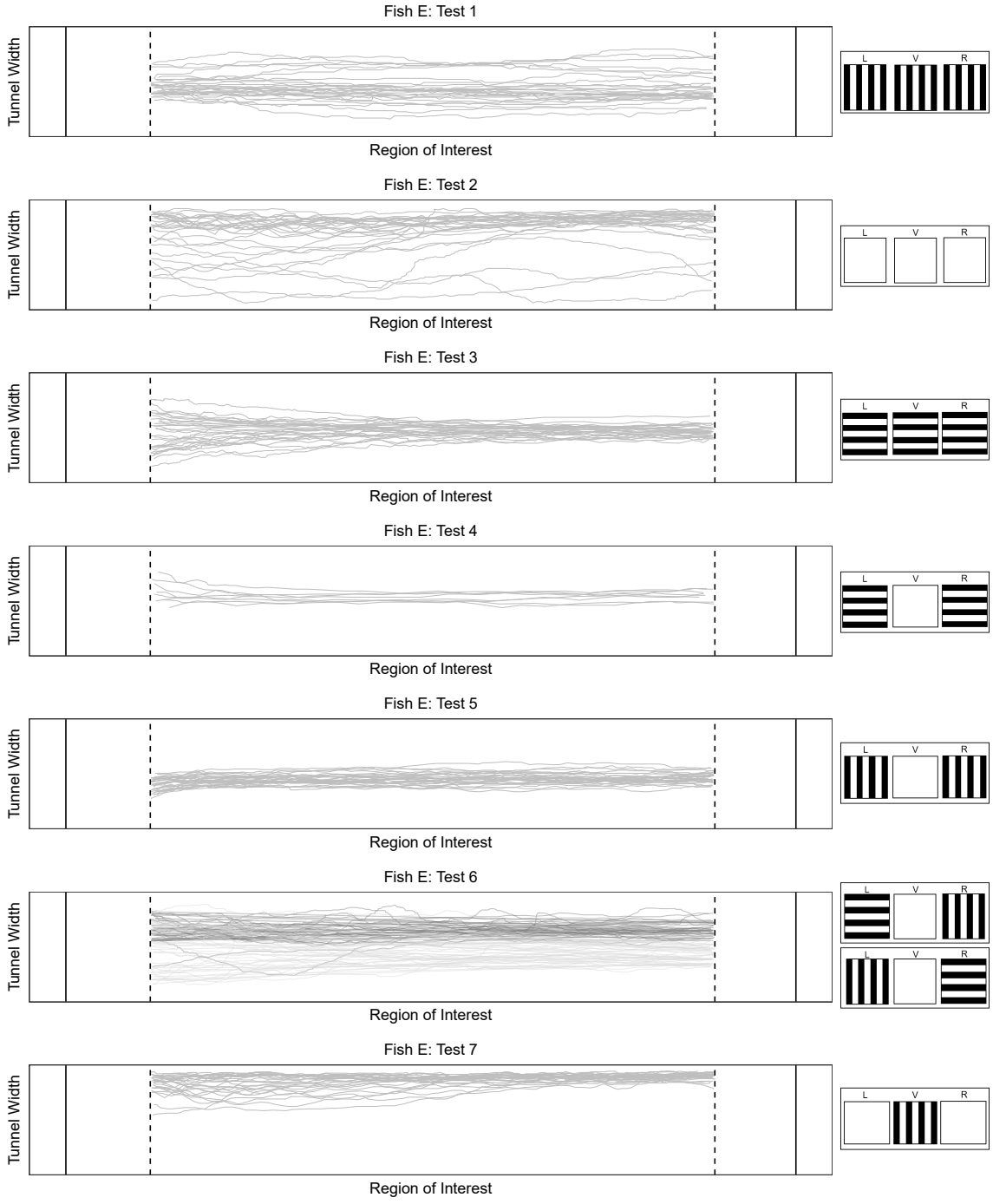


Figure 5: Individual tracks for Fish E between start areas across treatments. Tracks go from left to right. In test 6, tracks in light grey indicate test 6.1 (top image) and tracks in dark grey indicate test 6.2 (lower image). Only tracks from the region of interest, bounded by the vertical black dashed lines are shown.

3 Statistical model summaries

3.1 Model results: lateral position

Visual treatment did have a significant effect on the mean absolute deviation from the central line (GLMM (visual treatment - fixed effect; fish ID - random effect), Type III analysis of variance with Satterthwaite's method to determine degrees of freedom, $F_{7,1098}$ = 128, $p<0.001$), with some residual variance explained by the random effect of fish identity (Likelihood Ratio Test of the model with and without the random effect of fish = 176, $p<0.001$).

Visual treatment also had a significant effect on the mean deviation from the central line (GLMM (visual treatment - fixed effect; fish ID - random effect), Type III analysis of variance with Satterthwaite's method to deterimine degrees of freedom, $F_{7,1098}$ = 3.78, $p<0.001$), with some residual variance explained by the random effect of fish identity (Likelihood Ratio Test of the model with and without the random effect of fish = 187, $p<0.001$).

Individual track standard deviation was affected by visual treatment (GLMM (log-link gamma distribution; visual treatment - fixed effect; fish ID - random effect), Type II Wald Chisquare test, χ^2_7 = 203, $p<0.001$).

Finally, the residual of track position from the treatment mean was also affected by visual treatment (GLMM (log-link gamma distribution; visual treatment - fixed effect; fish ID - random effect), Type II Wald Chisquare test, χ^2_7 = 357, $p<0.001$).

3.2 Model results: swimming speed

Track swimming speed was affected by access to spatial frequency information (GLMM (visual treatment - fixed effect; fish ID - random effect), Type III analysis of variance using Satterthwaite's method for degrees of freedom: $F_{7,1098}$ = 119, $p<0.001$), with some residual variance explained by the random effect of fish identity (Likelihood Ratio Test of the model with and without the random effect of fish = 166, $p<0.001$).

Second, track residual speed from the treatment mean was also explained by access to spatial frequency information (GLMM (log-link gamma distribution; visual treatment - fixed effect; fish ID - random effect), Type II Wald Chisquare test, $\chi^2_7 = 640$, $p<0.001$).

Finally, the mixed effects model for the effect of visual treatment on the log of normalised dimensionless jerk indicated a significant effect of visual treatment (GLMM (visual treatment - fixed effect; fish ID - random effect), Type III analysis of variance using Satterthwaite's method for degrees of freedom: $F_{7,1098} = 90.0$, $p<0.001$), with some residual variance explained by the random effect of fish identity (Likelihood Ratio Test of the model with and without the random effect of fish = 147, $p<0.001$).

4 Testing model assumptions

We ascertained that models described in the analysis adhered to the assumptions of linear mixed effects modelling. Data was modelled to appropriate distributions according to the shape of the data. All data was fitted using a gaussian distribution, except for analyses of standard deviation and residual data that showed continuous positive right skew and were modelled using a gamma distribution with a log link.

Model residuals were then required to be normally distributed. Histograms of residuals and qqplots of standard normal quantiles against standardised residuals were visually inspected. Residuals were deemed to be normally distributed if the majority of points on the qqplot followed the central 1:1 straight line, but small deviations of the tails from the 1:1 line were permitted. Small deviations of tails in the same direction from the qqplot 1:1 line would indicate a slight left or a right skew, but tails deviating in opposite directions simply reflect 'fat' or 'thin' tails to the normal distribution.

The assumption of linearity was tested by plotting model residuals, ie the difference between the predicted model value and the actual value, against the model predictor (visual treatment for all models), and linearity was ascertained if no clear linear pattern emerged.

Finally, homogeneity of variance was assessed by plotting fitted data against the model residuals, and points should be equally distributed above and below the 0.00 line. Our analyses demonstrate that variance does differ across some visual treatments. However, mixed effects modelling and subsequent analysis of variance is sufficiently robust to deviations from exact equality of variance to make the deviations observed in our analyses acceptable to forming robust, reliable conclusions [2].

References

[1] Cohen J. *The Concepts of Power Analysis BT - Statistical Power Analysis for the Behavioral Sciences (Revised Edition)*. Hillsdale, N.J. : L. Erlbaum Associates, 1988. doi: 10.4324/9780203771587.

[2] Blanca M.J., Alarcón R., Arnau J., Bono R., and Bendayan R. Effect of variance ratio on ANOVA robustness: Might 1.5 be the limit? *Behavior Research Methods*, 50(3):937–962, Jun 2018. doi: 10.3758/s13428-017-0918-2.

Appendix D

Supplementary Information: A fish's frame of reference: distance estimation in variable flows.

Supplementary Information: A fish's frame of reference: distance estimation in variable flows

C. Karlsson[1], J.K. Willis[1], and T. Burt de Perera[1]

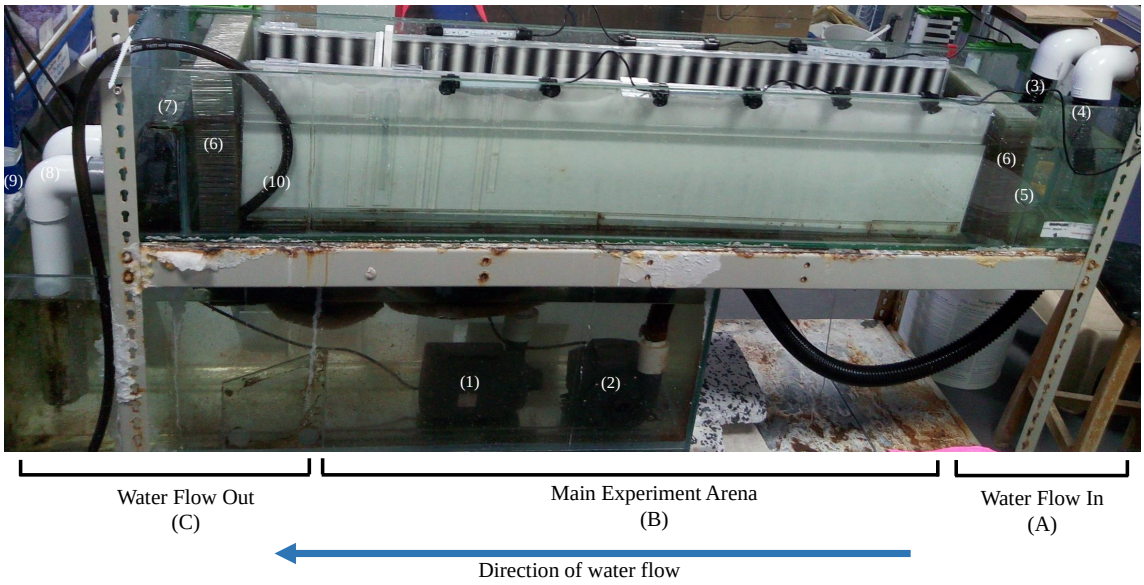
[1]Department of Zoology, Research and Administration Building, 11a Mansfield Road, Oxford, OX1 3SZ

Contents

1 Apparatus **i**

2 Fish illness report **v**

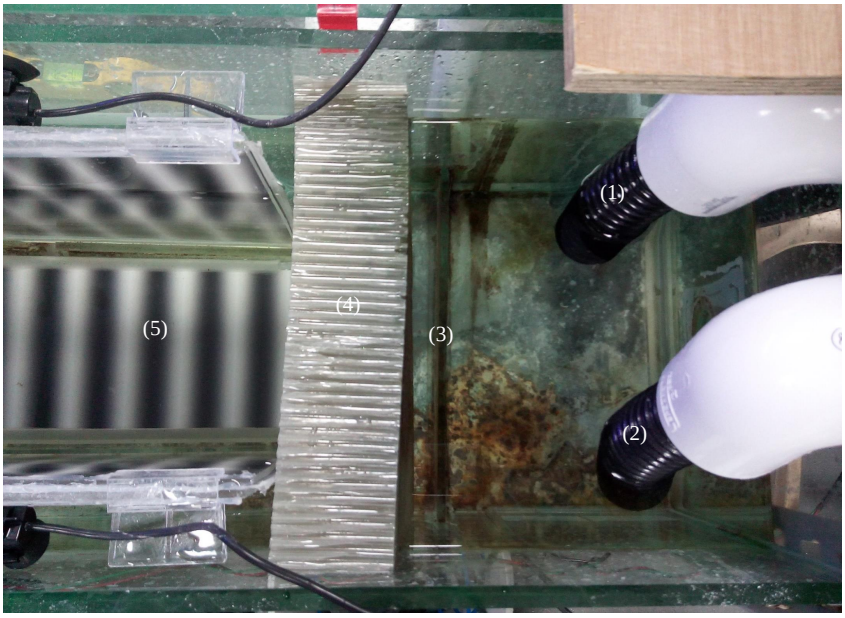
1 Apparatus



(1) Pump 1
(2) Pump 2
(3) Water flow in from pump 1
(4) Water flow in from pump 2
(5) Glass weir to maintain water depth
(6) Flow straighteners
(7) Glass weir to maintain water depth
(8) Water flow out to sump
(9) Passive water flow out to home aquarium system sump
(10)Water flow in from home aquarium system

Figure 1: Side view of full flume system, with three main regions: (A) Water flow in; (B) Main experiment arena; (C) Water flow out. The experiment system sump, experiment arena tank and home water system are all connected via a closed water system to maintain constant water parameters, namely salinity and temperature.

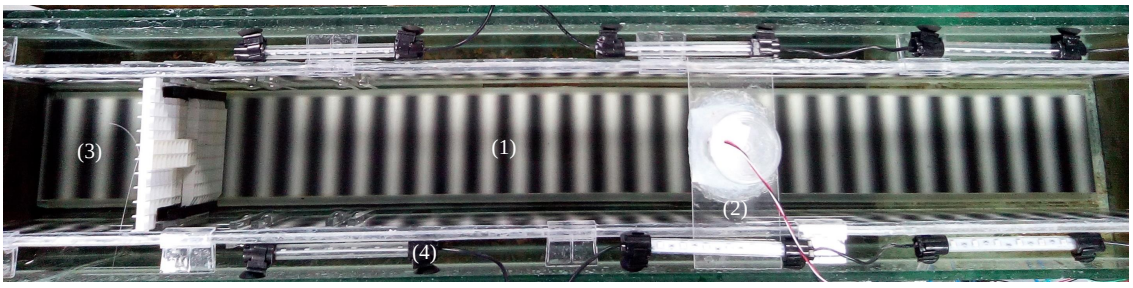
(A)



(1) Water flow in from pump 1
(2) Water flow in from pump 2
(3) Glass weir to maintain water depth
(4) Flow straightener
(5) Main experiment arena

Figure 2: Top-down view of region (A): water flow in. Water is fed in via two inlet pipes connected to pumps each capable of moving water at 150l/minute. A glass weir (3) maintains a minimum water depth, and a flow straightener (4) ensures laminar flow through the experiment arena (5).

(B)

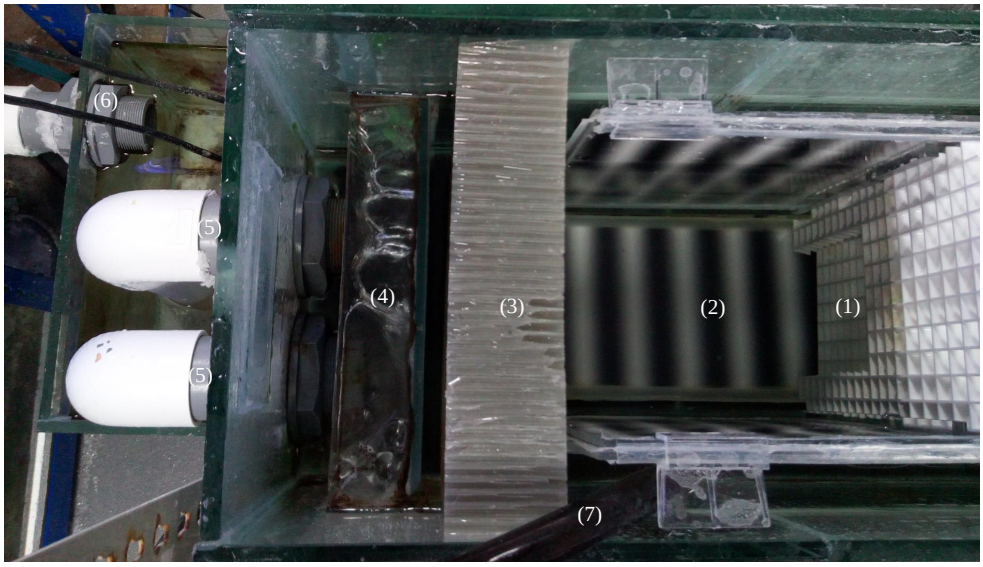


Direction of water flow

(1) Main experiment arena with training background of black and white sinusoidal stripes (grey background on reverse)
(2) Overhead infra-red proximity sensor (IR detector)
(3) Start Area
(4) Surrounding aquarium lights

Figure 3: Top-down view of region (B): the main experiment arena. The walls and floor are interchangeable between two different visual patterns: a black and white pattern with spatial contrast changing gradually according to a sinusoidal function, and a plain grey background when the walls are reversed. An overhead infrared detector (2) controls the surrounding aquarium lights (4) via an Arduino microprocessor. The start area doorway is perforated to ensure water can flow freely through it to the back of the tank where outlet pipes are located.

(C)



(1) Start area doorway
(2) Start area
(3) Flow straightener
(4) Glass weir to maintain minimum water depth
(5) Passive water flow out to experiment system sump
(6) Passive water flow out from experiment system to home aquarium system sump
(7) Water flow in from home aquarium system

Figure 4: Top-down view of region (C): the outlet system. A weir once more maintains a minimum depth (4) and water flows out over the weir and to the sump below via two large outlet pipes (5). A second outlet on the experiment system sump (5) allows water to passively flow into the home aquarium system sump. Water is pumped back from the home aquarium system to the experiment system via a small eheim pump moving 15l/minute (7).

2 Fish illness report

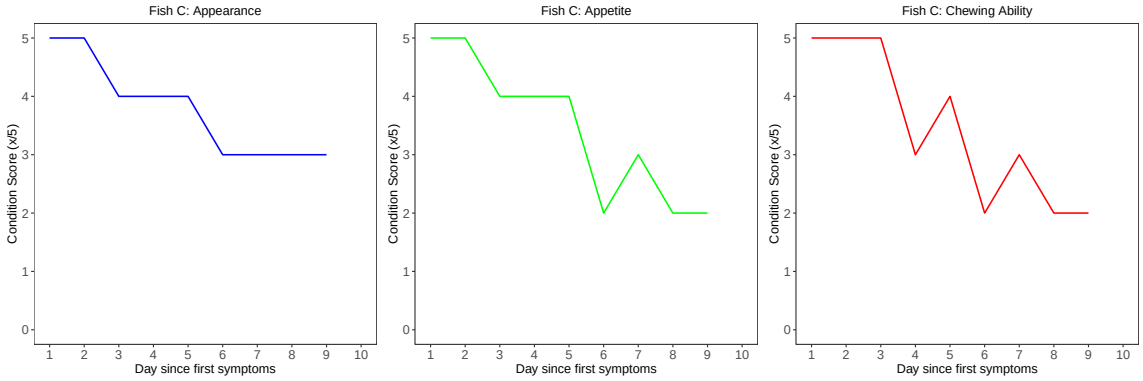
Five out of the six fish selected for this experiment were unable to complete either training or all testing stages due to a highly contagious infection spreading through the population. The illness was characterised primarily by a gradual decline in motivation in experiments followed by the sudden onset of chewing and swallowing difficulties. Fish became increasingly lethargic over time, and showed a gradual loss of body condition as a result of reduced food intake.

Fish were removed from further experimentation upon onset of any of the above symptoms, and were scored daily according to three measures to track disease progression: overall appearance (table 1), appetite (table 2), and chewing ability (table 3). All measures were scored out of 5, with 5 being normal and 1 being the lowest acceptible level prior to humane end point (schedule 1 killing using MS222).

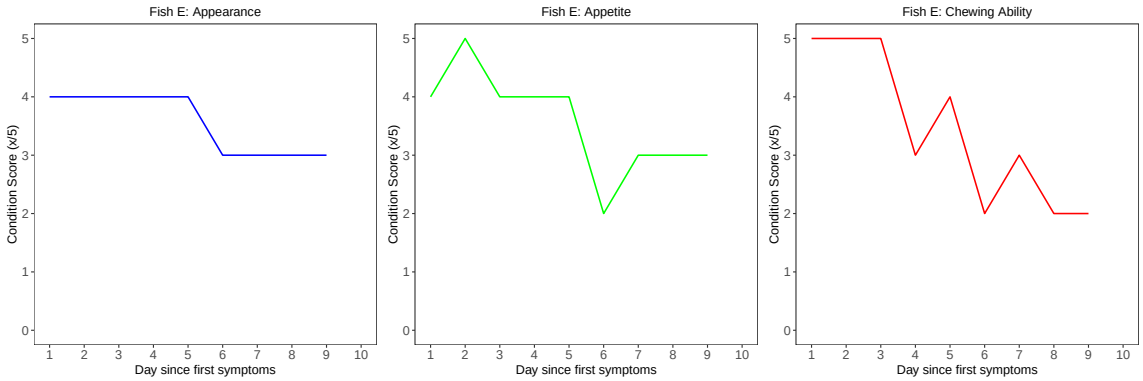
In an attempt to gain a diagnosis and the possibility of treating the majority of the affected population, the two initially worst affected individuals that demonstrated the most rapid decline in all three condition measures (Fish C and Fish E, fig. 5) were euthanised using an immersion of MS222 and post mortem analysis and histopathology were carried out. Individuals showed signs of hepatic lipidosis, reflected in severe discolouration and atrophy of the liver; reduced muscle mass; severe inflation of the swim bladder; a large increase in vascularisation to the liver, stomach and intestines; and, inflammation of the lymph nodes. The vascularisation could be a result of reactive hyperaemia with actual angiogenesis, reflecting a possible immune response to an infection.

None of the common stains used in histopathology were able to identify the specific pathogen responsible, but early evidence from giemsa staining suggests that it may be a novel myxozoan infection, hitherto unheard of in this fish species.

As no firm diagnosis or treatment was possible, Fish A, D and F continued to be monitored and condition scored daily. After 40 days with no significant improvement of the main symptoms, and a continuous decline in body condition (fig. 6), these individuals



(a)

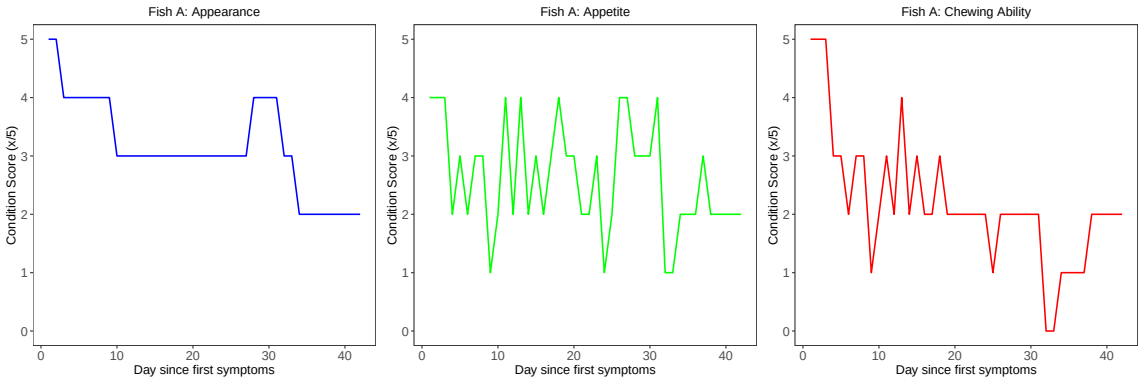


(b)

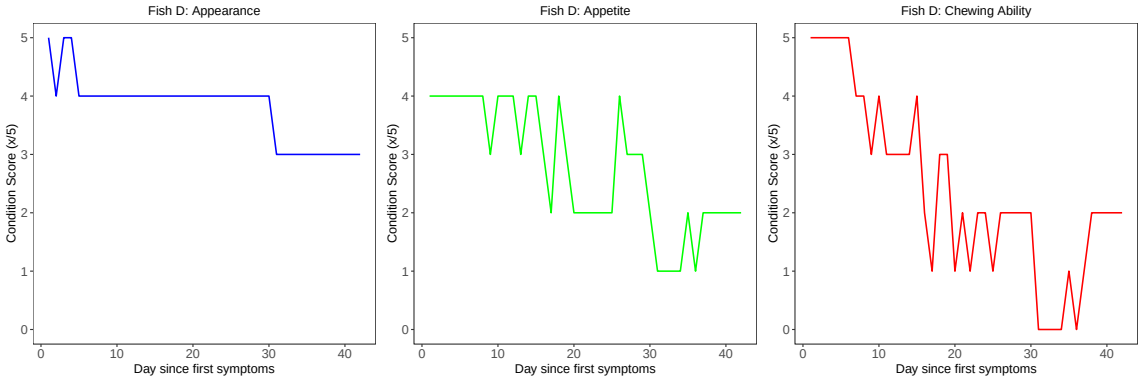
Figure 5: Change in condition scores over time for Fish E and C. All measures were scored out of 5, with a score of 5 indicating normal condition, and a score of 1 indicating the worst acceptable sustained condition prior to humane end point. Measures were as follows: Overall Appearance (blue), appetite (green), and chewing ability (red). Fish E and C were euthanised after 9 days of gradually worsening symptoms and used for diagnosis via post mortem and histopathology.

were also euthanised. Post mortems confirmed the same pathological signs noted in Fish C and E.

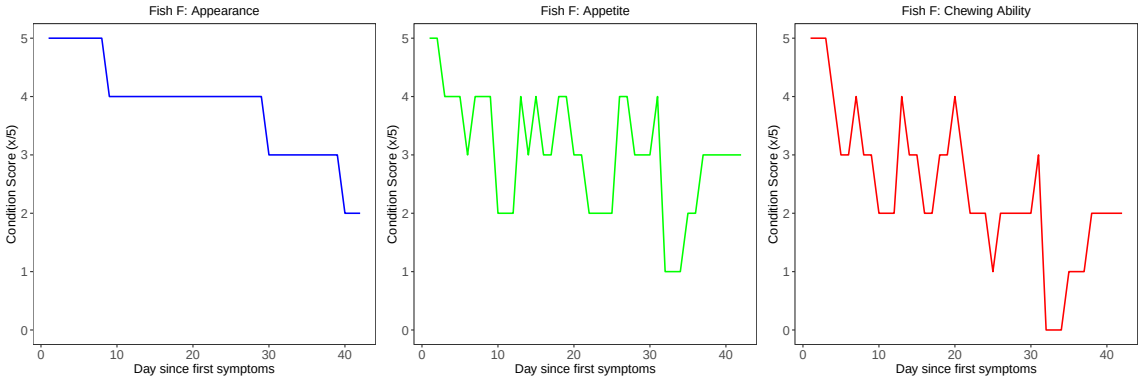
Unfortunately, replacement of these individuals from the wild to complete the sample size required for this experiment was not possible within the time-constraints present.



(a)



(b)



(c)

Figure 6: Change in condition scores over time for Fish A, D and E. All measures were scored out of 5, with a score of 5 indicating normal condition, and a score of 1 indicating the worst acceptable sustained condition prior to humane end point. Measures were as follows: Overall Appearance (blue), appetite (green), and chewing ability (red). Fish A, D and E were euthanised after 40 days of gradually worsening symptoms and post mortems were carried out to compare pathology with Fish E and C.

Condition Score	Description
5	Normal: High activity levels, well covered on chin, face, body area and tail. Colouration normal.
4	Some condition loss: pale in colouration, chin becoming more pronounced.
3	Pale skin, chin increasingly pronounced, and facial bones starting to protrude.
2	Pale skin, protruding chin and facial bones, stomach area hollowing out.
1	Emaciated: all facial bones protruding, hollow stomach area, loss of muscle on top line and tail area.

Table 1: Condition score table for fish overall appearance, with a score of 5 indicating normal appearnce, and a score of 1 indicating the worst acceptable appearance prior to humane end point.

Condition Score	Description
5	Normal appetite: begging for food, and quickly taking presented food directly from tweezers with no hesitation. Full food allowance consumed, with no display of satiation.
4	Reduced food begging behaviour. Some hesitation when presented with food from tweezers. Full food allowance consumed, but becoming satiated faster.
3	Needs encouragement to accept food from tweezers, and won't eat full food allowance, but still more than half.
2	Takes a long time to approach tweezers for food. Eats less than half of food allowance, no begging behaviours observed. May still slowly pick at a scatter feed.
1	No appetite: no interest in presented food, ignores a scatter feed.

Table 2: Condition score table for fish appetite, with a score of 5 indicating a normal appetite with classic begging behaviours, and a score of 1 indicating the worst acceptable sustained appetite levels prior to humane end point.

Condition Score	Description
5	Normal: rapidly chewing and swallowing food from tweezers with no noticeable problems (pellet and soft food). Larger fish will appear to swallow pellets whole.
4	Increased time taken between pellets. Even large fish will show visible chewing difficulties. Pellets may be spat out before being picked up again.
3	Showing visible difficulty with chewing: all pellet food is repeatedly spat out and recaptured. No issues with soft food.
2	Chewing takes an increasingly long time. Pellets repeatedly spat out and eventually abandoned. Chewing difficulties even with soft food.
1	Inability to chew or swallow pellets, accompanied by fish rapidly giving up on individual pellets. Takes a long time to chew even soft food. Un-eaten food is scattered around the tank.

Table 3: Condition score table for fish chewing abilities, with a score of 5 indicating normal chewing of soft and hard food, and a score of 1 indicating the worst acceptable sustained chewing and swallowing ability prior to humane end point.

$\sim$ Page left blank intentionally $\sim$

Appendix E

Supplementary Information: Development of methods - designing and testing a behavioural task for studying distance estimation in teleost fish.

Supplementary Information. Development of methods: designing and testing a behavioural task for studying distance estimation in teleost fish

C. Karlsson[1] and T. Burt de Perera[1]

[1]Department of Zoology, Research and Administration Building, 11a Mansfield Road, Oxford, OX1 3SZ

Contents

1 Arduino set-up **i**

1 Arduino set-up

To set up the automated lighting system, we connected a SHARP 2Y0A21 proximity sensor to an Arduino Uno microprocessor, which via a MOSFET power adaptor controlled the overhead aquarium lights.

First, the three wires to the SHARP 2Y0A21 proximity sensor were connected to 5V power, Ground and the A0 analog Pin on the main Arduino Uno circuit board (fig. 1, red arrows).

Next, a MOSFET power adaptor with a 10 ohm resistor was connected to the main Arduino circuit board via power connections to 5V and Ground (fig. 1, blue arrows) and a digital connection to digital pin 10 (fig. 1, green arrow).

The wiring of the two sets of aquarium lights were in turn connected to the +/- device connections on the MOSFET. The two sets of LED lights (Interpret Triple LED Lighting System, 0.75m) could then be plugged in as normal to a mains power supply (235V), but were controlled using the proximity sensory via the Arduino microprocessor, functioning at a much lower voltage (5V).

The Arduino itself was powered and controlled via the PC through a Matlab (Mathworks Inc) program. The voltage of the infrared proximity sensor varied between 0V and 3.5V depending on the strength of the reflection from objects which passed in front of it in the tunnel. We tested the response of the detector to objects in water and after this we set a threshold of 1.7V. As the fish passed beneath the detector, a voltage change was registered and when this exceeded 1.7V, the Matlab program caused the aquarium lights to be switched on.

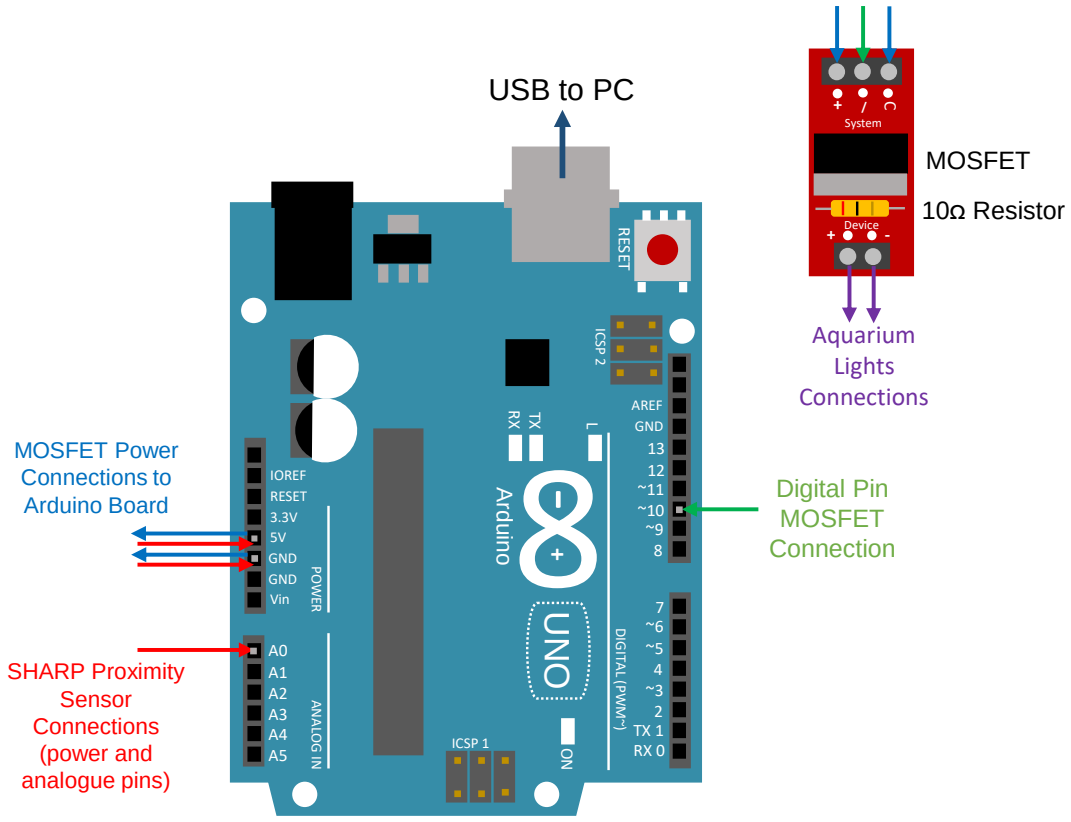


Figure 1: Arduino set-up for continuous distance estimation task with *Rhinecanthus aculeatus*. The SHARP 2Y0A21 Proximity sensory was connected to 5V power, ground and the A0 analog pin. The MOSFET transformer connecting the aquarium lights to the Arduino was connected to 5V power, Ground, and Digital Pin 10. The MOSFET transformed used a 10 ohm resistor.

Appendix F

Pilot experiment: Metric spatial memory in *Lamprologus ocellatus*.

Pilot experiment: Metric spatial memory in the shell-dwelling cichlid, *Lamprologus ocellatus*

C. Karlsson[1], J. Green[1], and T. Burt de Perera[1]

[1]Department of Zoology, Research and Administration Building, 11a Mansfield Road, Oxford, OX1 3SZ

Contents

1 Background and Aims **i**

2 Methods **ii**

2.1 Subjects ii

2.2 Experiment set-up iii

2.3 Training iii

2.4 Testing v

2.5 Analysis vi

3 Preliminary Results **vii**

3.1 Training vii

3.2 Testing: tracks vii

3.3 Testing: search areas viii

3.4 Testing: trajectories xi

4 Future work: experiment design for testing path integration in *Lamprologus ocellatus* **xii**

1 Background and Aims

Path integration involves the use of an internal reference of the distance and direction travelled during a journey to compute a direct trajectory back to a starting position (fig. 1a). This form of navigation allows an animal to navigate independently of allothetic informaton such as external landmarks or geometric cues from the environment.

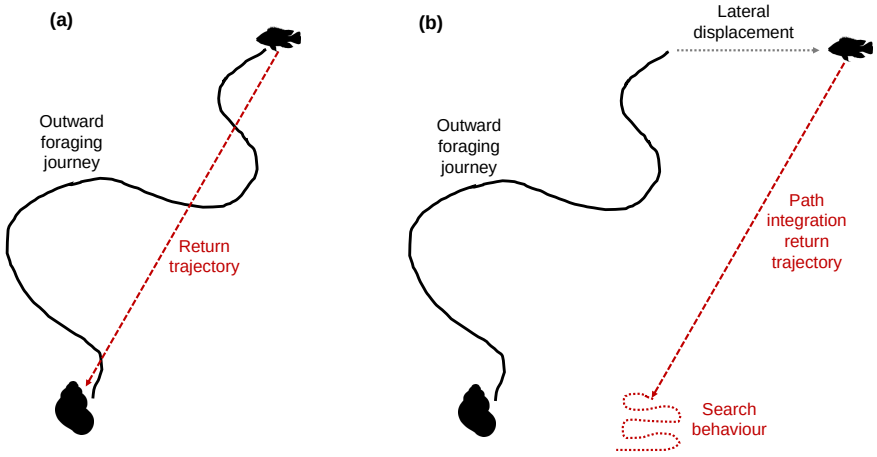


Figure 1: Displacement experiment to test path integration in central place foragers. (a) A path integrating animal will summate its outward movement vectors during a foraging journey (black trajectory) to compute a direct vector taking it directly back to its home nest (red arrow). (b) If the animal is experimentally displaced laterally prior to returning home from a foraging journey (grey arrow), it will still follow its internally computed vector parallel to the original correct path.

I have shown that teleost fish are able to estimate distance travelled, a central component of path integration navigation, using self-motion cues alone. However, whether this is part of a teleost path integrator remains unknown. In order to conclusively demonstrate that teleost fish are able to path integrate, we must test fish in a displacement experiment similar to that used to test the path integrators of terrestrial animals, such as the gerbil [1] and the desert ant [2] (fig. 1).

Path integration is most strongly used and easily demonstrated in central place foragers. These animals typically have a home nest or location and leave this home nest to

patrol their territory, move between foraging patches, or find mates. *Rhinecanthus aculeatus* is a central place forager and would therefore have been a good candidate for studying path integration in teleosts. However, their large size and tendency towards aggression and destroying experiment set-ups means we considered a different fish species to study teleost path integration using a maze set-up.

We predicted that path integration was likely to be important for the African radiation of shell-dwelling cichlids. These fish are also central place foragers, with both males and females aggressively defending a central home shell and additional peripheral sub-shells from predators and conspecifics [3]. Fish will leave their main shell for short foraging journeys to feed on small fish and crustaceans, patrol peripheral sub-shells, and for courtship and mating. The lake and river floors of their habitats are littered with visually indistinguishable shells, mostly of the gastropod *Neothauma tanganyicense*, from which they must be able to rapidly determine the location of their own shell. Having an internal vector containing information on the direct distance and direction back to their home shell is therefore likely to be advantageous.

In this pilot experiment with a small group of adult male *Lamprologus ocellatus* subjects, we aimed to explore whether these fish do use internally-computed distance and direction information to remember the relative position of a home shell. We also aimed to assess their suitability for training in operant conditioning tasks and testing in novel environments. Results from this experiment would then be used to inform a full experiment design for testing the path integration abilities of this species.

2 Methods

2.1 Subjects

Subjects were 8 *Lamprologus ocellatus* adult males from the Lake Tanganyika radiation of African shell-dwelling cichlids. Outside of experiments, fish were housed in individual tanks measuring 0.35m x 0.30m x 0.65m, and were provided with deep sand substrate and

a single home shell. Tanks were cleaned weekly and water quality tested twice weekly (nitrates were kept below 10ppm, nitrites and ammonia at 0ppm, kH at 12, gH at 25, and pH at 8.2). Water was prepared using RO water mixed with Seachem Cichlid lake salts and Seachem Malawi/Victoria Buffer to replicate the mineral content and pH in their natural lake habitat. A 12h/12h day/night light cycle was maintained through an automated overhead lighting system.

2.2 Experiment set-up

All experiments took place in a separate experiment tank measuring 0.80m (length) x 0.60m (width) x 0.45m (height). A sand bed of 0.07m depth was provided, using the same material as in their home tanks. The experiment tanks and home tanks were in the same room and shared a water supply to maintain constant water paramters.

The experiment tank was split into two regions: familiar area (width 0.20m), and unfamiliar area (width 0.60m), separated from each other by a removable clear perspex screen (fig. 7a and d). Within the unfamiliar area was an opaque holding chamber of diameter 0.10m, connected to a clear perspex L-shaped tube of side lengths 0.30m and diameter 0.07m. Side lengths of 0.30m were chosen because this produced a beeline distance of 0.42m, which is within the average range of inter-shell distances for this species [3]. The L-shaped tube connected directly to the familiar area. Doors prevented the fish from exiting the familiar area and opaque start area outside of training trials.

2.3 Training

Fish were split into two groups of 4 individuals: trained and control. Control fish were trained to swim voluntarily into a clear transport container for a food reward but did not undergo any main training phases. In contrast, following the same period of pre-training to voluntarily swim into the transport container, trained fish went through two key training phases.

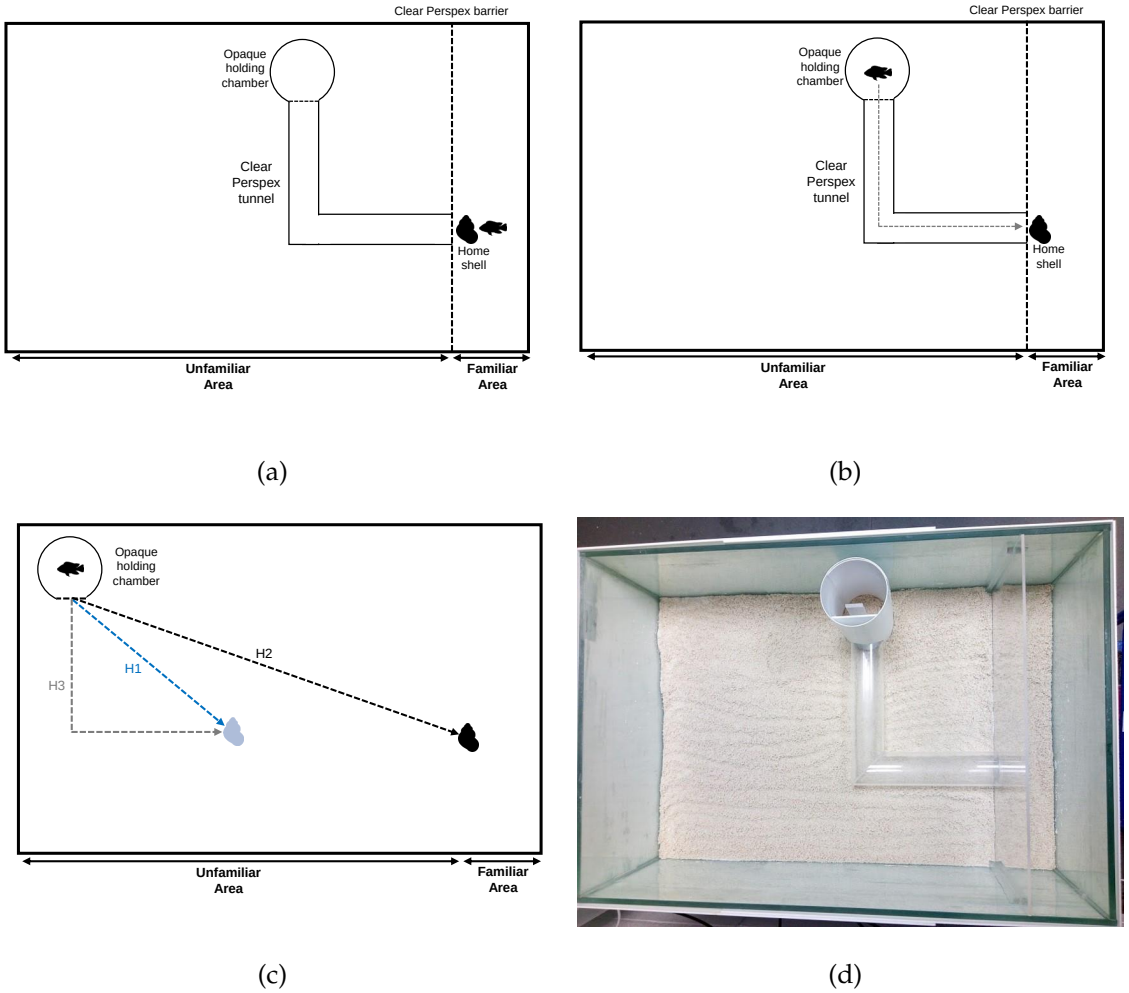


Figure 2: Training and testing in a metric spatial memory task with *Lamprologus ocellatus*. (a) Training stage 1: the fish is introduced to the familiar area with its home shell and is given 4 days to settle and form a territory. (b) Training stage 2: the fish is periodically displaced into an opaque holding chamber and is trained to swim through an L-shaped tunnel to return to its home shell (grey line). (c) Testing: The holding chamber is shifted to a novel position and the fish is released without the L-shaped tunnel guiding swimming trajectories. The shell has also been removed. H1 (black line) is the predicted trajectory if the fish is able to integrate the previously learned internal representation of distance and direction travelled to return to the percevied previous position of its shell (now removed). H2 (blue line) is the predicted trajectory if the fish returns along the most direct trajectory to the previous location of its shell as indicated by external allothetic cues. H3 (grey line) is the predicted trajectory if the fish swims along the previous trajectory as determined by the L-maze. (d) Photo of set-up in training configuration.

In training phase I (fig. 3a), the fish was placed in the familiar area of the experiment tank. Its home shell was placed adjacent to the entrance to the connecting L-tube entrance. Access to the tunnel was blocked by a door. The fish was then given 4 days to settle and form a territory. During this time, it was fed its normal diet twice daily.

In training phase II (fig. 3b), the fish was caught in a transport container and placed in the opaque holding chamber. The shell remained in its previous position within the familiar area. The fish was given 2 minutes to settle prior to the door to the L-shaped tube being opened, allowing the fish to swim down the L-tube to return to its shell. *Lamprologus ocellatus* males are strongly motivated to return to their shell once displaced from it. All training trials were filmed from above at 30fps using a Logitech c920 camera. Training trials were complete once the fish had returned to its home shell, or until the session limit of 20 minutes was reached, whichever came first. If the fish did not exit the holding chamber before the 20 minute time limit, it was captured and returned to the familiar area via the transport container. Fish completed 3 displacement trials per day, with at least 2 hours between each displacement to avoid causing stress.

Training was considered complete when fish exited the holding chamber within 5 seconds of the door being opened and then swam directly to their shell with no pauses or turns in the tunnel, across three consecutive training trials. This was considered to represent a shift from exploratory behaviour to evidence of learning the correct route to rapidly return to their shell. The number of displacements required to reach this testing criterion varied from 10 to 17 between fish.

2.4 Testing

During the testing phase (fig. 3c), the opaque holding chamber was shifted laterally by 0.30m to a novel position within the unfamiliar area. The connecting L-shaped tunnel was then removed. The fish was caught in the transport container as before and moved to the holding chamber. The fish was once again given 2 minutes to settle, and during this

time the perspex barrier separating the familiar and unfamiliar areas was removed, and its home shell was taken away. The sand substrate was also redispersed and levelled to remove any positional odour or landscape shape cues from the familiar area. The door to the holding chamber was then opened and the fish was given 5 minutes to freely swim in the experiment tank. Control fish completed the same testing sessions as the trained individuals, but had no prior experience of the experiment tank or the maze set-up. Testing sessions were filmed from above at 30fps using a Logitech c920 camera.

If fish were motivated to return to their home shell and had formed a spatial memory of the location of this shell, we could form three hypotheses about their tracks (fig. 3c): (i) Fish swim along a direct trajectory using an internal memory of the distance and direction of the shell relative to the previous position of the opaque start area to return to the *relative* previous position of the shell (H1), (ii) Fish swim along a direct trajectory using external positional cues such as the geometry of the tank to return to the *absolute* previous position of the shell (H2), (iii) Fish retrace a previous path and swim along the trajectory determined by the L-maze (H3).

2.5 Analysis

Using a video tracking program written in Matlab (Mathworks Inc), the position of the most anterior part of the fish was tracked for each frame of the testing video.

We subsequently plotted fish trajectories and quantified two measured: (i) the relative time spent in search area H1 and H2; (ii) the mean distance of the fish's exit trajectory from the holding chamber from the predicted trajectories defined by H1, H2 and H3 (fig. 3c).

Fish ID	No. of training sessions
D	17
E	10
F	15
H	11

Table 1: Number of training sessions completed by each fish prior to testing.

3 Preliminary Results

3.1 Training

During pre-training, fish showed a strong motivation for food rewards. Within five days of feeding from tweezers in the transport container, fish readily collected food rewards up to 0.30m from their home shell. This indicates that these fish could be trained in a more complicated training set-up using food rewards.

In the main training phases, fish showed few stress responses upon being moved to the holding chamber and rapidly learned the route through the L-maze to return to their home shell, with 17 being the highest number of displacements prior to testing (table 1).

3.2 Testing: tracks

Figure 3 shows the tracks of the four trained fish for the first 2.8m travelled upon release from the holding chamber and fig. 4 shows the tracks of the four control fish. Tracks were cropped to 2.8m as this was the total distance required to swim once around the tank perimeter and therefore accounted for the fish being able to enter both hypothesised search areas and return to the holding chamber. Analysis was therefore not biased towards the search area for hypothesis 1, which was closer to the holding chamber. All trained fish readily swam into the central area of the experiment tank, unlike control fish that showed a tendency to swim closer to the tank perimeter. Among both trained and

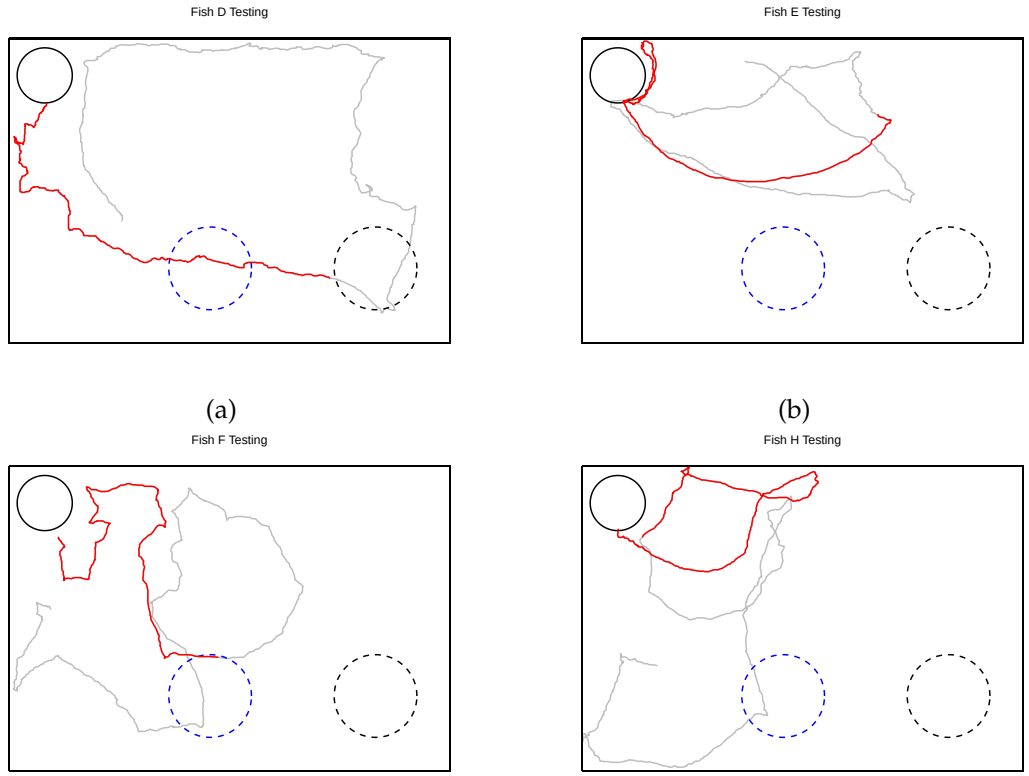


Figure 3: Tracks of the first 2.8m travelled (equivalent to once around the tank perimeter) upon release from the holding chamber for trained fish. The first 1m of each track is coloured in red. The black solid circle indicates the actual position of the holding chamber during testing. The blue dashed circle indicates the predicted search region for H1 (use of internal distance and direction information), and the black dashed circle indicates the predicted search region for H2 (use of external cues).

control fish, only one individual from each group (Fish D - trained, Fish I - control) entered the previous familiar area, with the remaining fish exploring only the unfamiliar area.

3.3 Testing: search areas

First, we explored whether fish preferentially moved into search area H1 (green circle in fig. 3) or into search area H2 (blue circle in fig. 3). Search areas were defined as a 0.15m diameter circle with the hypothesised position of the shell occupying the centre of each circle. 0.15m was chosen as predators coming within this distance to a shell will

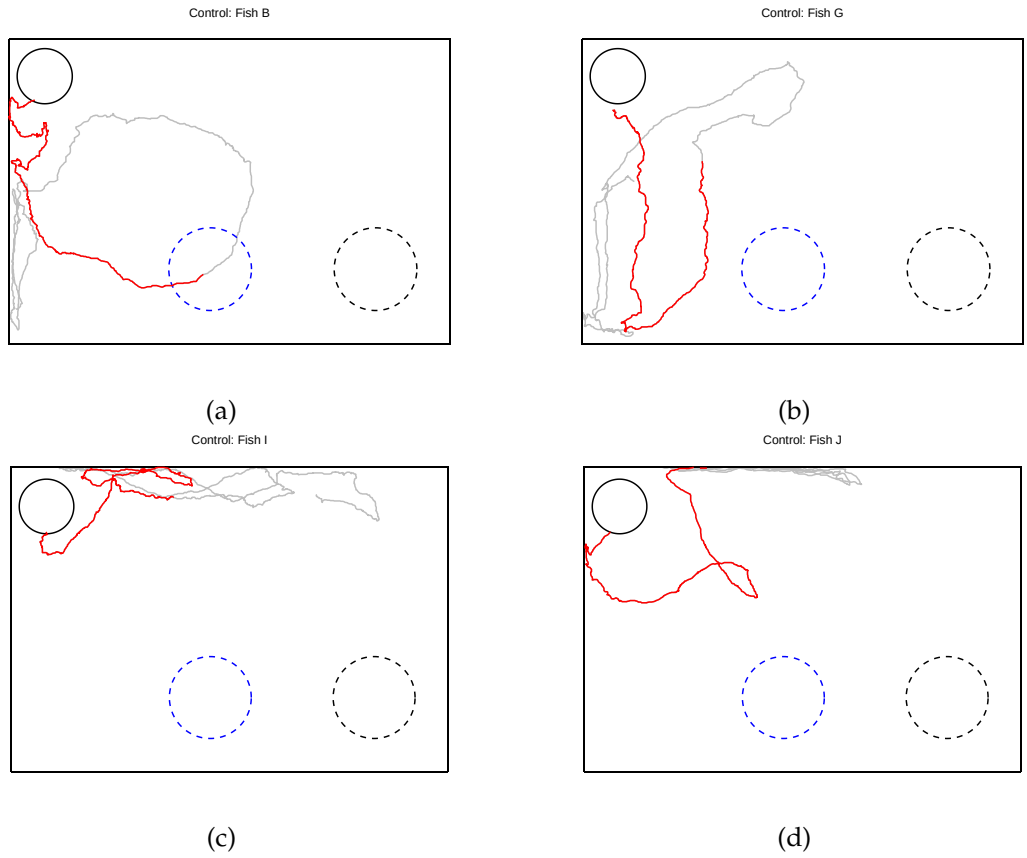


Figure 4: Tracks of the first 2.8m travelled (equivalent to once around the tank perimeter) upon release from the holding chamber for control (untrained) fish. The first 1m of each track is coloured in red. The black solid circle indicates the actual position of the holding chamber during testing. The blue dashed circle indicates the predicted search region for H1 (use of internal distance and direction information), and the black dashed circle indicates the predicted search region for H2 (use of external cues).

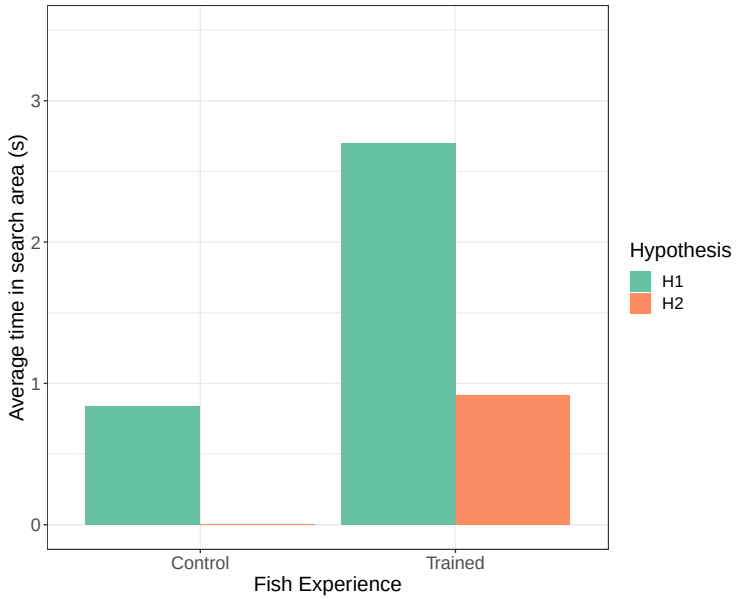


Figure 5: Total time spent in each pre-defined search area for H1 (using an internal reference of the previously learned distance and direction of the shell relative to the holding chamber) and H2 (using the absolute previous position of the shell within the experiment tank) for testing and control fish during the first 2.8m travelled following release from the holding chamber.

illicite territorial aggression responses in male *Lamprologus ocellatus* subjects [4]. We could therefore assume that this area covered the territory range of that particular shell.

We quantified the total time spent in each search area for each fish's 2.8m trajectory (fig. 5). Overall, both trained and control fish spent more time in search area H1 than search area H2. Among control fish, only one fish (Fish B, fig. 4a) entered either of the two start areas, with the remaining three fish preferentially swimming close to the tank walls. Among trained fish, three out of four tested individuals entered search area H1, and only one fish entered search area H2. The comparisons made therefore represent very small sample sizes. However, the trends in fig. 5 do indicate that trained fish spent a greater amount of in search area H1 compared to the untrained controls.

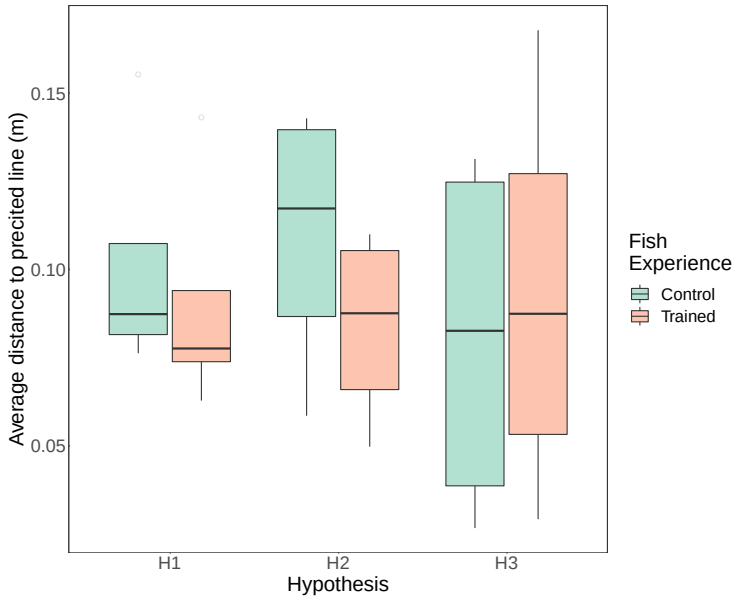
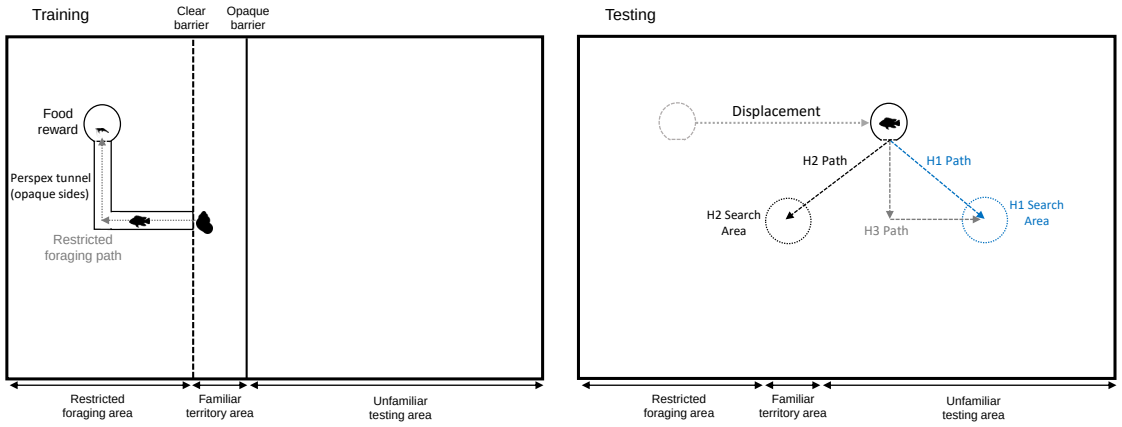


Figure 6: Average distance of fish exit paths from each of the predicted trajectories, split according to control and trained groups.

3.4 Testing: trajectories

Second, we explored how similar the exit track from the holding chamber was compared to the predicted trajectories as defined by H1, H2 and H3 in fig. 3c. The exit track was defined as the first 1m travelled upon exiting the holding chamber (highlighted in red in fig. 3 and fig. 4). 1m was chosen because it was the total length of the diagonal of the tank if the fish travelled from one corner of the tank to the opposite corner.

We calculated the shortest distance between each point on the fish's trajectory and each of the predicted trajectories according to hypotheses H1, H2 and H3. We then calculated the mean distance from the predicted trajectories for each fish's exit path. This was done for both control and trained fish and summarised results are shown in fig. 6. Trends in fig. 6 indicate that the trained fish are closer to both H1 and H2 than the control fish, with trained and control fish both slightly closer to H1 than H2. However, these effect sizes are very small, indicating that under the current set-up distinguishing between hypotheses H1 and H2 will require a large sample size and a modification to the experiment design.



(a) (b)

Figure 7: Training and testing in a path integration dispalcement task with *Lamprologus ocellatus*. (a) Training: Following a period of territory establishment in the familiar area, the fish is trained to swim through a perspex L-shaped tunnel to claim a high quality food reward (grey path). The fish is trained to have the door to the food reward chamber closed behind it as it consumes the food reward. It is then released and permitted to retrace its steps to its shell. (b) Testing: Upon having swum down the L-tube to claim its food reward, the door to the reward chamber is closed and the fish is displaced laterally to a novel position within the unfamiliar area. The L-maze, perspex barriers and shell are removed. The fish is then released from the reward chamber by removing the lateral walls. The exit bearing upon leaving the reward chamber, exit trajectory and preferential use of predicted search areas will be assessed. There are three hypothesised trajectories to find its lost shell. H1 (blue): the integrated trajectory based on summation of the outward movement vectors. H2 (black): the trajectory if allocentric landmark or environment geometry cues are used. H3 (grey): the trajectory if the fish retraces previous steps as if the L-maze was still there.

4 Future work: experiment design for testing path integration in *Lamprologus ocellatus*

Overall, this pilot study with *Lamprologus ocellatus* provided some indication that this species does learn and remember the previous distance and direction of their home shell relative to a starting position, rather than beaconing directly to the previous absolute position of their home shell based on allothetic cues from their environment. Using the results from this study, and observations during training, we propose an experiment set-up and

training protocol to comprehensively explore path integration in this species.

Results from the trajectory similarity analysis and search area analysis indicate a requirement for a geometric change in the experiment set-up. Trajectories H1 and H2 under the present set-up are likely to be too similar to adequately distinguish between use of either of these predicted paths. Moreover, as both control and trained fish preferentially explore the region closest to their release point, we cannot exclude the possibility that H1 is occupied more often due to its proximity to the holding chamber. Figure 7 proposes a new experiment set-up in which trajectories H1 and H2 are in opposite directions upon exiting the holding chamber, and search areas H1 and H2 are equidistant from the holding chamber.

This species has shown to be highly trainable using food rewards, indicated by the rapidly learned association of swimming into the transport container to obtain food. Moreover, it is robust to being placed in novel environments, as exhibited by the control fish readily exploring the experiment tank during testing despite no prior experience, and the trained fish upon being displaced to a novel position in the unfamiliar environment. Trained fish also rapidly learned the path down the L-tunnel to return to their home shell. These observations indicate that *Lamprologus ocellatus* subjects can be trained in a more complicated operant conditioning task to assess path integration. We propose that instead of fish being experimentally displaced to the holding chamber during training, the fish is instead trained to actively swim to the holding chamber via a path constrained by the L-tube to claim a food reward, and is then permitted to return to its shell via the same path (fig. 7a). This is crucial for testing path integration, as during path integration movement vectors are summated during the outward foraging journey. During testing, the fish is similarly allowed to move down the L-tube to claim its food reward, but prior to being allowed to return home via the same path, the fish is shut inside the holding chamber. This chamber, as before, will be displaced to a novel position in the experiment tank and the L-tube, perspex barrier and shell are removed (fig. 7b). The fish will then be released from the reward chamber. However, the exit direction will not be constrained - the fish

will have all walls of the holding chamber removed from around it. This will allow us to test the unconstrained exit bearing from the holding chamber, as well as the exit trajectory and search areas.

References

[1] Mittelstaedt M. L. and Mittelstaedt H. Homing by path integration in a mammal. *Naturwissenschaften*, 67(11):566–567, 1980.

[2] Müller M. and Wehner R. Path integration in desert ants, Cataglyphis fortis. *Proceedings of the National Academy of Sciences (PNAS)*, 85(14):5287–90, 1988.

[3] Bills I.R. *Eco-ethology of shell-dwelling cichlids in Lake Tanganyika*. PhD thesis, Rhodes University, 1996.

[4] Ota K. Fight, fatigue and flight: Narrowing of attention to a threat compensates for decreased anti-predator vigilance. *Journal of Experimental Biology*, 221(7), 2018.